TABLE OF CONTENTS

Summary of Section 7, Flood Risk Analysis

Purpose:

Section 7 assesses the probability of levee failures in the Delta under flood events.

Methods of Analysis:

Section 7.1 through 7.4 provide a summary of the flood risks from storm inflows and tides and estimate their corresponding stages throughout the Delta and Suisun Marsh. Section 7.5 presents the results of flood-related levee breaches and island flooding since 1900. Sections 7.6 though 7.14 discuss the flood-related failure modes and the procedures and method used to develop the levees' conditional probabilities of failure given flood stage.

Main Findings:

- Blankets of 15 feet or less in thickness have the highest impacts on under-seepage.
- The drainage ditch contribution to under-seepage is significant for blankets of 15 feet or less in thickness.
- Blankets of 20 feet or more in thickness are not impacted by the presence of a drainage ditch, which is assumed to be 5 feet deep or less.
- The presence or absence of slough sediments has a significant impact on under-seepage. However, it is difficult to map the presence, thickness, and composition of slough sediments knowing that their state is changing with flow velocities and channel dredging. This parameter is highly variable with time.
- Other contributors to under-seepage and through-seepage cannot be formally accounted for or explicitly modeled. These contributors include random and elusive weaknesses in the levees and their foundations (e.g., burrowing animals, human activities, or weak zones). We believe that these "weak links" are more pronounced in non-engineered levees.
- The use of empirical models and the calibration of the models against observations help account implicitly for these pre-existing and difficult-to-investigate weak links.

TABLE OF CONTENTS

Section 7 Flood Risk Analysis 7-1

7.1 Delta Inflow 7-1
7.2 Flow-Frequency Analysis 7-4
7.3 Delta Inflow Patterns 7-4
7.4 Delta Water Surface Elevations 7-6
7.4.1 Data 7-6
7.4.2 Data Review and Adjustments 7-6
7.4.3 Regression Analysis of Water Surface Elevations 7-7
7.5 Delta Levees and Historical Failures 7-7
7.6 Definition of Failure Modes 7-9
7.7 Probability of Failure due to Under-seepage 7-9
7.7.1 Definition of Vulnerability Classes 7-10
7.7.2 Material Properties and Random Variables 7-12
7.7.3 Methodology for Developing Flood Fragility Functions 7-14
7.7.4 Evaluation of Levee Response Functions 7-14
7.7.5 Evaluation of Conditional Probability Failure Functions 7-23
7.7.6 Evaluation of Fragility Functions 7-24
7.8 Probability of Failure due to Through-Seepage 7-25
7.9 Probability of Failure due to Overtopping 7-26
7.10 Probability of Failure due to Wind/Wave 7-26
7.11 Spatial Modeling of Physical Response of Levees to Flood Events 7-27
7.12 Island Failure Probability Under Multiple Failure Modes 7-28
7.13 Probability of Damage but No Breach 7-28
7.14 Length Effects on Probability of Levee Failures 7-28
7.15 Summary of Findings and Observations 7-29
7.15.1 General Observations 7-29
7.15.2 Findings 7-30

Tables

7-1 Partial List of Major Dams and Reservoirs in Tributary Watersheds to the San Francisco Bay-Delta
7-2 Summary of Delta Inflows
7-3 Statistical Analysis of Annual Peak Inflows
7-4 Annual Peak Delta Inflows (cfs), 1956–2005
7-5 Results of Log Pearson Type III Frequency Analyses
7-6 Parameters Used in Log Pearson Type III Distribution
7-7 Inflow Ranges (Bins) and Confidence Limit Probabilities for the High Inflow Season – Year 2000
7-8 Results of Logistic Regressions
7-9a Islands/Tracts Flooded Since 1900
7-9b Chronologic List of Flooded Islands Since 1900

7-9c Annual Peak Day Delta Inflows of Record (WY 1956 Through 2005)
7-10 Vulnerability Classes for Under-Seepage Analyses
7-11 Reported Permeability Data for Organic Soils
7-12 Reported Permeability Data for Sandy Soils and Silt
7-13 Permeability Coefficients Used for Initial Seepage Analysis
7-14 Initial Analysis Results for Terminous Tract
7-15 Estimated Vertical Gradients for Grand Island Under-seepage Problem
7-16 Evaluated Permeability Coefficients Used for Model Analyses

Figures

7-1 Flow Stations Used with Flood Hazard Analysis
7-2 Historical Delta Inflows
7-3 Temporal Distribution of Peak Delta Inflows
7-4 All Seasons Flow Frequency
7-5 High Runoff Season – Inflow Frequency
7-6 Low Runoff Season – Inflow Frequency
7-7 Comparison Between Inflow-Frequency Curves, CL = 50%
7-8 Flow in Sacramento River Plus Yolo Bypass Versus Total Delta Inflow
7-9 Relationship Between Flow in Yolo Bypass and Total Flow in the Sacramento River
7-10 Comparison Between Predicted and Observed Flow in San Joaquin River
7-11 Comparison Between Predicted and Observed Flows in MISC Inflow
7-12 Comparison between Predicted and Observed Flows in the Cosumnes River
7-13 Comparison between Measured and Predicted Flows in the Sacramento River and Yolo Bypass
7-14 Comparison between Measured and Predicted Flows in the San Joaquin River
7-15 Comparison between Predicted and Measured Flows in the Miscellaneous Inflows
7-16 Comparison between Predicted and Measured Flows in the Cosumnes River
7-17 Stations Used for Regressions Analyses
7-18 Venice Island (VNI) Predicted and Measured vs. Date 1/5/1998 - 7/4/1998
7-19 Historic Island Breaches in the Delta and Suisun Marsh Since 1990
7-20 Locations of Levee Failures
7-21 Cumulative Number of Levee Failures Since 1900
7-22a Cumulative Number of Levee Failures Since 1950
7-22b Number of Levee Failures per Year Since 1950
7-22c Program Funding Level
7-22d Total Delta Inflows (cfs) Since 1955
7-23 Effect of Slough Width on Vertical Gradient
7-24 Effect of Aquifer Thickness on Vertical Gradient

7-25 Effect of Slough Sediment Thickness on Vertical Gradient

7-26 Effect of Slough Bottom Elevation on Vertical Gradient

7-27 Spatial Distribution of Under-seepage Vulnerability Classes

7-28 Probability of Failure versus Flood Stage

7-29 Idealized Soil Profile - Terminous Tract

7-30 Finite Element Mesh and Boundary Conditions - Model with Drainage Ditch - Terminous Tract

7-31 Finite Element Mesh and Boundary Conditions - Model without Drainage Ditch - Terminous Tract

7-32 Total Head and Vertical Gradient Contours for Slough Water EL: 0 ft –Terminous Tract

7-33 Total Head and Vertical Gradient Contours for Slough Water EL: +4 ft Terminous Tract

7-34 Total Head and Vertical Gradient Contours for Slough Water EL: +7 ft Terminous Tract

7-35 Total Head and Vertical Gradient Contours for Slough Water EL: 0 ft- Model without Drainage Ditch, Terminous Tract

7-36 Total Head and Vertical Gradient Contours for Slough Water EL: +4 ft- Model without Drainage Ditch, Terminous Tract

7-37 Total Head and Vertical Gradient Contours for Slough Water EL: +7 ft- Model without Drainage Ditch, Terminous Tract

7-38 Effect of Permeability of Peat - Initial Analyses - Terminous Tract

7-39 Effect of Permeability of Sand Aquifer- Initial Analysis -Terminous Tract

7-40 Effect of Slough Sediment - Initial Analysis -Terminous Tract

7-41 Effect of Drainage Ditch - Initial Analysis -Terminous Tract

7-42 Reported Problem Areas

7-43 Topography and Boring Data - Grand Island

7-44 Idealized Cross-Section - Grand Island

7-45 Monitored Slough Water Level at Walnut Grove Station (ID: 91650)

7-46 Finite Element Mesh and Boundary Conditions, Grand Island Under-seepage Problem

7-47 Total Head & Vertical Gradient Contours for $(k_h/k_v)_{peat}$ = 10, Grand Island Under-seepage Problem

7-48 Total Head & Vertical Gradient Contours for $(k_h/k_v)_{peat}$ = 100, Grand Island Under-seepage Problem

7-49 Total Head & Vertical Gradient Contours for $(k_h/k_v)_{peat}$ = 1000, Grand Island Under-seepage Problem

7-50 Thickness of Organic Materials

7-51 Typical Cross Section with Drainage Ditch and 25 ft Peat & Organic Layer

7-52 Typical Cross Section without Drainage Ditch and 25 ft Peat & Organic Layer

7-53	Finite Element Mesh & Boundary Conditions, Typical Cross Section with Drainage Ditch and 25 ft Peat & Organic Layer
7-54	Finite Element Mesh & Boundary Conditions, Typical Cross Section without Ditch and 25 ft Peat & Organic Layer
7-55	Total Head & Vertical Gradient Contours, Typical Cross Section with Drainage Ditch for 5 ft Peat
7-56	Total Head & Vertical Gradient Contours, Typical Cross Section with Drainage Ditch for 15 ft Peat
7-57	Total Head & Vertical Gradient Contours, Typical Cross Section with Drainage Ditch for 25 ft Peat
7-58	Total Head & Vertical Gradient Contours, Typical Cross Section with Drainage Ditch for 35 ft Peat
7-59	Vertical Gradients for 5 ft Peat/Organics - Typical Cross Section with Ditch
7-60	Vertical Gradients for 5 ft Peat/Organics - Typical Cross Section without Ditch
7-61	Vertical Gradients for 15 ft Peat/Organics - Typical Cross Section with Ditch
7-62	Vertical Gradients for 15 ft Peat/Organics - Typical Cross Section without Ditch
7-63	Vertical Gradients for 25 ft Peat/Organics - Typical Cross Section with Ditch
7-64	Vertical Gradients for 25 ft Peat/Organics - Typical Cross Section without Ditch
7-65	Vertical Gradients for 35 ft Peat/Organics - Typical Cross Section with Ditch
7-66	Vertical Gradients for 35 ft Peat/Organics - Typical Cross Section without Ditch
7-67	Typical Cross Section for Suisun Marsh Levees
7-68	Finite Element Mesh and Boundary Conditions - Typical Cross Section for Suisun Marsh
7-69	Total Head & Vertical Gradient Contours for 25 ft Peat & Organics – Typical Cross Section for Suisun Marsh
7-70	Vertical Gradients for 5, 25, and 45 ft Peat/Organics - Typical Cross Section for Suisun Marsh
7-71	Probability of Failure versus Exit Gradient – No Human Intervention
7-72	Probability of Failure versus Exit Gradient – With Human Intervention
7-73a	Estimated Failure Probability at 16%, 50%, and 84% Confidence Levels for Under-seepage, Vulnerability Classes 1, 2, 3 and 4
7-73b	Estimated Failure Probability at 16%, 50%, and 84% Confidence Levels for Under-seepage, Vulnerability Classes 5, 6, 7 and 8
7-73c	Estimated Failure Probability at 16%, 50%, and 84% Confidence Levels for Under-seepage, Vulnerability Classes 9, 10, 11 and 12
7-73d	Estimated Failure Probability at 16%, 50%, and 84% Confidence Levels for Under-seepage, Vulnerability Classes 13, 14, 15 and 16
7-73e	Estimated Failure Probability at 16%, 50%, and 84% Confidence Levels for Under-seepage, Vulnerability Classes 17, 18, 19 and 20
7-73f	Estimated Failure Probability at 16%, 50%, and 84% Confidence Levels for Under-seepage, Vulnerability Classes 21, 22, 23 and 24

7-74 Through-Seepage Case Histories
7-75 Probability of Failure versus Water Height over the Crest - Overtopping Failure Mode

This section presents a summary of the analyses and results of the flood risk analysis. Section 7.1 through 7.4 provide a summary of the flood risks from storm inflows and tides and estimate their corresponding stages throughout the Sacramento–San Joaquin River Delta (Delta) and Suisun Marsh. Section 7.5 presents the results of flood-related levee breaches and island flooding since 1900. Sections 7.6 though 7.14 discuss the flood-related failure modes and the procedures and method used to develop the levees' conditional probabilities of failure given flood stage. Section 7.15 summarizes the findings and observations of the flood risk analysis. Detailed discussion of the flood risk can be found in the Flood Hazard Technical Memorandum (TM) (URS/JBA 2008a), and historical levee failures and the levee vulnerability analyses are discussed in the Levee Vulnerability TM (URS/JBA 2008c).

7.1 DELTA INFLOW

Average daily inflows into the Delta are available from the California Department of Water Resources (DWR) web site for the 50 water years (WYs) from October 1, 1955, through September 30, 2005 (WYs 1956 through 2005). These data include average daily inflows for all major streams entering the Delta and the total inflow into the Delta (DWR 2006). The major streams or stream groups included in the dataset are Sacramento River, Yolo Bypass, Cosumnes River, Mokelumne River, San Joaquin River, and miscellaneous streams. Flows in miscellaneous streams are primarily Calaveras River flows. The locations of the stations used in the analysis are shown on Figure 7-1. Measured average daily inflows into the Delta are summarized graphically on Figure 7-2. Figure 7-2a presents total inflows into the Delta for the period of record. Figure 7-2b presents inflows from Sacramento River and Yolo Bypass, the major contributors to total inflow (>80 percent). Figure 7-2c presents inflows from San Joaquin River, the third-largest contributor to total inflow (approximately 10 percent).

One of the objectives of these studies is to develop estimates of hydrologic characteristics of the Delta under current conditions in the tributary watersheds. Thus, it was necessary to examine the available Delta inflow data to determine if these data adequately reflect current watershed conditions or if the statistical characteristics of the data have significantly changed during the period of recorded data due to new reservoirs in the watersheds, developments in the watershed, land use changes, and other factors.

As shown on Figure 7-2, the period from approximately 1987 to 1993 had relatively fewer large flood inflow events than before 1987. This six-year period had below-average precipitation and is the longest period of below-average rainfall between 1955 and 2005. This pattern suggests that during the 50-year period of record, more drought years occurred in the recent period of record than in earlier years. It is, therefore, desirable to use the entire period of available inflow record to avoid or reduce any statistical bias caused by the recent drought years.

Several dams and reservoirs, developments, and other changes have been constructed in the watersheds tributary to the Delta, and the impacts of these changes on inflows into the Delta were reviewed in the Delta Risk Management Strategy (DRMS) studies. Construction of new dams and reservoirs in the tributary watersheds could be a large contributor to changes in characteristics of runoff to the Delta. However, as discussed in the following paragraphs and in more detail in the Flood Hazard TM (URS/JBA 2008a), it is believed that changes related to reservoirs and watershed developments are associated with water supply and environmental flow releases from the reservoirs and have minimal impact on flood inflows into the Delta.

Table 7-1 is a partial list of dams and reservoirs that have been constructed in the tributary watersheds. As shown in Table 7-1, the reservoirs behind Oroville and New Melones dams are two of the largest reservoirs constructed during the period of available inflow measurements. Analyses were made to determine if Oroville Dam and other watershed changes since construction of the dam had a significant impact on Delta inflows from Sacramento River and Yolo Bypass. Similar analyses were made with regard to San Joaquin River since construction of New Melones Dam.

As shown on Figure 7-2, the incremental addition of reservoirs in the Sacramento or San Joaquin River watersheds between the beginning of the Delta inflow record (1955) and the essential completion of reservoir construction in the watersheds (1968 for the Sacramento River, and 1978 for the San Joaquin River) did not have a noticeable impact on lowering annual peak day Delta inflows. Although new reservoirs constructed during the early years of the inflow record undoubtedly provided some incremental increase in flood protection (by reducing flows at and downstream from the new dams), it is possible that some of the flood attenuation provided by the new reservoirs may have occurred anyway due to floodplain storage, thereby reducing the apparent impact of the reservoirs on Delta inflows. This result is generally consistent with the results presented by Florsheim and Dettinger (2007), which showed that the pattern of levee breaks in the Delta was the same in the first half of the twentieth century (before major dam construction) as it was in the last half of the twentieth century (after major dam construction).

Table 7-2 summarizes the measured Delta inflows for three periods. For the Sacramento watershed, the periods are the pre-Oroville Dam period (1956–1968), the post-Oroville Dam period (1969–2005), and the entire period of record. For the San Joaquin River watershed, the periods are the pre- and post-New Melones Dam periods (1956–1979 and 1980–2005, respectively), and the entire period of record. Because no major storage projects have been developed on the Delta tributaries since construction of New Melones Dam, the post-New Melones Dam period is considered to represent current conditions. As shown in Table 7-2, the average number of days per year with high Delta inflows (>100,000 cubic feet per second [cfs]) from San Joaquin River is greater during current conditions in the watershed than before New Melones Dam was constructed, and the average number of days per year of low Delta inflows (<100,000 cfs) is less. This situation is contrary to what would be expected if New Melones Dam and reservoir had a significant impact on flood inflows. Similarly, Table 7-2 shows more high (>100,000 cfs) and fewer low (<100,000 cfs) total inflows into the Delta from the Sacramento River watershed since the construction of Oroville Dam.

A statistical analysis was performed to compare the annual peak day Delta inflows for the following stations between two potentially distinct periods:

- Sacramento River + Yolo Bypass: Before 1968 versus after 1968
- San Joaquin River: Before 1979 versus after 1979

The data were tested by Shapiro-Wilk W test and were found to be lognormally distributed. Also, the variances were approximately equal between the two periods. Hence, the parametric *t*-Test, using the log-transformed data, was used to test whether data from the aforementioned periods were different from each other.

The statistical results are presented in Table 7-3. The *p*-values of the *t*-Test were above 0.05, indicating that the annual peak day Delta inflows were not significantly different from each other

for the two periods, at the 5 percent significance level (i.e., 95 percent confidence level). Therefore, it is reasonable to combine data from all years together for subsequent analysis.

In summary, it was concluded that the available 50-year period of record data (WYs 1956 through 2005) should be used for the DRMS studies without adjustment for the following reasons:

1. Use of the entire period of available inflow record will reduce any statistical bias caused by the 1987 to 1993 drought years.
2. During major flood events before new reservoir construction, some, if not most flood attenuations were provided by floodplain storage, thereby reducing the impact of new reservoirs on Delta inflows and tending to make the 50-year data set more homogeneous.
3. No major changes in the Sacramento River watershed have occurred since 1968; thus, 38 years of the 50-year period of record represent approximate current watershed conditions.
4. Eleven of the largest 15 annual peak day Delta inflows from the Sacramento River and Yolo Bypass occurred during approximate current watershed conditions (see Flood Hazard TM [URS/JBA 2008a] for discussion).
5. Most of the major reservoirs in the San Joaquin River watershed were completed by 1979, meaning over half of the annual peak day Delta inflows during the 50-year period of record occurred during approximate current watershed conditions.
6. Eight of the largest 15 annual peak day Delta inflows from San Joaquin River occurred during approximate current watershed conditions (see Flood Hazard TM [URS/JBA 2008a] for discussion).
7. Additions to reservoir storage in the San Joaquin River watershed may not have significantly changed inflows into the Delta during major flood events but instead only reduced the amount of floodplain storage that has historically occurred.
8. Analyses of the annual peak day inflow data indicate no statistically significant changes in the data during the period of record.
9. Adjustment of the 50-year inflow record to reflect current watershed conditions would require numerous assumptions regarding reservoir operations and, more important, assumptions regarding downstream levee failures and floodplain storage and would probably incur more error than would result from using the inflow record without adjustment.

Another consideration in the DRMS studies is the season of high inflows into the Delta. It is anticipated that repairing damages in the Delta, due to any cause, will be more difficult during the high-inflow season and the repairs likely will take longer. Additionally, the possible impacts on Delta exports caused by damages may be different depending upon the time of year that the damage occurs. Thus, hydrologic characteristics in the Delta during different inflow seasons were considered in the studies. Figure 7-3 presents average daily Delta inflow versus time of the year for the period of record inflows. As shown on Figure 7-3, high inflows begin near the end of December and last until approximately mid-April. Between April 15 and December 15 maximum daily inflows are less than 200,000 cfs, and most of the time maximum daily inflows are less than 100,000 cfs, with the exception of one flood that occurred during October 14–17, 1962. Thus, only two inflow seasons are considered in these studies: the high-inflow season (December 16 through April 15) and the low-inflow season (April 16 through December 15).

7.2 FLOW-FREQUENCY ANALYSIS

The magnitude of the Total Delta Inflow (TDI) for a hydrologic event of a given probability can be estimated from a frequency analysis of the measured annual peak inflow events. Table 7-4 summarizes the annual peak TDIs for each of the 50 WYs of record, the 50 high-inflow seasons in the period of record, and the 49 low-inflow seasons in the period of record.

A commonly accepted frequency distribution of hydrologic events is the Log Pearson Type III (LPIII) distribution. This frequency distribution is recommended by the Hydrology Subcommittee of the Interagency Advisory Committee on Water Data published by the U.S. Geological Survey (1982). LPIII uses three distribution parameters: mean, standard deviation, and skew. Annual probabilities were calculated by using the data in Table 7-4 to estimate the distribution parameters.

Results of the LPIII analyses are presented in Table 7-5, and on Figures 7-4, 7-5, and 7-6 for all WYs (all seasons), high-inflow seasons, and low-inflow seasons, respectively. The distributions of seasonal peak daily inflows into the Delta are compared to the all-seasons distribution on Figure 7-7. Table 7-6 presents the estimated parameters for each distribution.

The frequency analyses of Delta inflows described above was divided into 50 ranges or bins of TDI, with each bin assigned the annual probability for the midpoint of the bin. The bins are equally spaced in log-space. Estimates are provided for five different confidence limits, ranging from 5 percent confidence that the inflow will not be exceeded to 95 percent confidence that the inflow will not be exceeded. The estimated probability of an inflow being in each of the 50 ranges is presented in Table 7-7 for each of the five confidence limits.

The 50 bins resulting from the above analysis represent the range of inflows likely to occur in the Delta (i.e., from 0 to 2,000,000 cfs). The Risk Analysis will use the flow from each bin in the risk analysis to cover the range of possible inflows. Each flow is associated with an annual probability that the flow will occur (the probabilities are included in Table 7-7). Because uncertainty exists in the assessment of the annual probability that a given flow will occur, the risk analysis will also associate a confidence bound with each annual probability.

7.3 DELTA INFLOW PATTERNS

Flood frequency as used in this risk assessment has a slightly different definition than the definition typically used in Delta flood studies. For purposes of the risk assessment, flood frequency in these studies provides a measure of the annual probability that the total inflow into the Delta will be equal or exceeded. Many different inflow patterns into the Delta can produce any selected annual probability of occurrence, each of which could have its own set of water surface elevations (WSEs) in the Delta. For example, four storm events in the period of record have peak total daily inflows to the Delta that exceeded the 10-year event. For the largest storm of record, February 1986, San Joaquin River was not a significant contributor to the storm event, and Cosumnes and Calaveras rivers were. For the second-largest storm, January 1997, both Cosumnes and San Joaquin rivers experienced extreme events, and Calaveras River did not. The third-largest storm occurred only on Sacramento River. Finally, for the fourth-largest storm, March 1983, an extreme event occurred only on San Joaquin River. The risk assessment needs to be able to account for all of these possible inflow patterns.

As described above, inflow to the Delta is from several sources, including the Yolo Bypass (Yolo), Sacramento River (Sac), Cosumnes River (CSMR), Mokelumne River (Moke), San Joaquin River (SJR), and miscellaneous streams (misc), primarily the Calaveras River. The sum of these sources of inflow is defined as the TDI. Given the variability of flows in the streams making up TDI, many combinations of flows that could account for any TDI observed are possible. This section describes a method for developing different combinations of Delta inflow patterns that could account for any selected TDI.

A somewhat arbitrary cutoff value of 80,000 cfs was selected to eliminate nonstorm event flow rates. A TDI of 80,000 cfs corresponds to a 50 percent confidence peak annual return period flow of less than two years.

Daily average flows in Sacramento River are not highly variable (the coefficient of variation is only 0.084), and most of the variability is due to flows in Yolo Bypass. Flows in these two channels are not independent because the flows originate from the same watershed. Upstream of the City of Sacramento, when the stage in Sacramento River reaches the crest of Fremont Weir, flow in Sacramento River spills over the weir into Yolo Bypass. This spill condition occurs at a flow of about 55,000 cfs in Sacramento River, as measured below the weir. Most of the increase in flow above 55,000 cfs goes over the weir into Yolo Bypass. The Yolo Bypass Working Group et al. (2001) developed a relationship between flows in the Sacramento River below Fremont Weir and spills over the weir. The relationship indicates that it is necessary only to predict one of the stream flows (Sacramento River or Yolo Bypass), and the other stream flow can be estimated. For this reason, the method presented below is used to predict the sum of flow in Sacramento River and Yolo Bypass.

The methodology for estimating flow in any of the contributing tributaries to the Delta given a specified TDI is to use a logistic regression relationship for each contributing inflow. The regression was structured such that the flow predicted from the regression could never exceed the flow possible in the tributary. The dependence between relationships was maintained by applying only the relationship to that portion of the flow not yet explained by any previously used relationship.

Table 7-8 lists the results of the logistic regression. The low r^2 values result from the large variability in the data. However, even with these small correlations, the equations reproduce the mean values for the flow distributions.

Figure 7-8 shows the results for the Sacramento River plus Yolo Bypass Delta inflow. The correlation coefficient for the fit is 0.94.

In addition to the above results, a relationship between the flow in Sacramento River and Yolo Bypass is needed to separate these two flows from the total. The correlation coefficient for the fit is 0.65. Figure 7-9 shows the relationship.

Figure 7-10 presents the results for San Joaquin River. The regression equations provide a reasonable fit, thought it slightly under predicts the main body of the data, due to the small number of cases where the remaining flow is large and the fraction of flow in San Joaquin River is small (approximately 10 percent of values). These events represent cases where a storm occurred on the Cosumnes River, but not the San Joaquin River.

Figure 7-11 presents the results for the miscellaneous inflows. The fit has an r^2 value of 0.94.

Figure 7-12 shows the results for the Cosumnes River. The r^2 value for the fit is 0.96, though it underestimates the peak annual flows.

The regression relationships reproduce the mean and median of the data well, except for the median of Cosumnes River inflows. For most of the rivers, the mean flow is centered within the bulk of the observed flows (e.g., halfway between the 25th and 75th percentiles), whereas, for Cosumnes River, the mean is almost at the 75th percentile. This percentile implies that the distribution of inflows from Cosumnes River is more skewed than the inflows from other rivers and, therefore, the regression will not reproduce the median values as well. Figures 7-13 through 7-16 compare measured to predicted flow for the Sacramento River plus Yolo Bypass, San Joaquin River, miscellaneous inflows, and Cosumnes River, respectively. All of the figures show a very good fit between the measured and predicted flows, except for the San Joaquin River cases in which the flows in other streams exceeded the flow in San Joaquin River. These values do not fit the relationship and need to be captured as part of the uncertainty analysis.

7.4 DELTA WATER SURFACE ELEVATIONS

WSEs throughout the Delta that are associated with various flood magnitudes and inflow patterns are needed to estimate risks of levee failure due to overtopping and/or high water. Delta WSEs were estimated from data on historic water levels measured at selected Delta gauging stations. Water levels, or stages, at the selected gauging stations were then used to interpolate stages at intermediate locations in the Delta.

7.4.1 Data

Tide data used in these analyses are tide elevations measured at the Golden Gate Bridge (NOAA 2005). The Golden Gate Bridge tide station was chosen for its long record of unbroken tide data dating back approximately 150 years. Tide levels at the Golden Gate station are independent of inflows into the Delta, but provide a geographically relevant measure of tailwater conditions that influence water levels in the Delta.

The California Data Exchange Center (CDEC) provides information on an extensive hydrologic data collection network, including automatic river stage sensors in the Delta. River stage data are provided primarily from the stations maintained by DWR and the U.S. Geological Survey. This stage data can be downloaded from CDEC's web site (http://cdec.water.ca.gov/).

Stage data, since 1984, are provided on an hourly basis. For some gauging stations, 15-minute stage levels have been recorded for some inflow events since 1995. Figure 7-17 shows the stage gauging station locations selected for use in these studies, and presents the period of record for hourly and event data for each station. Gauging stations were selected based on station location, and length and reliability of available record.

7.4.2 Data Review and Adjustments

Stage records for the selected gauging stations contained some inconsistent data significant enough to have an impact on the analysis results. To assist in evaluation of the stage data, plots of daily stage versus time were created for each measuring station. These plots provide a picture of the normal stage range and also show apparent inconsistencies in the data. The data records

were evaluated and, when possible, adjusted to eliminate apparent invalid data. The data records were reviewed to adjust or eliminate the following inconsistent data:

- Changes in station datum
- Measured stages greater than flood stage
- Missing and known invalid data
- Constant stage measurements
- Invalid recording intervals
- Incomplete daily records
- Conversion of data to common datum

7.4.3 Regression Analysis of Water Surface Elevations

Once maximum daily stage data were reviewed, invalid records removed, and conversion to North American Vertical Datum 88 (NAVD88) datum estimated for each station, the daily stage data for flood inflows were matched to the corresponding maximum daily tide data and the mean daily inflow data. The resulting data set is a daily record of maximum daily stage (NAVD88), maximum daily tide, and mean daily inflow from each of the six tributary inflows into the Delta.

This study focuses on the threat from high stages occurring during flood events. Most of the inflow data in the data sets represent low-inflow nonflood events. To minimize bias in the statistical analyses of WSEs, the inflow data sets were reduced to include only high-inflow events. Based on review of the data it was judged that only TDI magnitudes greater than 57,000 cfs should be included in the regression analyses.

Using the data on maximum daily tide, mean daily inflow, and measured adjusted stages at the gauging stations, multiple regression analyses were made for each of the stage-measuring stations. The regression analyses were made to determine best fit coefficients. Details on the regression analysis are provided in the Flood Hazard TM (URS/JBA 2008a).

At each station the measured WSE was compared to the WSE calculated using the coefficients developed from the regression. Figure 7-18 compares the calculated stage with the measured stage at Venice Island. Similar comparisons for other stations are provided in Appendix A of the Flood Hazard TM (URS/JBA 2008a). In addition, the observed annual peak at each station is compared to the predicted annual peak for stations with four or more years of data. For most stations, the root mean square error is equal to 0.34 feet or less. Only two stations, Benson's Ferry and Liberty Island, have root mean square errors greater than one foot.

7.5 DELTA LEVEES AND HISTORICAL FAILURES

Delta levees were constructed over the past 150 years largely by farmers and reclamation groups who used light equipment and local, uncompacted sediments and organic matters, and did little or no foundation preparation. Foundations are composed of a complex mélange of river sediments and organic (peat) materials consisting of coarse-grained sediments, including gravels and loose, clean sands to soft, fine-grained materials such as silts, clays, and organics, including

fibrous peat. The levee material consists of interfingered layers of loose sands, soft silts and clays, and peat.

Since 1900, 158 islands have been flooded as a result of levee breaches in the Delta (not including failures in Suisun Marsh). Records on Suisun Marsh levee failures are incomplete and consequently not included in the historical failures database. Failures in Suisun Marsh are more frequent due to the lower crest elevations of it levees. During the winter of 2005-06, Simmons Wheeler, Honker Bay Club, Fay and Van Sickle islands flooded during a relatively mild winter storm. These frequent floods have caused multiple overtopping of the Suisun Marsh levees. In a few places, the levees have been lowered to allow tidal exchange and tidal wetland restoration. Table 7-9a lists the number of island/tract breaches and their corresponding years of occurrence. A limited (and recent) number of failures in Suisun Marsh are listed at the bottom of Table 7-9a. Figure 7-19 illustrates the number of times islands or tracts have breached since 1900. Table 7-9b provides a chronological list of flooded islands since 1900. Figure 7-20 identifies the locations (when available) of the levee breaches that resulted in island/tract flooding. Most breach locations have been mapped except for few cases where information was not available.

In recent years, the levees have been built up to contain larger floods and have been upgraded and maintained to meet certain engineering standards (freeboard and geometry). Part of the recent changes include (1) raising levees to meet higher flood protection level; (2) raising levees to compensate for foundation consolidation and settlement; (3) raising levees to mitigate for the continued subsidence (peat and organic marsh deposits) as a result of farming practices; (4) and improving/increasing maintenance to mitigate/contain the higher stresses on the levee system due to higher hydrostatic heads. A plot of island cumulative breach trend is presented on Figure 7-21 for the last 106 years. For the period between 1900 and 2006, the mean annual frequency of island flooding corresponds to about 1.31 for all events, excluding earthquakes. The trend of the mean annual frequency of levee failures is about 1.19 for the period from 1900 to 1949 compared to 1.36 for the period from 1950 to 2006, showing a relatively similar trend between the 50 years before 1950 and the 56 years since 1950.

Figure 7-22a shows the cumulative number of levee breaches resulting in island flooding since 1950, and Figure 7-22b shows the numbers of flooded islands per annum since 1950. The “sunny weather” island flooding events are not included in these numbers. Data cutoff at 1950 was intentionally selected to remove older historical events during which levee configurations were different from current levees. These more-recent years represent a better data set for comparison with results of the predictive levee vulnerability numerical models. One should recognize that, since 1950, the levee geometry and crest elevation continued, nonetheless, to change slowly with time.

Further examination of the data (Figure 7-22a) indicates a mean annual frequency of island failures of 1.39 for the period between 1980 and 2006, compared to 0.80 for the period between 1950 and 1980. These trends indicate that during the last 26 years, the Delta levees have experienced a higher rate of levee failure than the period between 1950 and 1980 (30 years), despite the increasing maintenance efforts and subvention programs shown in Figure 7-22c.

A plot of the mean daily total Delta inflow (since 1955, the earliest date of available records) is presented on Figures 7-22d and 7-2(a). The storms of records for that period are shown in Table 7-9c. Although the cumulative daily mean inflow is constant for the period between 1955 and 2006 (red line in Figure 7-2[a]), the last 26 years experienced a prolonged drought between 1987

and 1993. The total mean daily inflow graph shows larger total daily storm inflows during the winters of 1983, 1986 and 1997 than during the period between 1950 and 1980. The storm events associated with the high Delta inflows since 1980 correlate with the higher number of simultaneously flooded islands/tracts. These particular floods include events in 1980 (6 islands flooded), 1983 (11 islands flooded), 1986 (9 islands flooded), and 1997 (11 islands flooded), as shown in Table 7-9b. Higher storm events tend to cause a disproportionate number of simultaneous levee failures.

7.6 DEFINITION OF FAILURE MODES

Three potential modes of failure—under-seepage, through-seepage, and overtopping—are considered in this analysis. Erosion was not considered a main failure mode. The mode of failure associated with stream flow erosion and wind-wave induced erosion is addressed in the Wind-Wave Hazard TM (URS/JBA 2008g) and the Emergency Response and Repair TM (URS/JBA 2008d).

Under-seepage refers to water flowing under the levee through the foundation materials, often emanating from the bottom of the landside slope and ground surface and extending landward from the landside toe of the levee. Through-seepage refers to water flowing through the levee prism directly, often emanating from the landside slope of the levee. Both conditions can lead to failure by several mechanisms, including excessive water pressures causing foundation heave and slope instabilities, slow progressing internal erosion and piping leading to levee slumping. Overtopping failure occurs when the flood water level rises above the crest of a levee. The representation of the failure modes and the evaluation of the probability of levee failures for each mode are discussed in the remaining sections.

When empirical data exist, model development relies heavily on calibration against past performance. In this context, the analysis team devoted its initial effort in collecting information on the levee performance under flood hazards. The information collection included review of relevant and available reports, DWR geographic information system (GIS) database, and interviews with local and state engineers. For most failures, information regarding the specific mode of failure, time and date of failure, and the water levels in the slough was either not available or incomplete, as discussed in Sections 2 and 4 of the Levee Vulnerability TM (URS/JBA 2008c). In cases of seepage-induced failures, the effort to attribute them to under-seepage or through-seepage cannot be made at this stage because of the absence of post-event detailed documentation.

7.7 PROBABILITY OF FAILURE DUE TO UNDER-SEEPAGE

This section describes the approach used to develop the fragility functions for the under-seepage mode of failure. The variables used to define the vulnerability classes should not be confused with the random variables that define the statistical variation of the parameters used to develop the probabilistic model to estimate the response of the levee and foundation conditions making a given class. The variables used to define the vulnerability classes are those spatial variables that can be discretized throughout the Delta and Suisun Mash regions to generate small enough “similar” reaches of levees and foundation that would have the same response if subjected to the same load. Within each class there is a range of random variables that are treated statistically to represent the aleatory uncertainties in the probabilistic model representation.

7.7.1 Definition of Vulnerability Classes

The area covered by the Delta and Suisun Marsh is very large, and the conditions of the levees and their foundations vary substantially across the region. Because of the extent of this variability of the levees and their foundations, the study area was divided into finer and "similar" zones. These zones are referred to as vulnerability classes (VCs). The VCs are defined as reaches of levees that would yield the same probability of failure when subjected to the same flood stage. The primary factors identified to potentially contribute to the definition of the VCs include:

- Blanket (peat/organic layer) thickness on the landside of the levee
- Slough width
- Sand aquifer thickness
- Presence of toe drainage ditches
- Presence of slough bottom sediment
- Slough bottom elevation
- Levee Geometry

The above list of potential parameters defining vulnerability classes was further examined to identify which parameters are clearly and readily distinguishable geographically (and, hence, will remain as parameters for defining VCs), and which should be treated as random variables due to the lack of clear geographic correlation. For this purpose, a sensitivity analysis was conducted to evaluate the effects of these factors. The sensitivity analyses were carried out using the seepage models for a typical cross-section with a 15-foot-thick peat layer.

Peat Thickness/Organic Soil-Blanket. The primary factor that affects the under-seepage conditions is the thickness of the peat and organic marsh deposits under and on the landside of the levee (blanket). This parameter is clearly distinguishable geographically and was mapped using the GIS models discussed in Section 2 of the Levee Vulnerability TM (URS/JBA 2008c). This variable was one of the primary parameters used to map the VCs into six bins of ranges of thicknesses. Further, within each bin, the peat thickness is considered as a random variable.

Slough Width. Slough width is clearly distinguishable geographically. A sensitivity analysis was conducted to evaluate the effects of slough width on the exit gradient for a range of values from 200 to 2,000 feet. The results are shown in Figure 7-23(a), assuming the presence of a drainage ditch, and in Figure 7-23(b), assuming the absence of a drainage ditch. Two curves are presented in each figure showing the trends associated with the presence or absence of slough sediments. Figure 7-23 shows that the exit gradient becomes insensitive to slough widths beyond 500 feet. As a result of these findings, the slough width was maintained as a parameter defining the vulnerability classes. To simplify the number of analysis cases, the slough width parameter was considered to have two possible outcomes: less than 500 feet, defined as "narrow slough," or larger than 500 feet, defined as "not narrow slough."

Aquifer Thickness. The effects of the aquifer thickness on the exit gradient on the landside of the levee were evaluated for a range of values from 5 to 55 feet. The results are shown in Figure 7-24(a), assuming the presence of a drainage ditch, and in Figure 7-24(b), assuming the absence of a drainage ditch. Two curves are presented in each figure showing the trends associated with the presence or absence of slough sediments. This analysis clearly shows that beyond 15 feet, the

thickness of the aquifer has little effect on the exit gradient. Based on these findings it was assumed that the presence or absence of the sand aquifer below the peat/organic blanket was sufficient to carry out the under-seepage analysis, and that no further discretization of the thickness of the aquifer was necessary.

Drainage Ditches. Seepage gradients and pressure heads in the levee foundation can be affected significantly by the thickness of a low-permeability layer on the landside of a levee. This layer is often referred to as the blanket. The effectiveness of the blanket can be reduced by any removal of material, such as a drainage ditch. Because agriculture in the Delta requires water levels to be maintained below the ground surface (2 to 3 feet), fields are often surrounded by drainage ditches near the levee toes, which drain water to pump stations. Development of a comprehensive catalogue of agricultural ditches throughout the Delta was beyond the scope of this study and was not entered into the DRMS database at this time. However, the presence of ditches have a strong affect on the exit gradients and under-seepage, as shown in Figures 7-23, 7-24, and 7-25. It should be noted, however, that the effects of a drainage ditch on under-seepage are stronger for thinner blankets and become less important for thicker blankets. For example, if a 25-foot-thick blanket without a drainage ditch is stable with respect to under-seepage, a 30-foot thick blanket with a 5-foot deep drainage ditch will also be stable. Consequently, it was decided to carry the analyses models for both instances assuming a 5-foot-deep drainage ditch when present in thin blankets (25 feet or less). Because the exact location of the drainage ditches is unknown at this time, the analysis was carried out assuming the presence of the drainage ditch to be random with 50 percent chance of being present.

Slough/River Channel Sediments. Flow regimes in the channel and sloughs generally cause scouring and movement of materials during high flows and deposition during low flows. As discussed in the Geomorphology TM (URS/JBA 2007c), the Delta can be divided into two generalized geomorphic provinces. In the northern portion of the Delta, where the river channel has higher gradients, higher flows, and higher velocities, much of the sediment that is transported and deposited is coarse-grained and relatively permeable. In the other portions of the Delta, especially those subject to tidal influences, river channel gradients and velocities are lower, leading to the transport and deposition of predominantly finer grained, lower permeability materials. These low-permeability materials can accumulate at the base of the river channel, often to great depths, and can act as a seepage barrier. There is some anecdotal evidence that dredging these “slough sediments” has led to increased seepage in the islands next to dredged channel. Development of a comprehensive catalogue of the location and thickness of fine-grained slough sediments is beyond the scope of this study. Because these sediments can affect the under-seepage gradients, models for levees with and without fine-grained sediments in the adjacent sloughs were developed and evaluated.

Figure 7-25 shows the results of analyses relating vertical exit gradient to the thickness of slough sediments for models with drainage ditch (Figure 7-25a) and without ditch (Figure 7-25b). Figure 7-25 also indicates that the slough sediments have a moderate impact on the computed vertical gradients. The calculated exit gradients are approximately 11 to 15 percent smaller when the slough sediments are present. The slough sediment is not a fixed parameter, and changes with time. During high-velocity flows, the slough sediment is removed, and during low-velocity flows, the reverse occurs. No continuous survey of slough bottoms is conducted regularly throughout the Delta. The analysis was then carried out assuming the presence of the slough sediments to be random and was assigned a 50 percent chance of being present.

Slough Bottom Elevation. Figure 7-26 presents the results of analyses relating vertical exit gradient to the bottom elevation of the slough for models with drainage ditch (Figure 7-26a) and without ditch (Figure 7-26b). As expected, Figure 7-26 indicates that the depth of the adjacent slough bottom does not have a significant effect on the exit gradient. This parameter was not further considered in the definition of the vulnerability classes.

Levee Geometry. The effects of the levee geometry on under-seepage are mostly controlled by levee crest elevation. The crest elevation was treated as a deterministic variable using the recent LiDAR survey (DWR 2007) as input data into the risk model for each reach and mile post. The model scans and reads the crest elevation at each levee reach and each mile-post where the analysis is performed. To simplify the rest of the analyses, the levee crest width and side slopes were assumed to be equal to the average values for the Delta and Suisun Marsh, respectively. These values are presented in Section 2 of the Levee Vulnerability TM (URS/JBA 2008c).

Conclusion. The above process was used to evaluate which factors contribute to the definition of the vulnerability and/or to the random nature of the Delta. The VCs for under-seepage were then defined as follows:

- Peat thickness/organic deposits - The peat/organic deposits were divided into six intervals representing the variation of the peat/organic thickness within the Delta region.

  1. No peat
  2. 0.1 to 5 feet
  3. 5.1 to 10 feet
  4. 10.1 to 15 feet
  5. 15.1 to 30 feet
  6. > 30 feet

- Slough width - Slough width was represented by two broad groups: less than 500 feet (narrow sloughs), and greater than 500 feet (not narrow sloughs).

Twelve VCs were developed to represent the levees in the Delta study region (VCs 1 through 12), and 12 VCs were developed to represent the levees in the Suisun Marsh area (VCs 13 through 24). Table 7-10 lists the VCs, their definitions, and the associated random variables. Figure 7-27 shows the distribution of the VCs in the study region.

7.7.2 Material Properties and Random Variables

7.7.2.1 Slough/River Water levels

A probabilistic model was developed to estimate the frequency of occurrence of various water stages in the Delta and Suisun Marsh sloughs and rivers (Flood Hazard TM [URS/JBA 2008a]). The model accounts for the combined effect of storm inflows and tides. The Flood Hazard TM estimates the probability of occurrence of various water stages in the Delta and Suisun Marsh. This section assesses the conditional probability of levee failures given flood stages.

7.7.2.2 Material Properties and Random Variables

The material properties used to describe and model the behavior of the various soils, included permeability values and their corresponding anisotropies, were obtained from laboratory test results from previous studies, published correlation relationships, and engineering judgment and experience. The selected parameters were then calibrated using actual levee performance during flood events at specific sites. The calibration of selected parameters is discussed in subsequent sections.

Numerous government, municipal, and private organizations were approached for information and data collection on the Delta and Suisun Marsh, as discussed in Section 2 of the Levee Vulnerability TM (URS/JBA 2008c). Except for few limited and site-specific investigations by others, no single study has conducted an extensive and comprehensive investigation of the peat and organic deposits throughout the Delta and Suisun Marsh. Tables 7-11 and 7-12 present summaries of reported vertical and horizontal permeability values of organic and sandy soils compiled by Harding Lawson Associates (HLA 1989, 1991, 1992) and others, as shown in Appendices A and B of the Levee Vulnerability TM (URS/JBA 2008c). These permeability values were obtained from laboratory tests and field pump tests. Also included in the tables are details of soil type, type of test, sample location, and other sampling details.

The reported permeability data for free-field peat/organic soils listed in Table 7-11 indicate that both horizontal and vertical laboratory-measured permeability values are approximately equal and on the order of 10^{-6} centimeters per second (cm/s). The Technical Advisory Committee (TAC) and the analysis team considered that the anisotropy should be higher than one, given the historical cycles of wetland vegetation growth and burial under sediment loads during run offs for the post ice-age sea-level rise period which started some 15,000 years ago. Further, these laboratory tests cannot support the TAC and analysis team's observations of high seepage flows in many locations in the Delta during non-flood high-tides conditions. The team's observations indicate that the horizontal permeability (k_h) of peat/organic soils is generally higher than the vertical permeability (k_v), especially if the peat is in a "free-field" condition, away from the consolidating loads of a constructed levee. Therefore, for the initial evaluations, the TAC members recommended using an anisotropy (k_h/ k_v) of 10, with a k_h of 1×10^{-4} and a k_v of 1×10^{-5} cm/s, for "free-field" peat/organic soil to be calibrated against case histories.

Peat/organic materials lying beneath the levee showed lower permeability than the free-field peat (Table 7-11), due to the consolidating effect of the weight of a constructed levee. For the initial analyses, the TAC members recommended using horizontal and vertical permeability values of 1×10^{-5} and 1×10^{-6} cm/s, respectively, one order of magnitude lower than the permeability of free-field peat/organic soils.

The permeability values of mineral silts and sands are well-tested and documented. Vast data, including empirical correlations, laboratory and field-performance data, are available for assessing the permeability of sandy soils (designated as SP or SM materials in the unified soils classification system or American Society for Testing and Materials ASTM-D2487). Table 7-12 contains results from both laboratory and field-pump tests from materials evaluated during previous Delta studies. These values are consistent with measurements and correlation relationships developed for these types of soils in other publications, including correlations from the United States Army Corps of Engineers (USACE) (1986, 1993), Terzaghi and Peck (1967), Freeze and Cherry (1979), and Cedergren (1979). For the initial analyses, the TAC and analysis

team members used values of horizontal permeability equal to 1×10^{-3} cm/s and a k_h/k_v ratio of 4 for these sandy materials.

As described above, low-permeability silt sediments deposited on slough bottoms can reduce the infiltration rate of water into underlying levee foundation materials, leading to beneficial reductions of seepage rates and water pressures below the levee. This phenomenon is often referred to as "entrance head losses." To model this condition, the TAC members and analysis team used a horizontal permeability of 1×10^{-5} cm/s with a k_h/k_v ratio of 1 for these fine-grained slough sediments, based on the above-published correlation relationships.

The peat/organic deposits and the sand aquifer permeability values were considered as random variables. The remaining parameters were considered as deterministic variables because they have a second order effect on the under-seepage results.

7.7.3 Methodology for Developing Flood Fragility Functions

Figure 7-28 illustrates the three-step method followed in developing the flood-fragility functions for under-seepage analysis of each vulnerability class.

The first step involves the evaluation of **levee response functions** (Section 7.7.4), which estimate the exit gradient as a function of water surface elevation (Figure 7-28a). The exit gradients are evaluated using generalized geotechnical models presented throughout this section.

The second step involves the development of the **conditional probability of failure functions** (Section 7.7.5), which relate the conditional probability of a levee breach given an exit gradient (Figure 7-28b). This step relied solely on expert elicitation. The range of expert elicitation was used to quantify the epistemic uncertainty in the assessed probability of failure.

The third and final step involves the development of the **levee fragility functions**, which relate the probability of failure to slough WSE, or equivalently freeboard [= crest elevation – WSE] for each VC (Figure 7-28c). This step combines the levee response functions with the conditional probability of failure functions, using Monte Carlo simulations, to generate the fragility functions.

Before the levee response functions are presented, a discussion on the analysis method (Section 7.7.4.1), numerical model development (Section 7.7.4.2), comparison to simplified procedure (Section 7.7.4.3), validations against known seepage cases (Section 7.7.4.4), and comparisons to historical cases (Section 7.7.4.5) are addressed first.

7.7.4 Evaluation of Levee Response Functions

The levee response functions represent the levee ability to withstand the forces applied by the hydrostatic pressures on the channel bottom and levee waterside slopes. The hydrostatic pressures will generate a flow path through the levee foundation substrates, and hydraulic gradients through those foundation layers. The hydraulic gradients represent the pressure head differential between two points along the flow path of the water, normalized by the length traveled by the water molecule between these two points.

The gradient is a measure of the force of the water velocity within each substrate that will try to move soil particles. Very often the word vertical exit gradient is used in conjunction with under-seepage. When the water, moving through the levee foundation reaches the ground surface on the

landside of the levee, the vector direction of the gradient will point upward, and hence the reference to the "vertical exit gradient". Under the levee, the water flows in a horizontal direction and consequently the vector of the gradient points to the horizontal direction. In other words, the vector of the gradient will point to the direction of the flow lines along which the water molecules travel from the river side until they exit on the landside of the levee.

When dealing with through-seepage, we often refer to horizontal or downward exit gradient. Similarly to the above definition, the water flow lines run parallel or downward (at varying angles) when they cross the levee fill. At the point of exit on the face of the landside slopes of the levees, the vectors of the exits gradients will point to horizontal or slightly downward directions (depending on which flow line is tracked) consistent with the flow lines.

7.7.4.1 Analysis Method and Model Development

Seepage analyses were conducted using a two-dimensional finite-element procedure (SEEP/W, Geo-Slope International Ltd. 2004) under steady-state flow conditions. The computer program SEEP/W allows for modeling multiple soil types, anisotropic hydraulic conductivity, irregular contacts between soil layers, and a variety of boundary conditions.

Boundary conditions in the steady-state analyses included constant head, no-flow, constant or variable flow, and infinite boundaries for modeling long landside basins.

Water levels in the low-lying Delta islands are maintained 2 to 3 feet below land surface by an extensive network of drainage ditches. Water collected by drainage ditches is pumped through or over the levees into the local stream channels. It is, therefore, reasonable to assume that steady-state seepage conditions exist in the tidal Delta. In the northern Delta and in the Delta fringes, flood waters may rise and drop so quickly that full steady-state conditions may not always develop in every area, especially if the foundation materials are of low permeability. In these locations, steady-state analyses may slightly overestimate seepage conditions; but because of the low permeability, these areas will not likely be vulnerable to significant under-seepage problems. Conversely, based on observations during past floods, most, if not all, of the levees experiencing under-seepage problems are founded on materials that are relatively permeable. In these cases, steady-state seepage analyses are appropriate.

7.7.4.2 Finite Element Model Details: Mesh Development and Boundary Conditions

Mesh development. Actual site data were used to develop idealized cross-sections at selected locations. The idealized cross-sections were then discretized into finite elements for performing seepage analysis using SEEP/W.

Boundary conditions. The following boundary conditions were used in all of the seepage models:

- To avoid boundary effects and to model conditions more accurately at the levee itself, the landside lateral boundary (left side of the models) was set approximately 1,000 feet from the levee crest.
- On the river/slough side (right side of the models), to portray seepage conditions below the mud line, the analysis sections were extended to the middle of the river, and a no-flow

boundary condition at the vertical face of the elements below the mud line was set as an axis of symmetry.

- A fixed, total-head-boundary condition was used to model the contact between the water and the riverbank and levee.
- Fixed, constant-head boundary conditions were used to model the drainage ditch water levels and was set to two feet below the top of the ditch.
- Fixed, head-boundary conditions were used to model far-field groundwater levels at the left boundary of the models. On the far-field left boundary, the water level was assumed to be at two feet below the ground surface.
- Other portions of the levee and the ground surface were modeled using "review nodes." The SEEP/W program assigns a flux-type boundary condition to all review nodes. After the heads are computed for all nodes, the head at the review node is modified if any have a computed head greater than the elevation of the node. Use of these nodes allows the water table to rise above or fall below the nodes, which leads to a more-accurate assessment of the location of the phreatic surface and allows seepage to flow at the free face.

Typical finite element meshes are shown in Figures 7-53 and 7-54.

7.7.4.3 Model Results Comparison to Simplified Hand Calculations

After the seepage models were created and the material properties (i.e., permeability values) assigned, the seepage analyses were performed for steady-state conditions for different water levels in the slough/river. The results were used to evaluate average gradients, exit gradients, steady-state phreatic surface location, the total head distribution throughout the model, and flow paths. Special attention was given to calculate gradients at several key locations, including the landside levee toe for cases without drainage ditches, and directly below and away from the drainage ditch for cases with a ditch.

To confirm the validity of the finite element model results, exit gradients calculated from SEEP/W were compared to average gradients calculated using the simplified "blanket theory." The blanket theory is a semi-empirical, hand-calculation method developed by USACE (1956, 1999b) and calibrated against the past experience. The blanket theory uses performance data and measured seepage conditions from numerous sites in the Mississippi Valley combined with a theoretically based model, to develop predictions for under-seepage flow conditions, pressures, and failure potential as a function of flood-level. The sites evaluated in those studies and used to develop the blanket theory are characterized as having a relatively thin layer of relatively low-permeability soil (i.e., the blanket) overlying a more permeable material directly connected to the river. Expectedly, the results of the FEM model and the blanket theory are very similar and hence it was confirmed that the finite element model was producing comparable results. The blanket theory has been widely used by private consultants and USACE to evaluate seepage conditions and cross-check the results of finite-element seepage models in this region. The finite element model is more versatile in representing irregular geometries and was used to carry the rest of the analyses.

7.7.4.4 Initial Seepage Analyses (Calibration and Verification)

To perform a "reality check" on the model, and especially to better ground-truth the results and validate the material properties, several initial seepage analyses were performed using information from sites where data and past performance were readily available. This part of the analysis was conducted to confirm that results of the levee response functions model are reasonable, and consistent with the empirical observations.

Several analysis sections were derived from information contained in the 1956–1958 California Department of Water Resources Salinity Control Barrier study (DWR 1958). Specifically, cross-sections at Bradford Island, Sherman Island, and Terminous Tract were considered. The cross-sections and boring logs describing the subsurface material types from these sites are presented in Appendix A of the Levee Vulnerability TM (URS/JBA 2008c). Not every site had information regarding slough-side subsurface materials. For these sites, the peat/organic layer present on the landside was assumed to extend horizontally into the waterside, intersected only the bathymetric profile of the channel bottom. Cross-sections on Bouldin Island, Byron Tract, and Union Island were also developed using data obtained from USACE (1987), the Mark Group (1992), and DWR (1994), respectively.

Table 7-13 presents values of horizontal permeability and anisotropy ratios used in the initial analyses. The uncertainties associated with the subsurface material properties, in particular the permeability values of the blanket layer (often composed of peat/organic materials in the central Delta) and the underlying sandy soil strata, were evaluated by conducting statistical analyses using mean estimated and distribution around the mean.

Because of the similarity of the results from the above cases evaluated in the initial analyses, and to avoid too much redundancy on this subject, only the evaluation process and results from the analysis of Terminous Tract are presented herein. These results are considered representative of the other islands, mentioned above. Below is a bulleted list of basis data and assumptions used for the modeling of these initial (calibration/verification) analysis cases.

- An idealized soil profile was developed based on the cross-section and boring log information from the 1958 DWR report (for Terminous Island) and other reports for the other cases, which are presented in Appendix A of the Levee Vulnerability TM (URS/JBA 2008c). In some locations, additional information from adjacent deep borings was used to supplement any information gaps.
- Because subsidence of peat/organic soil has been an ongoing process in the Delta, the cross-section data from the 1956 study are likely under representing the current ground-surface conditions. The data is likely representative of the elevation at the bottom of the peat/organic layer and foundation sand layer. The topography of the cross-section was corrected using recently surveyed IFSAR topography data (DWR survey provided with the GIS database). To better evaluate current slope profiles below the slough water levels, bathymetric data available from the DWR GIS database were used.
- For the model cases with slough sediments, a 2-foot-thick silt sediment layer was assumed to exist at the bottom of the channel slough.
- An analysis cross-section was developed, based on the above data and interpretation, as illustrated in Figure 7-29.

- Using the above cross-section, a finite-element model was developed using SEEP/W. It was often difficult to confirm whether drainage ditches abutting the landside levee toe were present or had been filled in after problems were identified during the 1986 and 1997 floods. Therefore, models were developed for both "with ditch" and "without ditch" conditions, as illustrated in Figures 7-30 and 7-31.
- The models were then executed using three different slough water elevations: 0, +4, and +7 feet NAVD88, representing low-tide, high-tide, and flood-water-level conditions, respectively, as illustrated in Figures 7-32 through 7-37.

The results of these initial analyses are briefly summarized below and making reference to the appropriate figures and results.

Figures 7-32 through 7-34 show the total head distribution and vertical gradient contours for the "with ditch" condition for the three slough water elevations (0, +4, and +7 feet, respectively).

Figures 7-35 through 7-37 show the total head distribution and vertical gradient contours for the "without ditch" condition for the three slough water elevations (0, +4, and +7 feet, respectively).

For the "with ditch" condition, gradients at Point A, located directly below the ditch, are significantly higher than at Point B, located approximately 100 feet from the toe of the levee (Figures 7-32 through 7-34). Except for the gradient at the bottom of the ditch, the "with ditch" and "without ditch" models, produce approximately the same vertical gradients near the landside toe of the levee and at Point B 100 feet away from the toe of the levee (Figures 7-35 through 7-37). These results indicate that the presence of a ditch next to a levee has a significant impact on seepage conditions with exit gradient of 0.8 when water stage is near +7 feet elevation. For the same +7 feet water stage, the exit gradient is 0.4 without drainage ditch. The analysis of the lower water stages indicates no adverse conditions at Terminous Tract, supporting the historical performance of Terminous Tract, which has experienced no failure since 1958.

To assess the contribution of the variation of the material properties around the mean values (uncertainties), the "with ditch" model as described below was analyzed:

- Mean-minus-one standard deviation value of permeability for the blanket layer (peat/organics)
- Mean-plus-one standard deviation value of permeability for the blanket layer (peat/organics)
- Mean-minus-one standard deviation value of permeability for the underlying higher permeability (SP/SM) foundation sand
- Mean-plus-one standard deviation value of permeability for the underlying higher permeability (SP/SM) foundation sand
- No slough sediment layer

The analysis results are summarized in Table 7-14 and presented in Figures 7-38 through 7-41. For comparison purposes, Table 7-14 also presents a summary of the results from analyses conducted for the "with ditch" and slough sediments case for the initial mean values of permeability, using estimated values of permeability for peat/organic or fine-grained blanket soils.

Table 7-14 and Figure 7-38 indicate that the blanket (peat) permeability has a direct and highly significant impact on computed gradients. Computed gradients increased by approximately 50 percent for a one standard deviation decrease in permeability and decreased by approximately 50 percent for a one standard deviation increase in permeability.

Table 7-14 and Figure 7-39 indicate that in the case of low-permeability sand for the model with sediments, the sand permeability has a less obvious impact on computed gradients. The computed gradients decreased by approximately 50 percent for an increase by one standard deviation and also decreased by less than 10 percent by decreasing the permeability by one standard deviation. In this situation, the sand layer is effectively "capped" on both the water entry on the slough side and water exit on the landside by the lower permeability of the slough sediment and blanket layer. Therefore, in the seepage model, these two impervious top layers have counteracting impacts, yielding a more-complex relationship and skewed distribution around the mean. Because of the strong contrast between the permeability of the blanket and the sand aquifer, the variation of the permeability of the sand was found to be of second-order effect (as long as its permeability is one to two log cycles below that of the blanket) and hence, the best estimate values only were used.

Table 7-14 and Figure 7-40 indicate that the presence of slough sediments has a potentially important impact on computed gradients. Computed gradients increased by about 25 percent when slough sediment is removed. Although slough sediment presence was found to be a potentially important and should be included as a random variable in the development of under-seepage fragility functions, unfortunately, confirmation of the presence of slough sediments at each location throughout the Delta was beyond the scope of this study. Because of this shortcoming, the slough sediment was modeled as random variable with 50 percent chance of being present. Slough sediments are more likely to exist in smaller channels and backwaters and less likely to exist in large, main flow, and dredged channels. Further assessment of the extent and thickness of slough sediments throughout the Delta is recommended.

Table 7-14 and Figure 7-41 indicate that the presence of a ditch has a potentially important impact on computed gradients at the ditch and little impact on computed gradients away from the ditch. Computed gradients increased by more than 100 percent near the levee when a ditch was present but increased by less than 5 percent about 100 feet away from the levee when a ditch was present. The ditch has the same impacts as the slough sediments on the exit gradient. Unfortunately, confirmation of the presence of ditches at each location throughout the Delta was beyond the scope of this study and could not be used as a deterministic feature during the development of the risk model. The presence of ditches is a potentially important factor and should be included in developing under-seepage fragility functions. In the best conditions, it must be modeled as a deterministic parameter defining the cross-section geometry for each vulnerability classes since it would be geographically defined. It should be noted however, that the presence of the drainage ditch becomes insignificant for cross-sections with peat thickness of 20 feet or more.

Findings from the initial analyses. Overall, the initial analyses for the selected specific cases in the Delta, indicate that calculated gradients are not showing adverse under-seepage conditions for normal water stages (excluding storm events) as expected. For the worst-case condition (mean-minus-one standard deviation blanket permeability, "with ditch" and slough water at +7 feet), the maximum computed vertical gradient is approximately 1.0, which is near the point of

initiation of under-seepage problems. This is generally consistent with observed seeps and boils throughout the Delta during high-water events.

7.7.4.5 Comparisons with Areas with Known Seepage Problems

As previously discussed, approximately 74 levee failures have resulted in island flooding since 1950 (Figure 7-22a and 7-22b). A compilation of eyewitness accounts and documented reports of seepage problems in the Delta were recorded on a map, as shown in Figure 7-42. In general, the observations represent reliable empirical data to gage the seepage model results against (verification of fatal flows). The analysis team identified sites where known under-seepage problems could be used to compare to the seepage model results.

These sites included a number of reported sites of observed seepage problems. The under-seepage problems observed during the 1997 flood at the east levee of Grand Island and the under-seepage reported at Woodward Island after the Upper Jones Tract failure in June 2004 are discussed below.

Grand Island. Topographical data derived from IFSAR and bathymetric data sets (provided in the DWR GIS database) were used to develop the geometry of the cross-section at that site. No ditches exist next to the levee at the problem area based on private communication with Mr. Gilbert Cosio (Consulting engineer to local Reclamation Districts 2007). Subsurface data from nearby borings (stick logs), shown in Figure 7-43, were used to develop a representative cross-section for analysis. A cross-section representing the geometry and subsurface conditions during the 1997 flood was developed, as shown in Figure 7-44.

To evaluate water levels during the 1997 flood, flood elevation data were obtained from DWR monitoring station B91650 on the Sacramento River at Walnut Grove. The station is approximately 2 miles upstream and is the closest station to the site (see recorded water elevation at the time of the event in Figure 7-45). The distance is short enough that a water-level distance correction was not considered necessary. Based on these data, a water elevation of +16 feet was used in the seepage model. In addition, because the seepage problem was observed during a flooding event when the flow velocity in the slough would be higher than normal, it was assumed that slough sediment was not present.

Figure 7-46 presents the finite-element model and boundary conditions at the site. Analyses were performed for a blanket anisotropy of 10, 100, and 1,000. The results are presented in Figures 7-47, 7-48, and 7-49, respectively. Computed gradients near the landside toe and away from the toe (Point B) are also summarized in Table 7-15. The results of the analysis indicate that the exit gradient at the toe of the levee is approximately 0.4, 0.5 and 0.6 for k_h/ k_v, of 10, 100, and 1000, respectively. The results for anisotropy of 10 indicate that the calculated vertical exit gradient (i_{vert} = 0.4) would be insufficient to initiate an under-seepage problem during the 1997 flood. For an anisotropy of 100, the exit gradient was calculated to be i_{vert} = 0.5, the value at which typical seepage starts to become a concern. An anisotropy of 100 was then adopted for the next steps of the analysis. It should be noted, however, that the change in the vertical exit gradient is not very sensitive to the increased anisotropy of the blanket (0.4 to 0.6).

Woodward Island. The properties from the above analysis with an anisotropy of 100 were used at the observed seeps and boils site at the southeastern corner of Woodward Island. During the

June 3, 2004 breach of the Upper Jones Tract, the slough water was at elevation +6.85 feet (NAVD88). One of two boring logs at the southeastern corner shows the presence of an upper, about 5- to 7-foot thick, soft organic clay layer with more than 30 percent organic content overlaying a thick sand deposit. The levee landside toe was at elevation –7.5 feet. The analysis with no slough sediment and no drainage ditch, showed that the exit gradient at this location was estimated to be approximately 2.0, clearly confirming the observed sand boils and consistent with the model prediction (see Figure 7-60 at point A near the toe of the levee). During the Jones Tract failure, the breach caused high-flow velocities which scoured the channel extensively as reported in the repair and construction documents (provided by DWR 2004), and hence removed any recent silt deposits and exposed the sand layer.

Based on the above initial verifications and the results of this calibration, the values listed in Table 7-16 were adopted as representative conditions throughout the Delta, and were then used for the production runs.

7.7.4.6 Levee Response Functions for the Delta

To develop levee response functions representative of conditions throughout the Delta, seepage models with the range of subsurface conditions throughout the Delta were developed. Based on the previously discussed review of cross-section data (Section 2.0 of the Levee Vulnerability TM [URS/JBA 2008c]) and with the aid of the GIS mapping, levee geometries and subsurface conditions were developed for each vulnerability class.

As shown on the peat/organics thickness map (Figure 7-50), the thickness of a landside blanket layer varies throughout the Delta. Levee reaches with ranges of thickness from no peat to over 35 feet were developed from the GIS model. For each of these reaches, “with ditch” and “without ditch” models were considered. Figure 7-51 shows a typical cross-section for a “with ditch” model and a 25-foot-thick peat layer. Figure 7-52 shows a typical cross-section for a “without ditch” model and a 25-foot-thick peat layer.

Based on the depth of the channels and sloughs (-25 feet to -34 feet elevation within the central western Delta) and the high velocity flows in the confined channel, it was assumed that the peat/organic layer (blanket) terminates below the waterside toe of the slope as the channels are incised. To model the landside downward slope of the ground surface away from most Delta levees, a slope of approximately 500 horizontal to 1 vertical (500H:1V), away from the levee, was used based on the general topographic contour maps of the interior of the islands. If the section was modeled with drainage ditch, the ditch was modeled as 5 feet deep and approximately 100 feet away from the levee centerline or near the toe, whichever is more distant. When slough bottom sediment was considered, a 2-foot-thick layer was used.

Figures 7-53 and 7-54 present typical finite element models used to estimate seepage conditions as a function of flood water levels and to develop fragility curves. Typical results from these models are presented in Figures 7-55 through 7-58, showing only the “with ditch,” with slough sediments, and slough water at elevation +4 feet, for peat/organic deposit thickness of 5 feet, 15 feet, 25 feet, and 35 feet, respectively.

Figures 7-59a and 7-59b present the computed vertical gradients (below the ditch and 100 feet from the ditch, respectively) versus water level (from +0 feet to levee crest elevation) for a levee founded on a 5-foot-thick blanket layer with a ditch. Maximum vertical gradients are found

below the ditch, which cuts completely through the peat layer. This is a special case for this series of models. In this situation, the ditch completely pierces the blanket layer and acts as a drain to the underlying sandy layer. While seepage flow rates into the ditch may be high, the pressures in the sand layer are greatly relieved, lowering the gradients to subcritical levels (i.e., <~0.24), particle movement is still a concern.

In contrast, for the model with a 5-foot-thick blanket layer and without a ditch (Figures 7-60a and 7-60b), the gradients at the toe (Figure 7-60a) and away from the toe (Figure 7-60b) show a substantial increase in the calculated vertical gradients (1.2 to 2.4 and 1.0 to 2.0, respectively). For this condition, the exit gradients are mostly above 1.0, indicating a state of active failure. Separate fragility curves for both “with ditch” and “without ditch” have been produced for the mean and standard deviations.

Figures 7-61a, 7-61b, 7-62a, and 7-62b present the computed vertical gradients for 15-foot-thick blanket layer as a function of river/slough water levels for “with ditch” and “without ditch,” respectively. The results indicate that the vertical gradient under the ditch increased to values ranging from 0.8 to 1.6 as a function of higher water levels (Figure 7-61a), effectively representing the average gradient through a 10-foot-thick blanket. Conversely, the vertical gradients calculated for “without ditch” are smaller and range from 0.4 to 0.9 near the toe (Figure 7-62a) and 0.3 to 0.8 away from the toe (Figure 7-62b).

The same calculations were conducted for blanket thicknesses of 25 and 35 feet, as shown in Figures 7-63 through 7-66. Generally, the results indicate that the vertical gradients are below 0.8 for “with ditch” and below 0.6 for “without ditch.” Therefore, blankets with 25 feet or more in thickness have less potential for under-seepage failures. It was also noted that the 84th percentile of the vertical gradients were constrained to values very close to the mean. Beyond a certain contrast between the sand and the blanket permeability coefficients, the vertical gradients become insensitive to further reduction of peat/organic permeability. or conversely further increase in the permeability of the aquifer

7.7.4.7 Levee Response Functions for Suisun Marsh

The available information indicates that the levees in the Suisun Marsh area have special characteristics that should be accounted for slightly differently than those in the main Delta. Most importantly, these levees are smaller and typically hold back lower flood levels. The landside ground elevation is also different from the Delta. The interior land elevations are much higher than the Delta and have not subsided much. Separate models were, therefore, developed to evaluate the relationships between flood levels and computed gradients.

Appendix A of the Levee Vulnerability TM (URS/JBA 2008c) contains cross-sectional and subsurface information on levees in the Suisun Marsh area. Figure 7-67 presents a typical cross-section for Suisun Marsh. Based on a review of available data, this cross-section was estimated to be representative of the conditions throughout Suisun Marsh. In a similar fashion to the process used for the main Delta, a model based on this section was developed and evaluated for a series of subsurface conditions and water levels. Figure 7-68 presents a typical finite element model of Suisun Marsh levees. Figure 7-69 presents the calculated values of head and gradient using this model and a water surface elevation of +4 feet (although the calculations were run for a full range of water elevations from 0 to +8 feet).

As with the Delta levees, sensitivity of the model to changing conditions was also evaluated. Figure 7-70 shows the relationship between computed vertical gradient as a function of blanket thickness and water level. All cases were run “without ditch” and 2-foot-thick slough sediment. Figure 7-70 indicates that the calculated gradients for Suisun Marsh are much smaller than those calculated for the main Delta. For example, the calculated vertical gradients for the 5-foot-thick blanket range from 0.4 to 1.1 for Suisun Marsh compared to 1.2 to 2.4 for the main Delta. The foremost reason for the difference with the main Delta is the higher surface elevation of the interior island floors in Suisun Marsh. Under-seepage at Suisun Marsh appears to be of lesser concern than for the main Delta, except for irregularities (e.g., sand seams, cracks, or burrowing animal holes).

7.7.5 Evaluation of Conditional Probability Failure Functions

The second step in the development of a fragility curve was to relate the predicted vertical gradient to a probability of failure. To complete this step, an expert elicitation process was used.

The members of the levee vulnerability team who had experience with the characteristics of the Delta and the experts from the Technical Advisory Committee were given a summary of the background work and data, model development methodology, and model results showing the computed gradients as a function of water levels and blanket permeability for each vulnerability class. The team of experts was also asked to consider the following assumptions in developing their opinion:

1. The objective behind the development of the conditional probability of failure curves is to characterize the likelihood that internal erosion and piping will progress to the point of full failure (breaching).
2. High water persists for one or more days with tides causing fluctuation.
3. In some cases, partial erosion degradation may already exist as a result of previous events.
4. Consider two options in the evaluation: (1) no human intervention to contain or mitigate the forming seeps and boils, and (2) human intervention.

The group of experts participating in the elicitation process included:

- Professor Ray Seed (UC Berkeley)
- Dr. Leslie Harder (DWR)
- Mr. Michael Driller (DWR)
- Dr. Ulrich Luscher (URS Consultant)
- Mr. Michael Ramsbotham (USACE)
- Mr. Gilbert Cosio (MBK Engineers)
- Mr. Kevin Tillis (Hultgren-Tillis)
- Mr. Edward Hultgren (Hultgren-Tillis)
- Dr. Said Salah-Mars (URS - Facilitator)

First the experts were briefed on the methodology and development process of the models discussed above in few briefing and questions and answers sessions. The experts were then asked to independently develop estimates of failure probability as a function of vertical gradient for the case of no human intervention, using the model results and assumptions provided above. Each expert submitted his recommendations separately. The experts were then asked to estimate failure probability for the same situation but using human intervention.

The proposed curves by the experts were treated as individual statistical values equally weighted and used to generate mean and standard deviations, representing the epistemic uncertainties for this failure mode.

Figure 7-71 is a summary of the exercise results assuming no human intervention. As shown, the mean value of the probability of failure is less than 50 percent for computed vertical gradients of less than 0.8. Probabilities of failure are expected to be greater than 80 percent when the vertical gradient is greater than approximately 1.1. This value is in general agreement with values suggested by USACE (1999b).

Figure 7-72 presents a summary of the results of the same exercise assuming human intervention. A comparison of Figure 7-71 with Figure 7-72 indicates that the panel believes that human intervention, assuming available emergency response resources, can significantly reduce the probability of levee failures**,** as indicated by the significant shift of the mean curve to the right of the graph in Figure 7-72.

During high flood stage when wind waves crash over the levee crest, emergency repair vehicles cannot access the crest roads. However, at lower flood stage, when levee crests are safe, emergency repair vehicles can access the levee crest to repair erosion damage, cracking, and levee slumps related to developing seepage or other problems. The experts recommend using two conditional probability-of-failure functions in the following manner: (1) use the “no human intervention” curve for the high flood stage with freeboard less than 2 feet, and (2) use the “with human intervention” curve for flood stage corresponding to more than 2 feet of freeboard.

7.7.6 Evaluation of Fragility Functions

The third and final step in developing levee fragility functions was to evaluate the under-seepage fragility functions, which was done by combining the levee response functions with the conditional probability of failure functions through Monte Carlo simulation. The levee fragility functions relate the probability of failure to slough water surface elevation (or in terms of freeboard [= crest elevation – WSE]) for each vulnerability class (Figure 7-28c). This step was performed using Monte Carlo simulations. The random variables used in the simulation are listed in Table 7-10 and described below.

- VCs 1 and 2 represent no-peat areas in the Delta. In the development of under-seepage fragility curves for these classes, presence of ditch and sediment were treated as random input variables.
- VCs 3 through 12 represent areas that have peat/organic blanket layer in the Delta. In the development of under-seepage fragility curves for these classes, presence of ditch, presence of sediment, peat thickness, and peat permeability were treated as random input variables.

- VCs 13 and 14 represent no-peat areas in the Suisun Marsh. In the development of under-seepage fragility curves for these classes, presence of sediment was treated as a random input variable.
- VCs 15 through 24 represent areas that have peat/organic blanket layer in the Suisun Marsh region. In the development of under-seepage fragility curves for these classes, presence of sediment, peat thickness, and peat permeability were treated as random input variables.
- Levee geometry and water level for a given flood event were treated as deterministic parameters. The model was run for a full range of water levels varying from the toe to the crest of the levee. In the overall risk analysis, the water level is treated probabilistically as discussed in the Flood Hazard TM (URS/JBA 2008a).

The vertical gradient versus water level curves (Figures 7-59 through 7-66 and Figure 7-70) are combined with the probability of failure versus gradient curves (Figures 7-71 or 7-72) to produce the probability of failure versus water level (or freeboard = crest elevation – water level) for the entire Delta and Suisun Marsh for each VC. The calculated under-seepage fragility functions for the Delta and Suisun Marsh region are shown in Figures 7-73a through 7-73f. The resulting curves will be used as input in the flood risk model.

7.8 PROBABILITY OF FAILURE DUE TO THROUGH-SEEPAGE

Calculations of through-seepage have yielded very low exit gradients through the levee landside slopes. The finite element models used to estimate exit gradients on the landside slope of the levees indicate that the exit horizontal gradients are on the order of 0.12 under flood stage condition (2 feet of freeboard).

This calculated exit gradient can easily be verified with a simple hand calculation. For a typical levee geometry consisting of a 20-foot-wide crest, 20 feet high, with 2.5H:1V and 3.5H:1V slopes on the waterside and landside, respectively, the water column will be 18 feet, leaving a 2-foot freeboard. The simplified one-dimensional flow equation for a sandy levee yields a horizontal exit gradient at the landside toe of the levee of approximately DH/DL=18/140=0.128.

The standard definition of critical gradient, and the safe-design gradient of 0.3 or less, do not apply in this case, where the horizontal flows through the levee tend to move the near-surface particles horizontally and down the landside slope of the levee. Unlike moving particles upward against gravity (as in the case of under-seepage), the seeping water through the levee will move particles horizontally with more ease and under a much-smaller gradient.

Because the analysis models show horizontal exit gradients values much smaller than 0.3, there were no standard procedures that establish failure probabilities as a function of exit gradient. The analysis team turned to expert elicitation and local knowledge to develop a procedure by which through-seepage levee failure prediction can be made for the Delta. Through-seepage failures are known to occur in the Delta by the local practicing engineers and researchers in that field.

The mechanism of through-seepage is known to evolve in a slow and progressive fashion as discussed below and illustrated with pictures of forming boils in Figure 7-74. We have observed many instances of unthreatening seeps and boils in the Delta and the Sacramento Basin as a whole (Bouldin Island 1983, Staten Island 2007, Sacramento River in the Natomas area 1986,

Sacramento Bypass South levee 1998), where fine particles are moved slowly and progressively over time, eroding the levee sandy fill of its finer particles.

As the finer particles are moved, the permeability of the levee increases, and flow velocities increases. This process takes time to develop, erodes fines with each high stage cycle, but will ultimately create a quasi-stable levee which will experience slumping and cracking (Staten Island, July 2007), and rapid erosion of the landside levee slope (Sacramento Bypass south levee, January 1998, and Sacramento River, Natomas area, 1986).

Because of the difficult nature of developing a reliable numerical model to predict through-seepage failures, the analysis team and the TAC recommended adopting the assumption that the annual frequency of failures by through-seepage is equal to that of under-seepage, based on their observations and long-standing experience with the Delta levees.

7.9 PROBABILITY OF FAILURE DUE TO OVERTOPPING

Water surface elevations were estimated based on in-Delta flows, tide condition, and wind set-up. A fragility curve was defined to assess the probability of overtopping as a function of freeboard, as shown in Figure 7-75.

Overtopping failure occurs when the floodwater level rises above the crest of a levee and erodes the levee to the point of breaching. The factors used to estimate the probability of failure by overtopping are levee crest elevation, the frequencies of floodwater levels above the levee crest, and the conditional probability of levee failure (breaching) as a function of the water height over the crest.

The probability of failure due to overtopping increases from zero (when the water level is at or below the levee crest), to one when the water level is at 2 feet above the levee crest. Figure 7-75 illustrates the fragility function assumed for the overtopping failure mode. Some amount of overflow can occur without complete failure of the levee. Human intervention can also prevent failure due to overtopping by raising the crests with sandbags during high-water periods and wind action. This approach was developed using an expert elicitation process similar to that used to relate predicted vertical exit gradient to probability of failure (see Section 7.7.5).

The flood levels for current and future years (in 50, 100, and 200 years) were developed in the Flood Hazard TM (URS/JBA 2008a) and the Climate Change TM (URS/JBA 2008b). The results of the probability of overtopping are combined with the probability of failure due to under-seepage and through-seepage and are presented in Section 13.

7.10 PROBABILITY OF FAILURE DUE TO WIND/WAVE

During non flood and non seismic conditions, the wind-wave action on the exterior slopes of the levees was not explicitly considered in the analysis. Excluding floods and earthquakes, and considering the existing waterside slope protection with rip rap and the human intervention, this particular hazard was considered relatively insignificant and, hence, was not considered explicitly. Furthermore, because these potential failures would occur during periods of no flood and no seismic conditions, they were implicitly included in the empirical data compiled for the normal failure conditions also referred to as “sunny-day failures” and discussed in Section 9.

However, when islands are flooded, the wind-wave action on the non protected interior slopes and the resulting erosion of the interior of the levees are represented in the risk model, and are addressed in the Wind-Wave Hazard TM (URS/JBA 2008g) and the Emergency Response and Repair TM (URS/JBA 2008d).

7.11 SPATIAL MODELING OF PHYSICAL RESPONSE OF LEVEES TO FLOOD EVENTS

Section 7.7 described the geotechnical model used to assess seepage gradients of individual levees in different vulnerability classes subjected to a given flood scenario, and the model to assess the probability of a breach of a levee reach given the estimated seepage gradient. To assess the risk of simultaneous, multiple levee failures under a given flood, the simultaneous physical behavior of all levees in the study area subjected to a specified flood event also needs to be modeled. Such a model needs to account for the spatial continuity of levees and define how levees within and across levee reaches are likely to behave in a given flood event.

This section first provides an overview of the spatial physical model of representing levees around different islands, and describes the key assumptions made in modeling the spatial behavior of levees during a flood event.

The geotechnical fragility model described in Section 7.7.6 provides a procedure to estimate the probability of under-seepage failure on individual reaches of an island. This procedure needs to be extended for estimating the probability of under-seepage failure of an island. The approach is based on the concept of the "weakest link," that is, the first failure of a system would occur at the weakest link. This assumption is appropriate for a linear system such as levees. It would not be known with certainty which levee reach is the weakest link. It is reasonable to assume that each reach has some probability of being the weakest link, and that probability is proportional to the vulnerability of the reach, as reflected in its conditional failure probability. That is, a reach with a higher failure probability would be more vulnerable to a failure, and would have a greater chance of being the weakest link and failing first. Using this assumption, the probability that each reach on an island is the weakest link is first estimated by making this probability proportional to the reach failure probability. This estimation can then be used to calculate the joint probability that a given reach would be the weakest link and would fail. This joint probability is summed over all reaches to estimate the probability of failure of the island.

This approach will honor three essential criteria: (1) It will be invariant with regard to the reach length. That is, regardless if an island is divided into 10 reaches or 100 reaches, the result would be the same. (2) It will preserve the concept of the weakest link. That is, the probability of island failure would not be simply an average value over all reaches. (3) Each reach will contribute to the overall probability of island failure. That is, the probability of island failure will not be controlled by a single reach that has the maximum failure probability. This approach simply reflects the fact that it is not known with certainty which reach is the weakest link; each reach could be the weakest link, with some probability, and could fail first.

Let

$P[R_{ij} \mid k]$ = conditional under-seepage failure probability of j-th reach on i-th island given k-th flood event and j-th reach is the "weakest" link

$P[I_i \mid k]$ = conditional under-seepage failure probability of i-th island given k-th flood event

$P[R^*_{ij} \mid k]$ = probability that j-th reach on i-th island is the "weakest" link given k-th event (that is, the link that would fail first under the given event)

$P[R^*_{ij} \mid k]$ is calculated as follows:

$$P\left[R^*_{ij} \mid k\right] = \frac{P\left[R_{ij} \mid k\right]}{\sum_j P\left[R_{ij} \mid k\right]} \quad (1)$$

The conditional under-seepage failure probability of the i-th island given k-th event is calculated taking into account the probability that each reach could be the weakest link and the conditional under-seepage failure probability of that reach given k-th event. Thus, $P[I_i \mid k]$ is calculated from:

$$P\left[I_i \mid k\right] = \sum_j P\left[R^*_{ij} \mid k\right] P\left[R_{ij} \mid k\right] \quad (2)$$

7.12 ISLAND FAILURE PROBABILITY UNDER MULTIPLE FAILURE MODES

The previous section was used to estimate the probability of an island failure in under-seepage for a given flood event. The probability of an island failure due to through-seepage was assumed to be equal to the probability of failure due to under-seepage, as discussed in Section 7.8. The probability of an island failure due to overtopping was estimated using the procedure described in Section 7.9 (i.e., using the fragility curve for overtopping). Overall probability of an island failure due to any of these three failure modes was calculated as follows:

$$P_f \text{ (island)} = 1 - ((1-P_{fUS}) \times (1-P_{fTS}) \times (1-P_{fOT})) \quad (3)$$

where,

P_f (island) = Probability of an island failure

P_{fUS} = Probability of an island failure in under-seepage

P_{fTS} = Probability of an island failure in through-seepage

P_{fTS} = Probability of an island failure in overtopping

7.13 PROBABILITY OF DAMAGE BUT NO BREACH

For the flood induced failure there is no condition of ,"damage but no breach" as with earthquake induced failures. The only secondary damage considered in the analysis is the interior slope erosion under wind/wave action when the island is flooded. The erosion of the landside slopes of flooded islands is discussed in the emergency response and repair section (Section 10).

7.14 LENGTH EFFECTS ON PROBABILITY OF LEVEE FAILURES

The procedure presented above for the estimation of an island failure probability does not account for the effect of length of levees within each island. A simplified procedure was

developed using historical island failures in the Delta islands to adjust the probability of failure considering the length of each island perimeter levee under consideration. To develop this simplified procedure, islands that have breached multiple times in the past were reviewed. Venice Island breached 8 times in the past 100 years, and was considered as the reference case where all contributing effects (including length) are included. Hence, the length effect is developed as a simple hyperbolic scaling function as described in Equation (4). This scaling factor (SF) is used to adjust the probability of failure of any given island.

$$SF = 1 + (L_i - L_r)/L_n \quad (4)$$

where

L_i = length of an island under consideration

L_r = length of a referenced island

L_n = length of the longest island in the study area

The analysis team adopted this approach after considering the 100-year record of Delta island flooding. The typical range of SF is about 0.7 to 1.7 for the Delta: 0.7 corresponds to an island with 1 mile of perimeter levee, and 1.7 corresponds to an island with 42 miles of perimeter levees such as Grand Island, which has perimeter levees that are 3.5 times longer than those on Venice Island.

7.15 SUMMARY OF FINDINGS AND OBSERVATIONS

7.15.1 General Observations

- About 158 islands have flooded in the Delta since 1900, and about 74 since 1950. The Suisun Marsh levees have lower elevation than those of the Delta and are prone to more frequent failures. The rate of island flooding in Suisun Marsh cannot be quantified because of absence of historical data going back to 1900.
- The Delta offers numerous case histories (although with incomplete details) for calibrating the levee flood-induced failure model. These case histories helped ground-truth the model used and the results.
- We observed that not all the details of historical flood events are recorded or available. It is recommended that failures in the Delta be fully documented in a formal and comprehensive way that covers the necessary details to reconstruct the events and verify them numerically. This documentation will provide increased validity to future modeling exercises.
- The data to collect should include, at a minimum, the following: the storm event date; the storm time; the type of storm; the Delta inflow measurements; the water stage readings before, during, and after the event; the crest elevation at the failure point (if failure occurred); visual observations (e.g., seeps, boils, ponding water, erosion, or overtopping); when the initiating conditions started and their type; a description of the flood fight, if any; and the actions taken.
- Field notes are essential in documenting the events and observations. These should be recorded and entered into the database that has been started in the context of this study.

- These observations will also help provide valuable information on the types of failure modes and, at a minimum, will allow the development of an empirical model to represent through-seepage failures.

7.15.2 Findings

- Because of the large contrast between the permeability of the organic/peat deposits and the pervious foundation sand layer, the uncertainties around the mean permeability values of the sand layer do not contribute substantially to the overall model uncertainties.
- Blankets of 15 feet or less in thickness have the highest impacts on under-seepage.
- The drainage ditch contribution to under-seepage is significant for blankets of 15 feet or less in thickness.
- Blankets of 20 feet or more in thickness are not impacted by the presence of a drainage ditch, which is assumed to be 5 feet deep or less.
- The presence or absence of slough sediments has a significant impact on under-seepage. However, it is difficult to map the presence, thickness, and composition of slough sediments knowing that their state is changing with flow velocities and channel dredging. This parameter is highly variable with time.
- Other contributors to under-seepage and through-seepage cannot be formally accounted for or explicitly modeled. These contributors include random and elusive weaknesses in the levees and their foundations (e.g., burrowing animals, human activities, or weak zones). We believe that these “weak links” are more pronounced in non engineered levees.
- The use of empirical models and the calibration of the models against observations help account implicitly for these pre-existing and difficult-to-investigate conditions.

Tables

Table 7-1 Partial List of Major Dams and Reservoirs in Tributary Watersheds to the San Francisco Bay-Delta

Dam Name	Watercourse	Tributary of	Reservoir	Year Original Construction Completed	Reservoir Capacity (acre-feet)
East Park	Little Stony Creek	Sacramento River	East Park	1910	
Daguerre Point	Yuba River	Sacramento River		1910	
Cache Creek	Cache Creek	Sacramento River	Clear Lake	1914	
Capay Diversion Dam	Cache Creek	Sacramento River		1914	
Stony Gorge	Stony Creek	Sacramento River	Stony Gorge	1928	
Pardee	Mokelumne River	San Joaquin River	Pardee	1929	210,000
Englebright	Yuba River	Sacramento River		1941	
Friant	San Joaquin River	San Joaquin River	Millerton Lake	1942	520,000
Shasta	Sacramento River	Sacramento River	Shasta Lake	1945	4,552,000
Martinez	off-stream storage		Martinez	1947	
Keswick	Sacramento River	Sacramento River	Keswick	1950	
Sly Park	Sly Park Creek	American / Sacramento River	Jenkinson Lake	1955	
Mormon Island Auxiliary Dam	Blue Ravine	American / Sacramento River	Folsom Lake	1956	
Folsom	American River	Sacramento River	Folsom Lake	1956	1,010,000
Tulloch	Stanislaus River	San Joaquin River	Tulloch	1957	68,000
Monticello	Putah Creek	Sacramento River	Lake Berryessa	1957	
Comanche	Mokelumne River	San Joaquin River	Comanche	1963	431,000
Whiskeytown	Clear Creek	Sacramento River	Whiskeytown Lake	1963	
Spring Creek Debris Dam	Spring Creek	Sacramento River	Spring Creek	1963	
Red Bluff (Diversion)	Sacramento River	Sacramento River	Lake Red Bluff	1964	
New Hogan	Calaveras River	San Joaquin River	New Hogan	1931, 1964	325,000
Los Banos (Detention)	Los Banos Creek	San Joaquin River	Los Banos	1965	

Table 7-1 Partial List of Major Dams and Reservoirs in Tributary Watersheds to the San Francisco Bay-Delta

Dam Name	Watercourse	Tributary of	Reservoir	Year Original Construction Completed	Reservoir Capacity (acre-feet)
Little Panoche (Detention)	Little Panoche Creek	San Joaquin River	Little Panoche	1966	
San Luis	San Luis Creek	Delta - Mendota Canal	San Luis	1967	
O'Neill	San Luis Creek	Delta - Mendota Canal	O'Neill Forebay	1967	
Contra Loma	off-stream storage		Contra Loma	1967	
Oroville	Feather River	Sacramento River	Lake Oroville	1968	3,537,580
New Exchequer	Merced River	San Joaquin River	Lake McClure	1926, 1968	1,026,000
New Bullards Bar	Yuba River	Sacramento River	New Bullards Bar	1969	
New Don Pedro	Tuolumne River	San Joaquin River	New Don Pedro	1923, 1971	2,030,000
Buchanan	Chowchilla River	San Joaquin River	Eastman Lake	1975	150,000
Indian Valley	N Fork Cache Creek	Sacramento River	Indian Valley	1976	300,600
New Melones	Stanislaus River	San Joaquin River	New Melones	1979	2,400,000
Sugar Pine	N Shirttail Creek	American / Sacramento River	Sugar Pine	1981	
Hidden	Fresno River	San Joaquin River	Hensley Lake		90,000
Almanor	N Fork Feather River	Sacramento River			

Table 7-2 Summary of Delta Inflows

Sacramento + Yolo Bypass Inflows	WY 1956 - 1968, pre-Oroville Dam	WY 1969 - 2005, ~Existing Conditions	WY 1956 - 2005, Period of Record
Average Daily Inflow, cfs	26,430	28,671	28,088
Avg. Annual Precip., inches[1]	17.4	18.1	18
Max. Annual Precip., inches	27.7	34.5	35
Inflow Range	**Number of Inflows in Q-Range**		
0-100K	4564	12924	17488
100K-200K	152	466	618
200K-300K	28	96	124
300K-400K	3	19	22
400K-500K	2	5	7
>500K	0	4	4
sum =	4749	13514	18263
Inflow Range	**No. of Days per Year With Inflows in Q-range**		
0-100K	351.1	349.3	349.8
100K-200K	11.7	12.6	12.4
200K-300K	2.2	2.6	2.5
300K-400K	0.2	0.5	0.4
400K-500K	0.2	0.1	0.1
>500K	0.0	0.1	0.1
sum =	365.3	365.2	365.3

San Joaquin River Inflows	WY 1956 - 1979, pre-New Melones Dam	WY 1980 - 2005, ~Existing Conditions	WY 1956 - 2005, Period of Record
Average Daily Inflow, cfs	4,416	4,809	4,416
Avg. Annual Precip., inches[2]	13.9	14.9	14.3
Max. Annual Precip., inches	25.9	27.5	27.5
Inflow Range	**Number of Inflows in Q-range**		
0-10K	8037	8270	16307
10K-20K	393	697	1090
20K-30K	247	336	583
30K-40K	74	171	245
40K-50K	15	22	37
>50K	0	1	1
sum =	8766	9497	18263
Inflow Range	**No. of Days per Year With Inflows in Q-range**		
0-10K	334.9	318.1	326.1
10K-20K	16.4	26.8	21.8
20K-30K	10.3	12.9	11.7
30K-40K	3.1	6.6	4.9
40K-50K	0.6	0.8	0.7
>50K	0.0	0.0	0.0
sum =	365.3	365.3	365.3

[1] Precipitation data from the Sacramento Airport, Station 47630.

[2] Friant Government Camp.

Table 7-3: Statistical Analysis of Annual Peak Inflows

Annual Peak Delta Inflows - Sacramento River & Yolo		
Annual Peak Inflows - Statistical Parameters	**WY 1956 - 1967, pre-Oroville Dam**	**WY 1968 - 2005, ~Existing Conditions**
No. of Years	12	38
Mean	188,164	160,107
Standard Deviation	128,500	140,928
Minimum	51,250	13,703
Median	137,681	108,106
Maximum	441,865	612,301
Distribution	Lognormal	
Statistical Test	t-Test (lognormal, equal variances)	
2-sided p-value	0.304	
Statistical Difference	No	

Annual Peak Delta Inflows - San Joaquin River		
Annual Peak Inflows - Statistical Parameters	**WY 1956 - 1978, pre-New Melones Dam**	**WY 1979 - 2005, ~Existing Conditions**
No. of Years	23	27
Mean	7,402	10,431
Standard Deviation	8,674	9,587
Minimum	960	1,280
Median	4,690	5,700
Maximum	41,700	41,800
Distribution	Lognormal	
Statistical Test	t-Test (lognormal, equal variances)	
2-sided p-value	0.227	
Statistical Difference	No	

Table 7-4 Annual Peak Delta Inflows (cfs), 1956-2005

Water Year	Water Year Oct. 1 to Sept. 30	High Runoff Season Dec 16 to Apr 15	Low Runoff Season Oct 1 to Dec 15, Apr 16 to Sep 30
1956	383,322	383,322	80,086
1957	127,125	127,125	77,800
1958	278,826	278,826	127,867
1959	122,938	122,938	18,357
1960	142,860	142,860	21,479
1961	52,585	52,585	35,461
1962	157,492	157,492	35,160
1963	350,859	350,859	232,438
1964	62,010	62,010	42,188
1965	470,122	470,122	90,923
1966	64,384	64,384	38,415
1967	237,831	237,831	115,781
1968	92,407	92,407	25,433
1969	283,710	283,710	86,471
1970	383,921	383,921	26,488
1971	118,608	110,400	118,608
1972	36,664	36,664	22,654
1973	222,801	222,801	43,742
1974	276,092	276,092	123,106
1975	127,364	127,364	44,033
1976	34,593	30,651	34,593
1977	14,908	14,908	12,438
1978	174,450	174,450	70,752
1979	101,046	101,046	27,774
1980	339,008	339,008	33,394
1981	64,268	64,268	33,434
1982	238,395	238,395	197,768
1983	422,213	422,213	127,334
1984	351,622	351,622	169,189
1985	49,820	44,937	49,820
1986	661,272	661,272	48,018

Table 7-4 Annual Peak Delta Inflows (cfs), 1956-2005

Water Year	Water Year Oct. 1 to Sept. 30	High Runoff Season Dec 16 to Apr 15	Low Runoff Season Oct 1 to Dec 15, Apr 16 to Sep 30
1987	44,060	44,060	26,604
1988	42,023	42,023	28,941
1989	77,384	77,384	30,508
1990	38,654	38,654	23,052
1991	56,926	56,926	13,399
1992	57,349	57,349	13,870
1993	143,649	143,649	54,362
1994	34,770	34,770	29,893
1995	387,177	387,177	176,174
1996	207,020	207,020	98,021
1997	561,989	561,989	130,890
1998	323,012	323,012	112,420
1999	141,418	141,418	69,997
2000	168,766	168,766	43,293
2001	57,684	57,684	18,567
2002	108,335	108,335	39,772
2003	93,766	93,766	71,627
2004	186,184	186,184	34,270
2005	96,699	73,956	96,699

Table 7-5 Results of Log Pearson Type III Frequency Analyses

Probability	Inflows For Various Percent Confidence That The Inflow Will Not Be Exceeded												
	CL = 99%	CL = 97.5%	CL = 95%	CL = 90%	CL = 80%	CL = 60%	CL = 50%	CL = 40%	CL = 20%	CL = 10%	CL = 5%	CL = 2.5%	CL = 1%
All Seasons Inflow													
0.5000	183,628	174,123	167,003	159,301	150,600	139,862	135,551	131,292	121,982	115,391	110,149	105,728	100,438
0.2000	417,743	384,177	362,404	340,001	316,076	288,481	280,047	267,913	246,965	232,973	222,322	213,661	205,125
0.1000	646,984	583,006	543,290	503,306	461,634	414,947	402,011	381,158	347,674	325,861	309,564	296,514	284,711
0.0500	925,781	819,574	755,468	691,963	626,943	555,619	536,997	505,080	455,965	424,523	401,337	382,966	367,245
0.0400	1,026,698	904,163	830,738	758,322	684,543	604,074	583,366	547,383	492,578	457,658	431,996	411,722	394,606
0.0250	1,257,855	1,096,264	1,000,731	907,312	813,021	711,305	685,788	640,424	572,582	529,736	498,454	473,871	453,614
0.0200	1,376,716	1,194,262	1,087,010	982,520	877,483	764,716	736,715	686,503	611,966	565,071	530,929	504,158	482,312
0.0100	1,784,960	1,527,536	1,378,571	1,234,957	1,092,240	941,059	904,505	837,586	740,151	679,497	635,677	601,532	574,362
0.0050	2,255,260	1,906,317	1,707,080	1,516,767	1,329,544	1,133,535	1,087,120	1,000,928	877,353	801,129	746,428	704,032	670,944
0.0020	2,978,735	2,480,798	2,200,802	1,936,227	1,679,002	1,413,366	1,351,820	1,236,059	1,072,812	973,177	902,221	847,564	805,745
0.0010	3,607,958	2,974,111	2,621,311	2,290,391	1,971,236	1,644,691	1,570,048	1,428,709	1,231,467	1,111,939	1,027,254	962,289	913,176
0.0005	4,312,097	3,520,576	3,084,102	2,677,476	2,288,198	1,893,304	1,804,086	1,634,300	1,399,532	1,258,192	1,158,523	1,082,350	1,025,346
0.0001	6,257,320	5,006,780	4,330,189	3,708,698	3,122,771	2,538,809	2,409,770	2,162,386	1,826,400	1,626,823	1,487,440	1,381,729	1,304,080
High Inflow Season													
0.5000	181,568	172,677	165,544	157,831	149,124	138,385	134,031	129,820	120,522	113,944	108,714	104,307	99,311
0.2000	413,058	384,136	362,145	339,533	315,401	287,591	276,906	266,882	245,805	231,739	221,037	212,338	202,824
0.1000	639,727	585,479	545,194	504,669	462,468	415,235	397,502	381,085	347,276	325,268	308,836	295,684	281,518
0.0500	915,397	825,972	760,721	696,137	630,079	557,696	530,974	506,465	456,730	424,919	401,476	382,913	363,125
0.0400	1,015,182	912,153	837,341	763,625	688,596	606,861	576,822	549,344	493,801	458,443	432,477	411,975	390,180
0.0250	1,243,746	1,108,170	1,010,641	915,363	819,299	715,802	678,096	643,769	574,902	531,453	499,753	474,855	448,526
0.0200	1,361,275	1,208,309	1,098,719	992,060	884,962	770,130	728,451	690,588	614,872	567,283	532,662	505,531	476,903
0.0100	1,764,939	1,549,465	1,396,870	1,249,918	1,104,061	949,770	894,360	844,316	745,139	683,467	638,948	604,280	567,919
0.0050	2,229,964	1,938,146	1,733,590	1,538,429	1,346,685	1,146,245	1,074,926	1,010,841	884,829	807,192	751,524	708,407	663,418
0.0020	2,945,324	2,529,142	2,240,895	1,968,875	1,704,783	1,432,499	1,336,657	1,251,046	1,084,220	982,528	910,174	854,479	796,708

Table 7-5 Results of Log Pearson Type III Frequency Analyses

Probability	Inflows For Various Percent Confidence That The Inflow Will Not Be Exceeded												
	CL = 99%	CL = 97.5%	CL = 95%	CL = 90%	CL = 80%	CL = 60%	CL = 50%	CL = 40%	CL = 20%	CL = 10%	CL = 5%	CL = 2.5%	CL = 1%
0.0010	3,567,490	3,037,795	2,673,925	2,333,085	2,004,848	1,669,586	1,552,438	1,448,212	1,246,349	1,124,182	1,037,709	971,422	902,933
0.0005	4,263,731	3,602,278	3,151,331	2,731,820	2,330,828	1,924,779	1,783,850	1,658,929	1,418,332	1,273,682	1,171,779	1,093,960	1,013,845
0.0001	6,187,136	5,141,778	4,440,231	3,796,821	3,191,257	2,588,905	2,382,741	2,201,376	1,856,069	1,651,259	1,508,377	1,400,104	1,289,453
Low Inflow Season													
0.5000	68,727	65,878	63,574	61,061	58,198	54,623	53,160	51,736	48,561	46,287	44,462	42,911	41,138
0.2000	139,955	131,575	125,144	118,473	111,284	102,898	99,645	96,576	90,066	85,675	82,306	79,549	76,513
0.1000	207,931	192,620	181,139	169,485	157,226	143,338	138,074	133,174	122,995	116,301	111,264	107,208	102,812
0.0500	290,229	265,260	246,858	228,475	209,477	188,403	180,547	173,303	158,476	148,897	141,785	136,120	130,045
0.0400	320,067	291,342	270,273	249,319	227,768	204,001	195,181	187,069	170,532	159,899	152,032	145,783	139,102
0.0250	388,659	350,886	323,437	296,368	268,789	238,708	227,642	217,513	197,019	183,960	174,362	166,780	158,715
0.0200	424,091	381,448	350,586	320,264	289,499	256,103	243,863	232,684	210,139	195,828	185,340	177,074	168,302
0.0100	546,819	486,453	443,268	401,289	359,189	314,108	297,761	282,918	253,258	234,632	221,091	210,485	199,300
0.0050	690,367	607,903	549,521	493,307	437,513	378,485	357,283	338,130	300,165	276,549	259,496	246,215	232,282
0.0020	916,000	796,528	712,991	633,460	555,491	474,173	445,288	419,355	368,429	337,098	314,656	297,288	279,181
0.0010	1,117,030	962,759	855,816	754,796	656,598	555,188	519,441	487,483	425,124	387,048	359,923	339,023	317,321
0.0005	1,347,193	1,151,399	1,016,766	890,518	768,770	644,191	600,590	561,764	486,453	440,790	408,423	383,584	357,892
0.0001	1,999,908	1,678,991	1,462,024	1,261,661	1,071,627	880,862	815,089	756,991	645,681	579,164	532,504	496,990	460,544

Table 7-6 Parameters Used in Log Pearson Type III Distribution

Season	Mean	Standard Deviation	Skew	Weighted Slew
All	5.12	0.383	-0.194	0.223
High	5.11	0.387	-0.184	-0.216
Low	4.72	0.325	0.0645	-0.0323

Weighted skew is a function of the generalized skew (-0.3000) and Mean Square Error of Generalized Skew (see p. 13, of Bulletin 17B)

Table 7-7 Inflow Ranges (Bins) and Confidence Limit Probabilities for the High Inflow Season - Year 2000

						50% Confidence Limit		80% Confidence Limit		20% Confidence Limit		95% Confidence Limit		5% Confidence Limit	
Bin #	LN (Lower Value)	LN (Upper Value)	Lower Value	Upper Value	Designated Bin Value[1]	Proabability of Exceedence	Probability of Being in Bin	Proabability of Exceedence	Probability of Being in Bin	Proabability of Exceedence	Probability of Being in Bin	Proabability of Exceedence	Probability of Being in Bin	Proabability of Exceedence	Probability of Being in Bin
			0	30,045		1.000		1.000		1.000		1.000		1.000	
1	10.310438	10.581243	30,045	39,389	34,717	0.940	0.060	1.000	0.000	1.000	0.000	1.000	0.000	1.000	0.000
2	10.581243	10.852048	39,389	51,640	45,514	0.865	0.072	0.970	0.030	1.000	0.010	1.000	0.000	0.970	0.030
3	10.852048	11.122853	51,640	67,701	59,670	0.780	0.084	0.911	0.059	1.000	0.025	1.000	0.000	0.920	0.050
4	11.122853	11.393658	67,701	88,757	78,229	0.685	0.095	0.817	0.094	0.900	0.060	0.830	0.100	0.840	0.080
5	11.393658	11.664463	88,757	116,362	102,560	0.565	0.105	0.673	0.144	0.800	0.100	0.680	0.150	0.735	0.105
6	11.664463	11.935268	116,362	152,553	134,458	0.445	0.113	0.498	0.175	0.650	0.154	0.530	0.220	0.617	0.118
7	11.935268	12.206073	152,553	200000	176,277	0.353	0.121	0.299	0.190	0.402	0.174	0.248	0.220	0.490	0.127
8	12.206073	12.476878	200,000	262,204	231,102	0.225	0.120	0.174	0.125	0.284	0.180	0.138	0.150	0.360	0.130
9	12.476878	12.747683	262,204	343,754	302,979	0.130	0.095	0.103	0.080	0.168	0.116	0.078	0.082	0.235	0.125
10	12.747683	13.018488	343,754	450,669	397,212	0.076	0.060	0.053	0.051	0.106	0.075	0.036	0.042	0.145	0.090
11	13.018488	13.289293	450,669	590,835	520,752	0.038	0.038	0.023	0.030	0.060	0.046	0.014	0.022	0.085	0.060
12	13.289293	13.560098	590,835	774,597	682,716	0.017	0.021	0.009	0.014	0.030	0.030	0.004	0.010	0.047	0.038
13	13.560098	13.830903	774,597	1,015,511	895,054	0.006	0.011	0.003	0.006	0.014	0.016	0.001	0.003	0.025	0.023
14	13.830903	14.101708	1,015,511	1,331,355	1,173,433	0.002	0.004	0.001	0.002	0.005	0.008	0.0002460	0.001	0.012	0.013
15	14.101708	14.372513	1,331,355	1,745,432	1,538,394	0.001	0.002	0.000	0.001	0.002	0.003	0.0000415	0.000	0.005	0.007
16	14.372513	14.643318	1,745,432	2,288,296	2,016,864	0.000	0.000	0.000	0.000	0.001	0.001	0.0000044	0.000	0.002	0.003
17	14.643318	14.914123	2,288,296	3,000,000	2,644,148	0.000	0.000	0.000	0.000	0.000	0.000	0.0000005	0.000	0.001	0.001
						Totals =	**1.000**		**1.000**		**0.9994**		**0.9998**		**0.9994**

[1] Designated Bin Value is average of Lower & Upper Value.

Table 7-8 Results of Logistic Regressions

River	a (Slope)	b (Intercept)	r^2	Standard Error of Regression
Sacramento + Yolo Bypass	.563	-5.21	0.054	0.530
San Joaquin River	0.430	-4.173	0.075	0.709
Miscellaneous Flows	0.379	-4.453	0.071	0.665
Cosumnes River	1.116	-9.670	0.358	0.714

Table 7-9a Islands/Tracts Flooded Since 1900				
	Location		Years	No. Of Failures
1	Bacon	Island	1938	1
2	Big Break	Island	1927	1
3	Bishop	Tract	1904	1
4	Brack	Tract	1904	1
5	Byron	Tract	1907	1
6	Coney	Island	1907	1
7	Donlon	Island	1937	1
8	Edgerly	Island	1983	1
9	Grand	Island	1955	1
10	Holland	Tract	1980	1
11	Little Holland	Tract	1963	1
12	Lower Roberts	Island	1906	1
13	Mandeville	Island	1938	1
14	Mc Donald	Island	1982	1
15	Medford	Island	1936	1
16	Palm	Tract	1907	1
17	Rd 1007	Tract	1925	1
18	Shima	Tract	1983	1
19	Union	Island	1906	1
20	Upper Jones	Tract	2004	1
21	Upper Roberts	Tract	1950	1
22	Walthall	Tract	1997	1
23	Wetherbee	Lake	1997	1
24	Bradford	Island	1950-1983	2
25	Cliftoncourt	Tract	1901-1907	2
26	Empire	Tract	1950-1955	2
27	Fabian	Tract	1901-1906	2
28	Fay	Island	1983-2006	2
29	Glanville	Island	1986-1997	2
30	Ida	Island	1950-1955	2
31	McMullin Ranch	Tract	1997-1950	2
32	Middle Roberts	Island	1920-1938	2
33	Rhode	Island	1938-1971	2
34	Sargent Barnhart	Tract	1904-1907	2
35	Staten	Island	1904-1907	2
36	Terminous	Tract	1907-1958	2
37	Victoria	Island	1901-1907	2
38	Webb	Tract	1950-1980	2
39	Little Mandeville	Island	1980-1986-1994	3
40	Ryer	Island	1904-1907-1986	3
41	Franks	Tract	1907-1936-1938	3

Table 7-9a Islands/Tracts Flooded Since 1900				
	Location		**Years**	**No. Of Failures**
42	Little Franks	Tract	1981-1982-1983	3
43	Lower Jones	Tract	1906-1907-1980-2004	3
44	Mildred	Island	1965-1969-1983	3
45	Mossdale Rd17	Tract	1901-1911-1950	3
46	Paradise	Junction	1920-1950-1997	3
47	Pescadero	Tract	1938-1950-1997	3
48	River Junction	Junction	1958-1983-1997	3
49	Stewart	Tract	1938-1950-1997	3
50	Twitchell	Island	1906-1907-1908	3
51	Tyler	Island	1904-1907-1986	3
52	Bethel	Island	1907-1908-1909-1911	4
53	Bouldin	Island	1904-1907-1908-1909	4
54	Jersey	Island	1900-1904-1907-1909	4
55	Quimby	Island	1936-1938-1950-1955	4
56	Shin Kee	Tract	1938-1958-1965-1986	4
57	Brannan-Andrus	Island	1902-1904-1907-1909-1972	5
58	Sherman	Island	1904-1906-1909-1937-1969	5
59	Dead Horse	Island	1950-1955-1958-1980-1986-1997	6
60	McCormack-Williamson	Tract	1938-1950-1955-1958-1964-1986-1997	7
61	New Hope	Tract	1900-1904-1907-1928-1950-1955-1986	7
62	Prospect	Island	1963-1980-1981-1982-1983-1986-1995-1997	8
63	Venice	Island	1904-1906-1907-1909-1932-1938-1950-1982	8
	Number of Delta Flooded Islands/Tracts			**158**
	Honker Bay Club	Island	2006	1
	Grizzly	Island	1983-1998	2
	Simmons Wheeler	Island	2005-2006	2
	Van Sickle	Island	1983-1998-2006	3
	Suisun Marsh		Incomplete record only few recent data points available	**NA**

Table 7-9b Chronologic List of Flooded Islands Since 1900

Island Flooded	Year	Island Flooded	Year
TERMINOUS	1907	HOLLAND	1980
CLIFTONCOURT	1907	LITTLE MANDEVILLE	1980
SARGENT BARNHART	1907	LOWER JONES	1980
STATEN	1907	WEBB	1980
VICTORIA	1907	DEAD HORSE	1980
FRANKS	1907	PROSPECT	1980
RYER	1907	LITTLE FRANKS	1981
TWITCHELL	1907	PROSPECT	1981
TYLER	1907	LITTLE FRANKS	1982
BETHEL	1907	MC DONALD	1982
BRANNAN-ANDRUS	1907	VENICE	1982
BOULDIN	1907	EDGERLY	1983
JERSEY	1907	SHIMA (2)	1983
NEW HOPE	1907	FAY	1983
VENICE	1907	GRIZZLY WEST	1983
BETHEL	1908	BRADFORD	1983
BOULDIN	1908	VAN SICKLE (2)	1983
BRANNAN-ANDRUS	1909	LITTLE FRANKS (U)	1983
BETHEL	1909	MILDRED (U)	1983
BOULDIN	1909	VAN SICKLE	1983
SHERMAN	1909	PROSPECT (2)	1983
VENICE	1909	RIVER JUNCTION	1983
MOSSDALE RD17	1911	GLANVILLE	1986
BETHEL	1911	RYER	1986
MIDDLE ROBERTS	1920	SHIN KEE	1986
PARADISE JUNCTION	1920	DEAD HORSE (2)	1986
RD 1007	1925	LITTLE MANDEVILLE	1986
BIG BREAK	1927	PROSPECT	1986
NEW HOPE	1928	MC CORMACK-WILLIA (2)	1986
VENICE	1932	NEW HOPE	1986
MEDFORD	1936	TYLER (2)	1986
FRANKS	1936	LITTLE MANDEVILLE (U)	1994

Table 7-9b Chronologic List of Flooded Islands Since 1900

Island Flooded	Year	Island Flooded	Year
QUIMBY	1936	PROSPECT	1995
DONLON	1937	DEAD HORSE	1997
SHERMAN	1937	MC CORMACK-WILLIA	1997
BACON	1938	PROSPECT	1997
MANDEVILLE	1938	MCMULLIN RANCH	1997
MIDDLE ROBERTS	1938	PARADISE JUNCTION	1997
RHODE	1938	RIVER JUNCTION	1997
PESCADERO	1938	WALTHALL (2)	1997
STEWART	1938	WETHERBEE	1997
FRANKS	1938	GLANVILLE	1997
SHIN KEE	1938	PESCADERO	1997
QUIMBY	1938	STEWART TRACT	1997
MC CORMACK-WILLIA	1938	GRIZZLY	1998
VENICE	1938	VAN SICKLE	1998
BRADFORD	1950	UPPER JONES	2004
EMPIRE	1950	SIMMONS WHEELER	2005
IDA	1950	HONKER BAY CLUB	2006
WEBB	1950	FAY ISLAND	2006
PESCADERO	1950	SIMMONS WHEELER	2006
STEWART	1950	VAN SICKLE	2006

Table 7-9c Annual Peak Day Delta Inflows of Record (WY 1956 Through 2005)

Water Year	Date, WY Peak Inflow Day	Peak Day Sacramento River, cfs	Peak Day Yolo Bypass, cfs	Peak Day Cosumnes River, cfs	Peak Day Mokelumne River, cfs	Peak Day Misc. Streams, cfs	Peak Day San Joaquin River, cfs	Peak Day Total Inflow, cfs	Average 5-day Peak Inflow, cfs	Ratio: Avg. 5-day Peak to Peak Day	5-Day Inflow Vol. Up Through Peak Day, ac-ft	5-Day Inflow Vol. Up Through Peak Day, ac-ft
1986	February 20, 1986	113,000	499,301	15,600	4,490	14,981	13,900	661,272	551,714	0.83	4,501,390.41	1,571,520
1997	January 3, 1997	113,000	395,140	19,200	4,250	5,699	24,700	561,989	493,338	0.88	3,641,896.86	959,768
1965	December 25, 1964	98,600	343,265	11,500	150	2,607	14,000	470,122	382,948	0.81	2,673,209.26	2,281,874
1983	March 4, 1983	83,100	274,300	6,490	3,350	13,173	41,800	422,213	381,167	0.90	3,127,846.61	797,068
1995	March 13, 1995	96,100	266,562	6,340	2,440	1,635	14,100	387,177	336,016	0.87	2,229,883.64	741,241
1970	January 25, 1970	93,000	255,600	5,970	4,330	3,821	21,200	383,921	362,105	0.94	3,304,076.03	455,516
1956	December 23, 1955	90,200	249,600	34,100	2,180	4,032	3,210	383,322	276,247	0.72	1,571,520.00	1,131,743
1984	December 28, 1983	92,700	221,988	7,010	3,840	7,484	18,600	351,622	305,986	0.87	2,345,680.66	1,190,319
1963	February 2, 1963	94,400	230,107	17,300	3,260	1,962	3,830	350,859	202,799	0.58	1,190,318.68	399,078
1980	February 22, 1980	94,100	202,145	9,190	1,730	11,543	20,300	339,008	303,426	0.90	2,285,049.92	2,673,209
1998	February 8, 1998	86,800	193,521	6,130	2,930	7,331	26,300	323,012	305,585	0.95	2,823,322.31	596,854
1969	January 27, 1969	87,000	134,770	10,600	4,160	5,480	41,700	283,710	259,060	0.91	2,608,720.66	1,807,500
1958	February 26, 1958	85,500	174,510	6,140	1,650	3,276	7,750	278,826	245,784	0.88	2,281,874.38	798,413
1974	January 20, 1974	94,200	165,350	4,360	2,250	1,642	8,290	276,092	251,157	0.91	1,960,831.74	2,608,721
1982	February 17, 1982	98,000	103,742	11,700	3,030	14,203	7,720	238,395	175,241	0.74	1,041,399.67	3,304,076
1967	February 1, 1967	90,100	132,590	6,060	93	918	8,070	237,831	211,254	0.89	1,807,499.50	923,631
1973	January 19, 1973	92,700	112,559	6,790	1,910	2,472	6,370	222,801	196,152	0.88	1,728,842.98	337,839
1996	February 23, 1996	86,800	93,818	2,900	2,840	5,262	15,400	207,020	193,127	0.93	1,647,205.29	1,728,843
2004	February 28, 2004	73,800	105,288	1,500	326	1,050	4,220	186,184	177,486	0.95	1,594,216.86	1,960,832
1978	January 18, 1978	75,000	85,024	5,100	114	5,062	4,150	174,450	158,930	0.91	1,310,340.50	1,126,078
2000	February 28, 2000	81,700	63,375	5,010	2,010	3,071	13,600	168,766	156,851	0.93	1,446,424.46	325,369
1962	February 16, 1962	70,100	68,679	7,520	547	2,826	7,820	157,492	137,722	0.87	1,131,742.81	122,450
1993	March 28, 1993	82,300	53,026	3,280	431	662	3,950	143,649	136,829	0.95	1,300,621.49	1,310,340
1960	February 10, 1960	69,100	67,482	3,280	156	712	2,130	142,860	108,434	0.76	741,240.99	838,080
1999	February 11, 1999	85,400	31,150	3,630	2,770	6,568	11,900	141,418	124,608	0.88	991,787.11	2,285,050
1975	March 26, 1975	73,800	36,228	6,340	895	3,171	6,930	127,364	118,869	0.93	1,126,078.02	525,396
1957	March 7, 1957	79,200	36,361	4,050	1,800	1,024	4,690	127,125	112,424	0.88	959,767.93	1,041,400
1959	February 20, 1959	67,300	46,902	1,830	662	1,404	4,840	122,938	105,502	0.86	797,067.77	3,127,847
1971	December 5, 1970	73,200	32,983	5,880	1,230	1,675	3,640	118,608	108,748	0.92	923,631.07	2,345,681
2002	January 6, 2002	65,567	34,528	725	194	3,097	4,224	108,335	91,437	0.84	802,131.57	461,516
1979	February 24, 1979	71,300	5,170	2,660	1,260	7,856	12,800	101,046	95,445	0.94	838,080.00	4,501,390
2005	May 22, 2005	74,100	6,668	1,590	2,090	151	12,100	96,699	90,974	0.94	769,348.76	331,279
2003	January 3, 2003	65,300	25,560	261	211	154	2,280	93,766	83,057	0.89	751,933.88	291,814
1968	February 25, 1968	66,200	18,648	1,350	838	1,251	4,120	92,407	88,976	0.96	798,412.56	578,604
1989	March 27, 1989	73,500	26	1,820	7	11	2,020	77,384	68,450	0.88	578,604.30	293,407
1966	January 10, 1966	53,600	4,085	377	436	536	5,350	64,384	61,741	0.96	596,854.21	398,339
1981	January 31, 1981	51,900	5,096	759	72	741	5,700	64,268	60,686	0.94	525,395.70	495,923
1964	January 23, 1964	52,200	2,841	2,780	624	455	3,110	62,010	54,099	0.87	399,078.35	1,300,621
2001	March 9, 2001	46,200	4,425	483	289	627	5,660	57,684	53,441	0.93	505,557.02	237,051
1992	February 17, 1992	46,800	2,456	1,290	177	1,516	5,110	57,349	53,943	0.94	495,923.31	2,229,884
1991	March 27, 1991	46,900	3,260	1,310	119	2,027	3,310	56,926	49,859	0.88	398,338.51	1,647,205
1961	February 14, 1961	49,500	1,750	228	111	36	960	52,585	51,222	0.97	455,516.03	3,641,897
1985	November 30, 1984	41,200	3,408	511	762	439	3,500	49,820	47,470	0.95	461,516.03	2,823,322
1987	March 16, 1987	38,000	1,686	840	91	443	3,000	44,060	40,764	0.93	331,279.34	991,787
1988	January 7, 1988	37,200	3,245	203	46	49	1,280	42,023	39,287	0.93	291,814.21	1,446,424
1990	January 16, 1990	36,900	25	284	45	30	1,370	38,654	33,325	0.86	293,406.94	505,557
1972	December 28, 1971	31,100	192	1,440	96	406	3,430	36,664	35,424	0.97	337,838.68	802,132
1994	February 10, 1994	29,900	1,686	190	150	64	2,780	34,770	29,317	0.84	237,050.58	751,934
1976	December 8, 1975	30,600	48	53	297	15	3,580	34,593	33,457	0.97	325,368.60	1,594,217
1977	January 5, 1977	13,700	3	76	37	12	1,080	14,908	13,128	0.88	122,449.59	769,349

Table 7-10 Vulnerability Classes for Under-Seepage Analyses

Geographic Region	Vulnerability Class Index	Peat Thickness (ft)	Slough Width	Random Input Variables
Delta	1	0	Narrow	Ditch, Sediment
	2	0	Not Narrow	Ditch, Sediment
	3	0.1-5	Narrow	Ditch, Sediment, Peat Thickness, Peat Permeability
	4	0.1-5	Not Narrow	Ditch, Sediment, Peat Thickness, Peat Permeability
	5	5.1-10	Narrow	Ditch, Sediment, Peat Thickness, Peat Permeability
	6	5.1-10	Not Narrow	Ditch, Sediment, Peat Thickness, Peat Permeability
	7	10.1-15	Narrow	Ditch, Sediment, Peat Thickness, Peat Permeability
	8	10.1-15	Not Narrow	Ditch, Sediment, Peat Thickness, Peat Permeability
	9	15.1-30	Narrow	Ditch, Sediment, Peat Thickness, Peat Permeability
	10	15.1-30	Not Narrow	Ditch, Sediment, Peat Thickness, Peat Permeability
	11	>30	Narrow	Ditch, Sediment, Peat Thickness, Peat Permeability
	12	>30	Not Narrow	Ditch, Sediment, Peat Thickness, Peat Permeability
Suisan Marsh	13	0	Narrow	Sediment
	14	0	Not Narrow	Sediment
	15	0.1-5	Narrow	Sediment, Peat Thickness, Peat Permeability
	16	0.1-5	Not Narrow	Sediment, Peat Thickness, Peat Permeability
	17	5.1-10	Narrow	Sediment, Peat Thickness, Peat Permeability
	18	5.1-10	Not Narrow	Sediment, Peat Thickness, Peat Permeability
	19	10.1-15	Narrow	Sediment, Peat Thickness, Peat Permeability
	20	10.1-15	Not Narrow	Sediment, Peat Thickness, Peat Permeability
	21	15.1-30	Narrow	Sediment, Peat Thickness, Peat Permeability
	22	15.1-30	Not Narrow	Sediment, Peat Thickness, Peat Permeability
	23	>30	Narrow	Sediment, Peat Thickness, Peat Permeability
	24	>30	Not Narrow	Sediment, Peat Thickness, Peat Permeability

Table 7-11 Reported Permeability Data for Organic Soils
(Source: HLA 1989, 1992)

Soil Type	k_h (cm/s)	k_v(cm/s)	Type of test	Location	Sampling detail
Black peat (PT) with fat clay	2.4×10^{-7}	-	Lab test	Levee, Bacon Island	1988, Sample depth = 22 ft
Black peat (PT) with fat clay	7.2×10^{-7}	-	Lab test	Levee, Web Tract	1988, Sample depth = 25 ft
Black Peat (PT)	4.7×10^{-6}	1.3×10^{-6}	Falling head lab test	Wilkerson Dam-Test fill, Bouldin Island	1989, Sample depth = 9 ft
Black Peat (PT)	5.5×10^{-6}	7.6×10^{-8}	Falling head lab test	Wilkerson Dam-Test fill, Bouldin Island	1989, Sample depth = 9 ft
Black Silty Peat (PT)	1.5×10^{-6}	2.1×10^{-6}	Falling head lab test	Wilkerson Dam-Bouldin Island	1989, Sample depth = 4 ft
Black Silty Peat (PT)	-	7.5×10^{-7}	Falling head lab test	Wilkerson Dam-Bouldin Island	1989, Sample depth = 5 ft
Black Silty Peat (PT)	1.9×10^{-6}	9.7×10^{-7}	Falling head lab test	Wilkerson Dam-Bouldin Island	1989, Sample depth = 11 ft
Black Silty Peat (PT)	2.6×10^{-6}	1.8×10^{-7}	Falling head lab test	Wilkerson Dam-Bouldin Island	1989, Sample depth = 10 ft
Black Silty Peat (PT)	8.8×10^{-7}	1.5×10^{-6}	Falling head lab test	Wilkerson Dam-Bouldin Island	1989, Sample depth = 5 ft
Brown elastic silt w/ peat (MH)	1.2×10^{-6}	3.2×10^{-7}	Falling head lab test	Wilkerson Dam-Bouldin Island	1989, Sample depth = 8 ft
Black organic silt (OH) contains peat		5.7×10^{-7}	Falling head lab test	Wilkerson Dam-Bouldin Island	1989, Sample depth = 15 ft

Table 7-12 Reported Permeability Data for Sandy Soils and Silt (Source: HLA 1989, 1991, 1992)

Soil Type	k_h (cm/s)	k_v(cm/s)	Type of test	Location	Sampling detail
Gray Silty sand (SM), fine to medium grained	2.2×10^{-5}	-	Lab test	Levee, Bacon Island	1988, Sample depth = 40 ft
Gray Silty sand (SM), fine to medium grained	3.3×10^{-4}	-	Lab test	Levee, Web Tract	1988, Sample depth = 45 ft
Brown silty sand (SM)	3.9×10^{-4}	-	Constant head lab test	Barrow pit, Bouldin Island	1991, Natural sample
Brown silty sand (SM)	1.2×10^{-4}	-	Constant head lab test	Barrow pit, Bouldin Island	1991, Natural sample
Brown poorly graded sand (SP)	6.9×10^{-4}	-	Constant head lab test	Barrow pit, Bouldin Island	1991, Washed sample
Brown poorly graded sand (SP)	8.6×10^{-4}	-	Constant head lab test	Barrow pit, Bouldin Island	1991, Washed sample
Brown silty graded sand (SP)	3.9×10^{-3}	-	Falling head lab test	Barrow pit, Bouldin Island	1991, Natural sample
Brown sand (SP)	6.4×10^{-3}	-	Falling head lab test	Barrow pit, Bouldin Island	1991, Washed sample
Brown silty sand (SM)	6.8×10^{-5}	-	Falling head lab test	Barrow pit, Bouldin Island	1991, Natural sample
Brown silty sand (SM)	1.1×10^{-5}	-	Falling head lab test	Barrow pit, Bouldin Island	1991, Natural sample
Brown poorly graded sand (SP)	5.6×10^{-4}	-	Constant head lab test	Barrow pit, Bouldin Island	1991, washed sample
Brown poorly graded sand (SP)	4.6×10^{-4}	-	Constant head lab test	Barrow pit, Bouldin Island	1991, Washed sample
Brown sand w/ silt (SP-SM)	1.1×10^{-3}	-	Constant head lab test	Barrow pit, Bouldin Island	1991, Natural sample
Brown sand w/ silt (SP-SM)	1.2×10^{-4}	-	Constant head lab test	Barrow pit, Bouldin Island	1991, Natural sample
Brown poorly graded sand (SP)	1.0×10^{-3}	-	Constant head lab test	Barrow pit, Bouldin Island	1991, washed sample
Brown poorly graded sand (SP)	1.9×10^{-3}	-	Constant head lab test	Barrow pit, Bouldin Island	1991, washed sample
Brown silty sand (SM)	2.4×10^{-5}	-	Constant head lab test	Test Fill, Bouldin Island	1991, natural sample
Brown silty sand (SM)	1.1×10^{-6}	-	Falling head lab test	Test Fill, Bouldin Island	1991, natural sample
Brown poorly graded sand (SP)	7.5×10^{-4}	-	Constant head lab test	Test Fill, Bouldin Island	1991, washed sample
Brown poorly graded sand (SP)	1.1×10^{-3}	-	Constant head lab test	Test Fill, Bouldin Island	1991, washed sample
Poorly graded sand (SP), very fine to fine grained, contains some silt	5.4×10^{-3}	-	Field pump test	Holland Tract	1989, Pumping rate = 30 GPM, Depth = 20 ft
Poorly graded sand (SP), very fine to fine grained, contains some silt	6.4×10^{-3}	-	Field pump test	Holland Tract	1989, Pumping rate = 30 GPM, Depth = 30 ft
Blue gray silty sand (SM, fine grained)	1.4×10^{-1}	-	Field pump test	McDonald Island	1989, Pumping rate = 215 GPM
Blue-gray elastic silt (MH)	3.1×10^{-6}	3.8×10^{-6}	Falling head lab test	Wilkerson Dam-Bouldin Island	1989, Sample depth = 20 ft
Blue-gray sandy silt (ML)	-	3.9×10^{-7}	Falling head lab test	Wilkerson Dam-Bouldin Island	1989, Sample depth = 25 ft
Blue-gray silt (ML)	-	1.1×10^{-5}	Falling head lab test	Wilkerson Dam-Bouldin Island	1989, Sample depth = 20 ft

Table 7-13 Permeability Coefficients Used for Initial Seepage Analysis

Material	k_h (cm/s)			k_h/k_v
	Mean - σ	Mean	Mean + σ	
Fill				
CL-ML (fill)	-	1×10^{-5}	-	4
SM (fill)	-	1×10^{-3}	-	4
Peat & Organics				
Free Field	1×10^{-5}	1×10^{-4}	1×10^{-3}	10
Under Levee	1×10^{-6}	1×10^{-5}	1×10^{-4}	10
Other Foundation Soils				
Sand (SM/SP)	5×10^{-4}	1×10^{-3}	5×10^{-3}	4
ML	-	1×10^{-4}	-	4
CL	-	1×10^{-6}	-	4
Sediment (at slough bottom)	-	1×10^{-5}	-	1

Table 7-14 Initial Analysis Results for Terminous Tract

Slough Water Elevation (ft) [NAVD88]	Analysis Case-Permeability	Ditch		No Ditch		Remarks
		i_y below ditch (Point A)	Ave. i_y at Point B	i_y (near toe)	Ave. i_y at Point B	
0	k_{mean}	0.46	0.17	0.22	0.178	model with sediment
4	k_{mean}	0.64	0.24	0.30	0.249	model with sediment
7	k_{mean}	0.75	0.29	0.36	0.301	model with sediment
0	$k_{(mean-\sigma)peat}$	0.57	0.25			model with sediment
4	$k_{(mean-\sigma)peat}$	0.82	0.38	-	-	model with sediment
7	$k_{(mean-\sigma)peat}$	1	0.47			model with sediment
0	$k_{(mean+\sigma)peat}$	0.26	0.05			model with sediment
4	$k_{(mean+\sigma)peat}$	0.36	0.07	-	-	model with sediment
7	$k_{(mean+\sigma)peat}$	0.42	0.08			model with sediment
0	$k_{(mean-\sigma)\ sand}$	0.44	0.14			model with sediment
4	$k_{(mean-\sigma)\ sand}$	0.6	0.20	-	-	model with sediment
7	$k_{(mean-\sigma)\ sand}$	0.7	0.24			model with sediment
0	$k_{(mean+\sigma)\ sand}$	0.25	0.07			model with sediment
4	$k_{(mean+\sigma)\ sand}$	0.41	0.15	-	-	model with sediment
7	$k_{(mean+\sigma)\ sand}$	0.52	0.21			model with sediment
0	k_{mean}	0.58	0.22			model without sediment
4	k_{mean}	0.79	0.31	-	-	model without sediment
7	k_{mean}	0.94	0.38			model without sediment

Table 7-15 Estimated Vertical Gradients for Grand Island Under-seepage Problem

(k_h/k_v)peat	Analysis Case: No Ditch & No Sediment	
	Ave. i_y near toe	Ave. i_y at Point B
10	0.42	0.26
100	0.59	0.50
1000	0.63	0.56

Table 7-16 Evaluated Permeability Coefficients Used for Model Analyses

Material	k_h (cm/s)			k_h/k_v
	Mean - σ	Mean	Mean + σ	
Fill				
SM (fill)	-	1×10^{-3}	-	4
Peat & Organics				
Free Field	1×10^{-5}	1×10^{-4}	1×10^{-3}	100
Under Levee	1×10^{-6}	1×10^{-5}	1×10^{-4}	100
Other Foundation Soils				
Sand (SM/SP)	-	1×10^{-3}	-	4
CL	-	1×10^{-6}	-	4
Sediment (at slough bottom)	-	1×10^{-5}	-	1

Figures

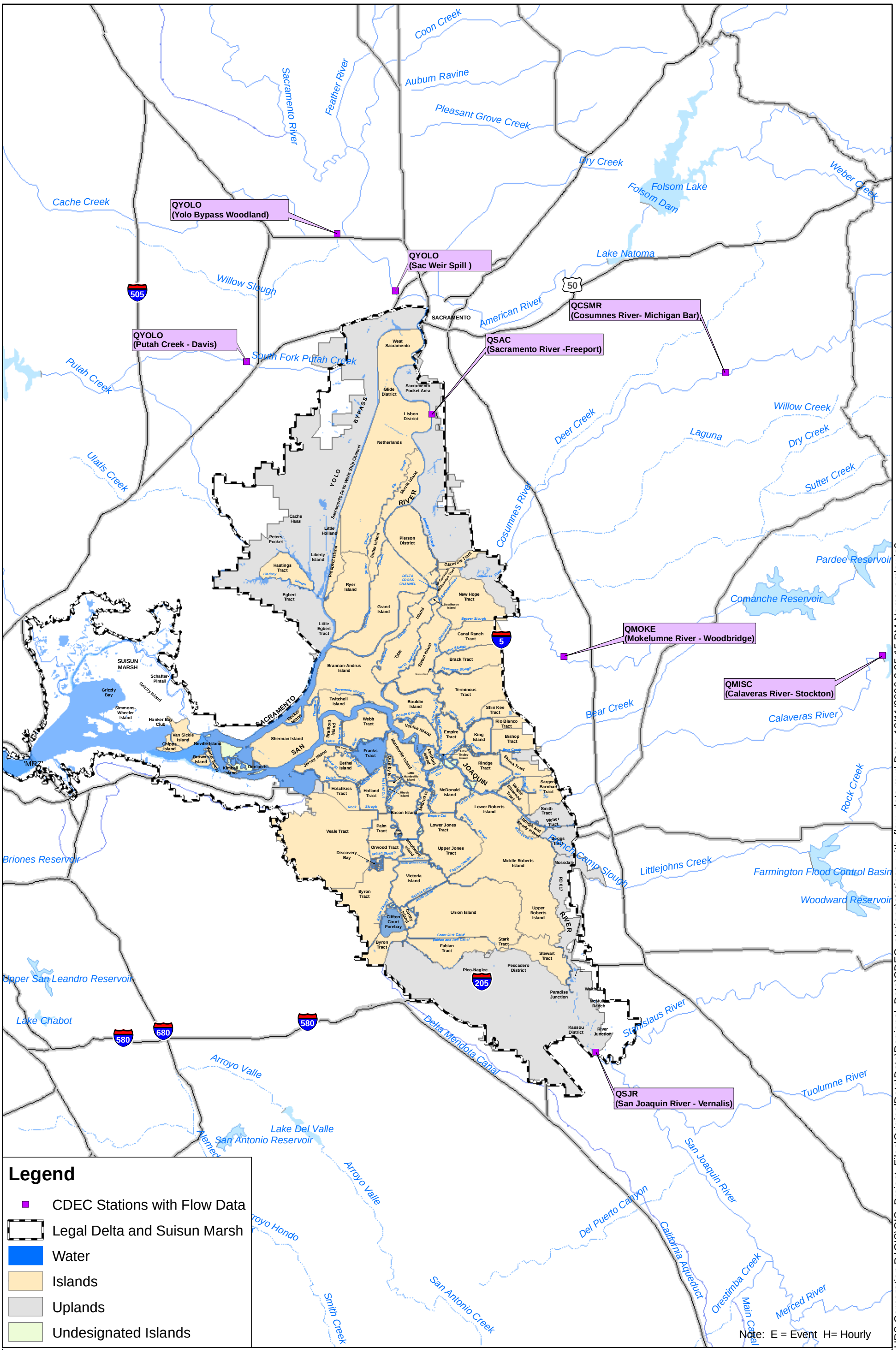

URS	DRMS	Flow Stations Used with Flood Hazard Analysis	Figure 7-1
	26815431		

URS Corporation P:\GIS\GIS_Project_Files\OriginalData\Data\Regional_Data\CDEC_stations\stations_with_flow_data.mxd Date: 12/11/2006 2:35:15 PM Name: smlewis0

Figure 7-2 Historical Delta Inflows

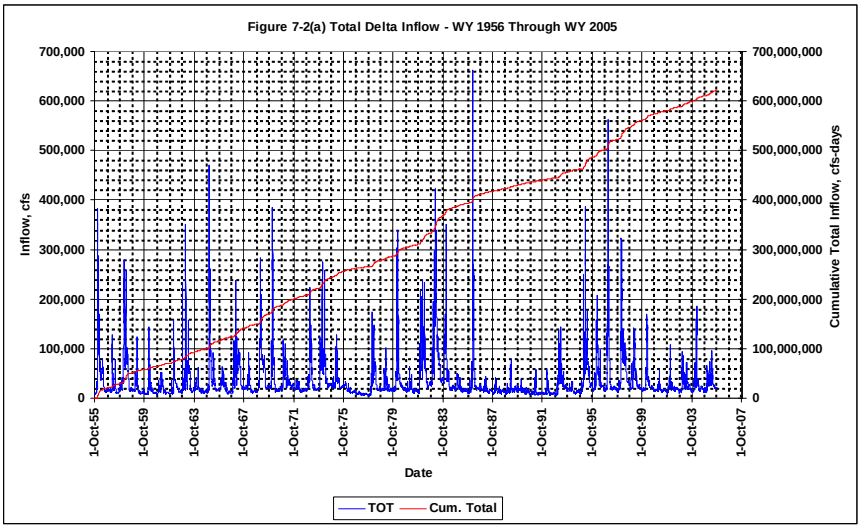

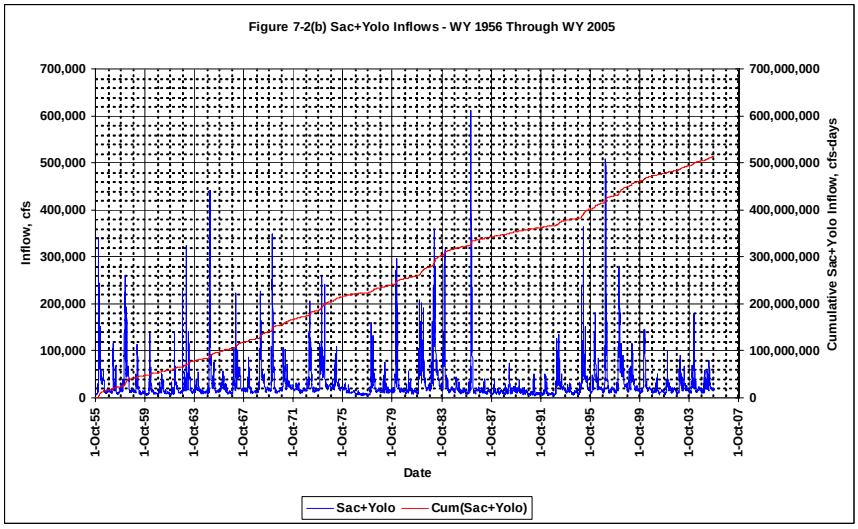

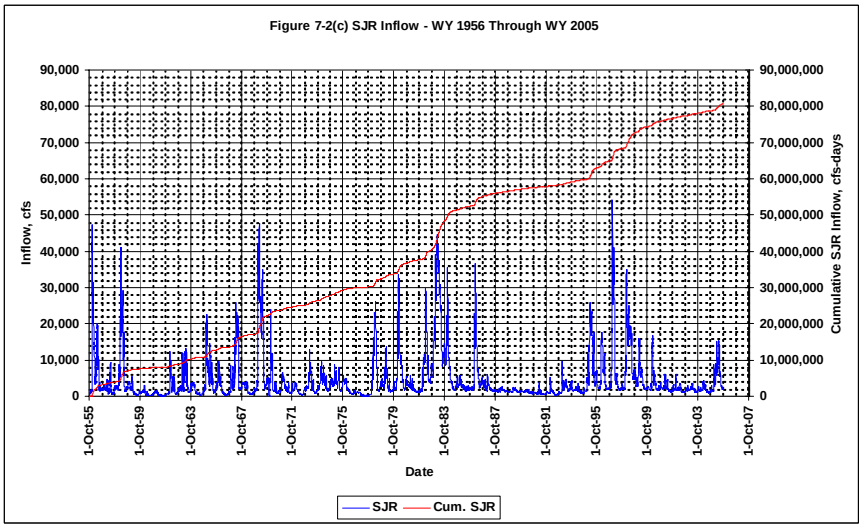

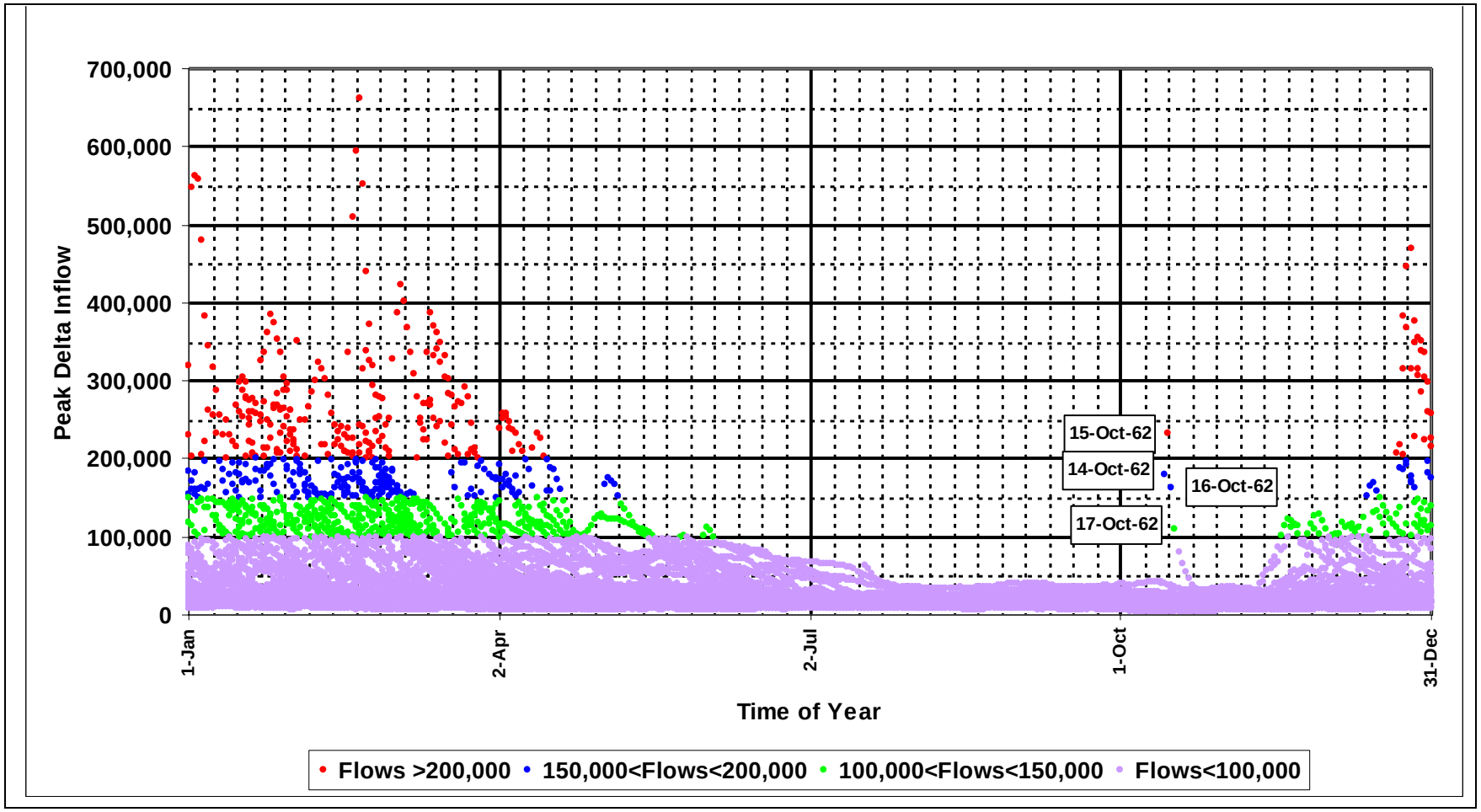

Figure 7-3 Temporal Distribution of Peak Delta Inflows

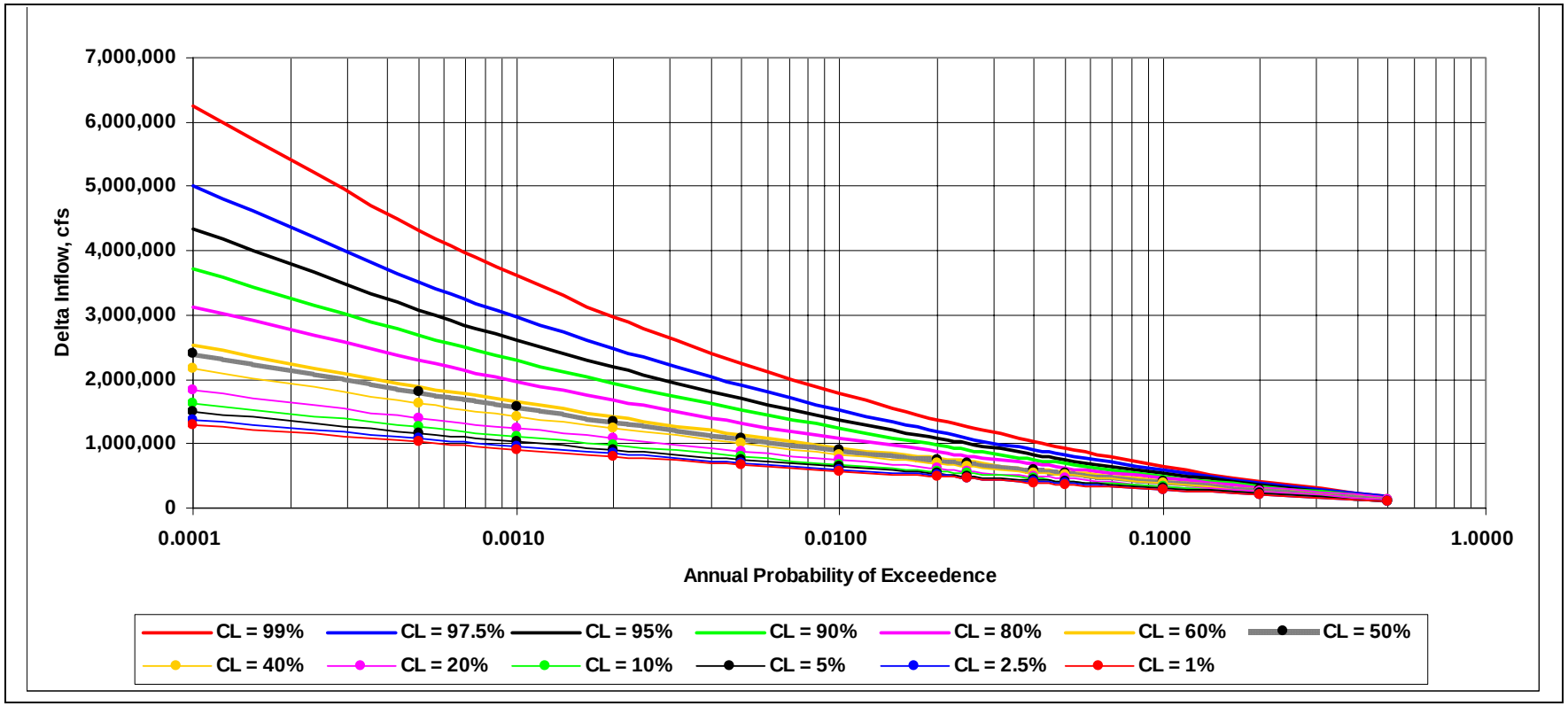

Figure 7-4 All Seasons Flow Frequency

(CL – Confidence Limit %)

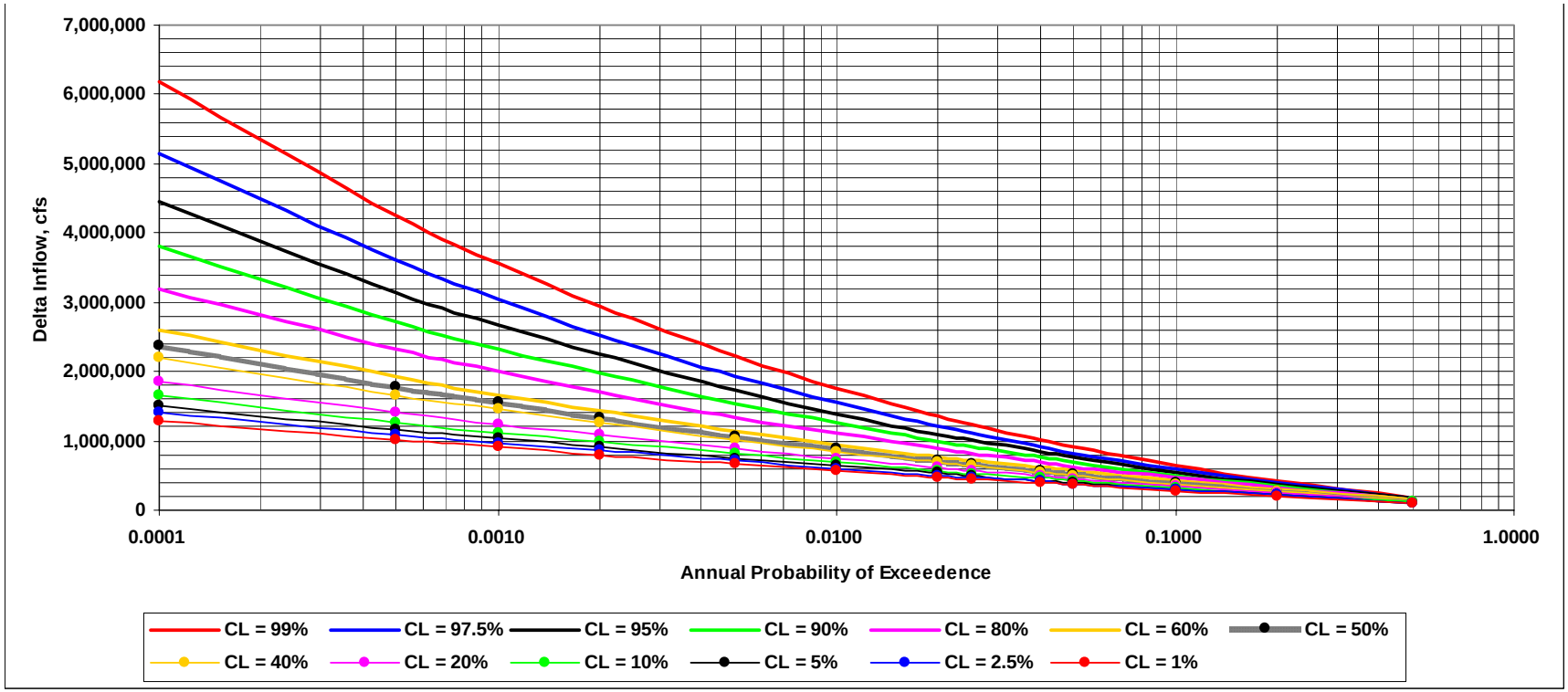

Figure 7-5 High Runoff Season – Inflow Frequency

(CL = Confidence Limit %)

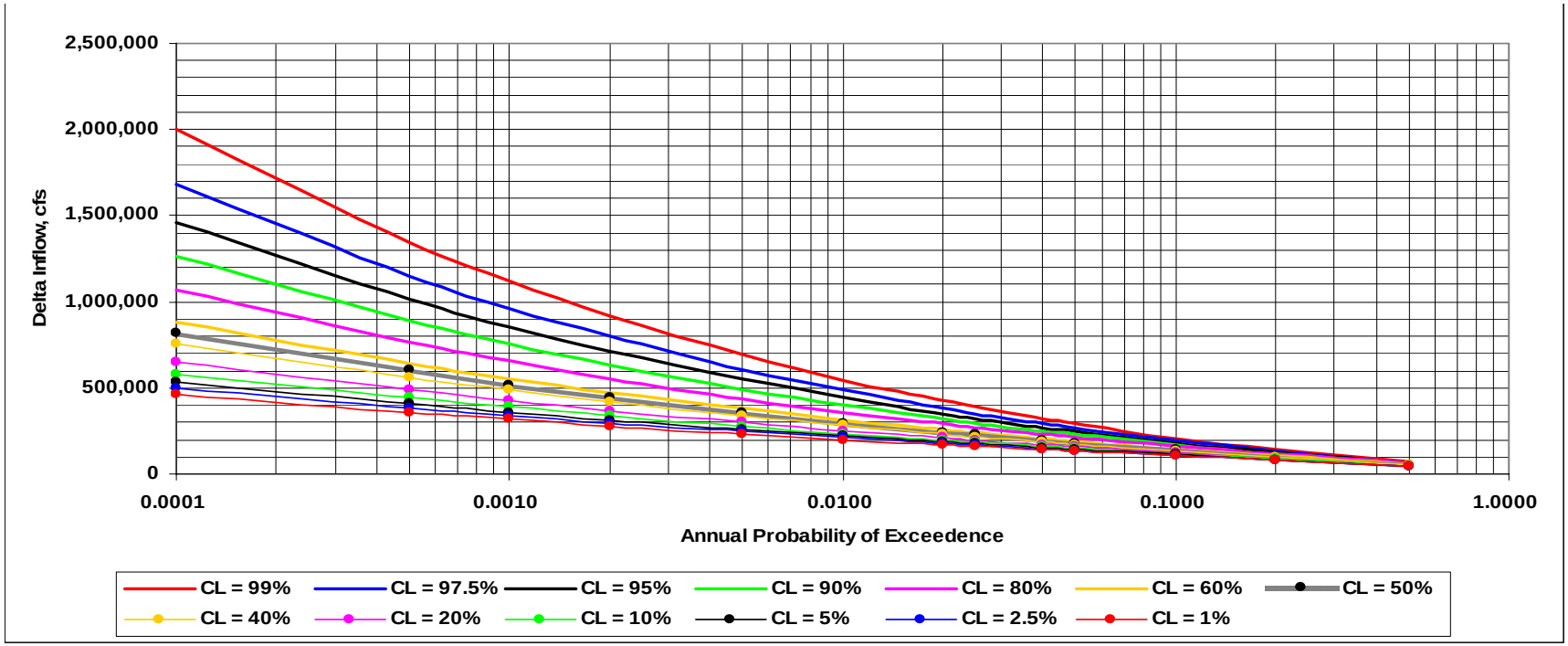

Figure 7-6 Low Runoff Season – Inflow Frequency

(CL = Confidence Limit %)

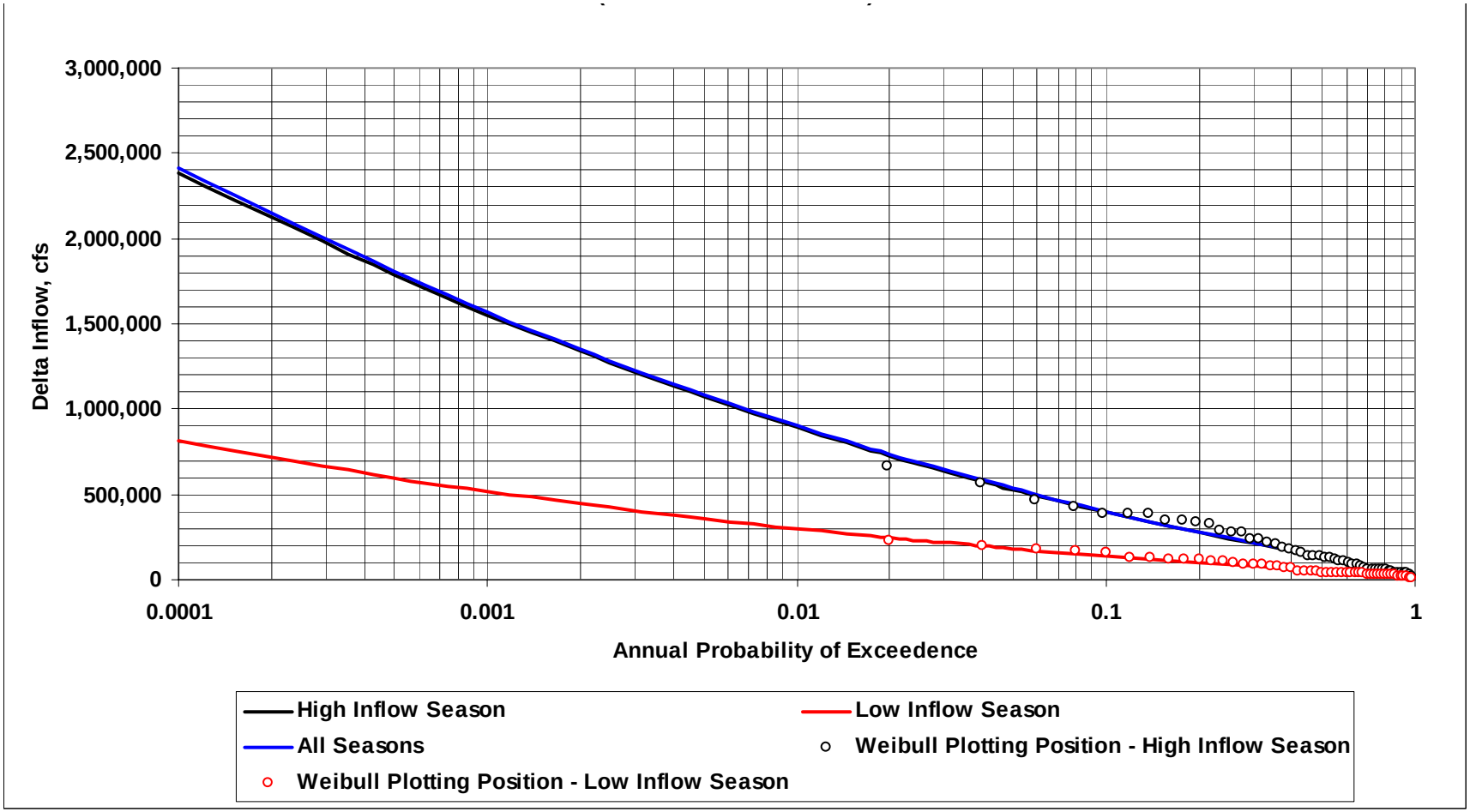

Figure 7-7 Comparison Between Inflow-Frequency Curves, CL = 50%

(CL = Confidence Limit %)

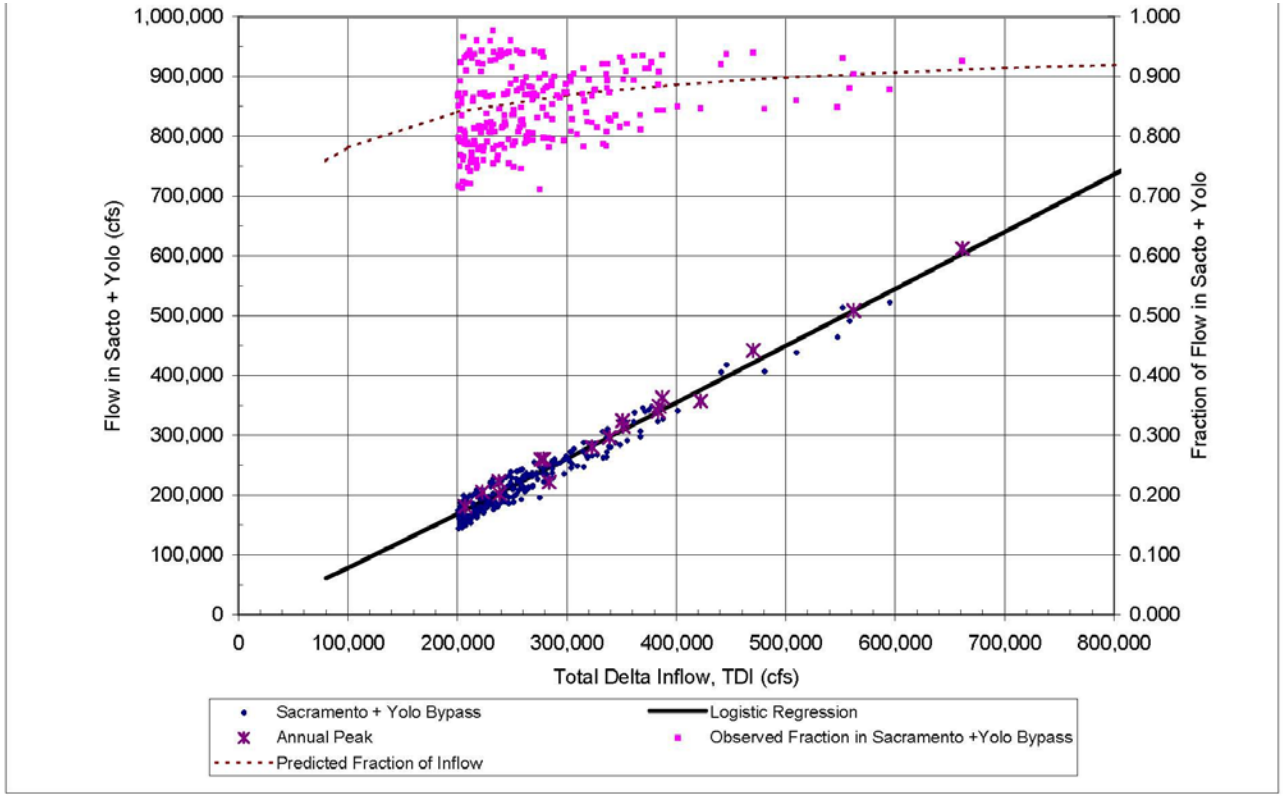

Figure 7-8 Flow in Sacramento River Plus Yolo Bypass Versus Total Delta Inflow

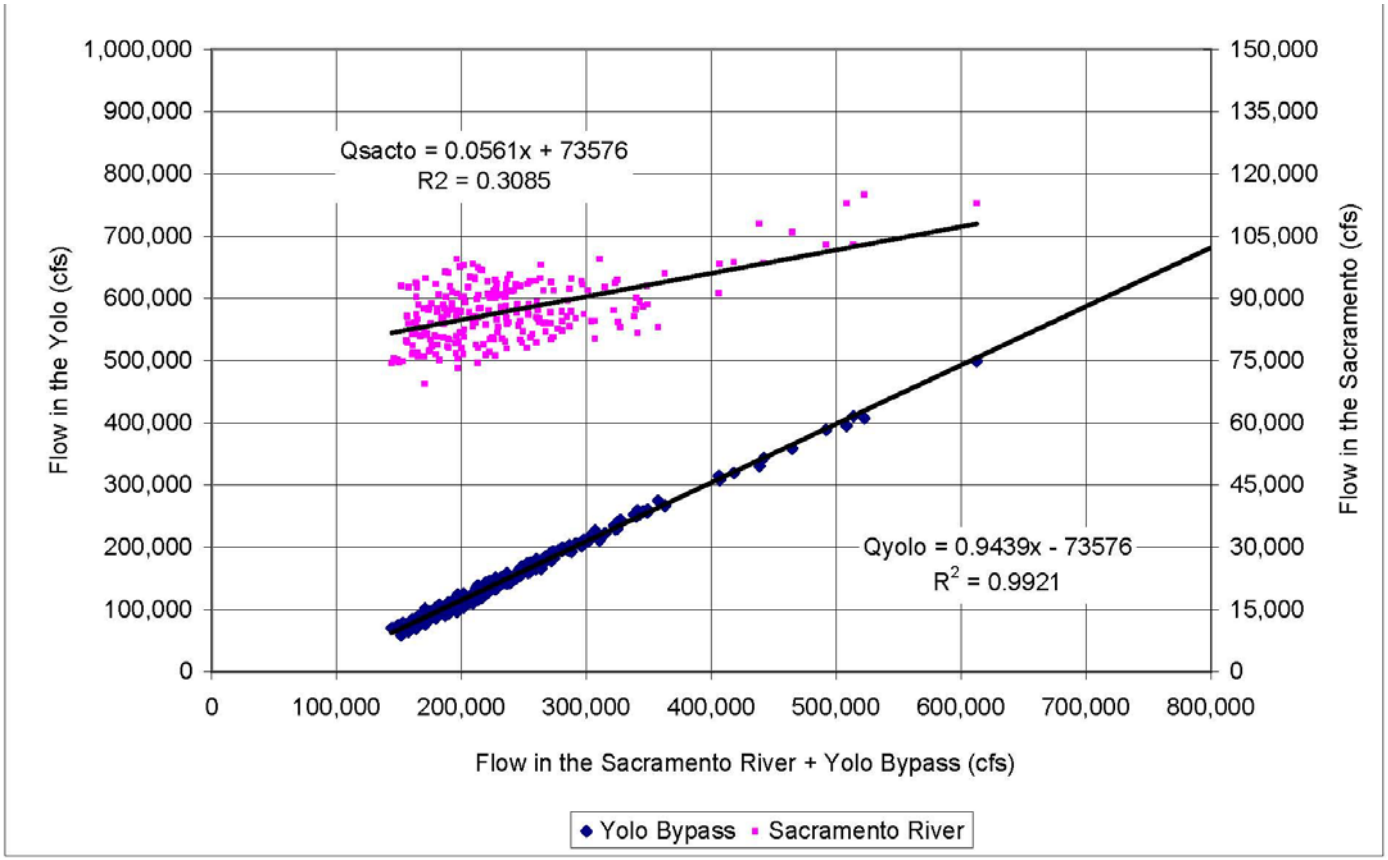

Figure 7-9 Relationship Between Flow in Yolo Bypass and Total Flow in the Sacramento River

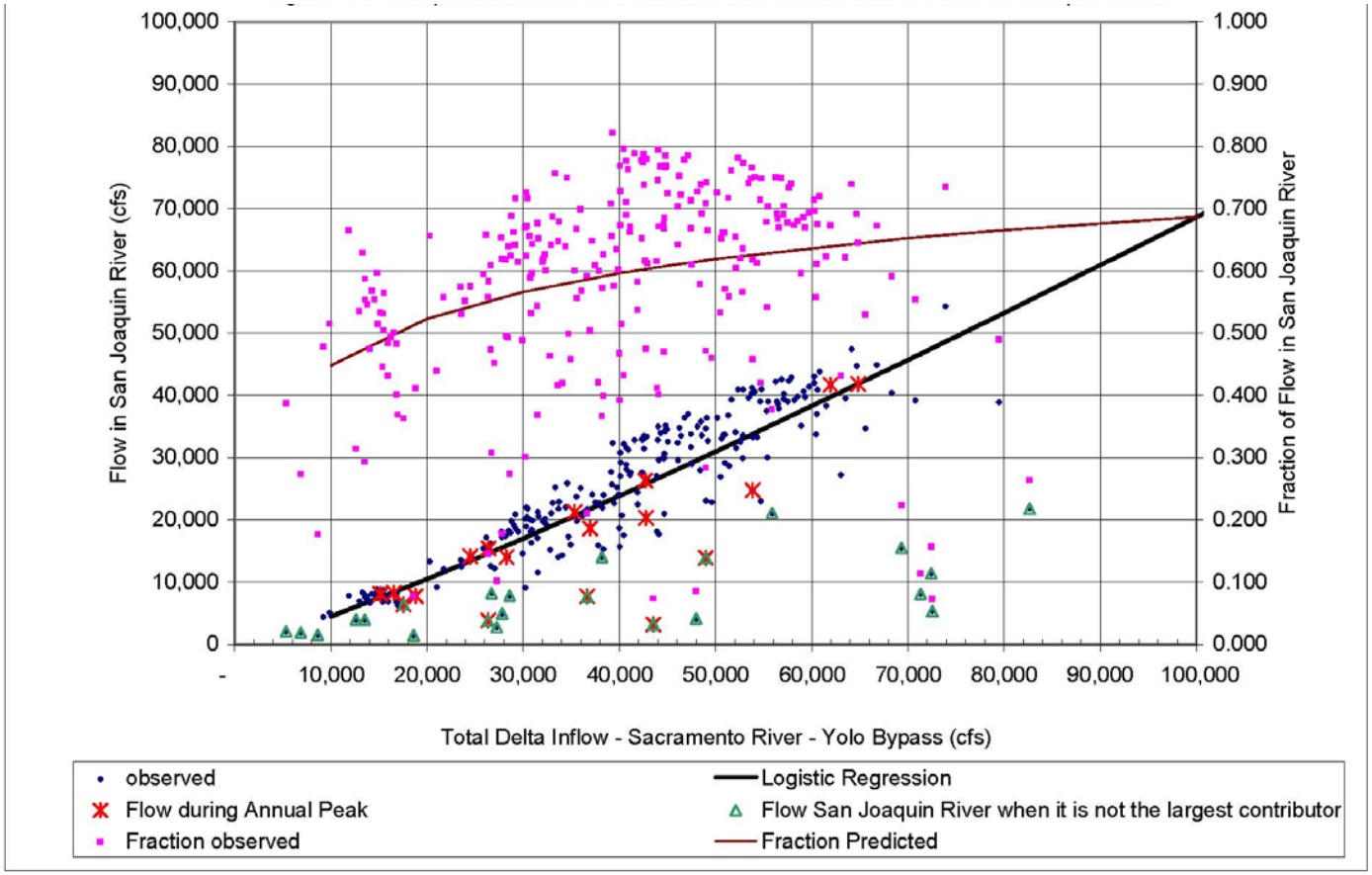

Figure 7-10 Comparison Between Predicted and Observed Flow in San Joaquin River

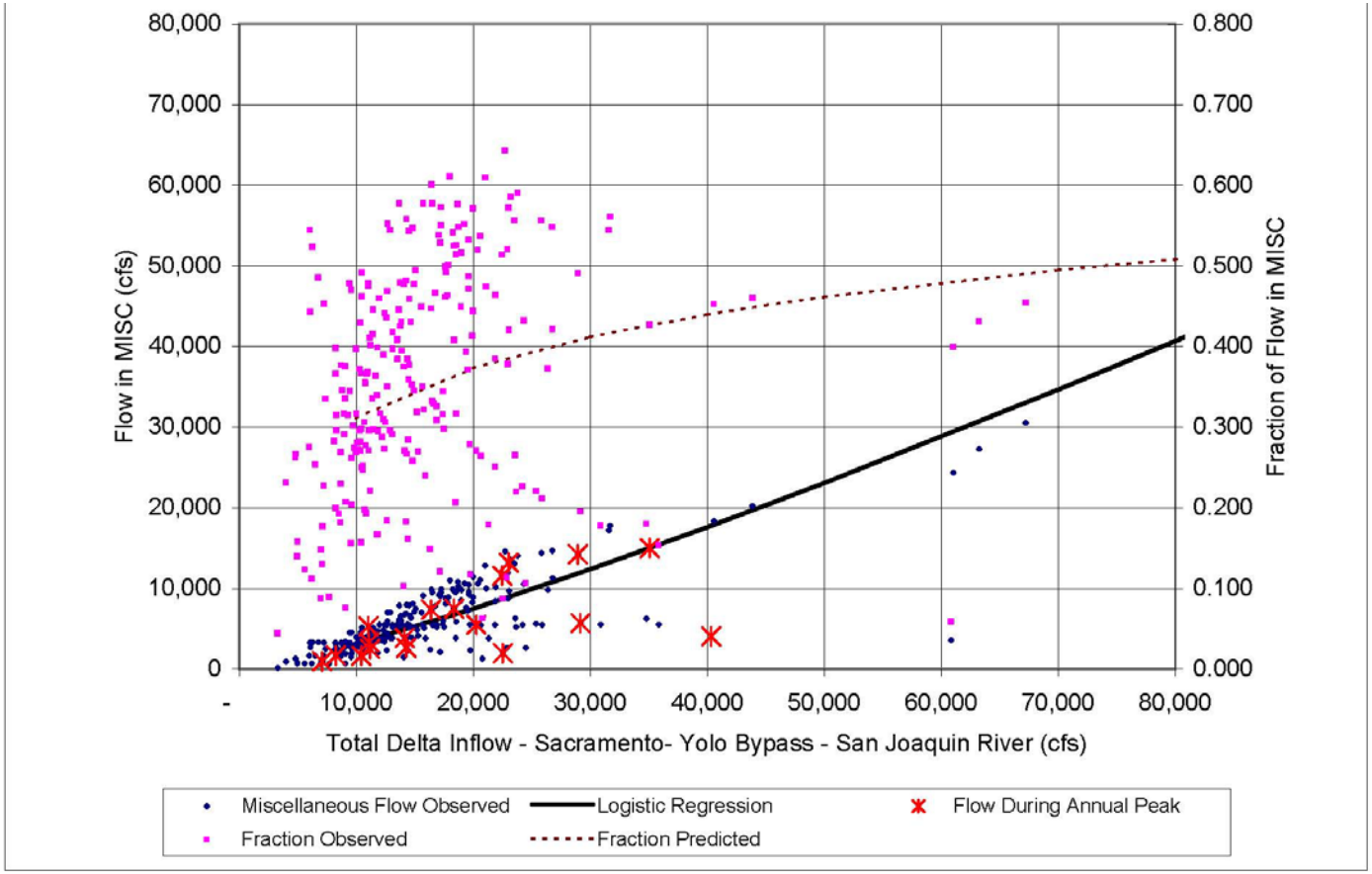

Figure 7-11 Comparison Between Predicted and Observed Flows in MISC Inflow

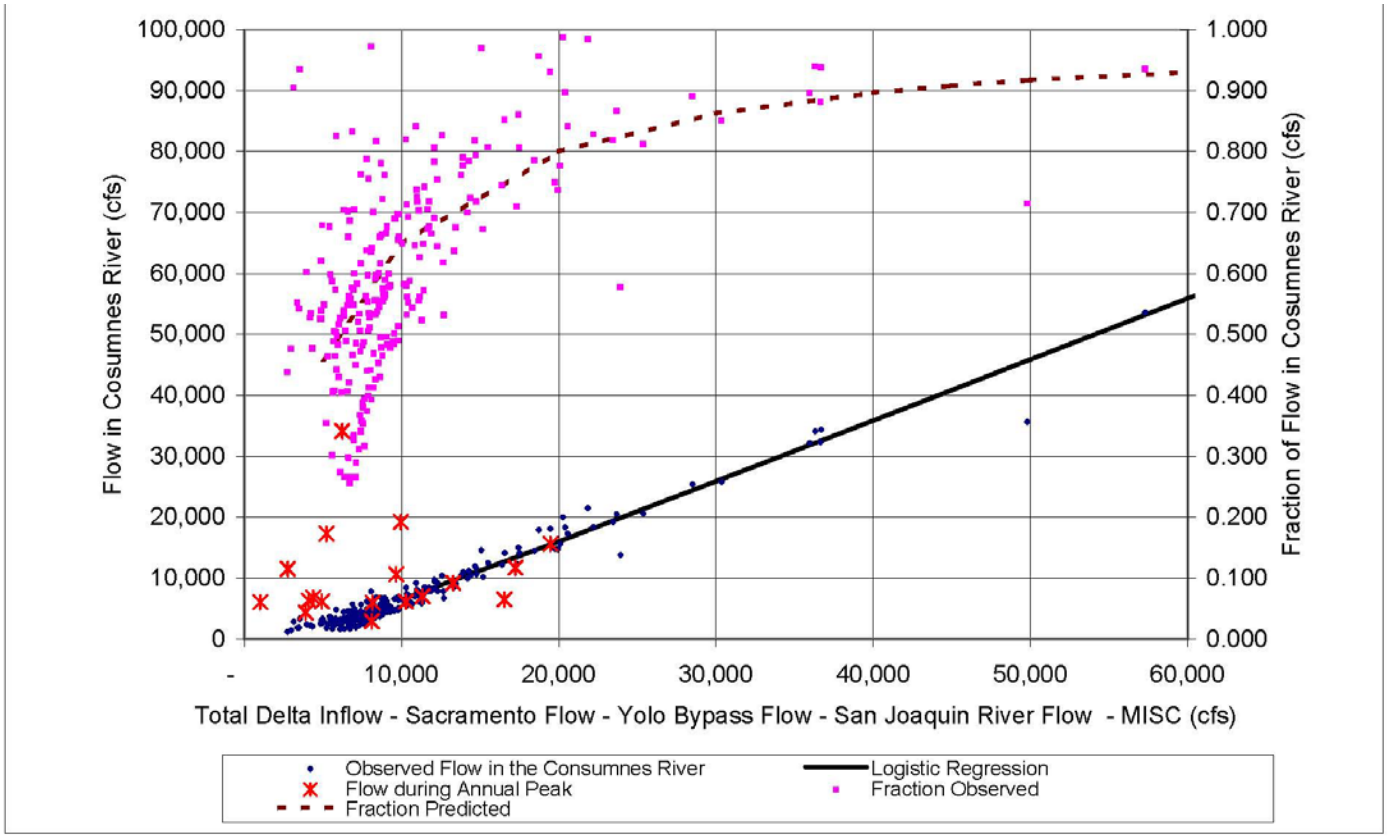

Figure 7-12 Comparison Between Predicted and Observed Flows in the Cosumnes River

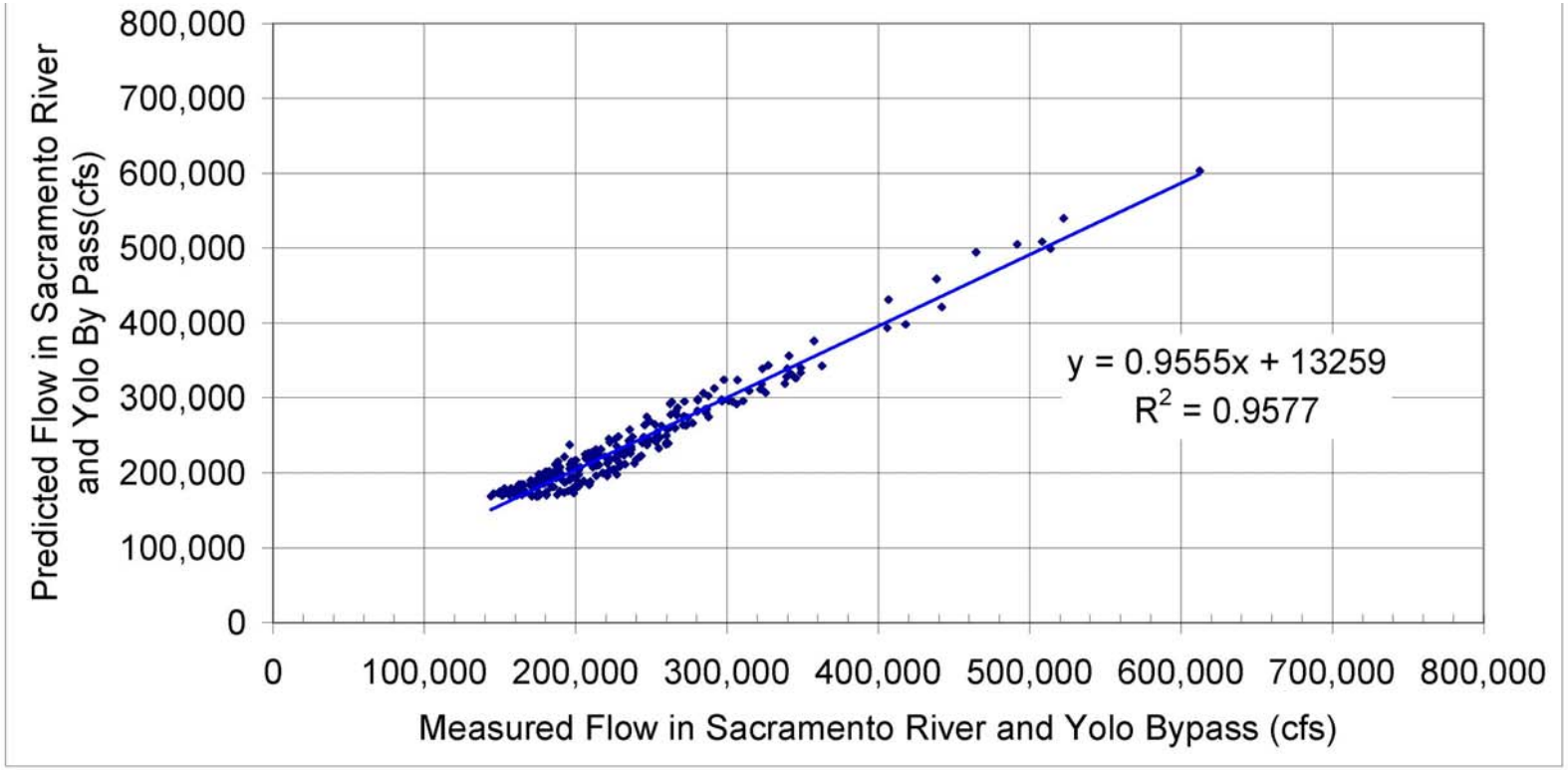

Figure 7-13 Comparison Between Measured and Predicted Flows in the Sacramento River and Yolo Bypass

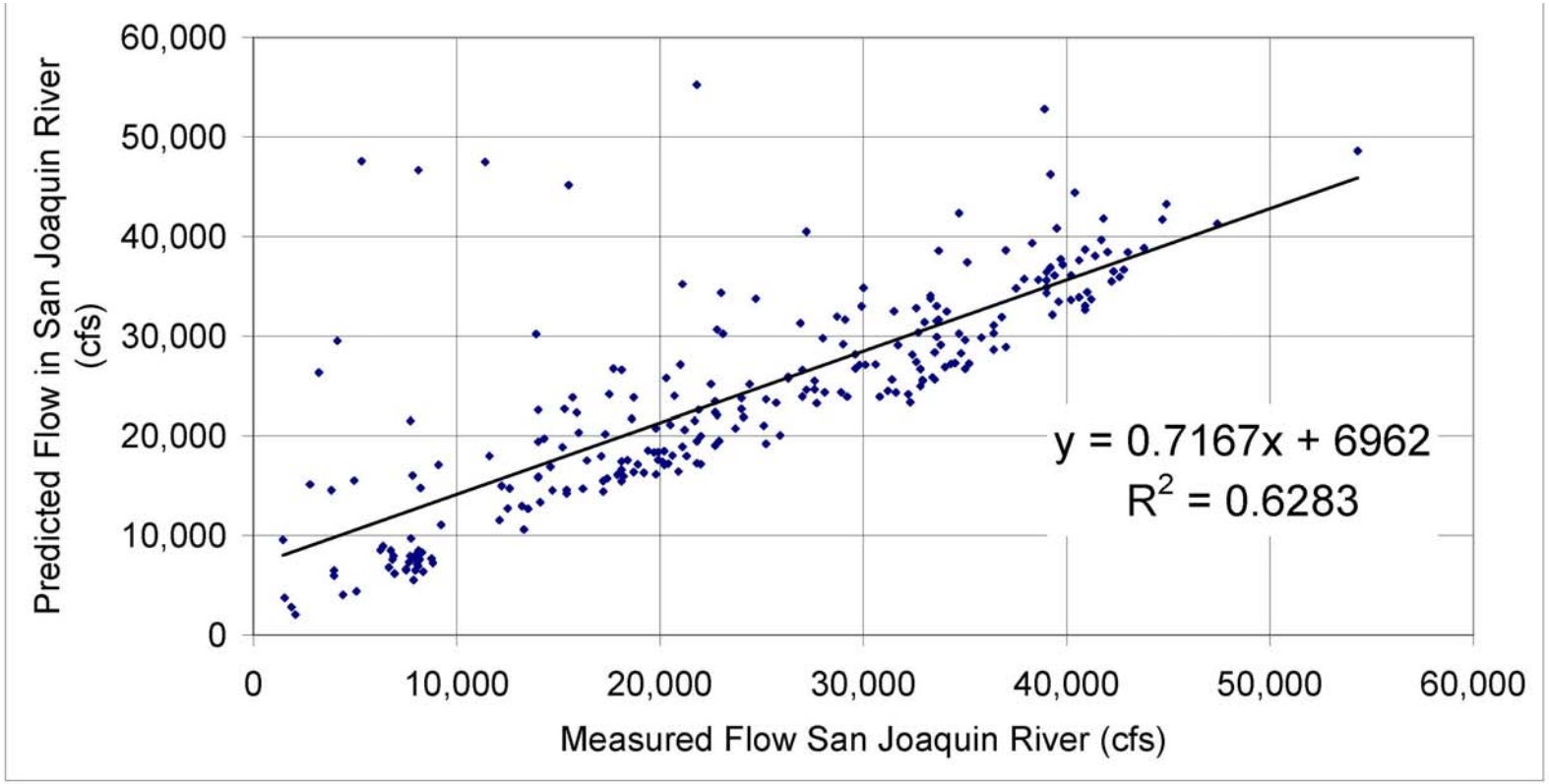

Figure 7-14 Comparison Between Measured and Predicted Flows in the San Joaquin River

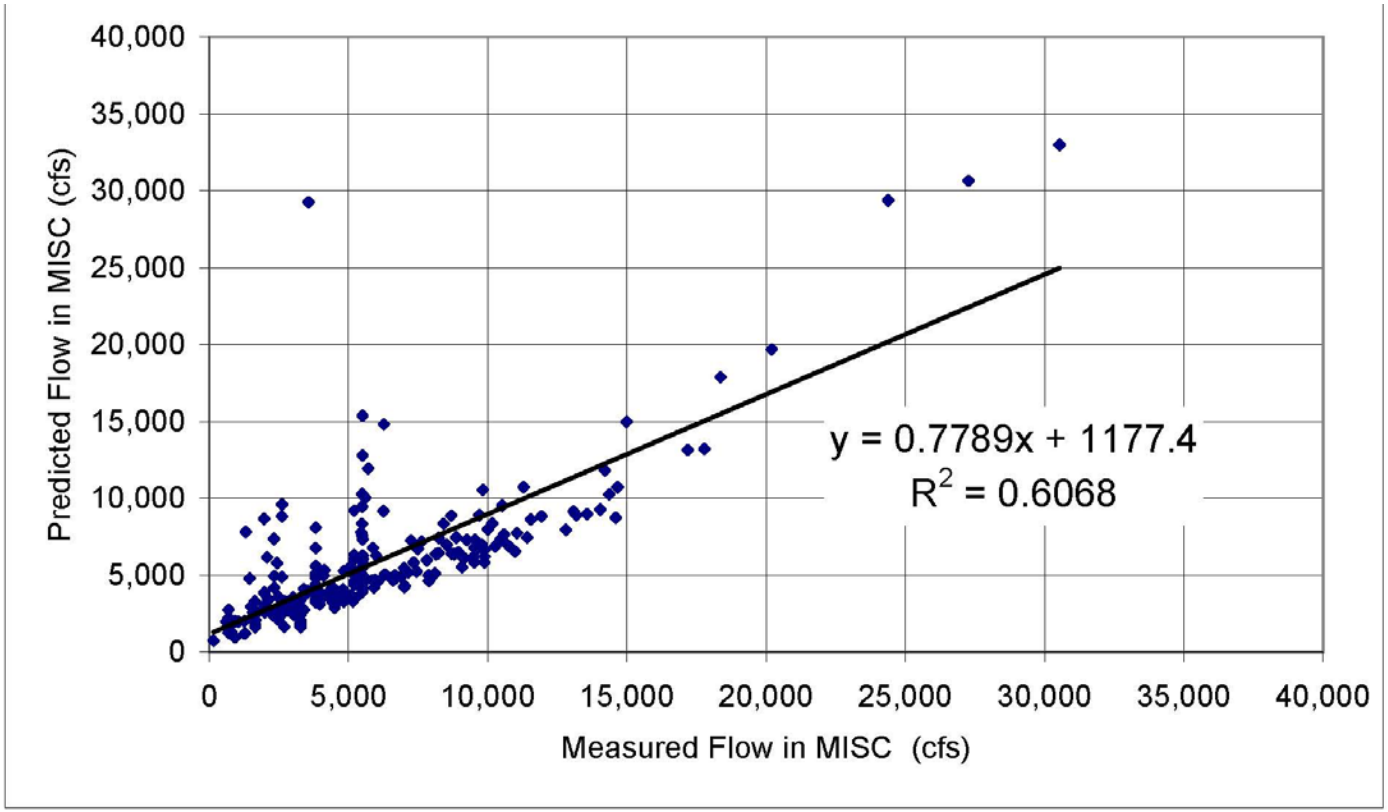

Figure 7-15 Comparison Between Predicted and Measured Flows in the Miscellaneous Inflows

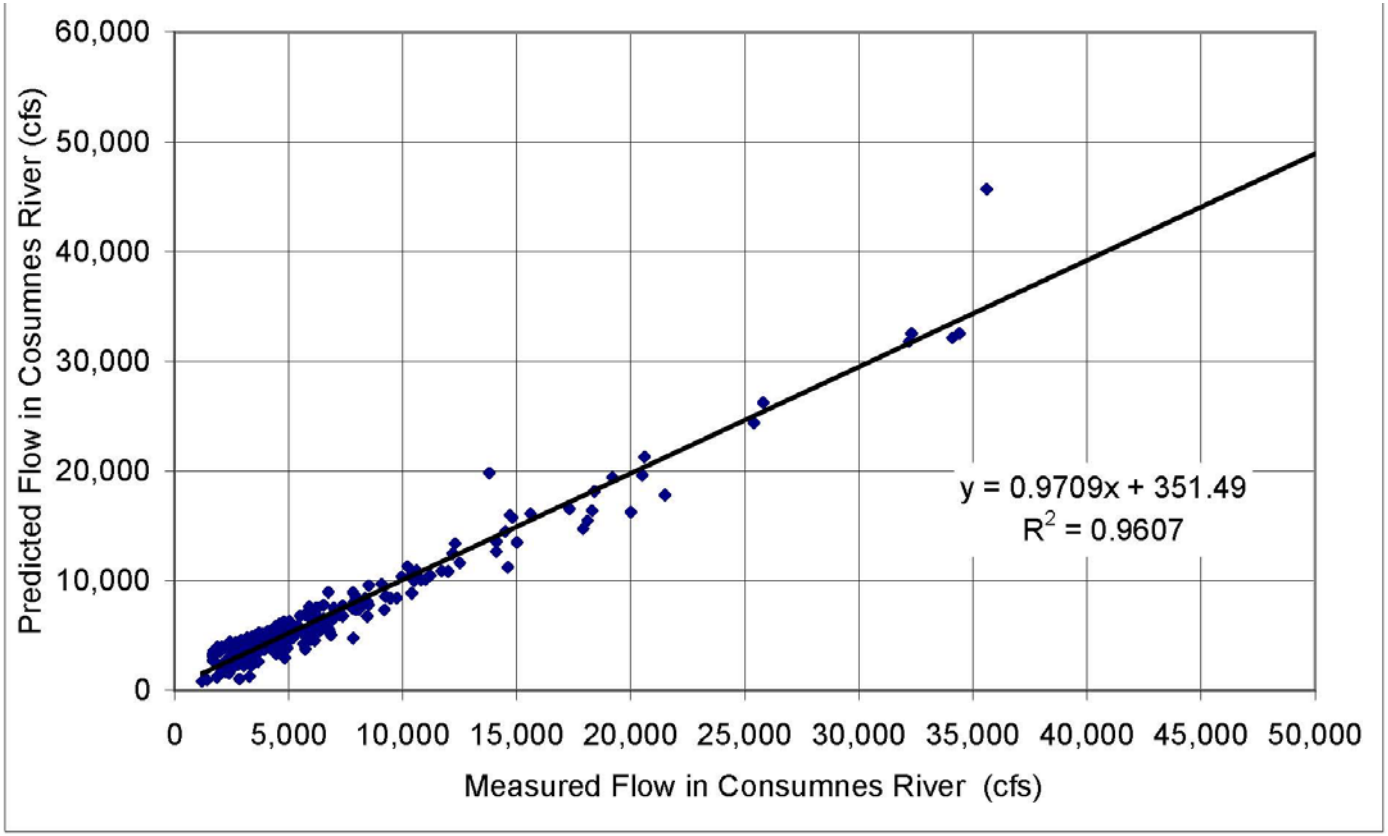

Figure 7-16 Comparison Between Predicted and Measured Flows in the Cosumnes River

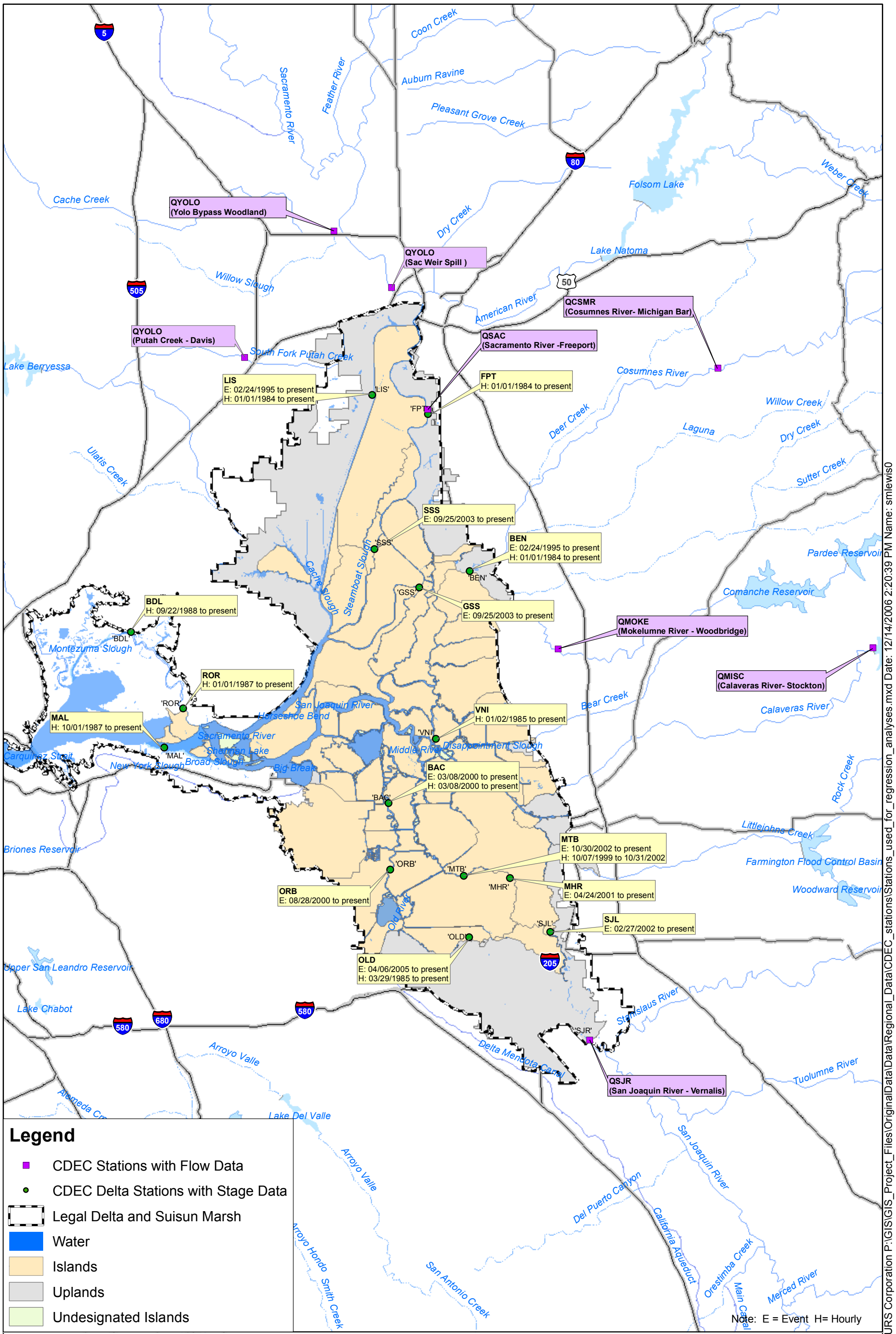

URS	DRMS 26815431	Stations Used for Regression Analyses	Figure 7-17

URS Corporation P:\GIS\GIS_Project_Files\OriginalData\Data\Regional_Data\CDEC_stations\Stations_used_for_regression_analyses.mxd Date: 12/14/2006 2:20:39 PM Name: smlewis0

Figure 7-18 Venice Island (VNI)
Predicted and Measured vs. Date
1/5/1998 - 7/4/1998

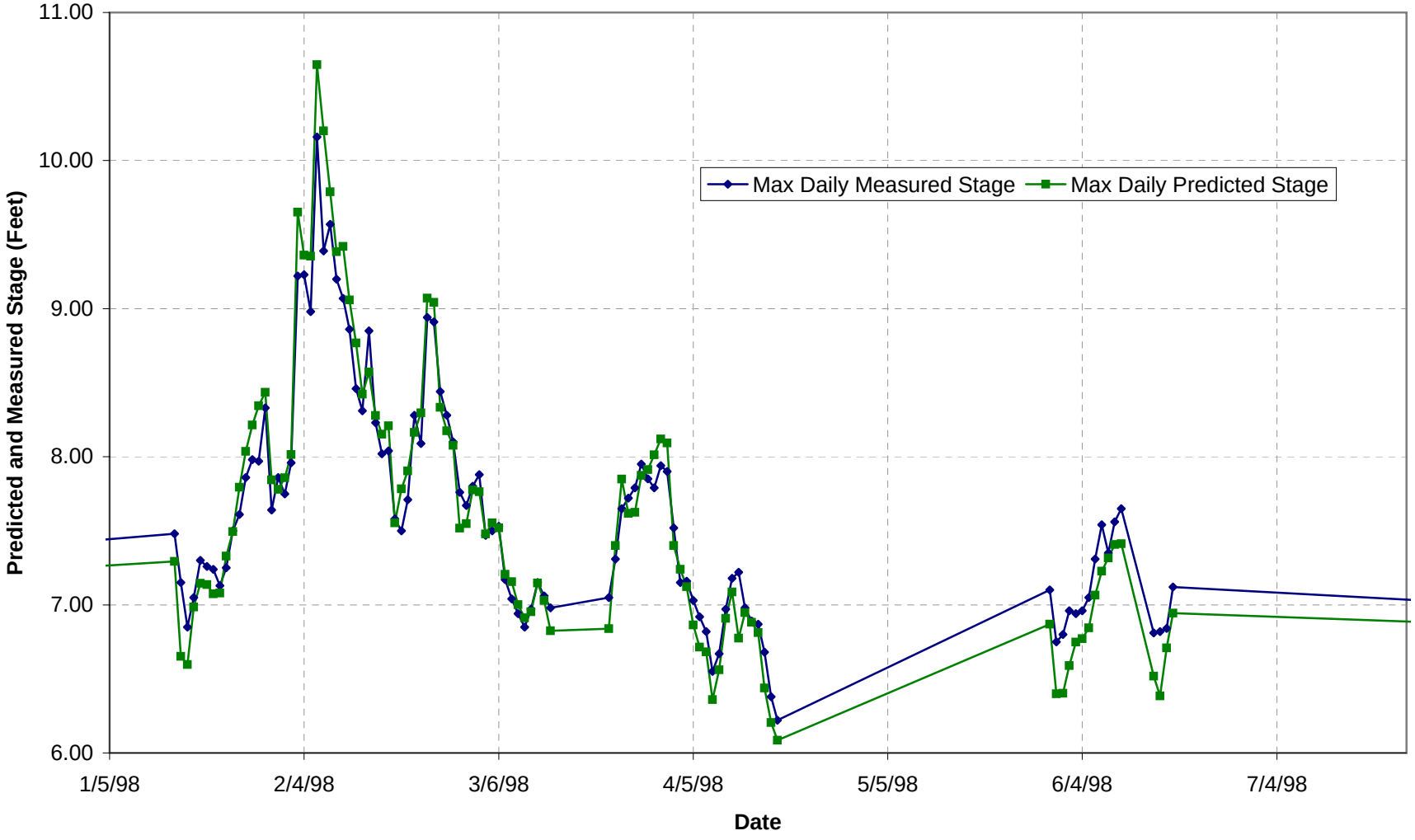

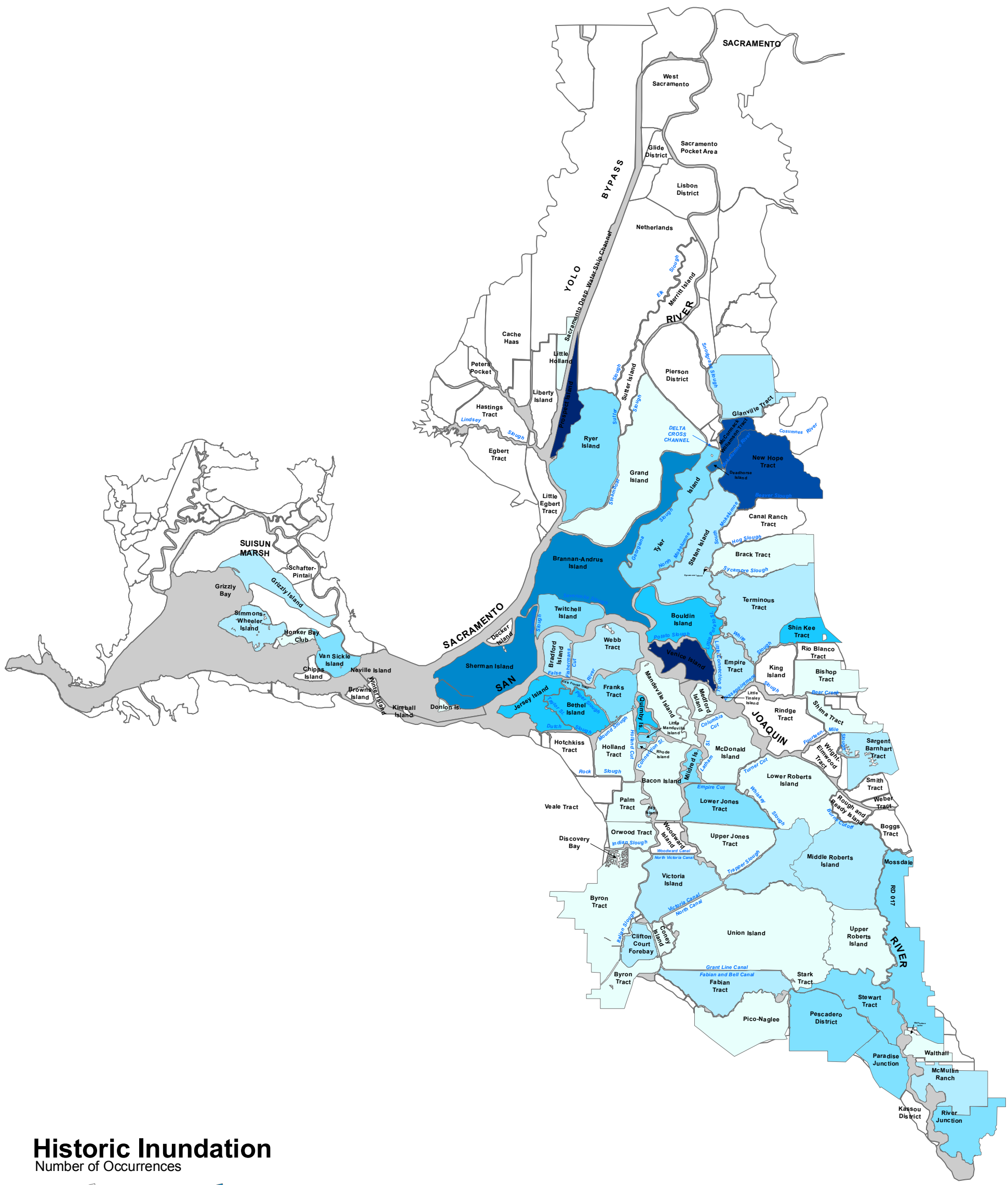

URS	DRMS	Historic Island Breaches in the Delta and Suisun Marsh Since 1900	Figure 7-19
	26815431		

URS Corporation P:\GIS\GIS_Project_Files\MXD\Analysis\Levee Failure Potential\Problem Areas, Failure Areas\Historical Inundation.mxd Date: 1/26/2007 8:03:43 AM Name: smitwe0

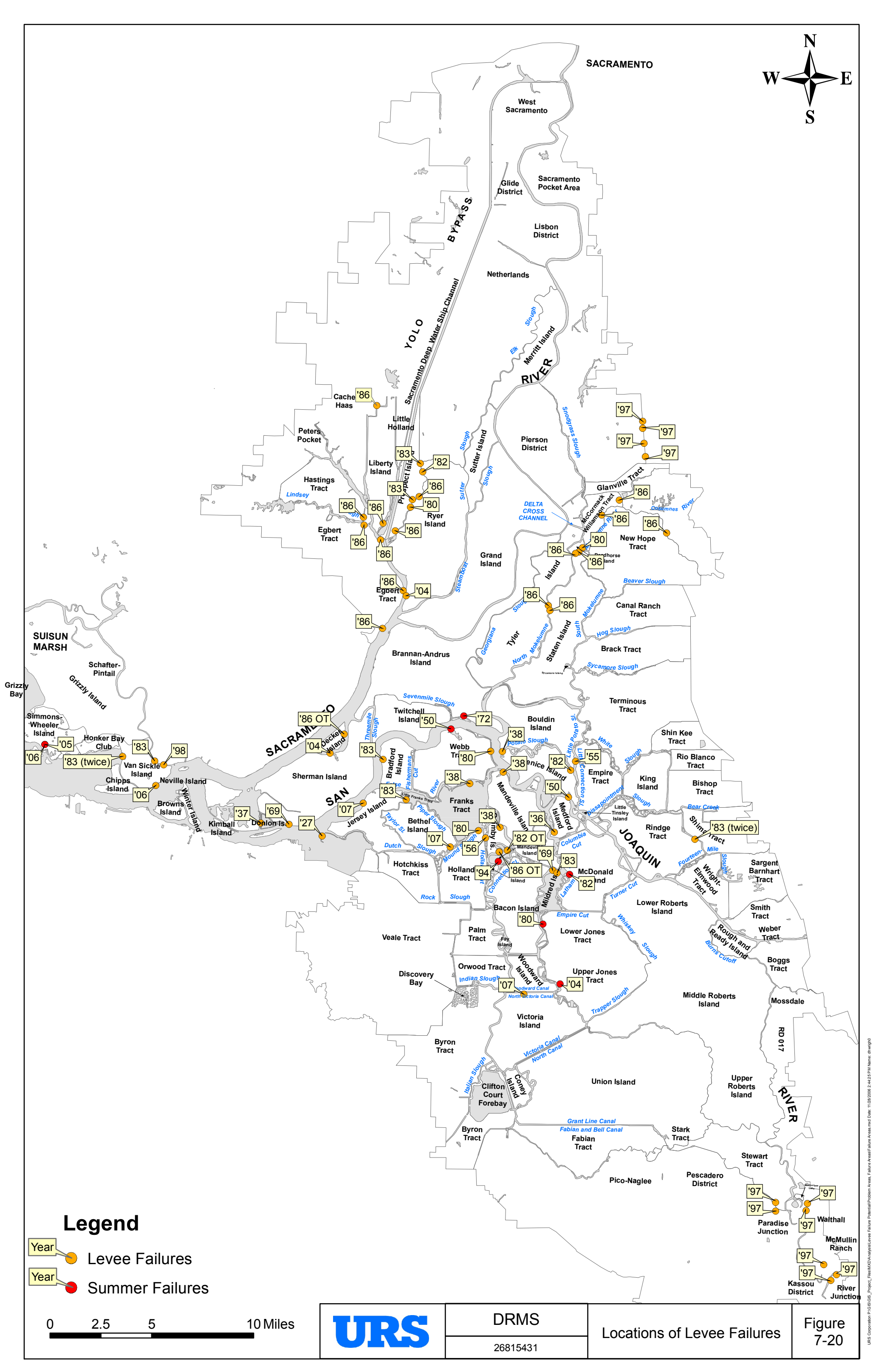

URS	DRMS	Locations of Levee Failures	Figure 7-20
	26815431		

URS Corporation P:\GIS\GIS_Project_Files\MXD\Analysis\Levee Failure Potential\Problem Areas, Failure Areas\Failure Areas.mxd Date: 11/28/2006 2:44:25 PM Name: dhwright0

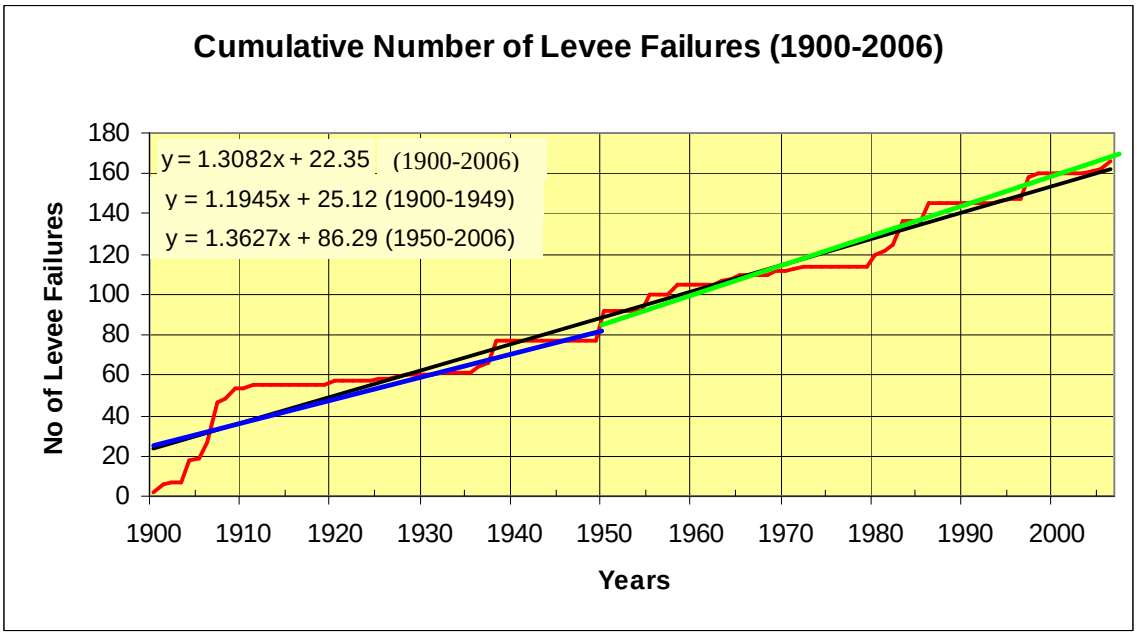

Figure 7-21 Cumulative Number of Levee Failures Since 1900

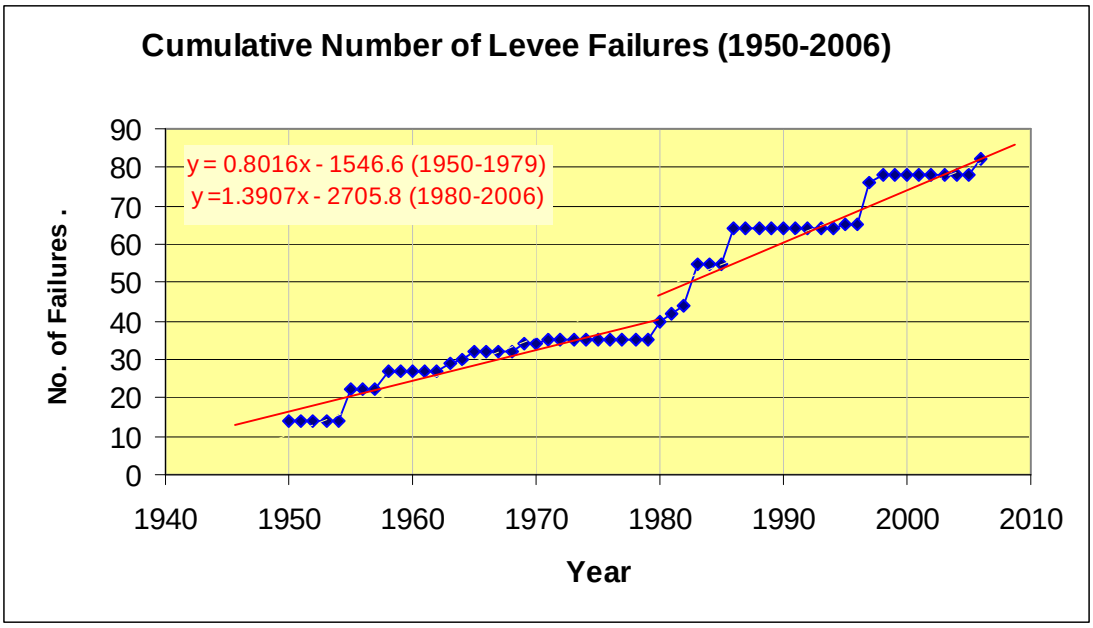

Figure 7-22a Cumulative Number of Levee Failures Since 1950

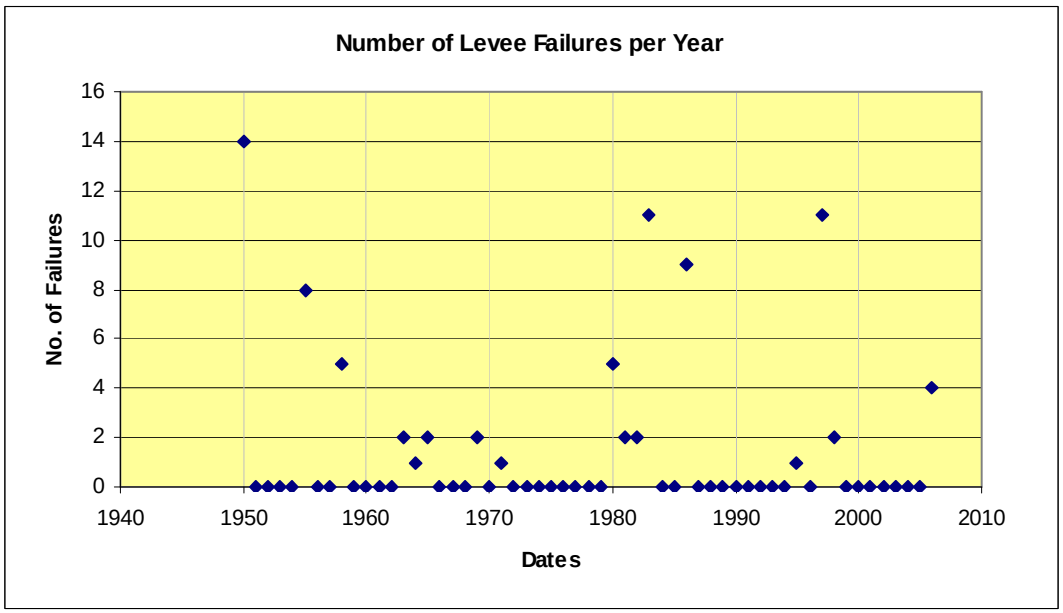

Figure 7-22b Number of Levee Failures per Year Since 1950

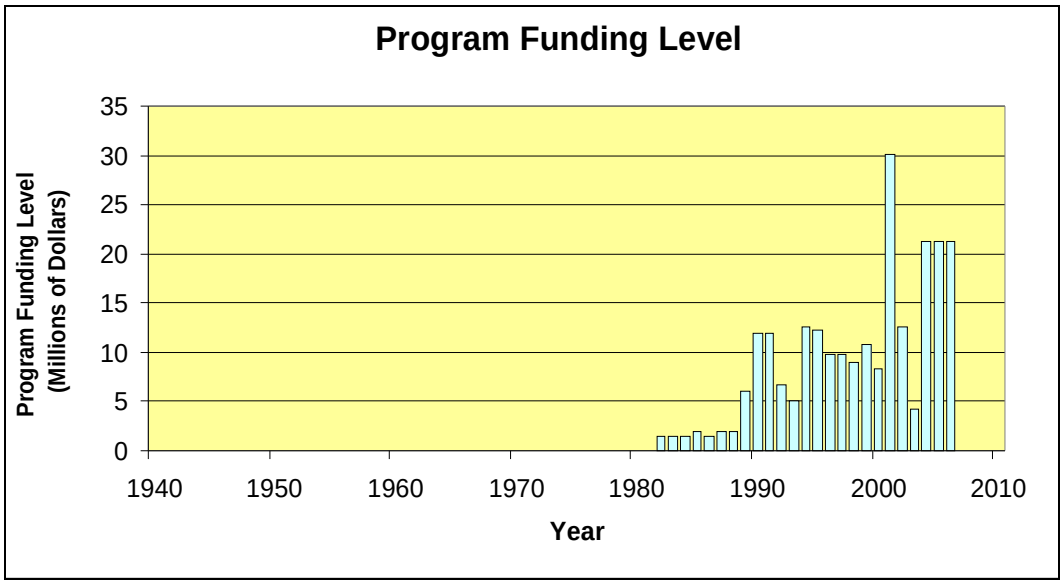

Figure 7-22c Program Funding Level

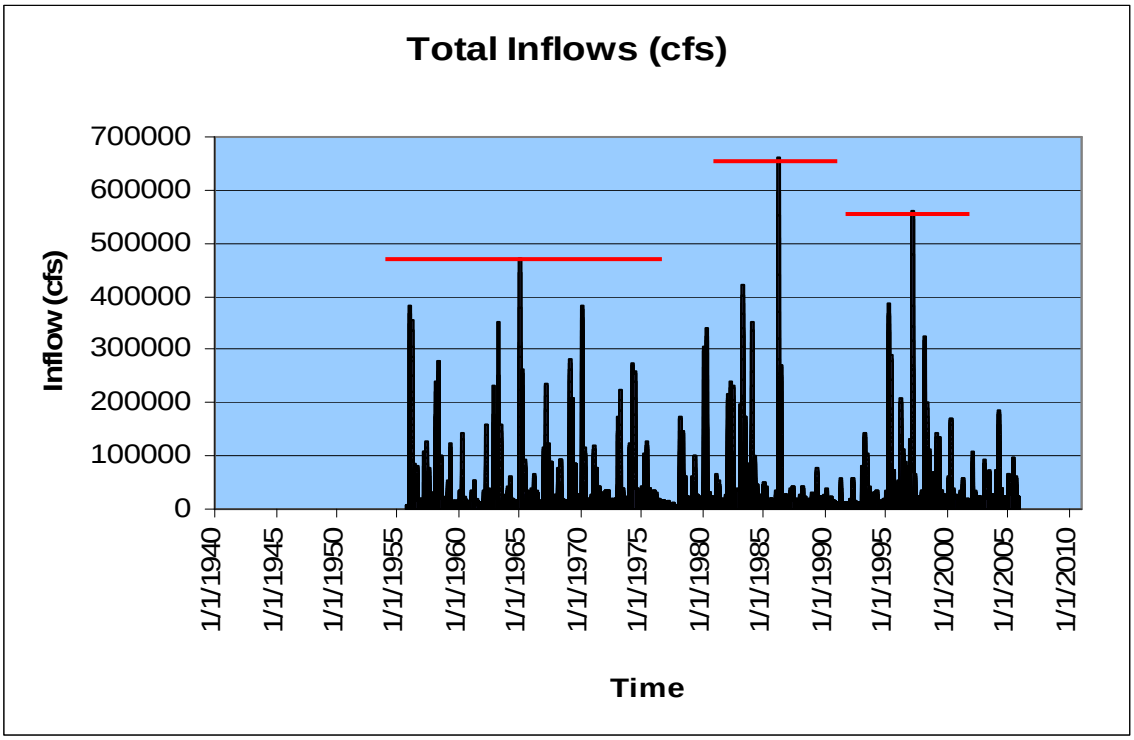

Figure 7-22d Total Delta Inflows (cfs) Since 1955

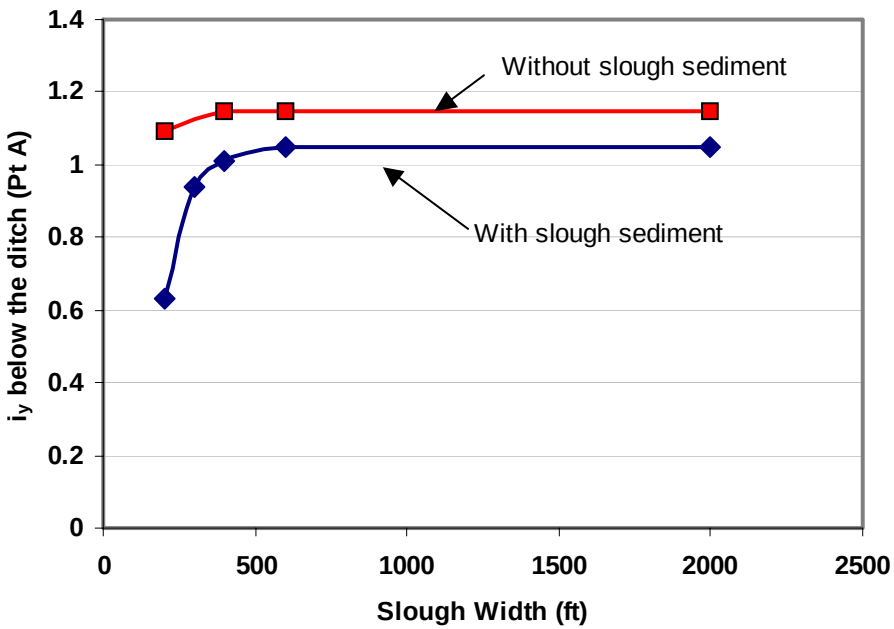

(a) Model with Ditch

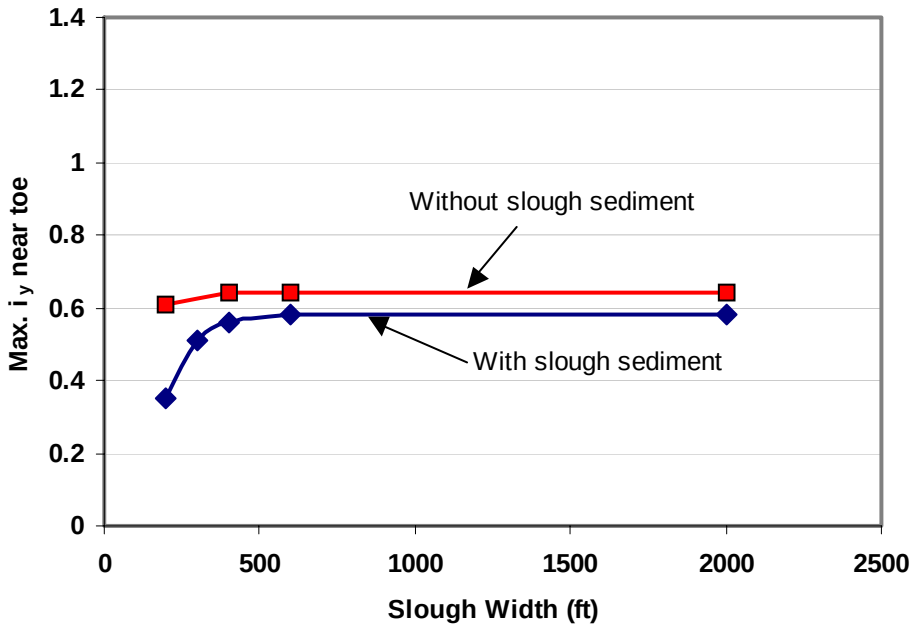

(b) Model without Ditch

Delta Risk Management Strategy (DRMS) Levee Fragility		Effect of Slough Width on Vertical Gradient	Figure 7-23
URS	Project No. 26815621		

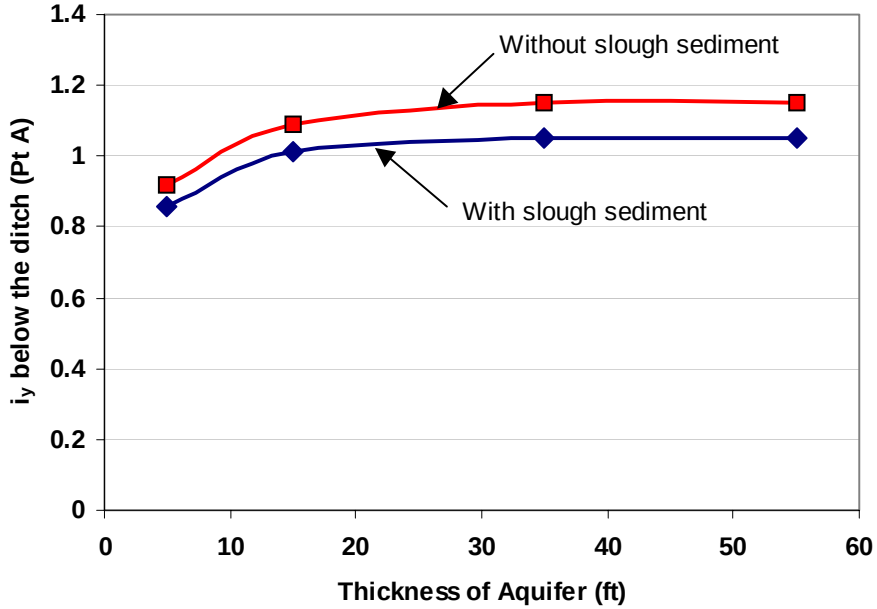

(a) Model with Ditch

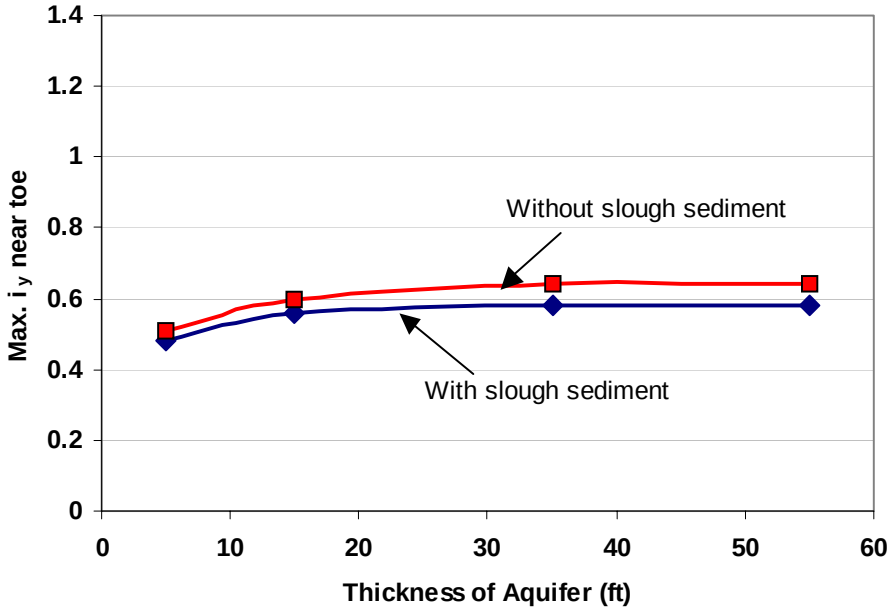

(b) Model without Ditch

Delta Risk Management Strategy (DRMS) Levee Fragility		Effect of Aquifer Thickness on Vertical Gradient	Figure 7-24
URS	Project No. 26815621		

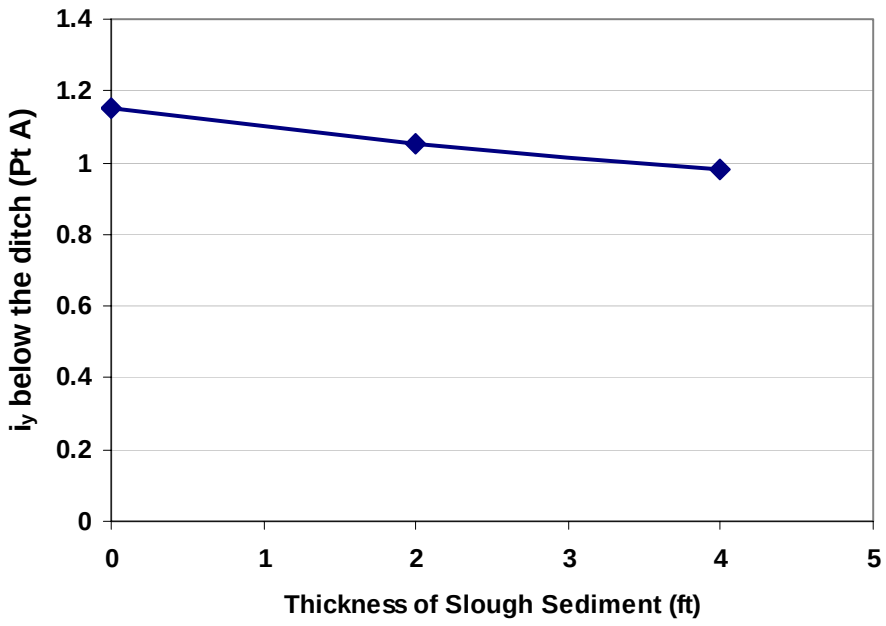

(a) Model with Ditch

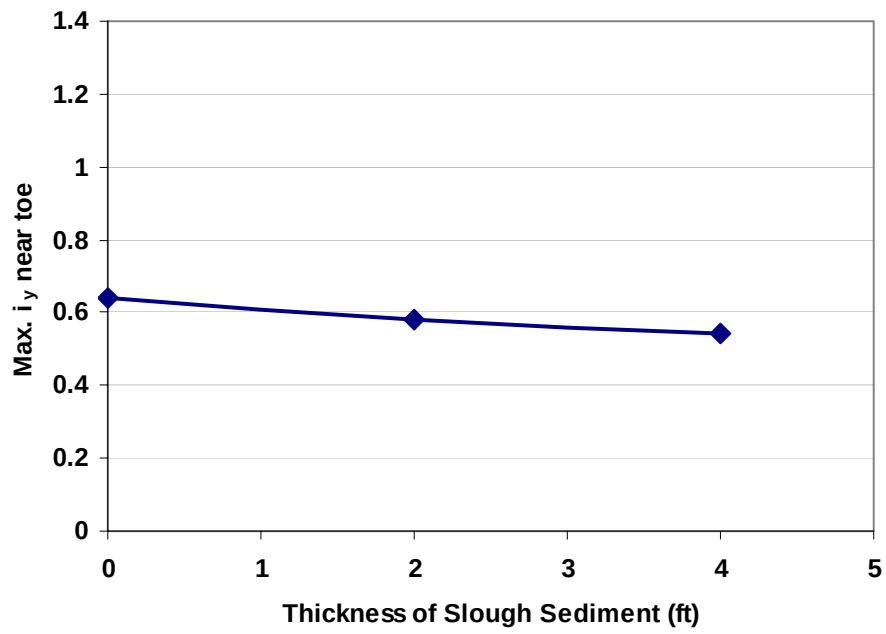

(b) Model without Ditch

Delta Risk Management Strategy (DRMS) Levee Fragility		Effect of Slough Sediment Thickness on Vertical Gradient	Figure 7-25
URS	Project No. 26815621		

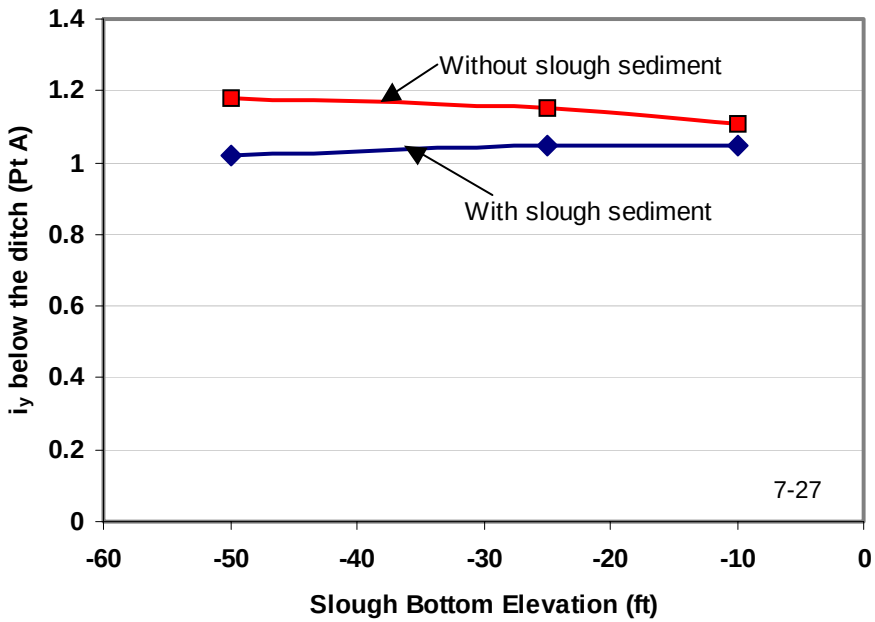

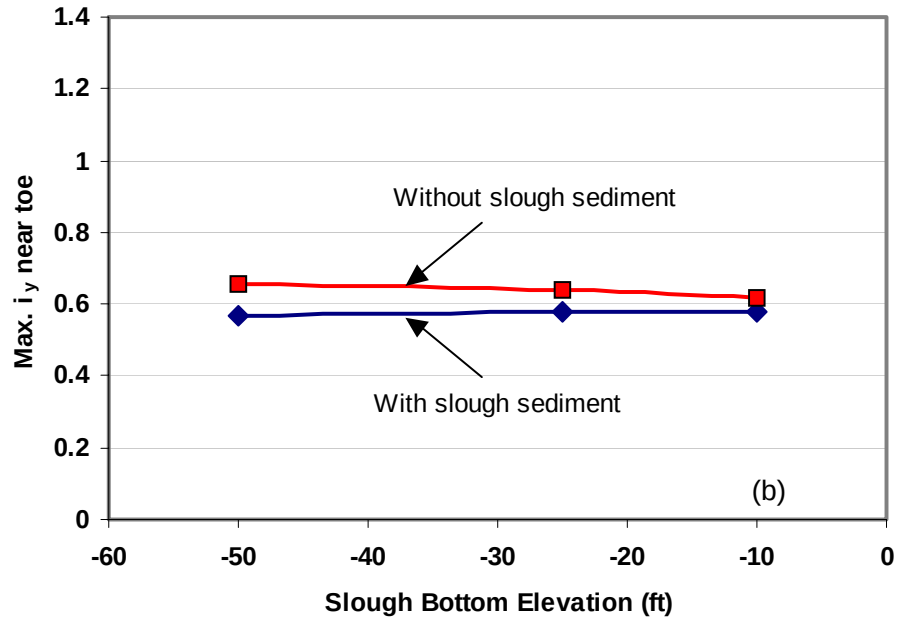

Note:
All elevations are referenced to NAVD88
(NAVD88 = NGVD29 + 2.5 ft)

Delta Risk Management Strategy (DRMS) Levee Fragility		Effect of Slough Bottom Elevation on Vertical Gradient	Figure 7-26
URS	Project No. 26815621		

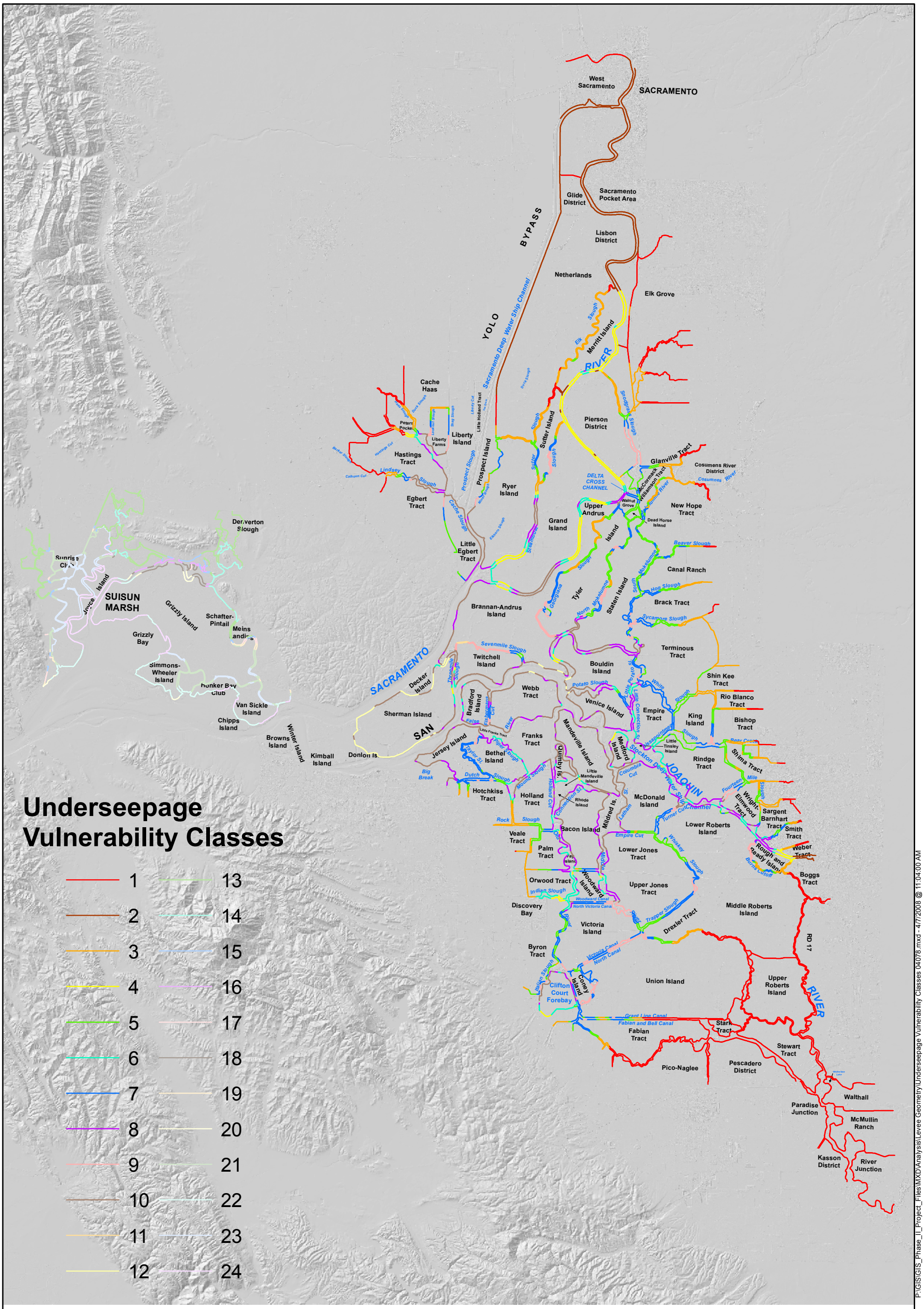
Underseepage Vulnerability Classes
1
2
3
4
5
6
7
8
9
10
11
12
13
14
15
16
17
18
19
20
21
22
23
24
West Sacramento
SACRAMENTO
Glide District
Sacramento Pocket Area
Lisbon District
Netherlands
Elk Grove
YOLO BYPASS
Sacramento Deep Water Ship Channel
Merritt Island
Cache Haas
Liberty Island
Little Holland Tract
Sutter Island
Pierson District
Hastings Tract
Prospect Island
Ryer Island
Glanville Tract
Cosumens River District
Egbert Tract
Grand Island
Upper Andrus Island
New Hope Tract
Derverton Slough
Little Egbert Tract
Canal Ranch
Brack Tract
Brannan-Andrus Island
Tyler
Staten Island
Terminous Tract
SUISUN MARSH
Grizzly Island
Schafter-Pintail
Grizzly Bay
Simmons-Wheeler Island
Twitchell Island
Bouldin Island
Shin Kee Tract
Rio Blanco Tract
Bishop Tract
Decker Island
Webb Tract
Venice Island
Empire Tract
King Island
Sherman Island
Bradford Island
Franks Tract
Mandeville Island
Rindge Tract
Shima Tract
Jersey Island
Bethel Island
Quimby Is.
Mildred Is.
McDonald Island
Hotchkiss Tract
Holland Tract
Bacon Island
Lower Roberts Island
Sargent Barnhart Tract
Smith Tract
Veale Tract
Palm Tract
Lower Jones Tract
Weber Tract
Boggs Tract
Orwood Tract
Upper Jones Tract
Discovery Bay
Middle Roberts Island
Drexler Tract
Victoria Island
Byron Tract
Union Island
Upper Roberts Island
Clifton Court Forebay
Coney Island
Fabian Tract
Stark Tract
Stewart Tract
Pico-Naglee
Pescadero District
Walthall
Paradise Junction
McMullin Ranch
Kasson District
River Junction
RD 17
SAN JOAQUIN RIVER
Donlon Is.
Kimball Island
Winter Island
Browns Island
Chipps Island
Van Sickle Island
Honker Bay Club
Joyce Island
Sunrise Club
Meins Landing
Little Mandeville Island
Rhode Island
Little Tinsley Island
Fourteen Mile Slough
Beaver Slough
Hog Slough
Sycamore Slough
Sevenmile Slough
Potato Slough
Dutch Slough
Rock Slough
Indian Slough
Trapper Slough
Grant Line Canal
Fabian and Bell Canal
Victoria Canal
North Canal
Woodward Canal
North Victoria Canal
Old River
Middle River
Whiskey Slough
Turner Cut
Empire Cut
Columbia Cut
Stockton Deep Water Ship Channel
Mokelumne River
Cosumnes River
DELTA CROSS CHANNEL
Walnut Grove
Dead Horse Island
McCormack-Williamson Tract
Elk Slough
Snodgrass Slough
Sutter Slough
Steamboat Slough
Georgiana Slough
North Mokelumne River
Lindsey Slough
Prospect Slough
Cache Slough
Elkhorn Slough
Barker Slough
Hastings Cut
Calhoun Cut
Liberty Cut
Duck Slough
Little Franks Tract
False River
Taylor Sl.
Piper Slough
Mound Slough
Big Break
Rough and Ready Island
Burns Cutoff
Bear Creek
Rio Vista
Isleton
Walnut Grove
Ryde
Hood
Courtland
Locke
Clarksburg
Freeport
Hood
Thornton
Walnut Grove
Isleton
Rio Vista
Ryde

For Vulnerability Class i,

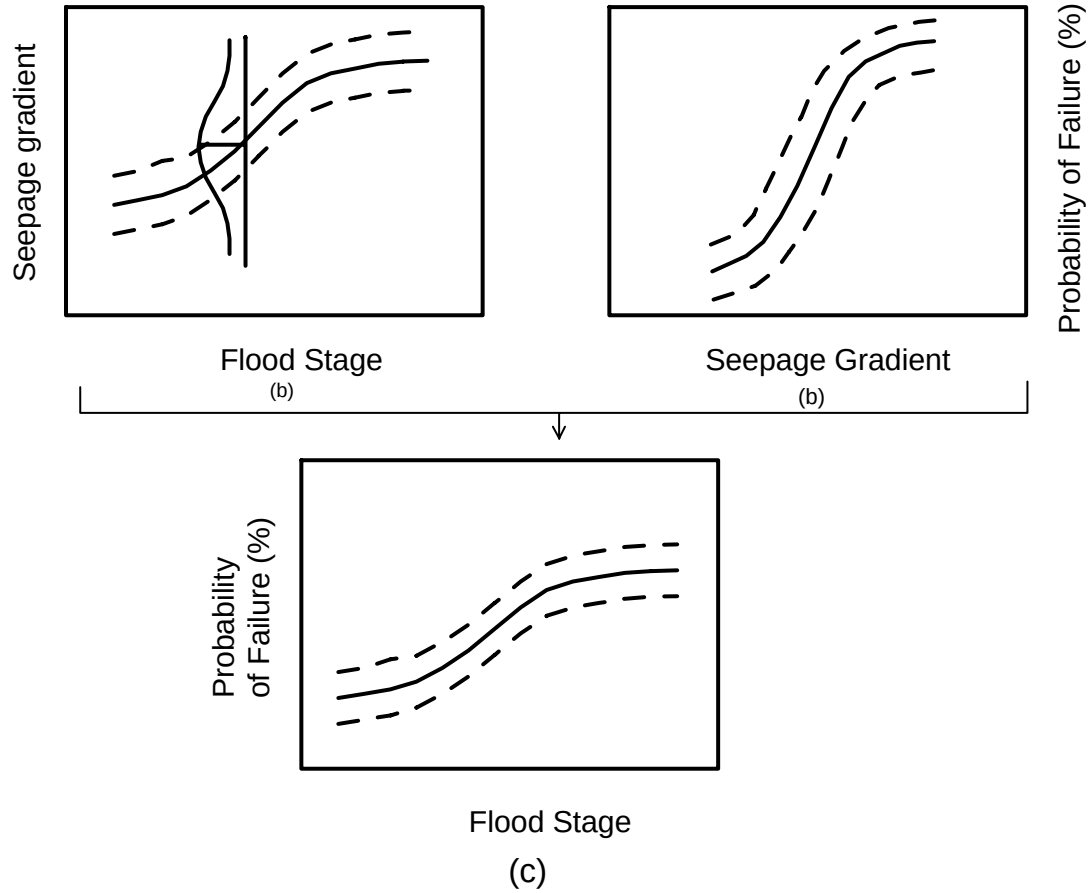

Delta Risk Management Strategy (DRMS) Levee Fragility		Probability of Failure versus Flood Stage	Figure 7-28
URS	Project No. 26815621		

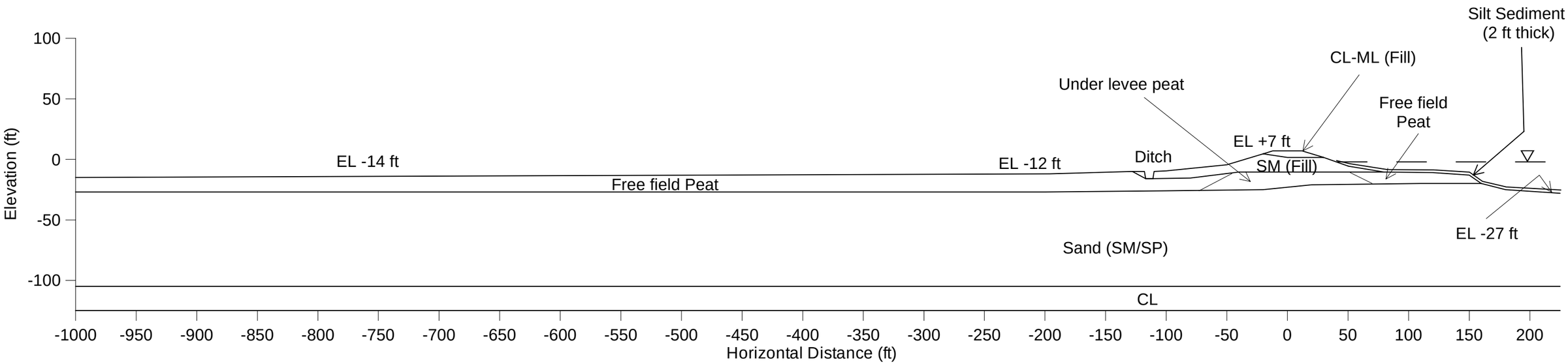

Note:
All elevations are referenced to NAVD88
(NAVD88 = NGVD29 + 2.5 ft)

Delta Risk Management Strategy (DRMS) Levee Fragility		Idealized Soil Profile - Terminous Tract	Figure 7-29
URS	Project No. 26815621		

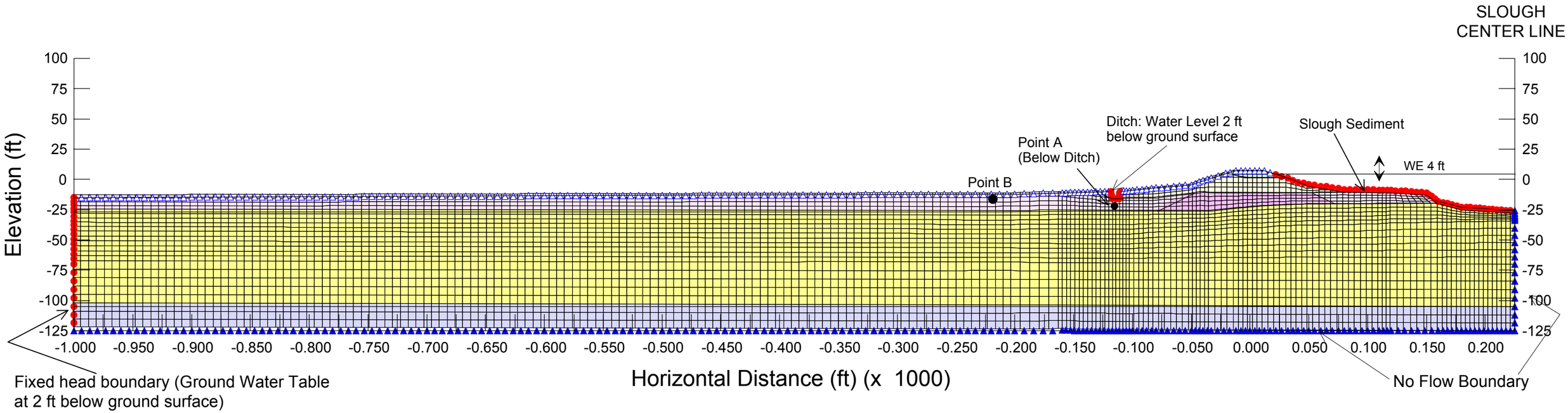

Legend

Boundary Conditions

- No flow
- Fixed head
- Review

Material Type

- CL-ML (Levee Fill)
- Sandy Levee Fill
- Free Field Peat
- Under Levee Peat
- Sand (SP/SM)
- Clay
- Slough Sediment

Hydraulic conductivities used for preliminary seepage analysis

Material	k_h (cm/s)			k_h/k_v
	Mean - σ	Mean	Mean + σ	
Fill				
CL-ML (fill)	-	1×10^{-5}	-	4
SM (fill)	-	1×10^{-3}	-	4
Peat & Organics				
Free Field	1×10^{-5}	1×10^{-4}	1×10^{-3}	10
Under Levee	1×10^{-6}	1×10^{-5}	1×10^{-4}	10
Other Foundation Soils				
Sand (SM/SP)	5×10^{-4}	1×10^{-3}	5×10^{-3}	4
ML	-	1×10^{-4}	-	4
CL	-	1×10^{-6}	-	4
Sediment (at slough bottom)	-	1×10^{-5}	-	1

Note:
All elevations are referenced to NAVD88
(NAVD88 = NGVD29 + 2.5 ft)

Delta Risk Management Strategy (DRMS) Levee Fragility		Finite Element Mesh and Boundary Conditions - Model with Drainage Ditch Terminous Tract	Figure 7-30
URS	Project No. 26815621		

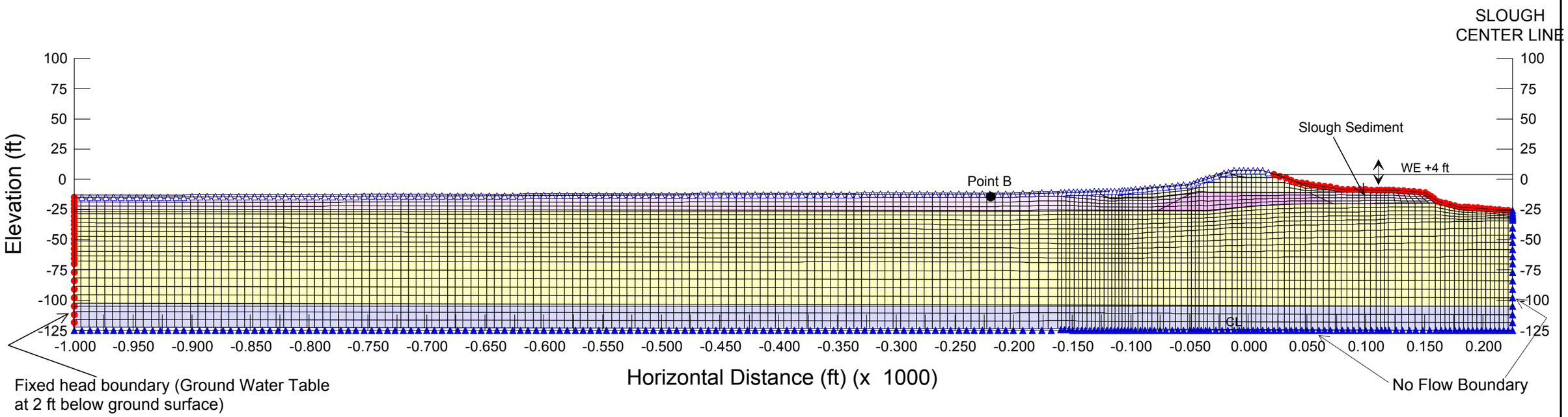

Legend

Boundary Conditions

- No flow
- Fixed head
- Review

Material Type

- CL-ML (Levee Fill)
- Sandy Levee Fill
- Free Field Peat
- Under Levee Peat
- Sand (SP/SM)
- Clay
- Slough Sediment

Hydraulic conductivities used for preliminary seepage analysis

Material	k_h (cm/s)			k_h/k_v
	Mean - σ	Mean	Mean + σ	
Fill				
CL-ML (fill)	-	1×10^{-5}	-	4
SM (fill)	-	1×10^{-3}	-	4
Peat & Organics				
Free Field	1×10^{-5}	1×10^{-4}	1×10^{-3}	10
Under Levee	1×10^{-6}	1×10^{-5}	1×10^{-4}	10
Other Foundation Soils				
Sand (SM/SP)	5×10^{-4}	1×10^{-3}	5×10^{-3}	4
ML	-	1×10^{-4}	-	4
CL	-	1×10^{-6}	-	4
Sediment (at slough bottom)	-	1×10^{-5}	-	1

Note:
All elevations are referenced to NAVD88
(NAVD88 = NGVD29 + 2.5 ft)

Delta Risk Management Strategy (DRMS) Levee Fragility		Finite Element Mesh and Boundary Conditions - Model without Drainage Ditch Terminous Tract	Figure 7-31
URS	Project No. 26815621		

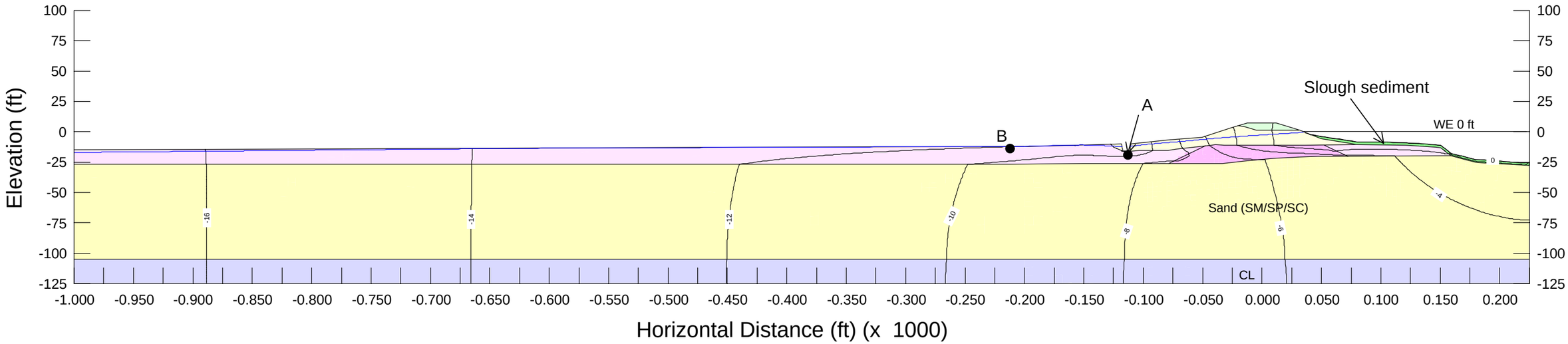

(a) Total head distribution contours

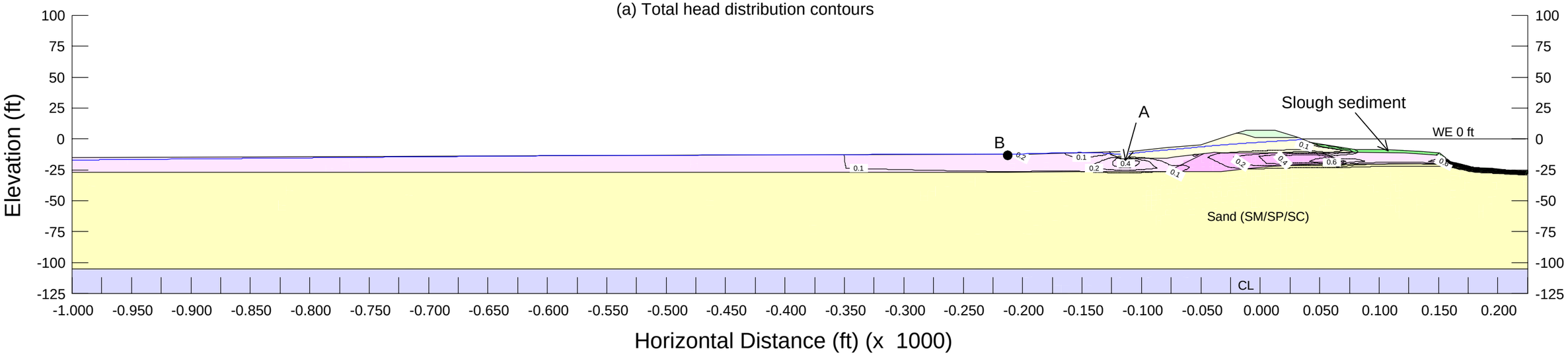

(b) Vertical gradient contours

Note:
All elevations are referenced to NAVD88
(NAVD88 = NGVD29 + 2.5 ft)

Delta Risk Management Strategy (DRMS) Levee Fragility		Total Head and Vertical Gradient Contours for Slough Water EL: 0 ft Terminous Tract	Figure 7-32
URS	Project No. 26815621		

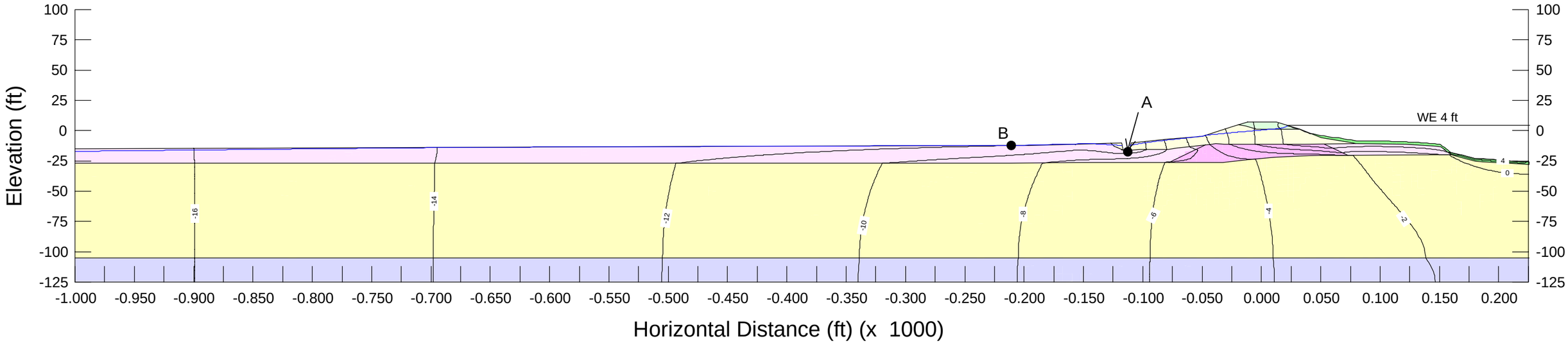

(a) Total head distribution contours

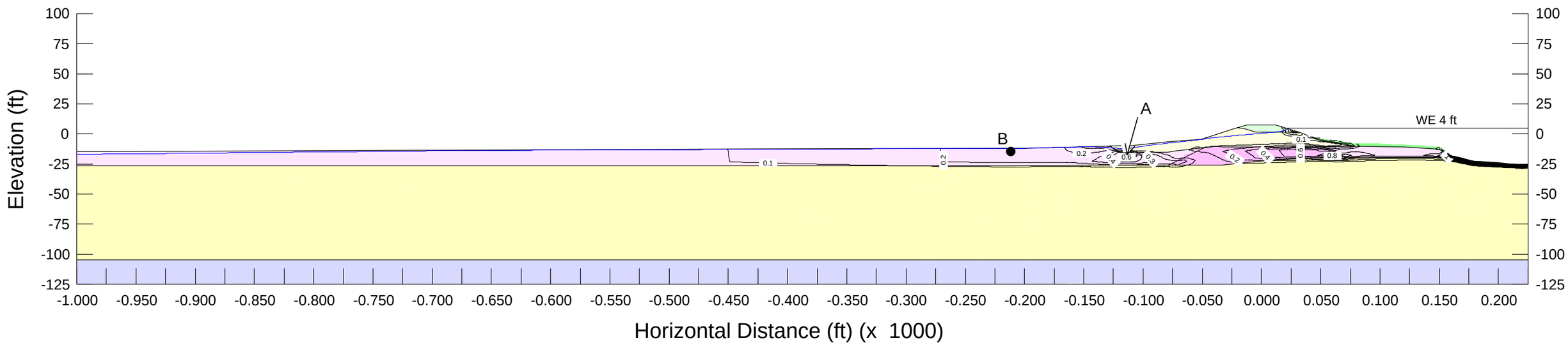

(b) Vertical gradient contours

Note:
All elevations are referenced to NAVD88
(NAVD88 = NGVD29 + 2.5 ft)

Delta Risk Management Strategy (DRMS) Levee Fragility		Total Head and Vertical Gradient Contours for Slough Water EL: +4 ft Terminous Tract	Figure 7-33
URS	Project No. 26815621		

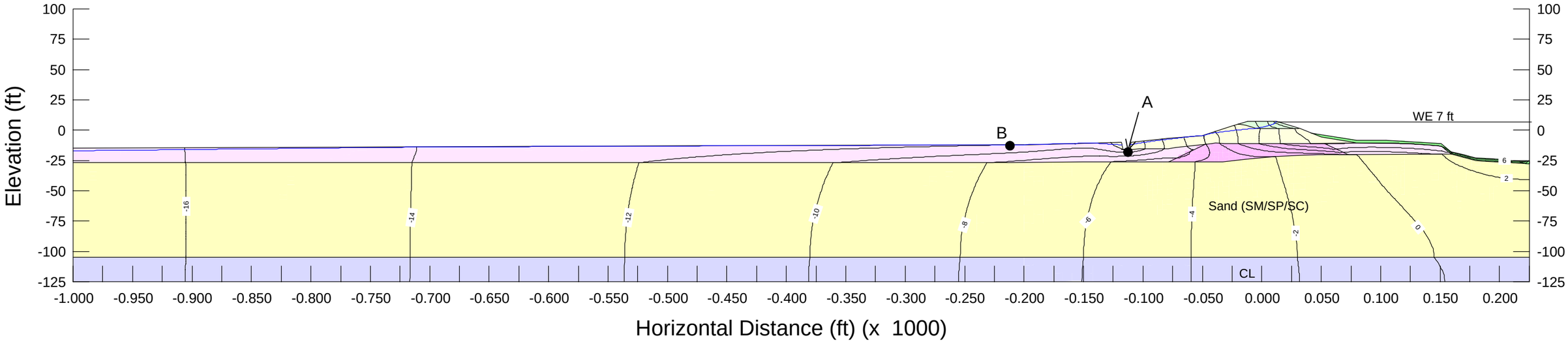

(a) Total head distribution contours

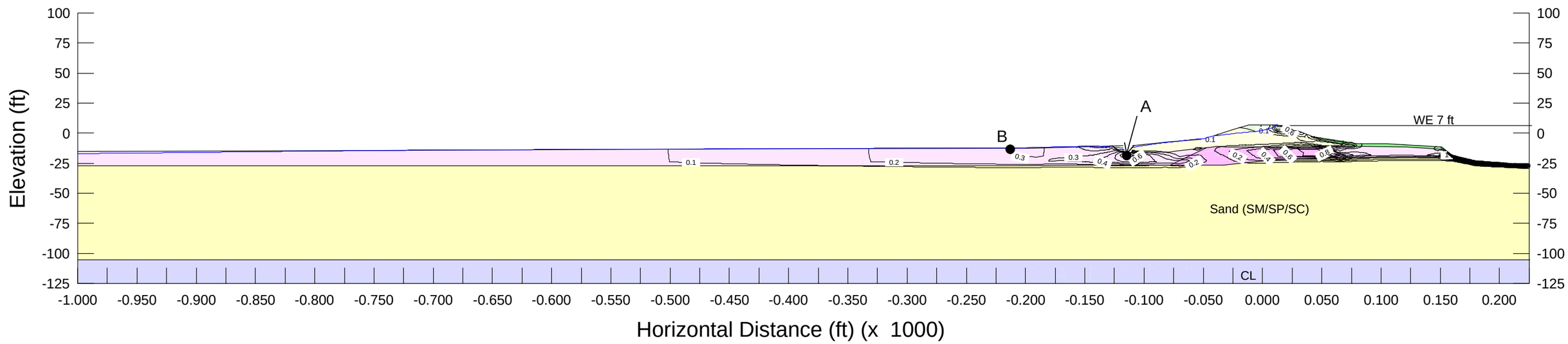

(b) Vertical gradient contours

Note:
All elevations are referenced to NAVD88
(NAVD88 = NGVD29 + 2.5 ft)

Delta Risk Management Strategy (DRMS) Levee Fragility		Total Head and Vertical Gradient Contours for Slough Water EL: +7 ft Terminous Tract	Figure 7-34
URS	Project No. 26815621		

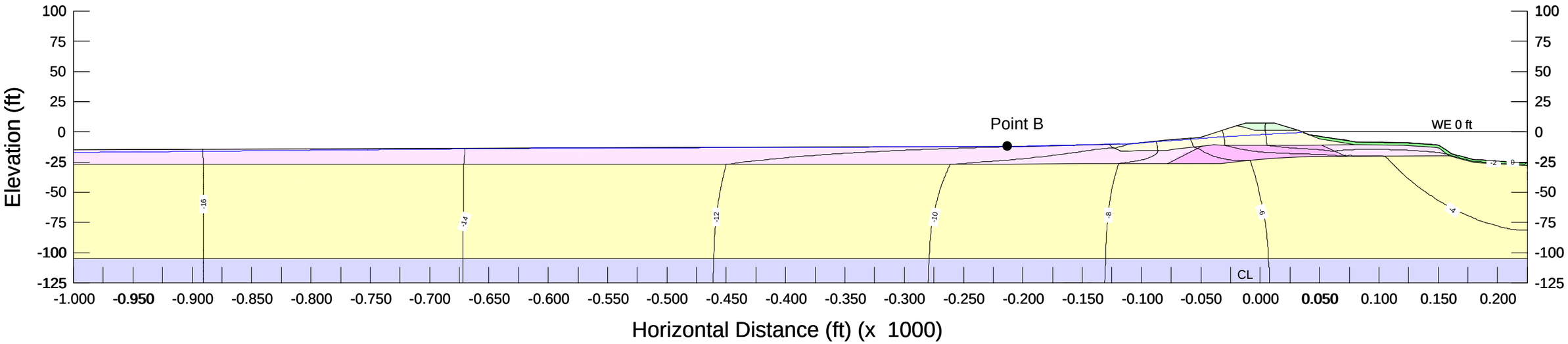

(a) Total head distribution contours

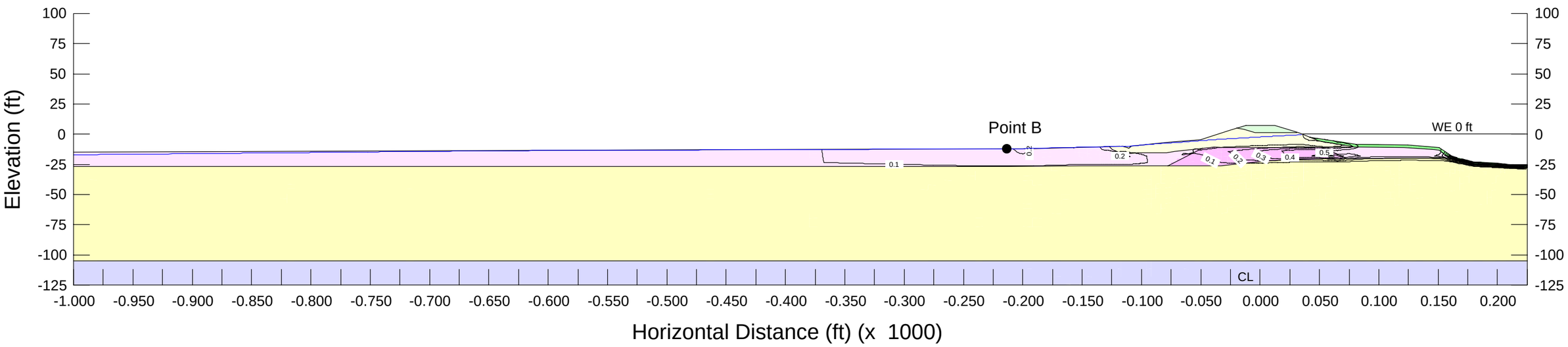

(b) Vertical gradient contours

Note:
All elevations are referenced to NAVD88
(NAVD88 = NGVD29 + 2.5 ft)

Delta Risk Management Strategy (DRMS) Levee Fragility		Total Head and Vertical Gradient Contours for Slough Water EL: 0 ft - Model without Drainage Ditch Terminous Tract	Figure 7-35
URS	Project No. 26815621		

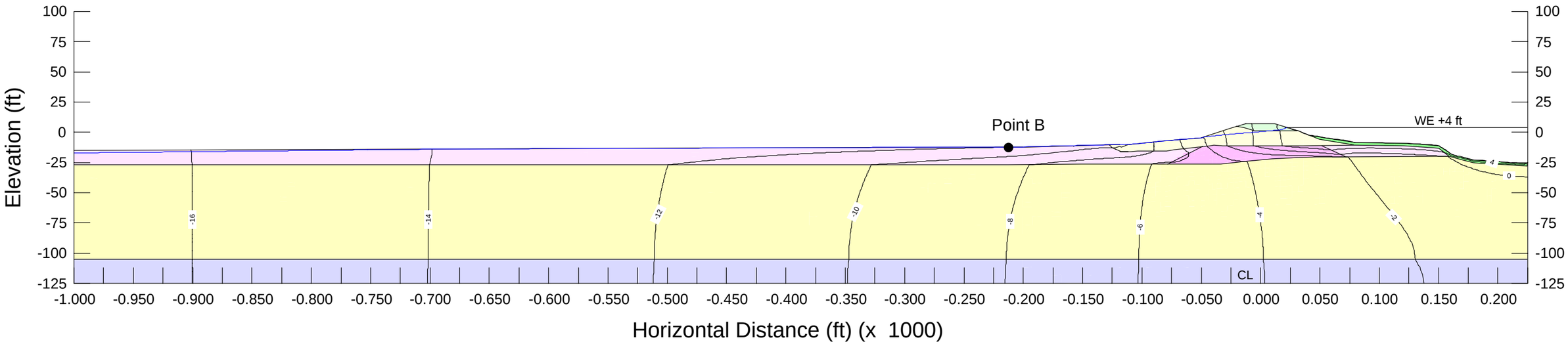

(a) Total head distribution contours

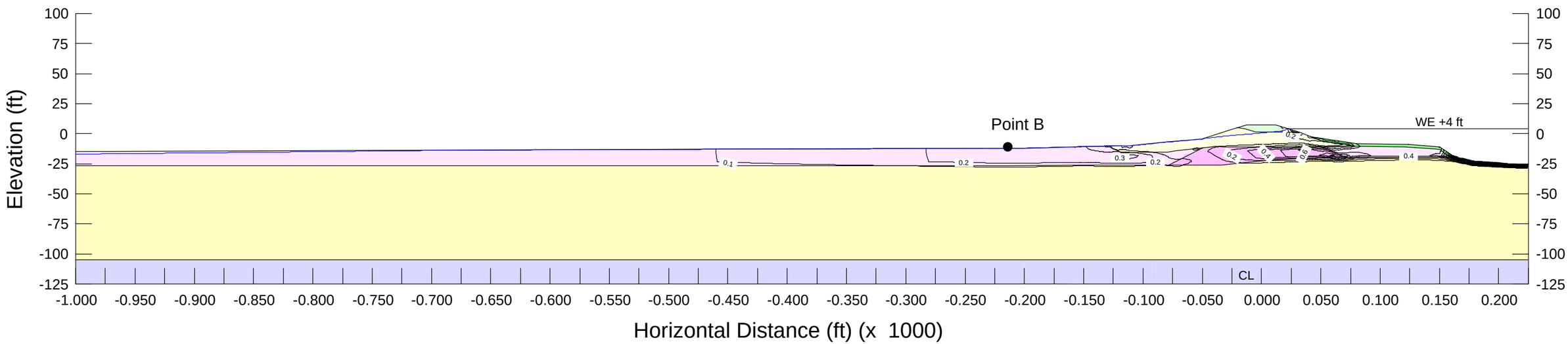

(b) Vertical gradient contours

Note:
All elevations are referenced to NAVD88
(NAVD88 = NGVD29 + 2.5 ft)

Delta Risk Management Strategy (DRMS) Levee Fragility		Total Head and Vertical Gradient Contours for Slough Water EL: +4 ft - Model without Drainage Ditch Terminous Tract	Figure 7-36
URS	Project No. 26815621		

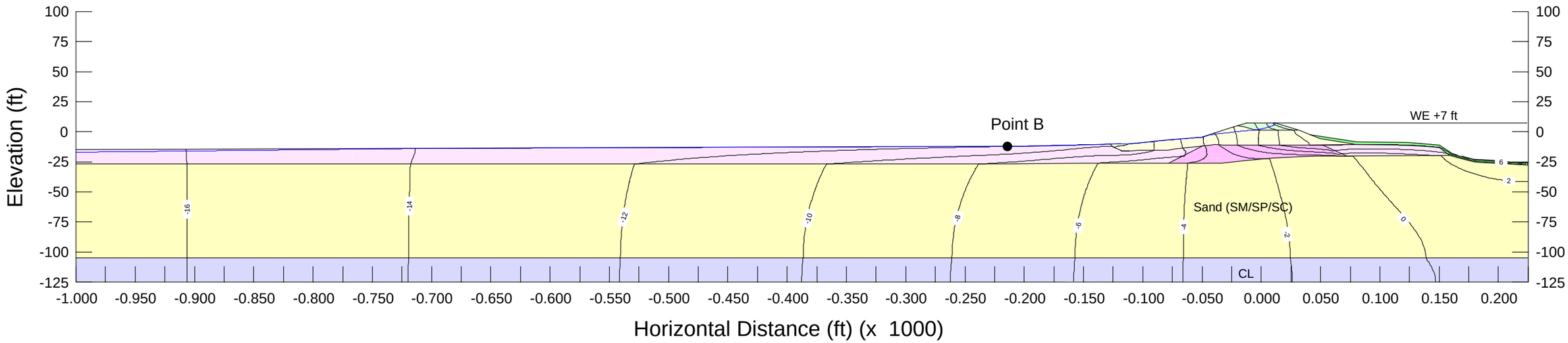

(a) Total head distribution contours

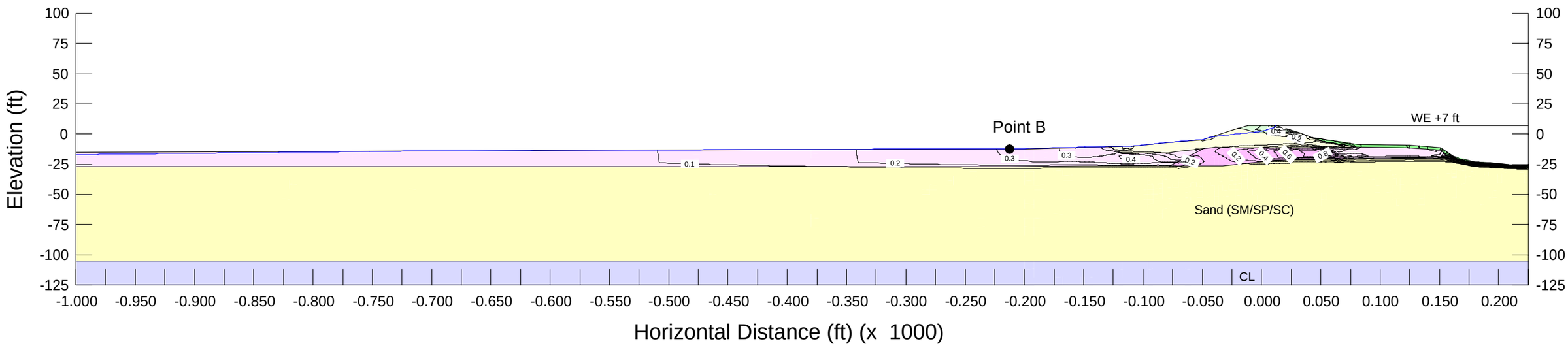

(b) Vertical gradient contours

Note:
All elevations are referenced to NAVD88
(NAVD88 = NGVD29 + 2.5 ft)

Delta Risk Management Strategy (DRMS) Levee Fragility		Total Head and Vertical Gradient Contours for Slough Water EL: +7 ft - Model without Drainage Ditch Terminous Tract	Figure 7-37
URS	Project No. 26815621		

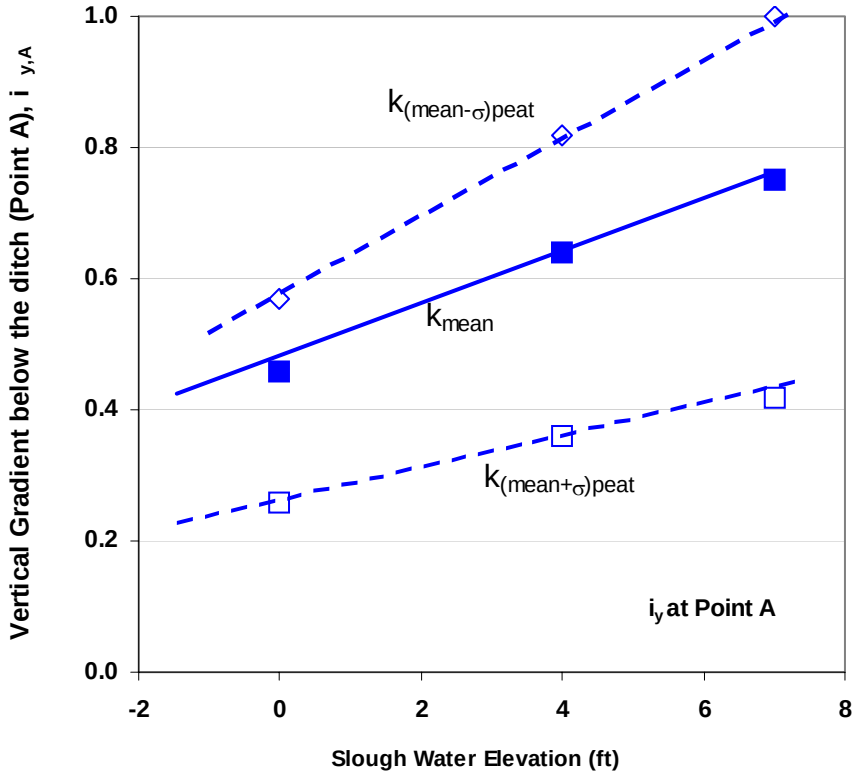

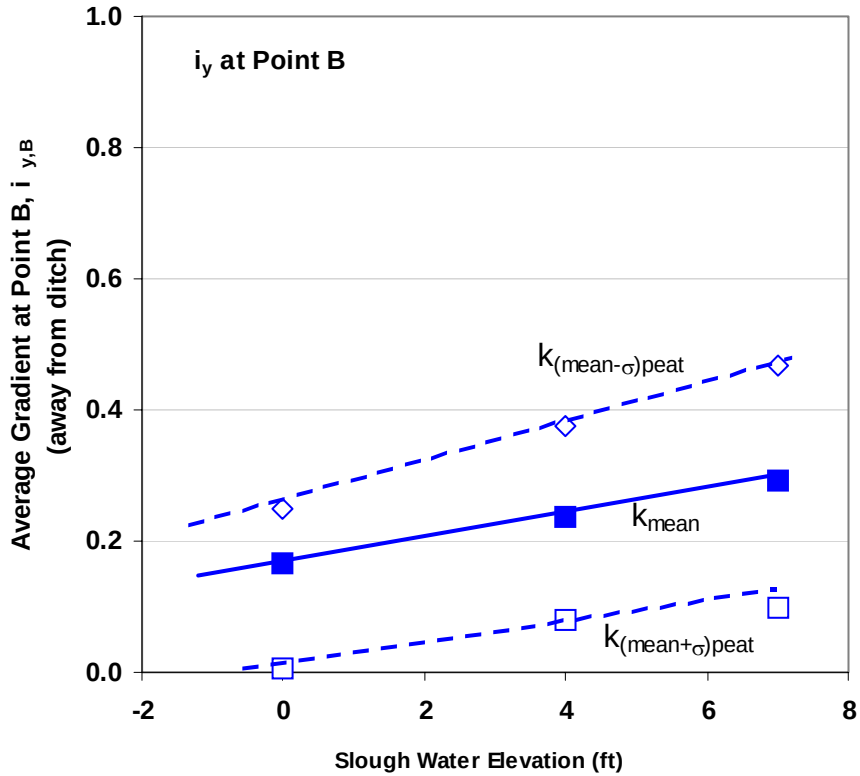

Note:

1. Gradients were calculated for seepage model with ditch and 2 ft silt sediment deposit at slough bottom.
2. All elevations are referenced to NAVD88 (NAVD88 = NGVD29 + 2.5 ft)

Delta Risk Management Strategy (DRMS) Levee Fragility		Effect of Permeability of Peat Initial Analysis -Terminous Tract	Figure 7-38
URS	Project No. 26815621		

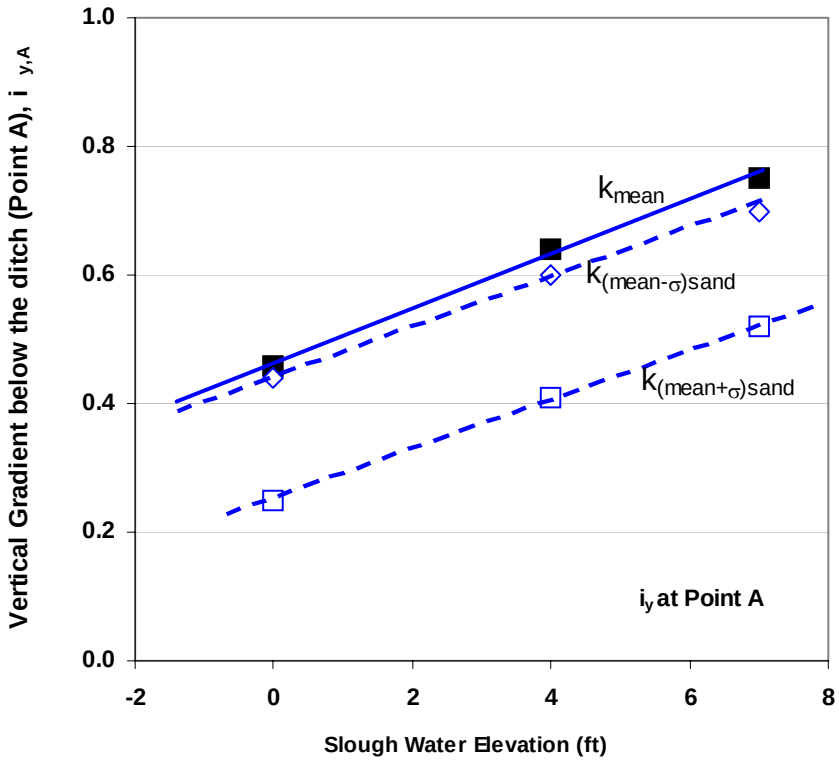

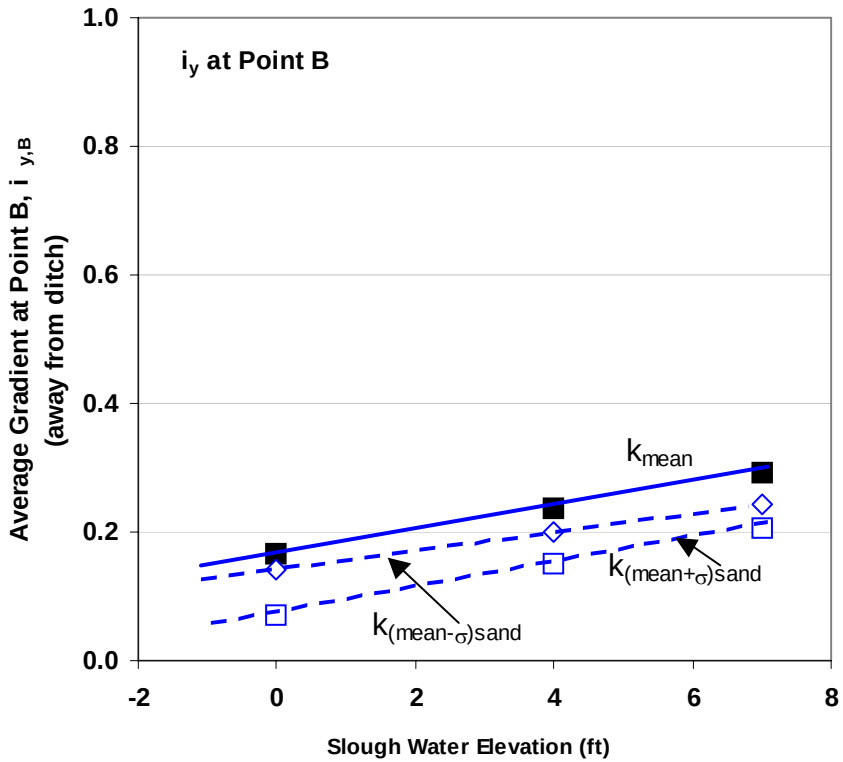

Note:

1. Gradients were calculated for seepage model with ditch and 2 ft silt sediment deposit at slough bottom.
2. All elevations are referenced to NAVD88
   (NAVD88 = NGVD29 + 2.5 ft)

Delta Risk Management Strategy (DRMS) Levee Fragility		Effect of Permeability of Sand Aquifer Initial Analysis -Terminous Tract	Figure 7-39
URS	Project No. 26815621		

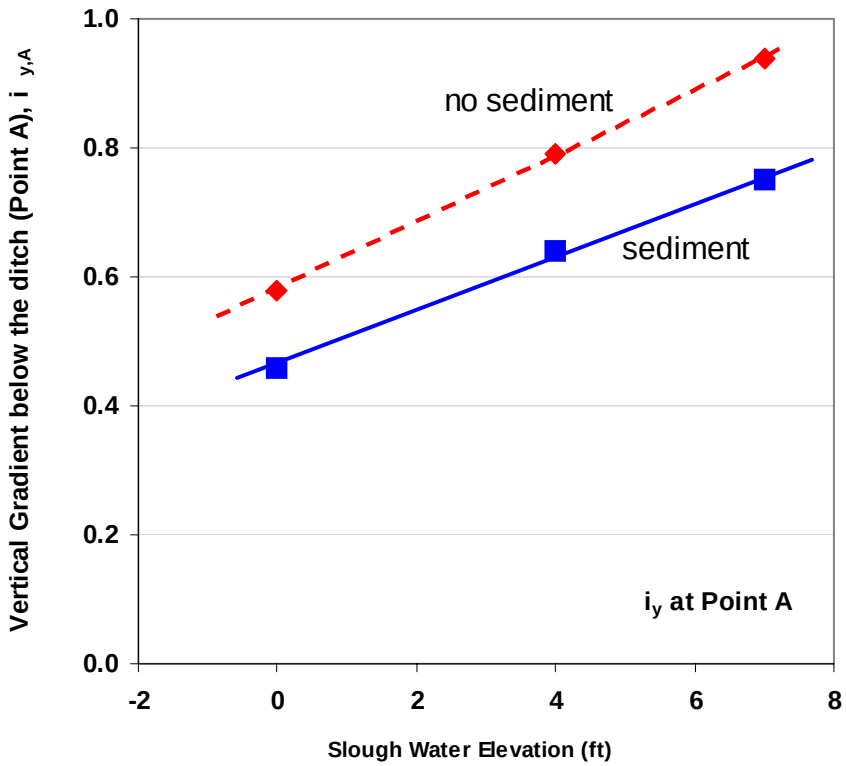

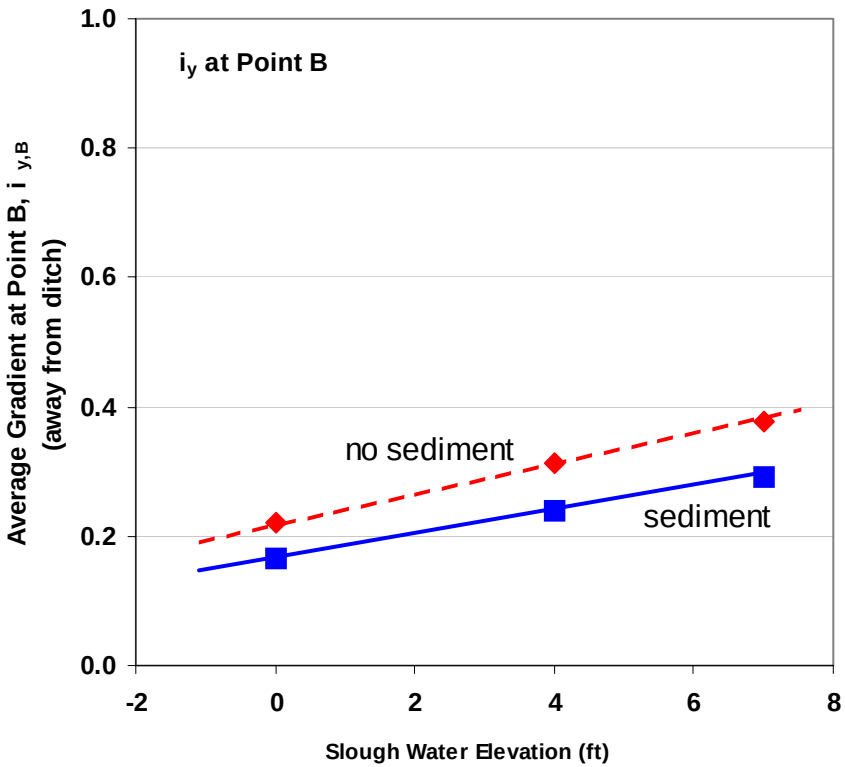

Note:
1. Gradients were calculated for seepage model with ditch.
2. All elevations are referenced to NAVD88
   (NAVD88 = NGVD29 + 2.5 ft)

Delta Risk Management Strategy (DRMS) Levee Fragility		Effect of Slough Sediment Initial Analysis -Terminous Tract	Figure 7-40
URS	Project No. 26815621		

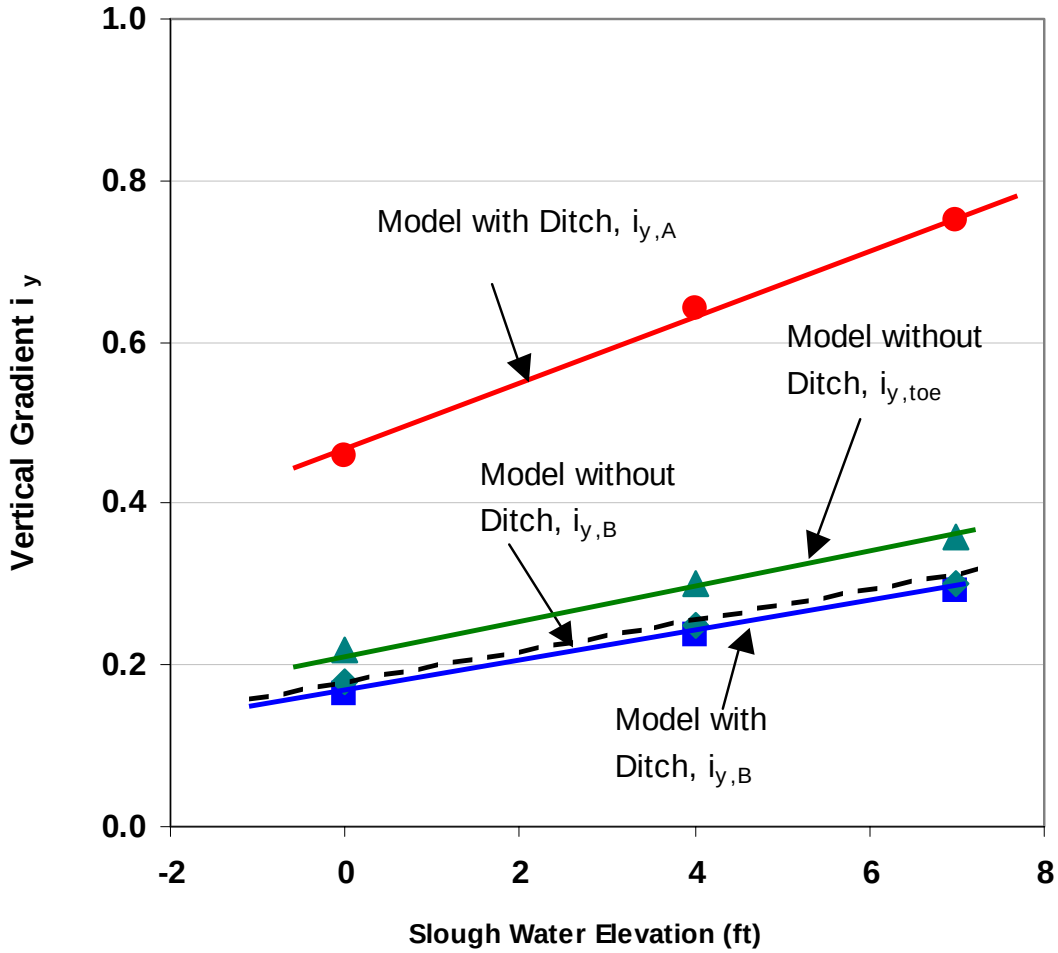

Note:
Gradients were calculated for seepage model with 2 ft silt sediment deposit at slough bottom.

Elevations are referenced to NAVD88

Delta Risk Management Strategy (DRMS) Levee Fragility		Effect of Drainage Ditch Initial Analysis -Terminous Tract	Figure 7-41
URS	Project No. 26815621		

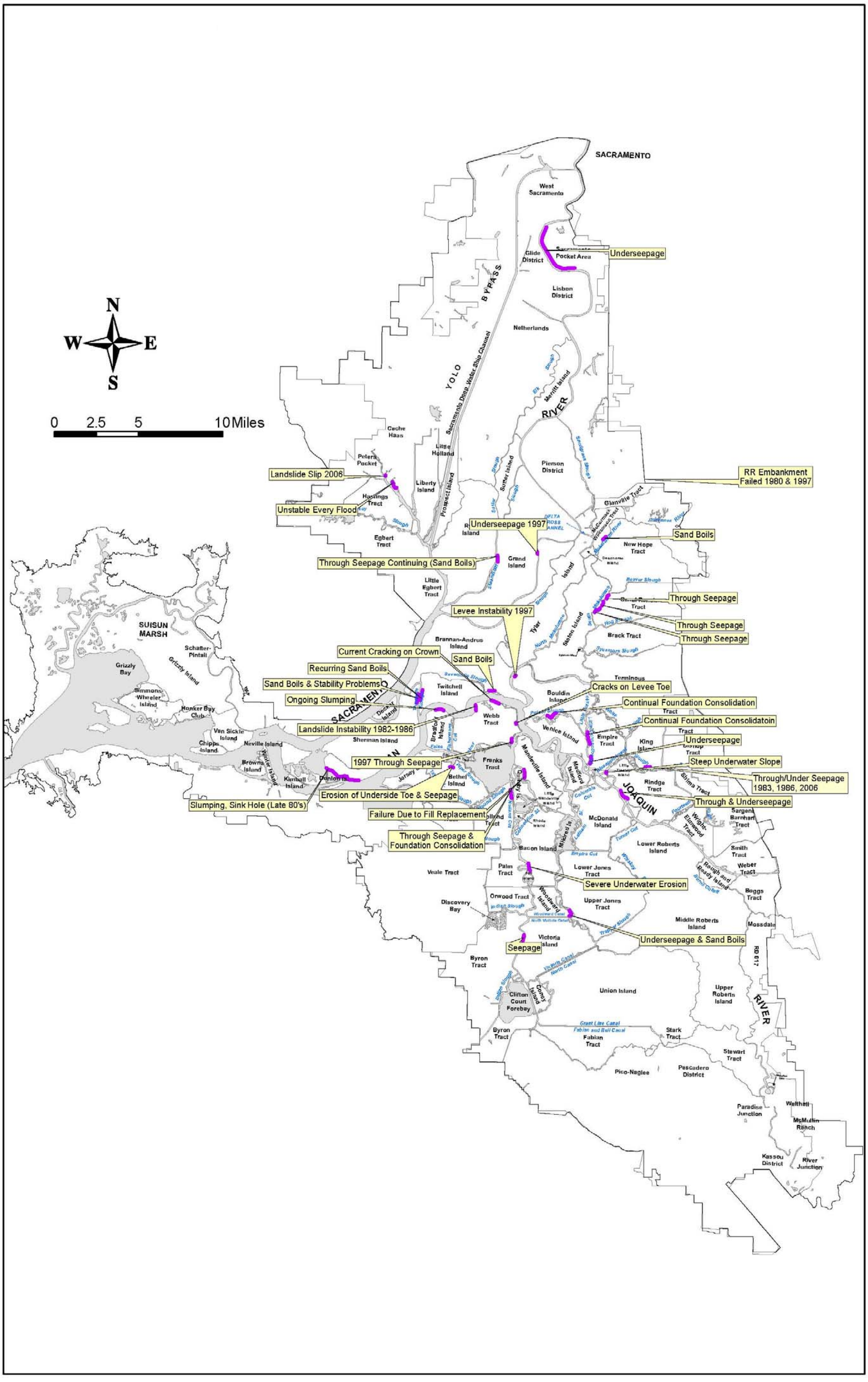

Delta Risk Management Strategy (DRMS) Levee Fragility		Reported Problem Areas	Figure 7-42
URS	Project No. 26815621		

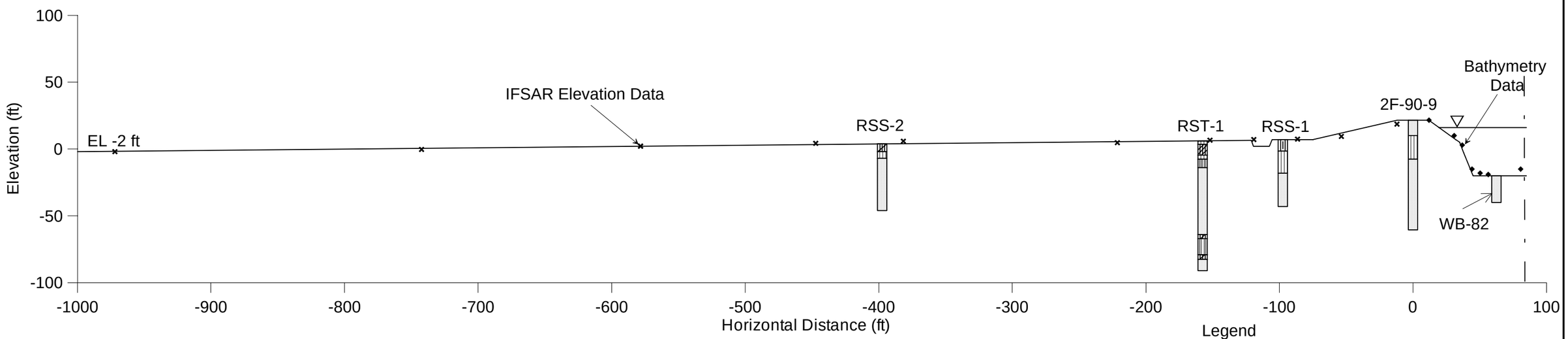

Legend

- Sand
- Silty Clay
- Silt
- Silty Sand
- Organic Silt

Note:
The above cross section was constructed based on boring data collected at/near the site.

Borings WB-82, RSS-1, RST-1, and RSS-2 were collected from "Salinity Control Barrier Investigation", DWR, 1958.

Boring 2F-90-9 was collected from "Sacramento River Flood Control System Evaluation, Lower Sacramento Area", COE, 1993.

Based on boring RSS-1 and Organic Thickness Map, it was conservatively assumed that the top foundation layer has 10 ft thick peat/organic material.

All elevations are referenced to NAVD88 (NAVD88 = NGVD29 + 2.5 ft)

Delta Risk Management Strategy (DRMS) Levee Fragility		Topography and Boring Data Grand Island	Figure 7-43
URS	Project No. 26815621		

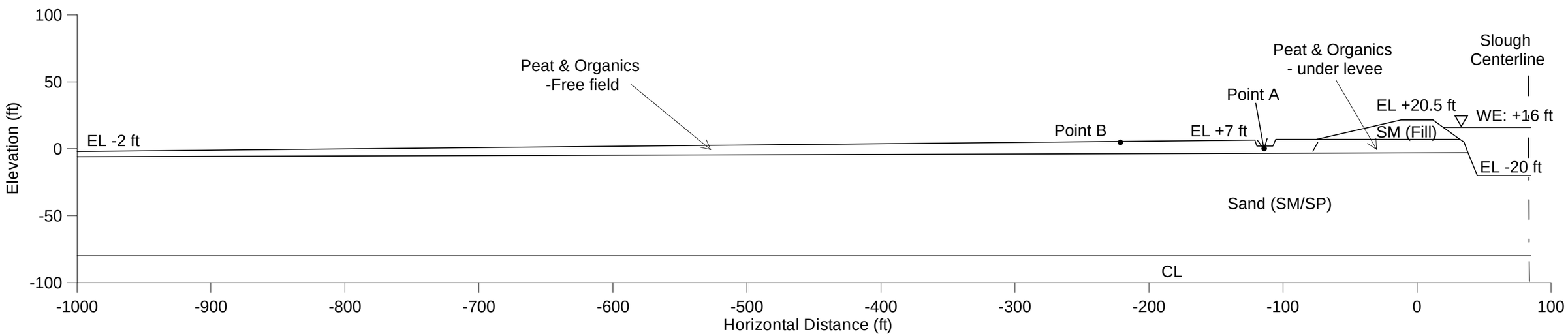

Note:
All elevations are referenced to NAVD88
(NAVD88 = NGVD29 + 2.5 ft)
Water Elevation: +16 ft (NAVD88)

Delta Risk Management Strategy (DRMS) Levee Fragility		Idealized Cross-section Grand Island	Figure 7-44
URS	Project No. 26815621		

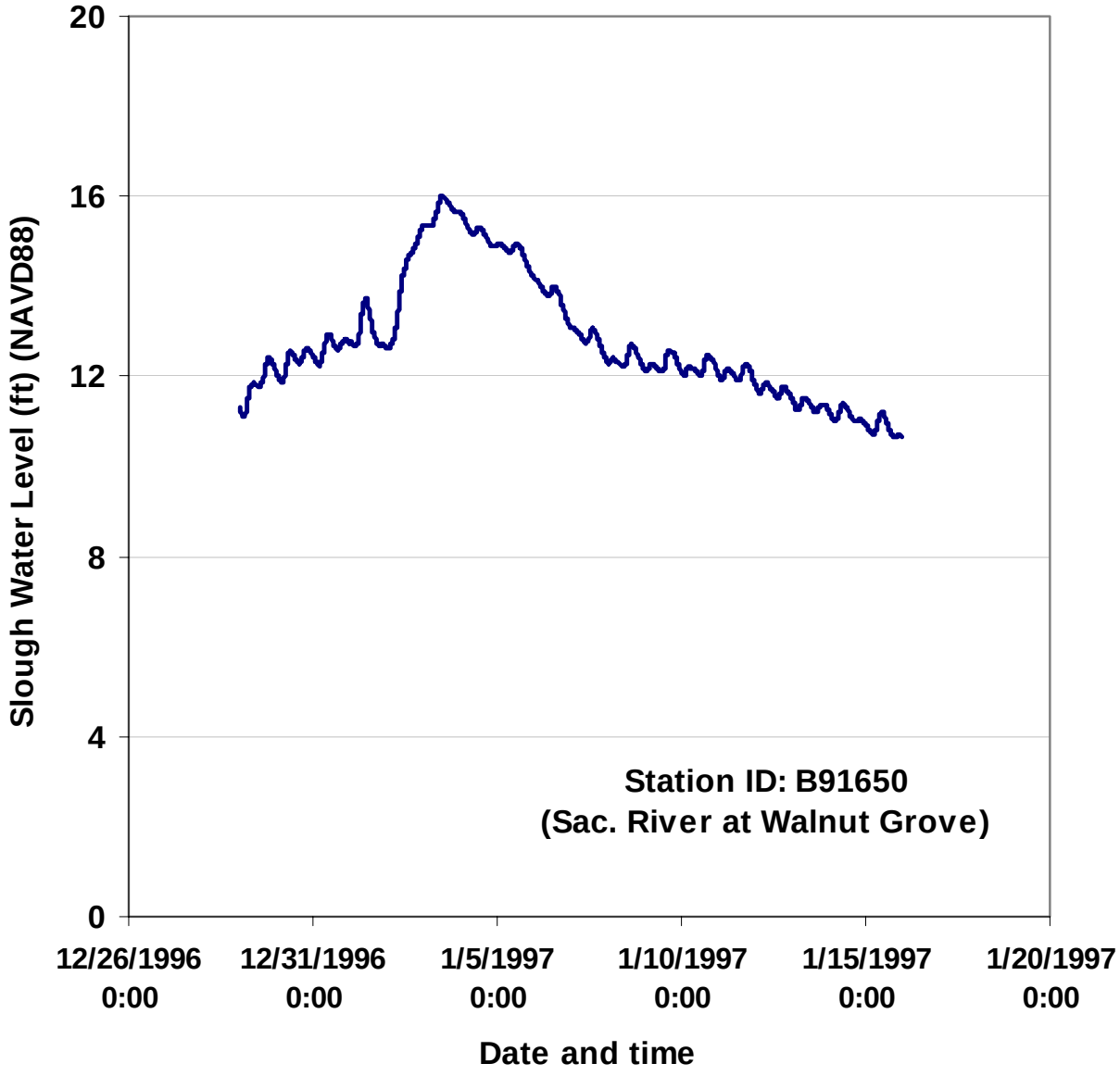

Delta Risk Management Strategy (DRMS) Levee Fragility		Monitored Slough Water Level at Walnut Grove Station (ID:91650)	Figure 7-45
URS	Project No. 26815621		

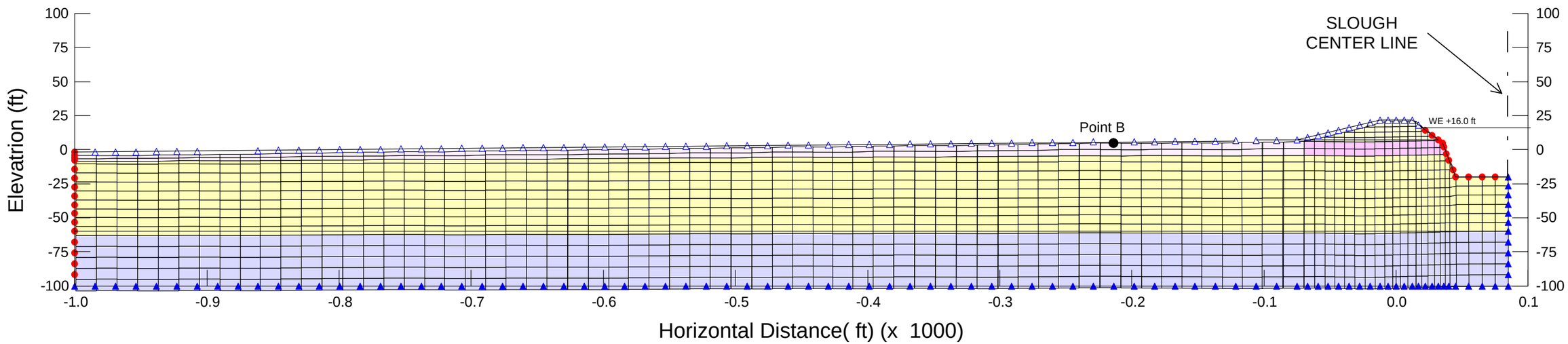

Seepage Model without Ditch

Legend

Boundary Conditions

- No flow
- Fixed head
- Review

Material Type

- Sandy Levee Fill
- Free Field Peat
- Under Levee Peat
- Sand (SP/SM)
- Clay

Delta Risk Management Strategy (DRMS) Levee Fragility		Finite Element Mesh and Boundary Conditions Grand Island Underseepage Problem	Figure 7-46
URS	Project No. 26815621		

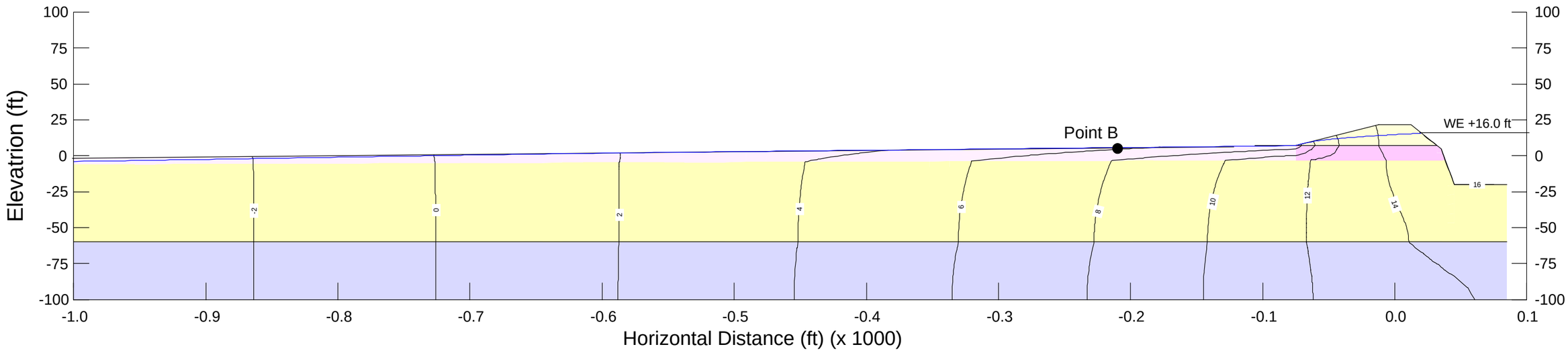

(a) Total head distribution contours

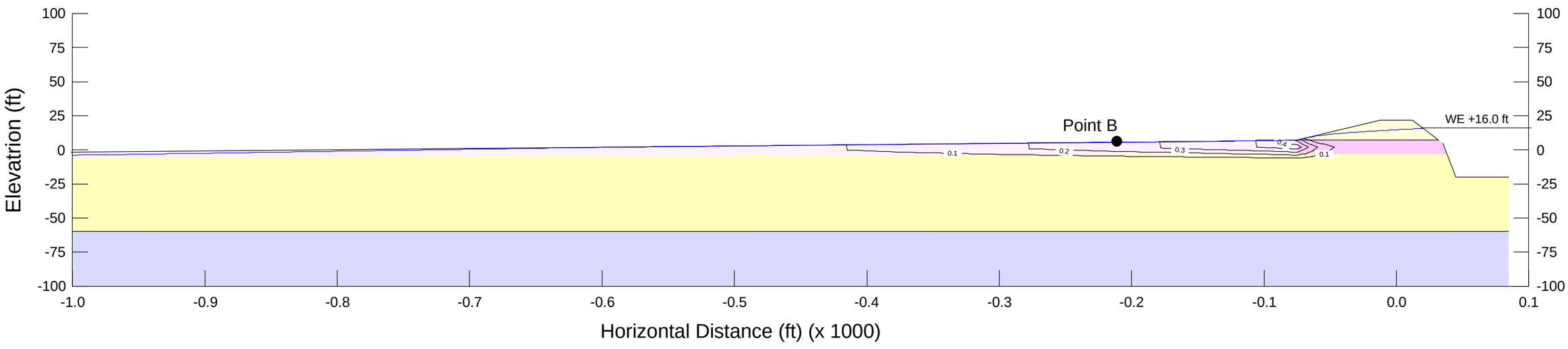

(b) Vertical gradient contours

Note:
All elevations are referenced to NAVD88
(NAVD88 = NGVD29 + 2.5 ft)

Delta Risk Management Strategy (DRMS) Levee Fragility		Total Head & Vertical Gradient Contours for $(k_h/k_v)_{peat}$ = 10 Grand Island Underseepage Problem	Figure 7-47
URS	Project No. 26815621		

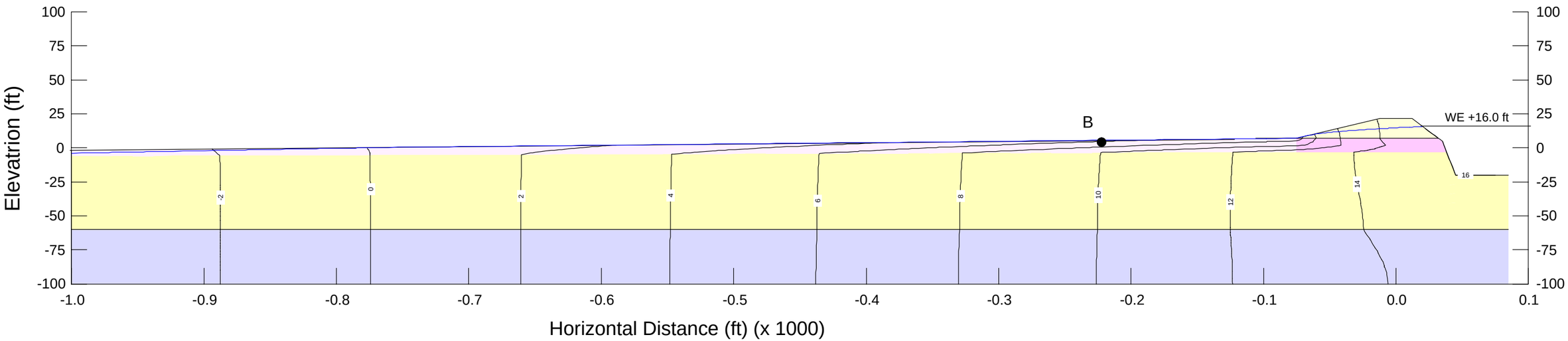

(a) Total head distribution contours

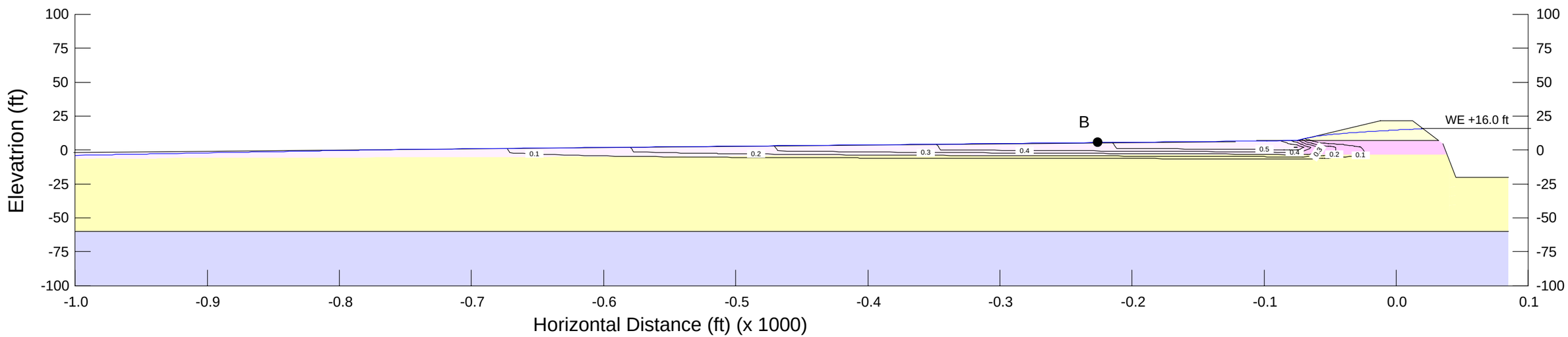

(b) Vertical gradient contours

Note:
All elevations are referenced to NAVD88

Delta Risk Management Strategy (DRMS) Levee Fragility		Total Head & Vertical Gradient Contours for $(k_h/k_v)_{peat}$ = 100 Grand Island Underseepage Problem	Figure 7-48
URS	Project No. 26815621		

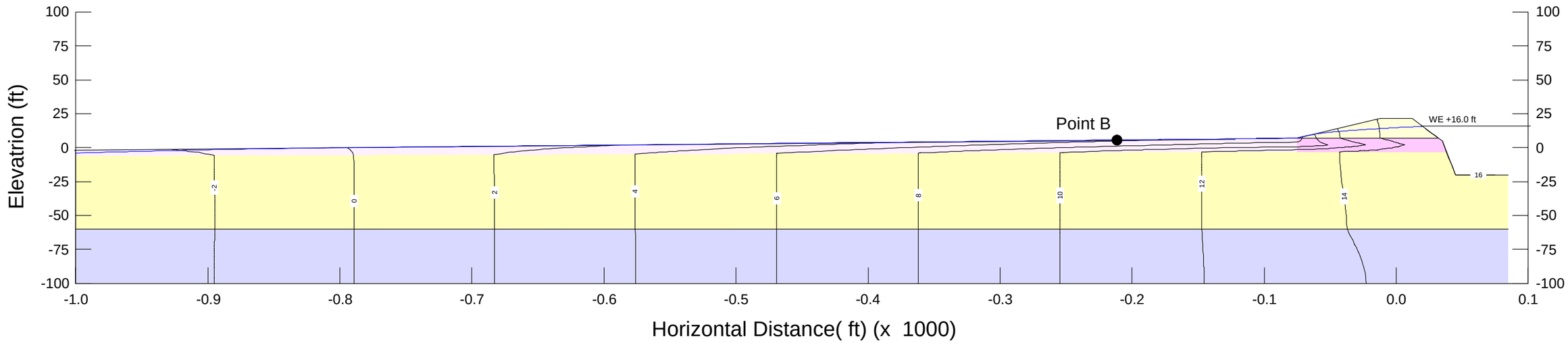

(a) Total head distribution contours

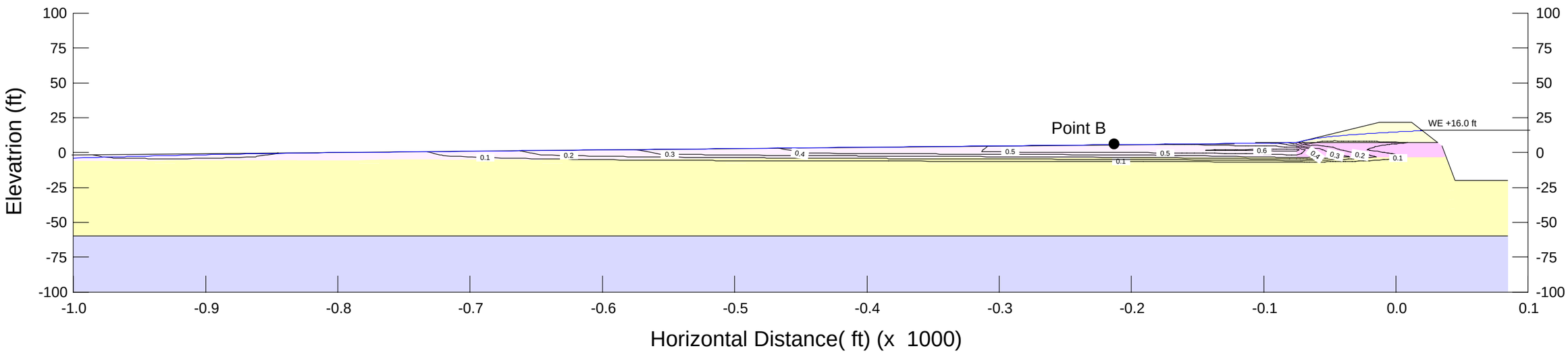

(b) Vertical gradient contours

Note:
All elevations are referenced to NAVD88
(NAVD88 = NGVD29 + 2.5 ft)

Delta Risk Management Strategy (DRMS) Levee Fragility		Total Head & Vertical Gradient Contours for $(k_h/k_v)_{peat}$ = 1000 Grand Island Underseepage Problem	Figure 7-49
URS	Project No. 26815621		

DRAFT

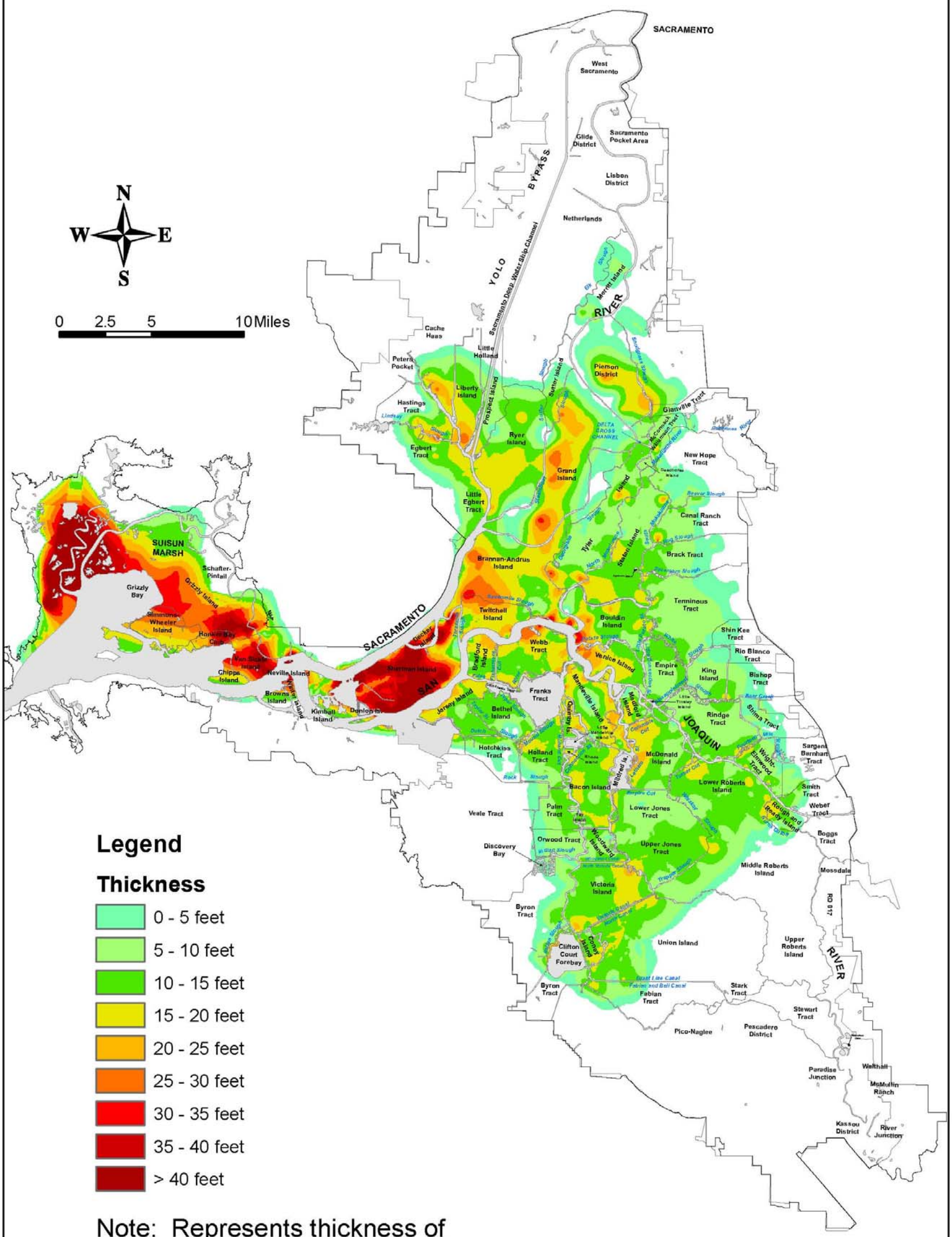

Note: Represents thickness of organic materials near levee toe.

Delta Risk Management Strategy (DRMS) Levee Fragility		Thickness of Organic Materials	Figure 7-50
URS	Project No. 26815621		

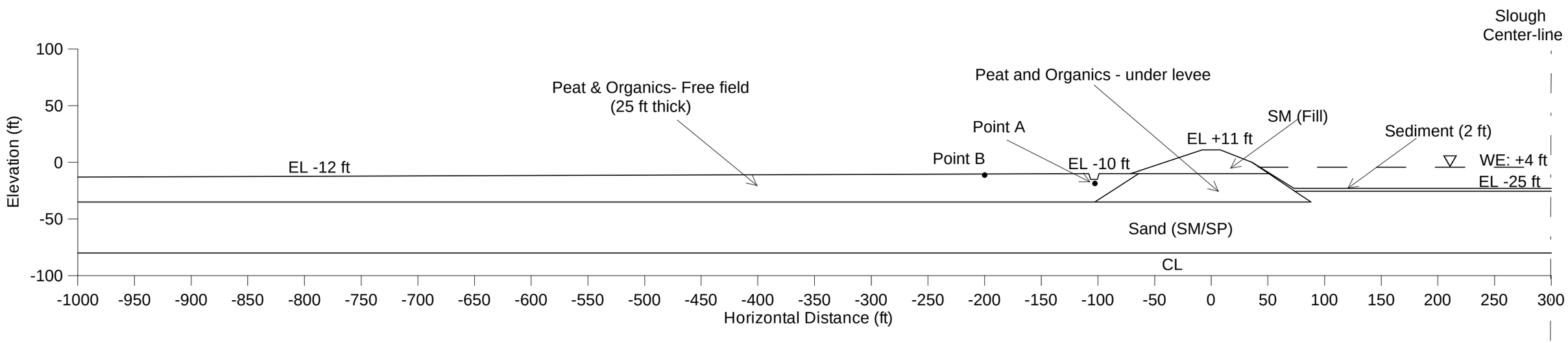

Note:
Typical cross section with drainage ditch and slough sediment
Landside slope: 3:1
Waterside slope: 2.5:1 from crest to EL 0 ft, and then 1.5:1
Crest width: 16 ft

All elevations are referenced to NAVD88
(NAVD88 = NGVD29 + 2.5 ft)

Delta Risk Management Strategy (DRMS) Levee Fragility		Typical Cross Section with Drainage Ditch and 25 ft Peat & Organic Layer	Figure 7-51
URS	Project No. 26815621		

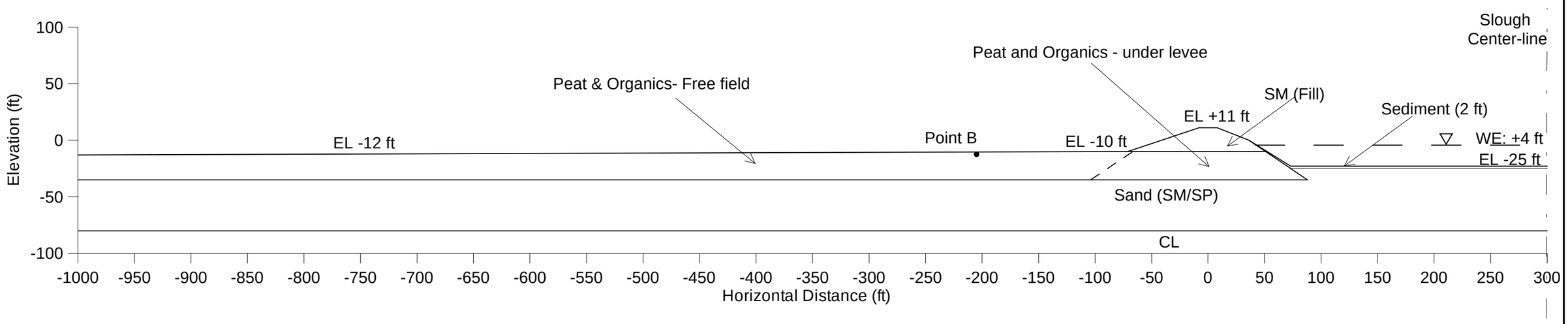

Note:
Model without drainage ditch and with slough sediment
Landside slope: 3:1
Waterside slope: 2.5:1 from crest to EL 0 ft, and then 1.5:1
Crest Width: 16 ft

All elevations are referenced to NAVD88
(NAVD88 = NGVD29 + 2.5 ft)

Delta Risk Management Strategy (DRMS) Levee Fragility		Typical Cross Section without Drainage Ditch and 25 ft Peat & Organic Layer	Figure 7-52
URS	Project No. 26815621		

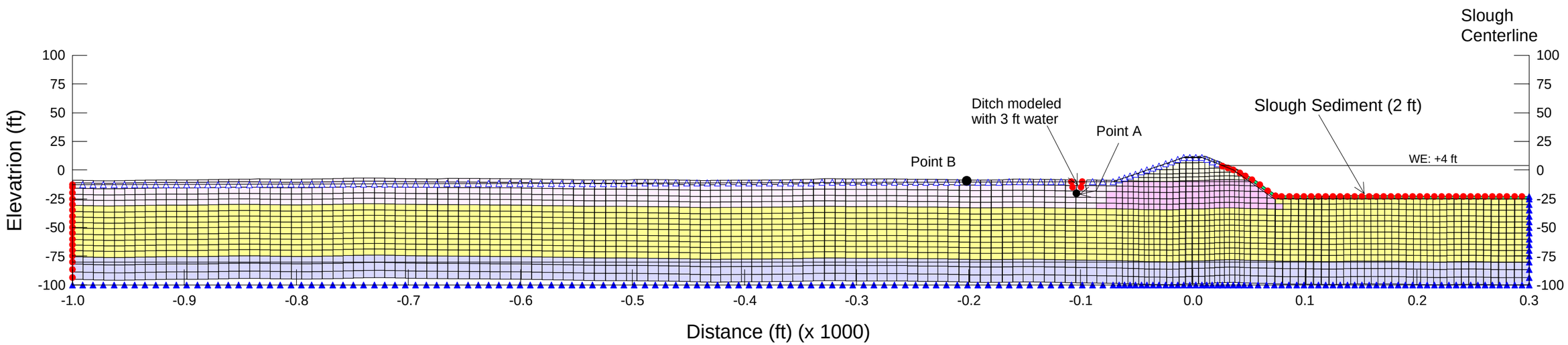

Legend

Boundary Conditions

- No flow
- Fixed head
- Review

Material Type

- Sandy Levee Fill
- Free Field Peat
- Under Levee Peat
- Sand (SP/SM)
- Clay
- Slough Sediment

Note:
All elevations are referenced to NAVD88
(NAVD88 = NGVD29 + 2.5 ft)

Delta Risk Management Strategy (DRMS) Levee Fragility		Finite Element Mesh & Boundary Conditions Typical Cross Section with Drainage Ditch and 25 ft Peat & Organic Layer	Figure 7-53
URS	Project No. 26815621		

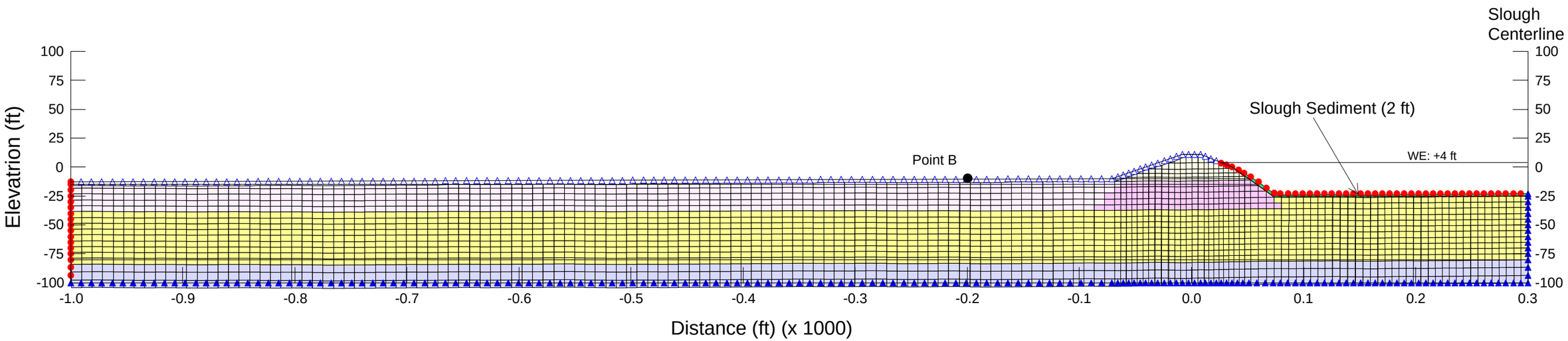

Legend

Boundary Conditions

- No flow
- Fixed head
- Review

Material Type

- Sandy Levee Fill
- Free Field Peat
- Under Levee Peat
- Sand (SP/SM)
- Clay
- Slough Sediment

Note:
All elevations are referenced to NAVD88
(NAVD88 = NGVD29 + 2.5 ft)

Delta Risk Management Strategy (DRMS) Levee Fragility		Finite Element Mesh & Boundary Conditions Typical Cross Section without Ditch and 25 ft Peat & Organic Layer	Figure 7-54
URS	Project No. 26815621		

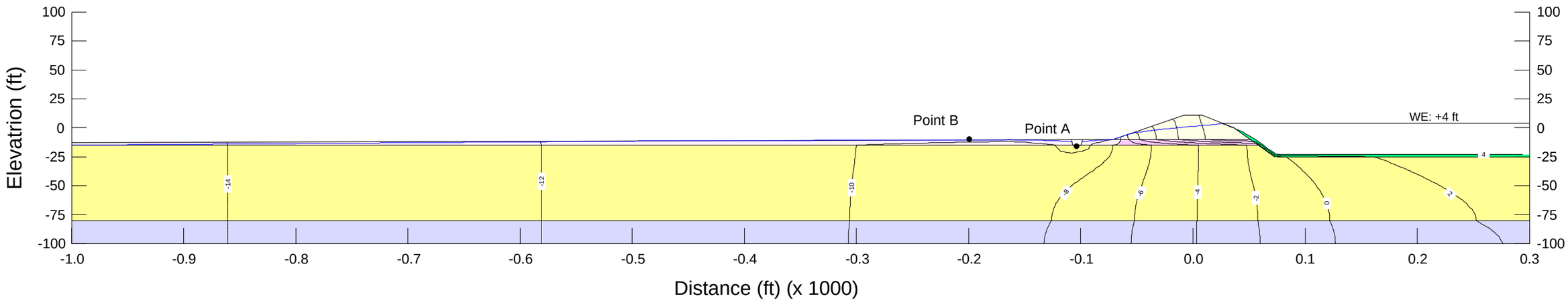

(a) Total head contours for slough water elevation of +4 ft

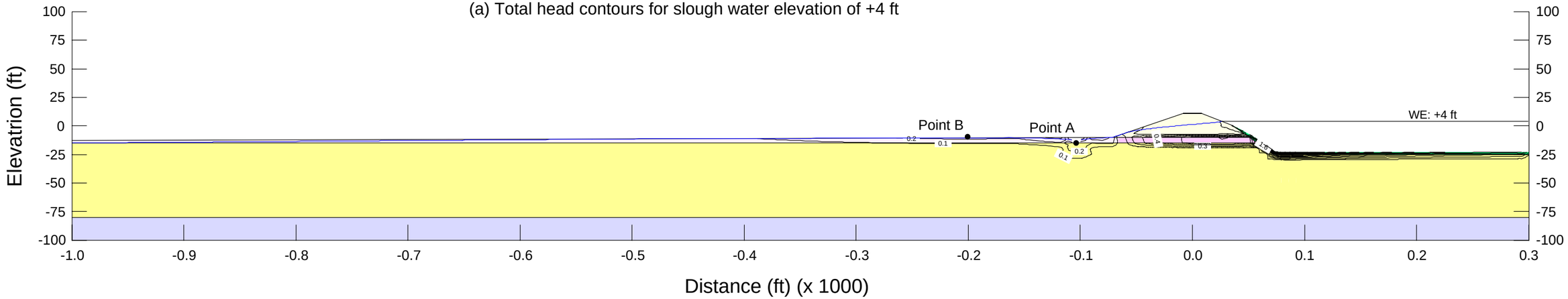

(b) Vertical exit gradient contours for slough water elevation of +4 ft

Note:
Analysis CAse:
Mean Permeability values, 5 feet peat/organics,
model with drainage ditch and with slough sediment

All elevations are referenced to NAVD88
(NAVD88 = NGVD29 + 2.5 ft)

Delta Risk Management Strategy (DRMS) Levee Fragility		Total Head & Vertical Gradient Contours Typical Cross Section with Drainage Ditch for 5 ft Peat	Figure 7-55
URS	Project No. 26815621		

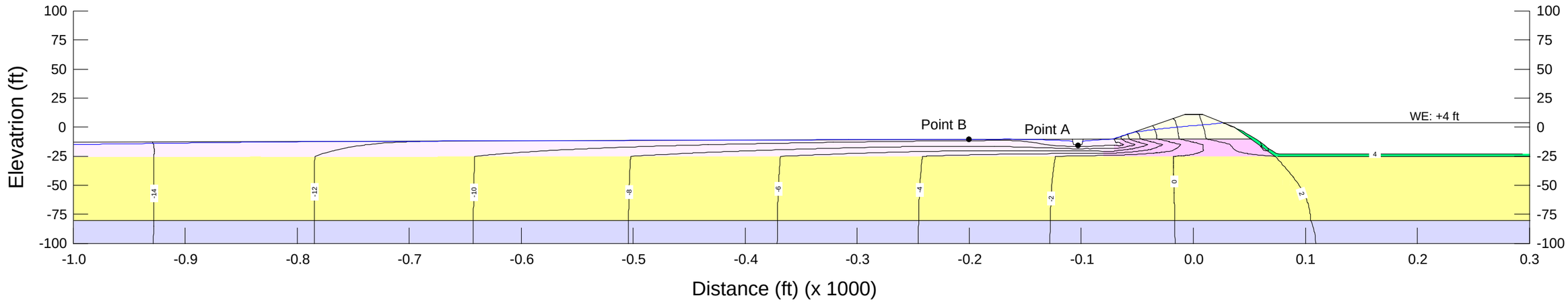

(a) Total head contours for slough water elevation of +4 ft

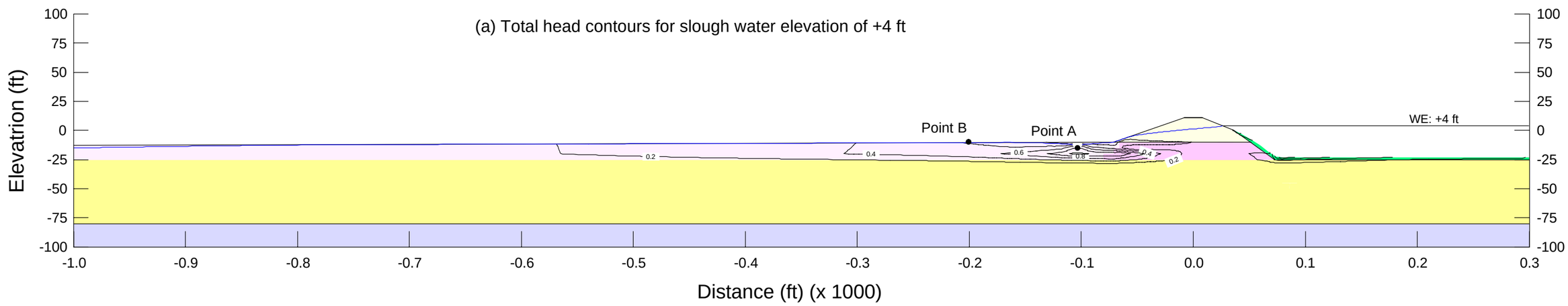

(b) Vertical exit gradient contours for slough water elevation of +4 ft

Note:
Analysis CAse:
Mean Permeability values, 15 feet peat/organics,
model with drainage ditch and with slough sediment

All elevations are referenced to NAVD88
(NAVD88 = NGVD29 + 2.5 ft)

Delta Risk Management Strategy (DRMS) Levee Fragility		Total Head & Vertical Gradient Contours Typical Cross Section with Drainage Ditch for 15 ft Peat	Figure 7-56
URS	Project No. 26815621		

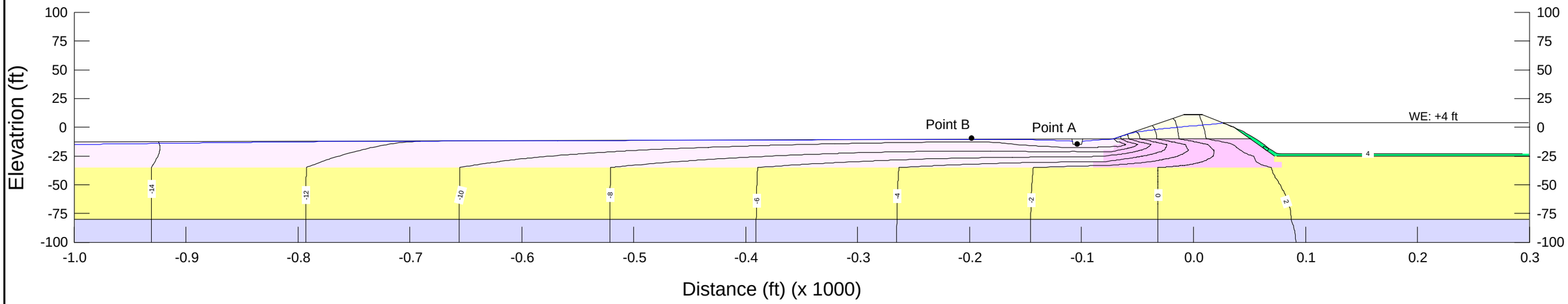

(a) Total head contours for slough water elevation of +4 ft

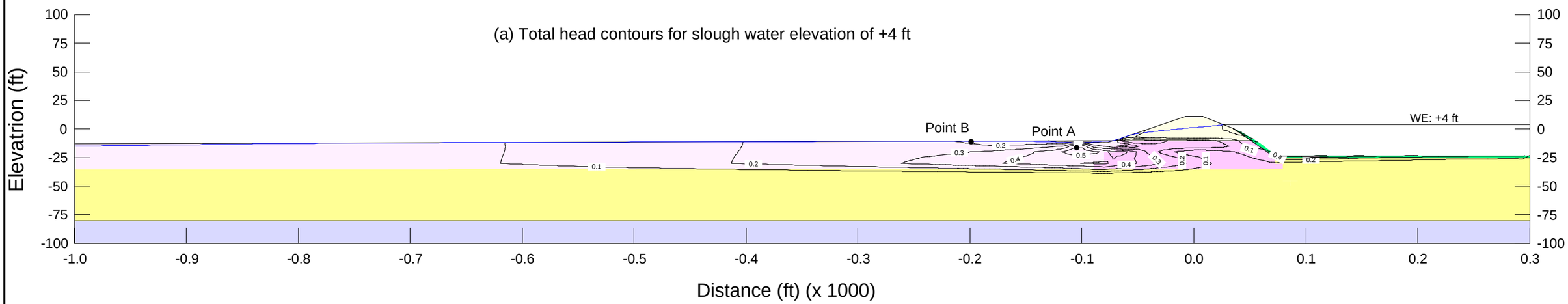

(b) Vertical exit gradient contours for slough water elevation of +4 ft

Note:
Analysis CAse:
Mean Permeability values, 25 feet peat/organics,
model with drainage ditch and with slough sediment

All elevations are referenced to NAVD88
(NAVD88 = NGVD29 + 2.5 ft)

Delta Risk Management Strategy (DRMS) Levee Fragility		Total Head & Vertical Gradient Contours Typical Cross Section with Drainage Ditch for 25 ft Peat	Figure 7-57
URS	Project No. 26815621		

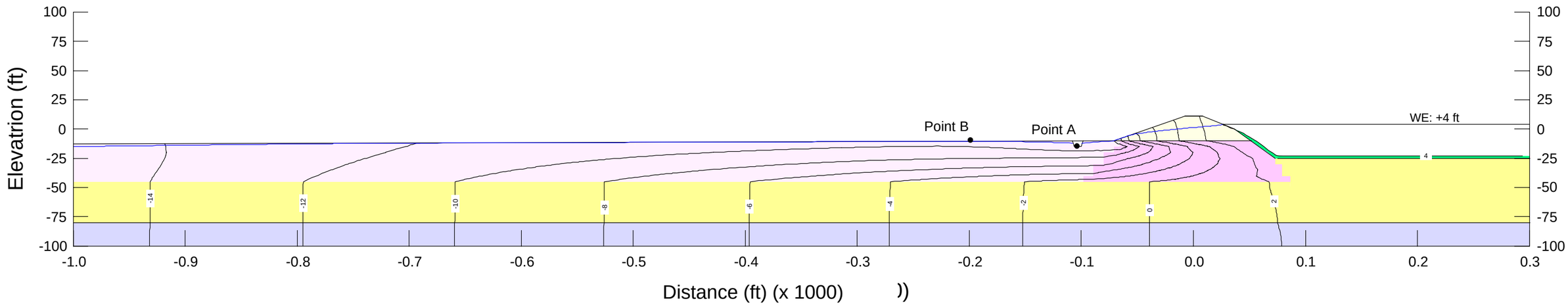

(a) Total head contours for slough water elevation of +4 ft

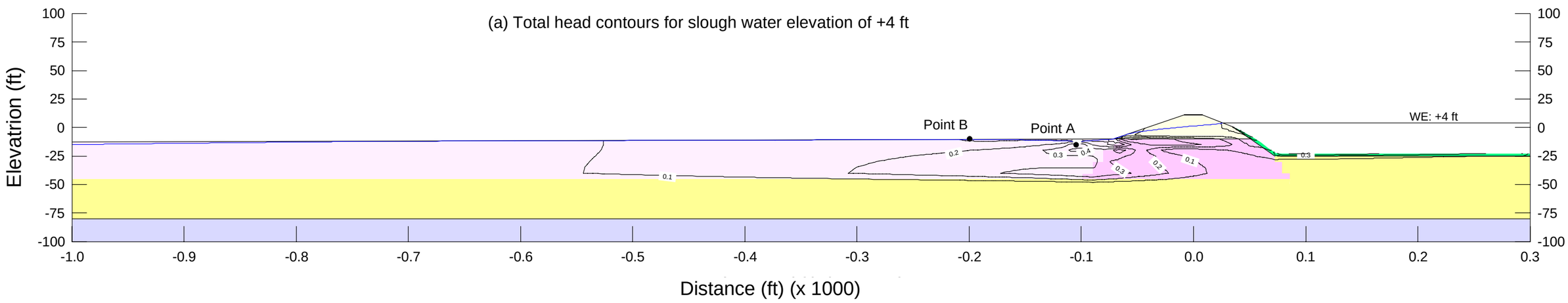

(b) Vertical exit gradient contours for slough water elevation of +4 ft

Note:
Analysis CAse:
Mean Permeability values, 35 feet peat/organics,
model with drainage ditch and with slough sediment

All elevations are referenced to NAVD88
(NAVD88 = NGVD29 + 2.5 ft)

Delta Risk Management Strategy (DRMS) Levee Fragility		Total Head & Vertical Gradient Contours Typical Cross Section with Drainage Ditch for 35 ft Peat	Figure 7-58
URS	Project No. 26815621		

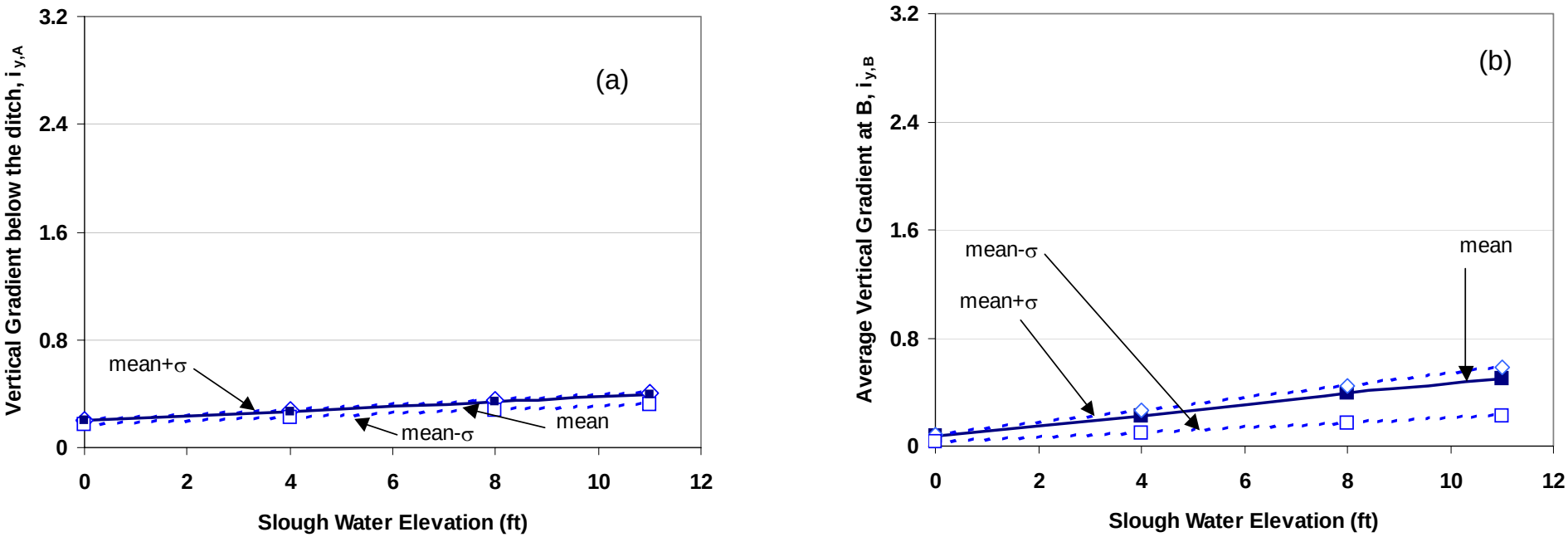

Note:
Analysis model: Typical cross section for Delta, 5 ft peat & organic layer, model with drainage ditch and slough sediment

All elevations are referenced to NAVD88
(NAVD88 = NGVD29+2.5 ft)

Delta Risk Management Strategy (DRMS) Levee Fragility		Vertical Gradients for 5 ft Peat/Organics - Typical Cross Section with Ditch	Figure 7-59
URS	Project No. 26815621		

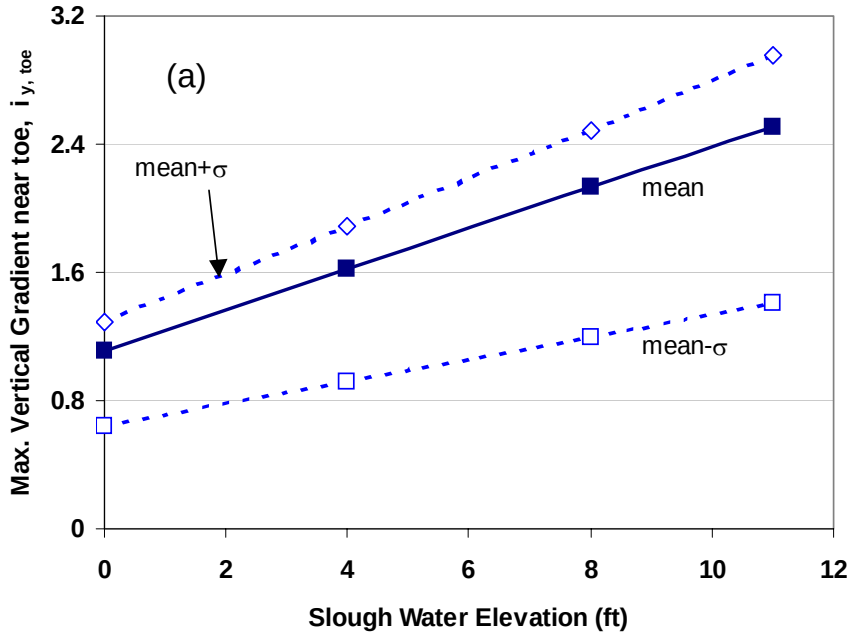

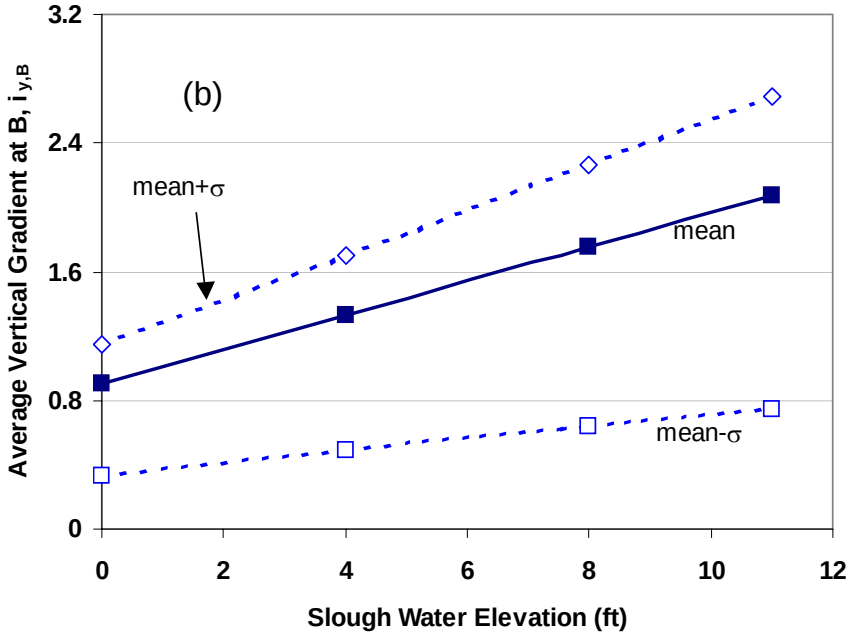

Note:
Analysis model: Typical cross section for Delta, 5 ft peat & organic layer, model without drainage ditch and slough sediment

All elevations are referenced to NAVD88
(NAVD88 = NGVD29+2.5 ft)

Delta Risk Management Strategy (DRMS) Levee Fragility		Vertical Gradients for 5 ft Peat/Organics - Typical Cross Section without Ditch	Figure 7-60
URS	Project No. 26815621		

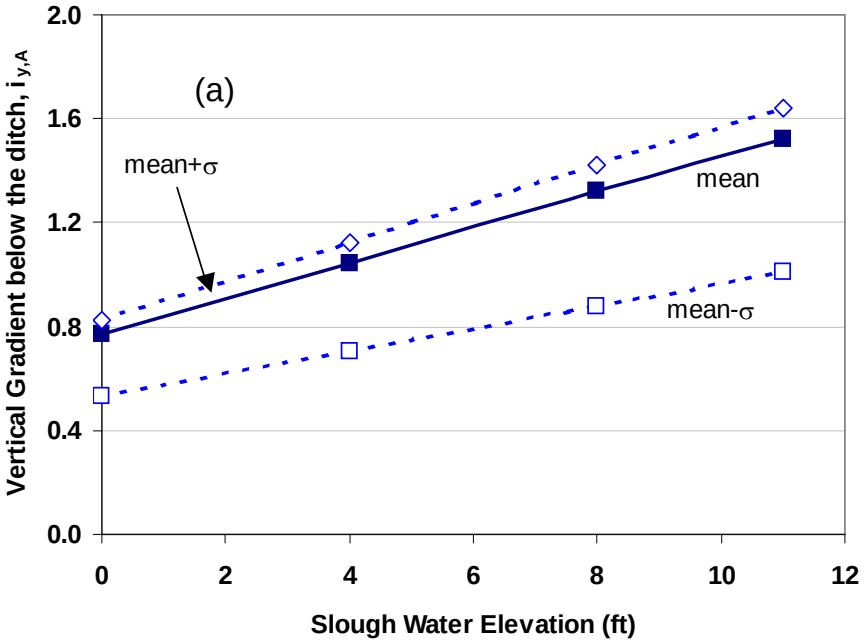

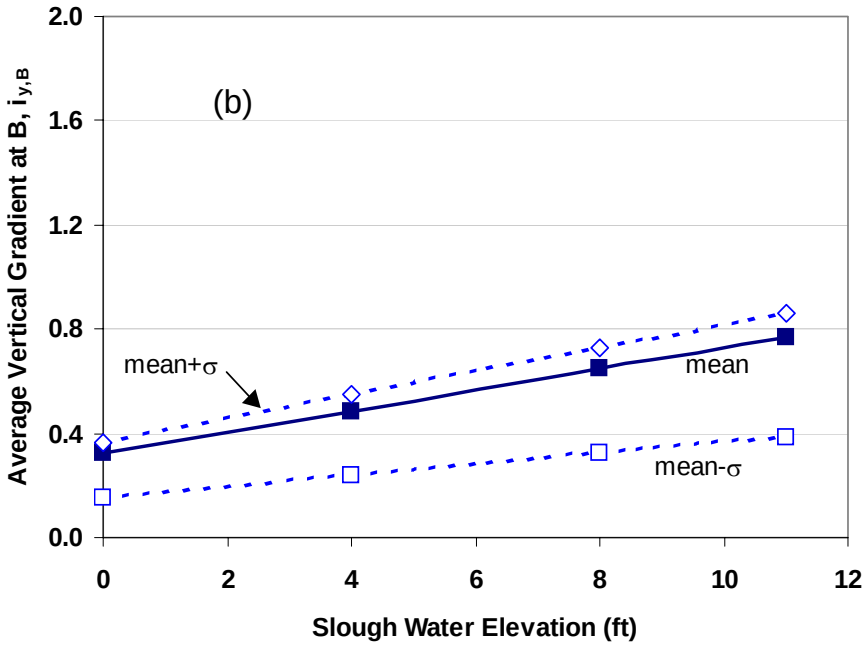

Note:
Analysis model: Typical cross section for Delta, 15 ft peat & organic layer, model with drainage ditch and slough sediment

All elevations are referenced to NAVD88
(NAVD88 = NGVD29+2.5 ft)

Delta Risk Management Strategy (DRMS) Levee Fragility		Vertical Gradients for 15 ft Peat/Organics - Typical Cross Section with Ditch	Figure 7-61
URS	Project No. 26815621		

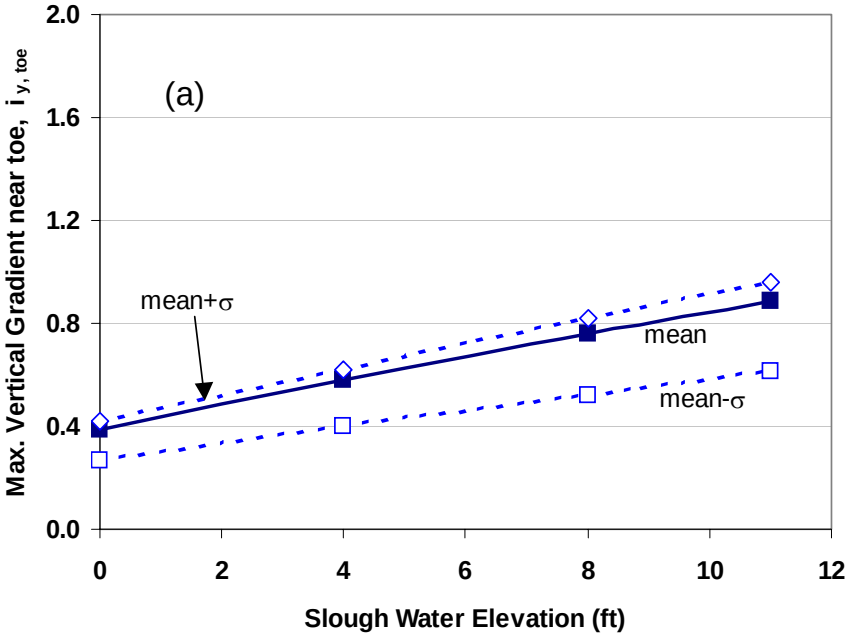

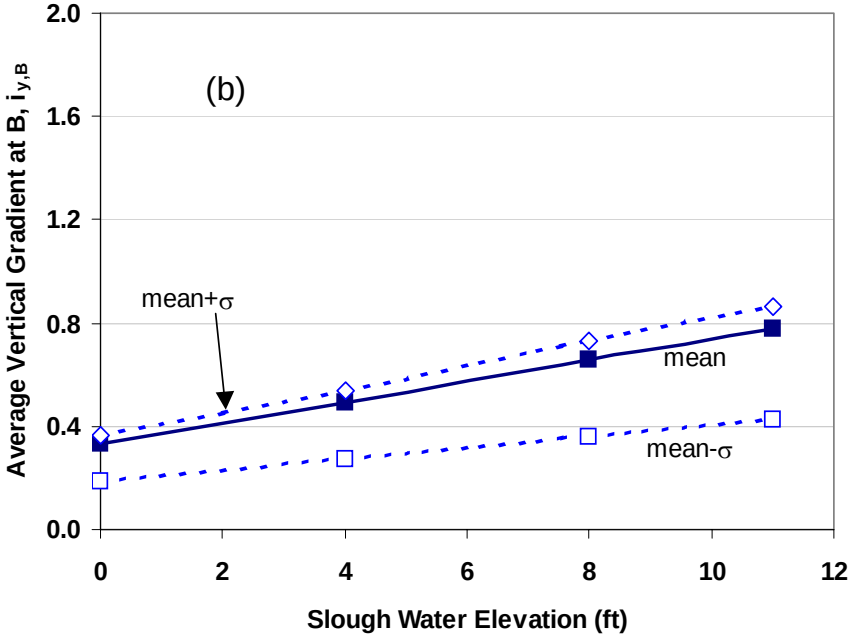

Note:
Analysis model: Typical cross section for Delta, 15 ft peat & organic layer, model without drainage ditch and slough sediment

All elevations are referenced to NAVD88
(NAVD88 = NGVD29+2.5 ft)

Delta Risk Management Strategy (DRMS) Levee Fragility		Vertical Gradients for 15 ft Peat/Organics - Typical Cross Section without Ditch	Figure 7-62
URS	Project No. 26815621		

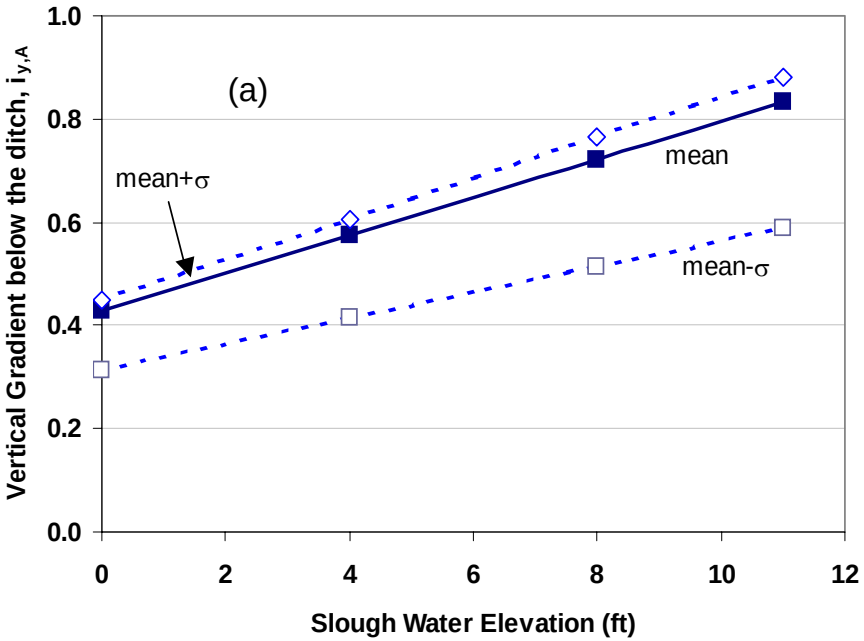

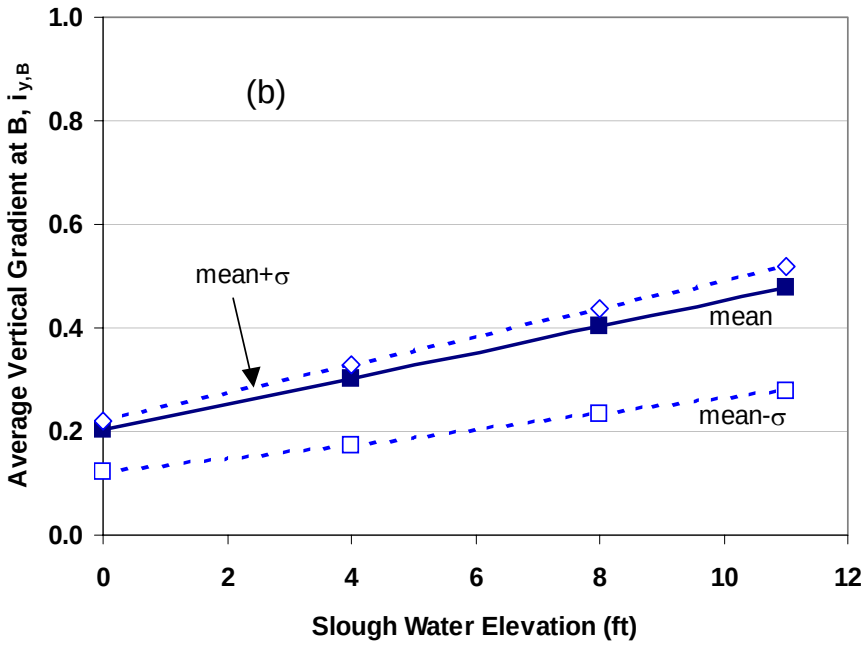

Note:
Analysis model: Typical cross section for Delta, 25 ft peat & organic layer, model with drainage ditch and slough sediment

All elevations are referenced to NAVD88
(NAVD88 = NGVD29+2.5 ft)

Delta Risk Management Strategy (DRMS) Levee Fragility		Vertical Gradients for 25 ft Peat/Organics - Typical Cross Section with Ditch	Figure 7-63
URS	Project No. 26815621		

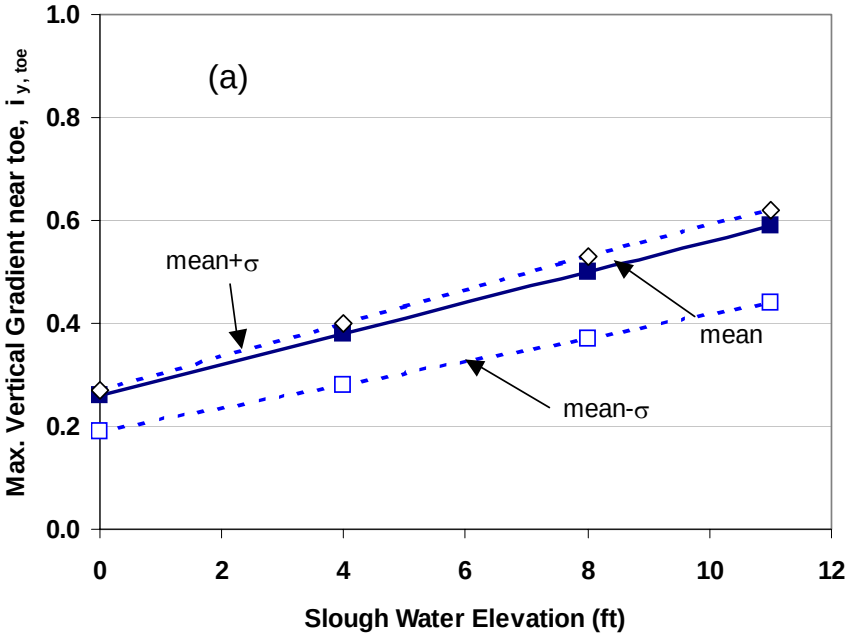

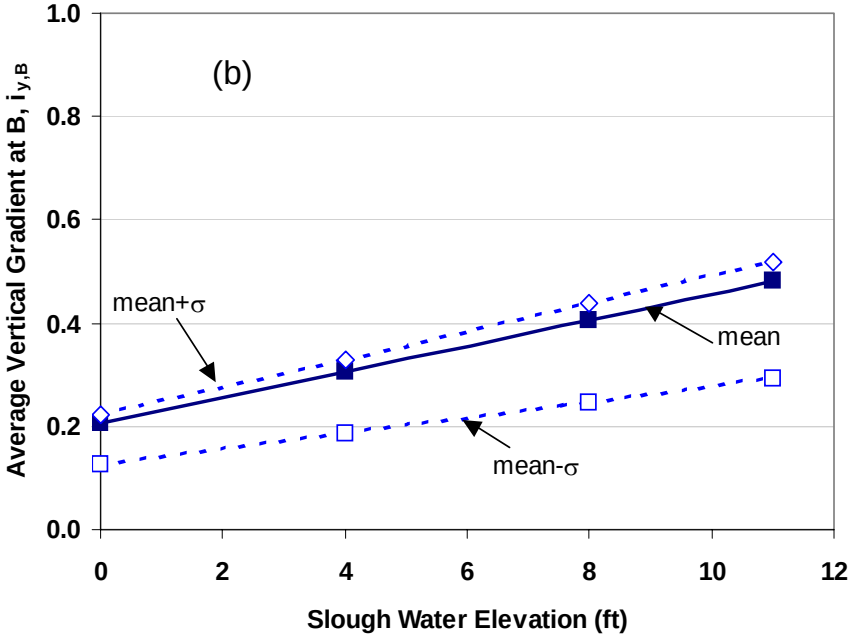

Note:
Analysis model: Typical cross section for Delta, 25 ft peat & organic layer, model without drainage ditch and slough sediment

All elevations are referenced to NAVD88
(NAVD88 = NGVD29+2.5 ft)

Delta Risk Management Strategy (DRMS) Levee Fragility		Vertical Gradients for 25 ft Peat/Organics - Typical Cross Section without Ditch	Figure 7-64
URS	Project No. 26815621		

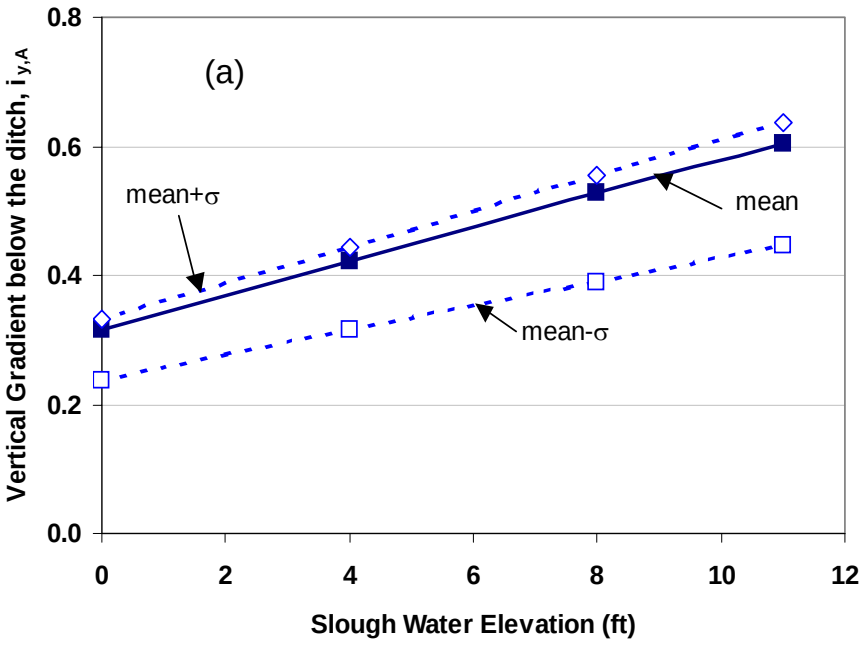

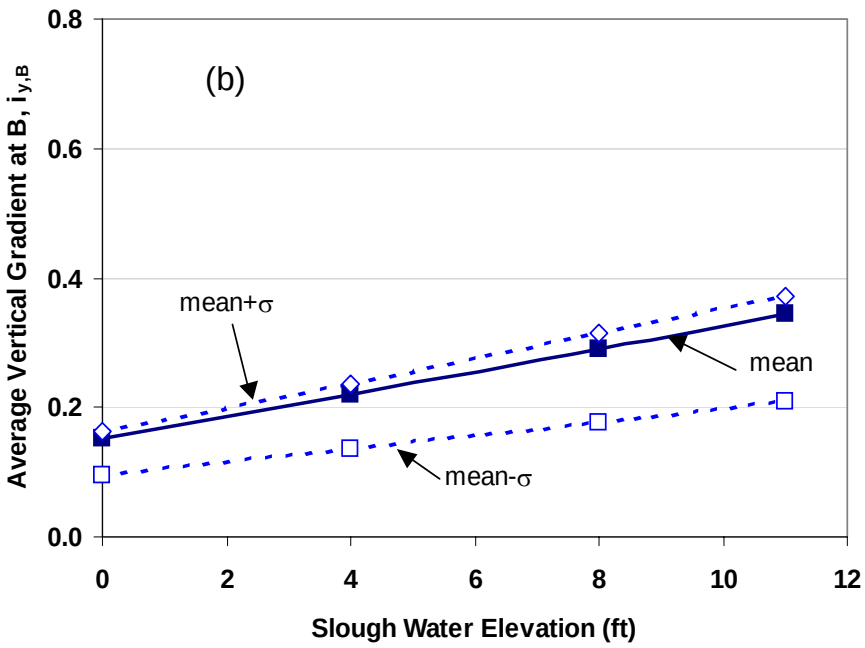

Note:
Analysis model: Typical cross section for Delta, 35 ft peat & organic layer, model with drainage ditch and slough sediment

All elevations are referenced to NAVD88
(NAVD88 = NGVD29+2.5 ft)

Delta Risk Management Strategy (DRMS) Levee Fragility		Vertical Gradients for 35 ft Peat/Organics - Typical Cross Section with Ditch	Figure 7-65
URS	Project No. 26815621		

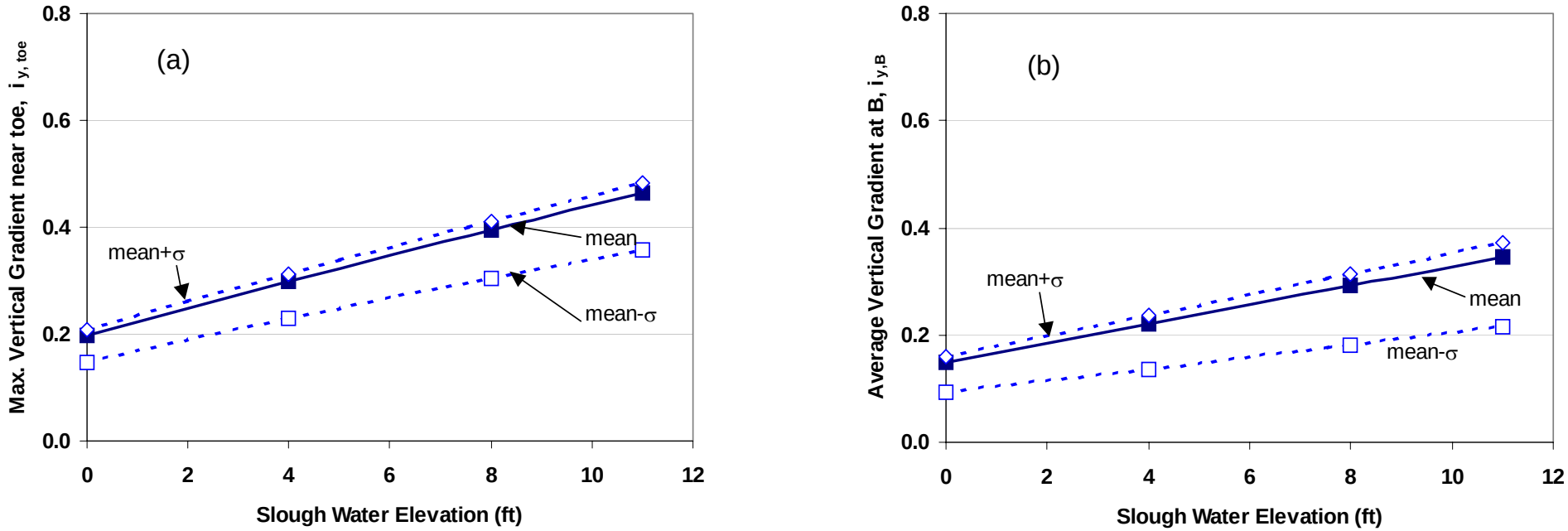

Note:
Analysis model: Typical cross section for Delta, 35 ft peat & organic layer, model without drainage ditch and slough sediment

All elevations are referenced to NAVD88
(NAVD88 = NGVD29+2.5 ft)

Delta Risk Management Strategy (DRMS) Levee Fragility		Vertical Gradients for 35 ft Peat/Organics - Typical Cross Section without Ditch	Figure 7-66
URS	Project No. 26815621		

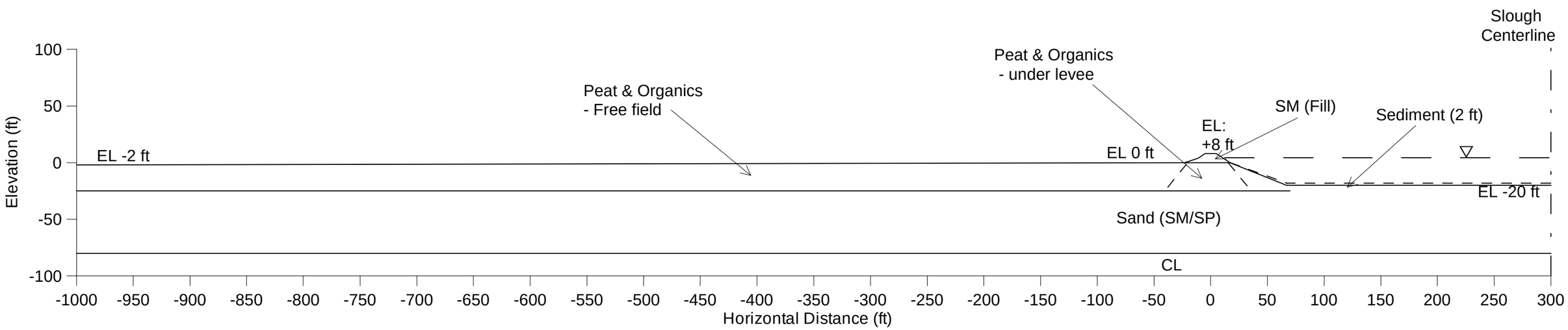

Note:
All elevations are referenced to NAVD88
(NAVD88 = NGVD29 + 2.5 ft)

Levee Geometry
Crest elevation +8 ft
Landside slope - From levee crest to EL+4 ft:1.5H:1V, followed by 3H:1V
Waterside slope - From levee crest to EL0 ft:1.5H:1V, followed by 2.5H:1V

Delta Risk Management Strategy (DRMS) Levee Fragility		Typical Cross Section for Suisun Marsh Levees	Figure 7-67
URS	Project No. 26815621		

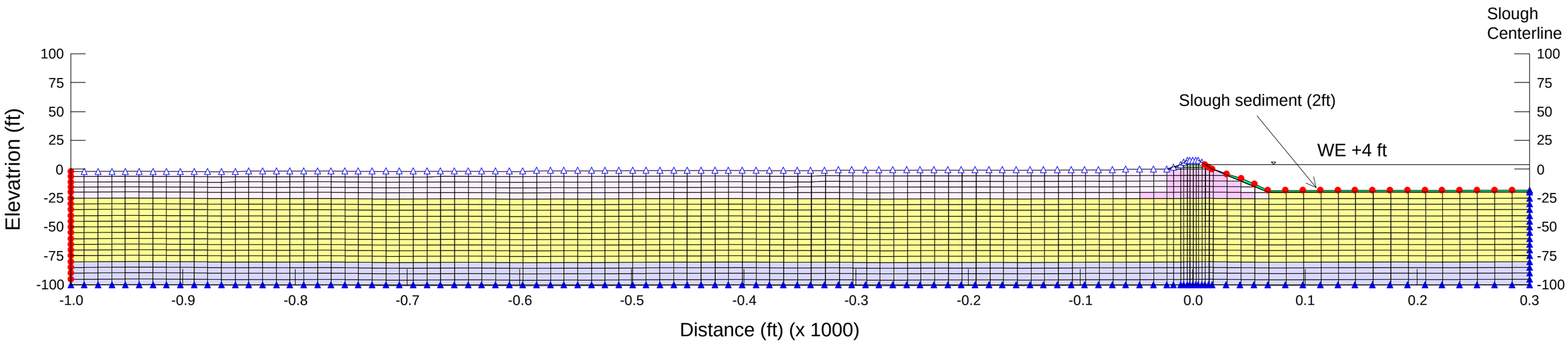

Legend

Boundary Conditions

- No flow
- Fixed head
- Review

Material Type

- Sandy Levee Fill
- Free Field Peat
- Under Levee Peat
- Sand (SP/SM)
- Clay
- Slough Sediment

Note:
All elevations are referenced to NAVD88
(NAVD88 = NGVD29 + 2.5 ft)

Model: Typical cross section for Suisun Marsh
with 25 ft peat & organics
(Case- with slough sediment and without ditch)

Delta Risk Management Strategy (DRMS) Levee Fragility		Finite Element Mesh & Boundary Conditions Typical Cross Section for Suisun Marsh	Figure 7-68
URS	Project No. 26815621		

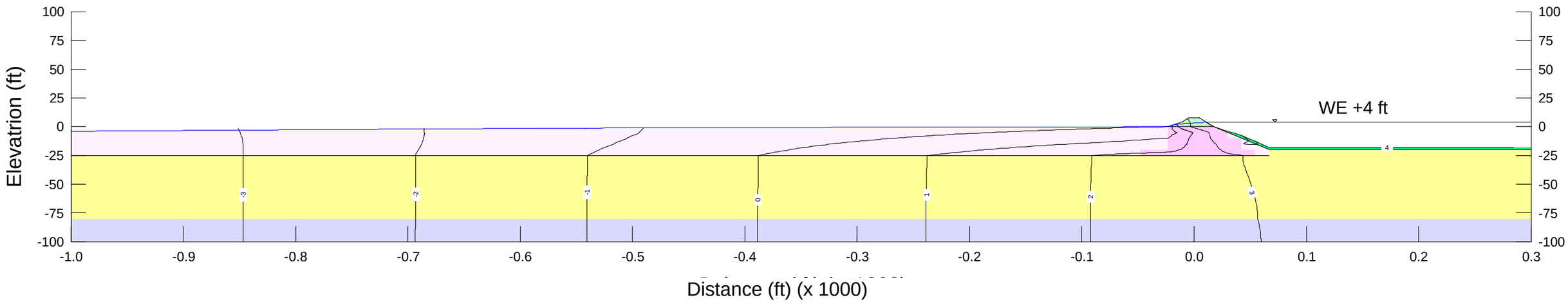

(a) Total head distribution contours

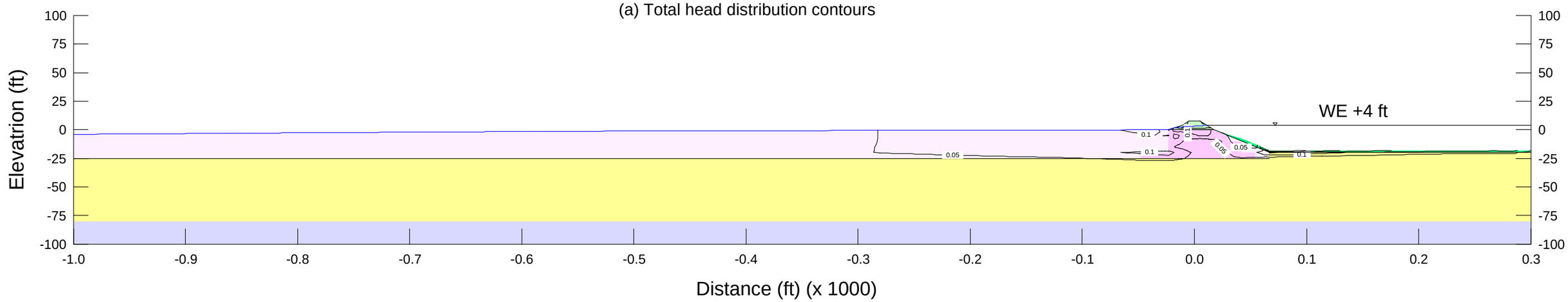

(b) Vertical gradient contours

Note:
All elevations are referenced to NAVD88
(NAVD88 = NGVD29 + 2.5 ft)

Analysis Case: Mean permeability veaues, Slough Water Elevation +4 ft,
Peat and Organic Thickness 25 ft, Model without Ditch , and
2 ft silt sediment presents at slough bottom

For Suisun Marsh,
Mean High Tide ~ +5.5 ft
Mean Low Tide ~ +0.3 ft

Delta Risk Management Strategy (DRMS) Levee Fragility		Total Head & Vertical Gradient Contours for 25 ft Peat & Organics Typical Cross Section for Suisun Marsh	Figure 7-69
URS	Project No. 26815621		

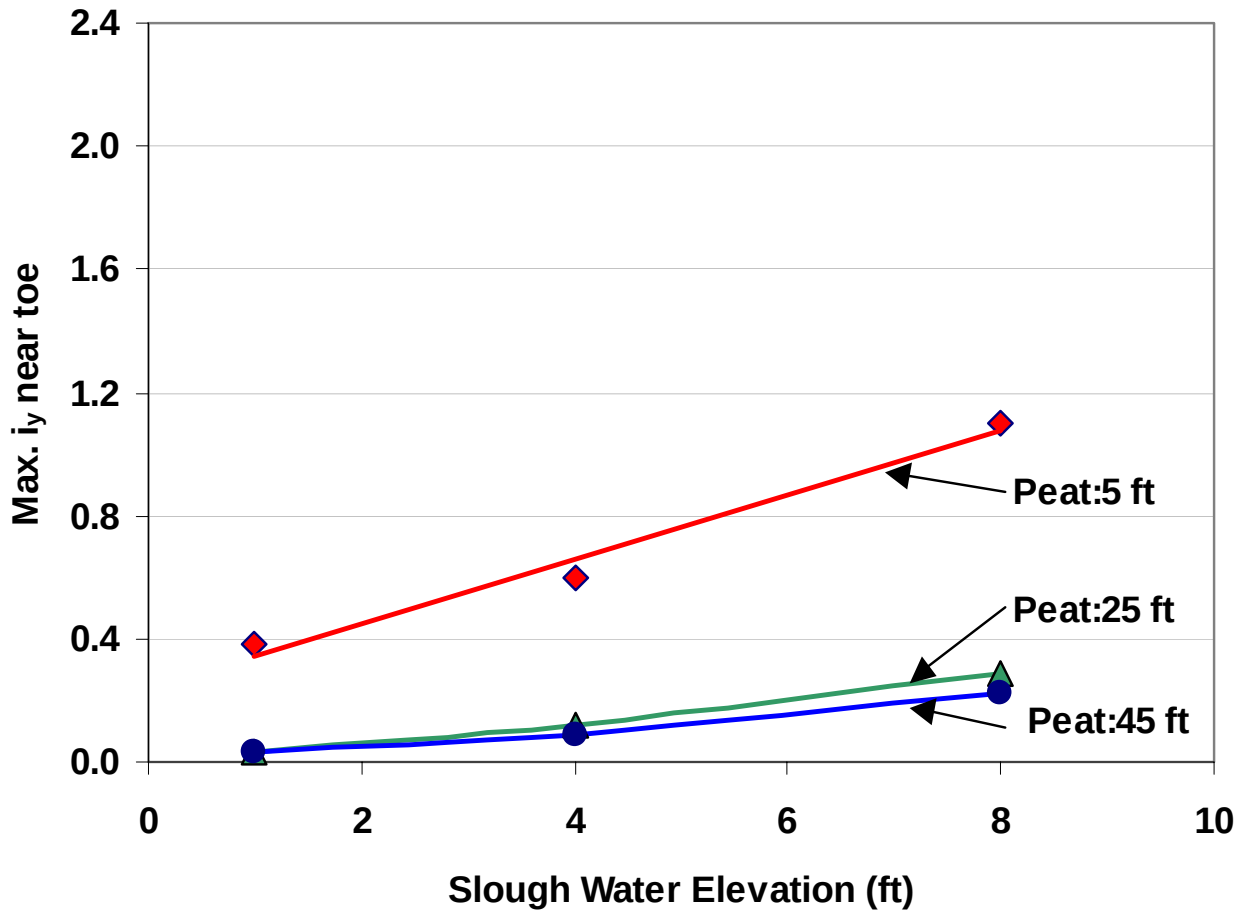

Note:
All elevations are referenced to NAVD88
(NAVD88 = NGVD29 + 2.5 ft)

Analysis Case: Model without ditch and with slough sediment

Delta Risk Management Strategy (DRMS) Levee Fragility		Vertical Gradients for 5, 25, and 45 ft Peat/Organics Typical Cross Section for Suisun Marsh	Figure 7-70
URS	Project No. 26815621		

Probability of Failure versus Vertical Exit Gradient for Under Seepage (smoothed)
-No Human Intervention

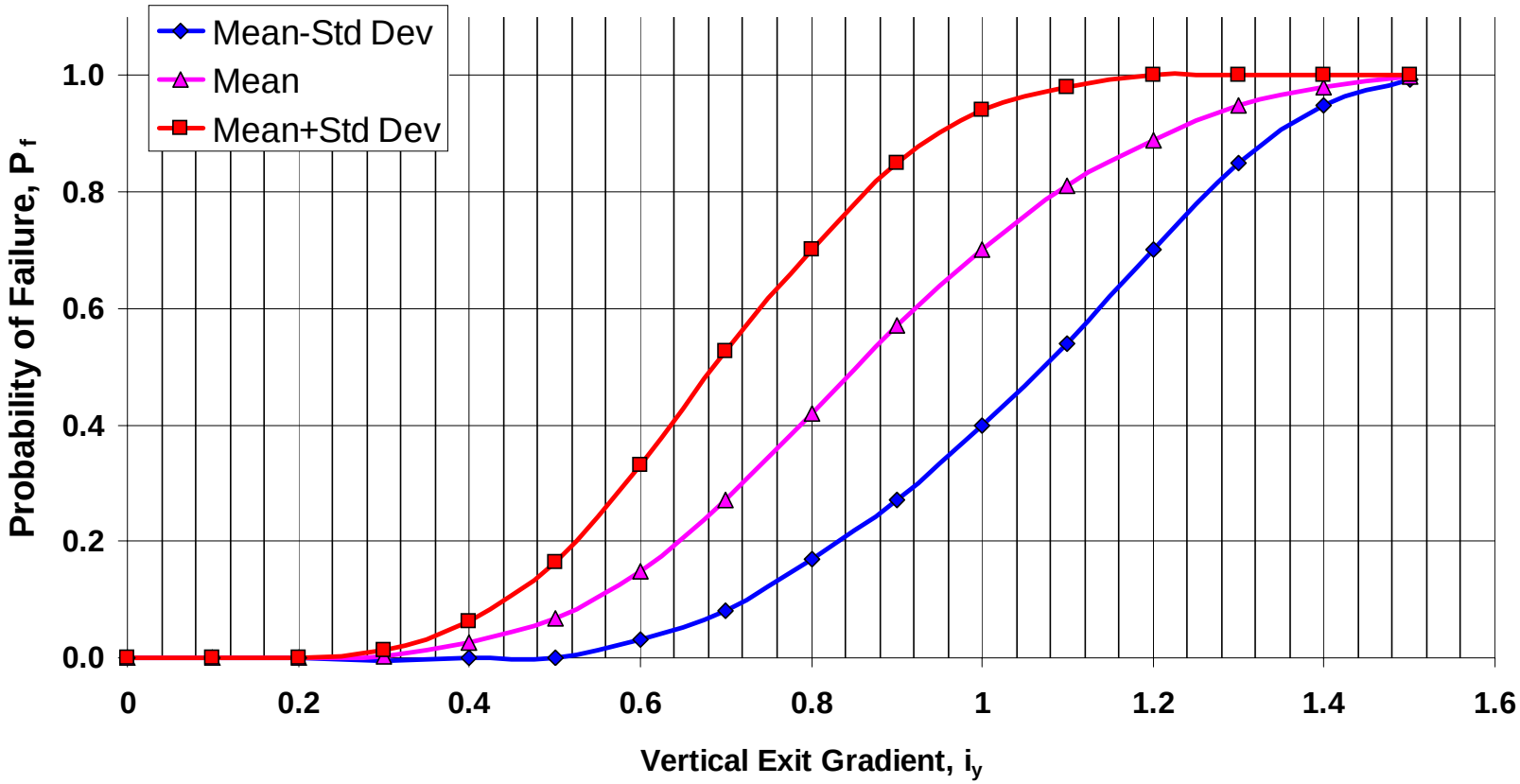

Delta Risk Management Strategy (DRMS) Levee Fragility		Probability of Failure versus Exit Gradient -No Human Intervention	Figure 7-71
URS	Project No. 26815621		

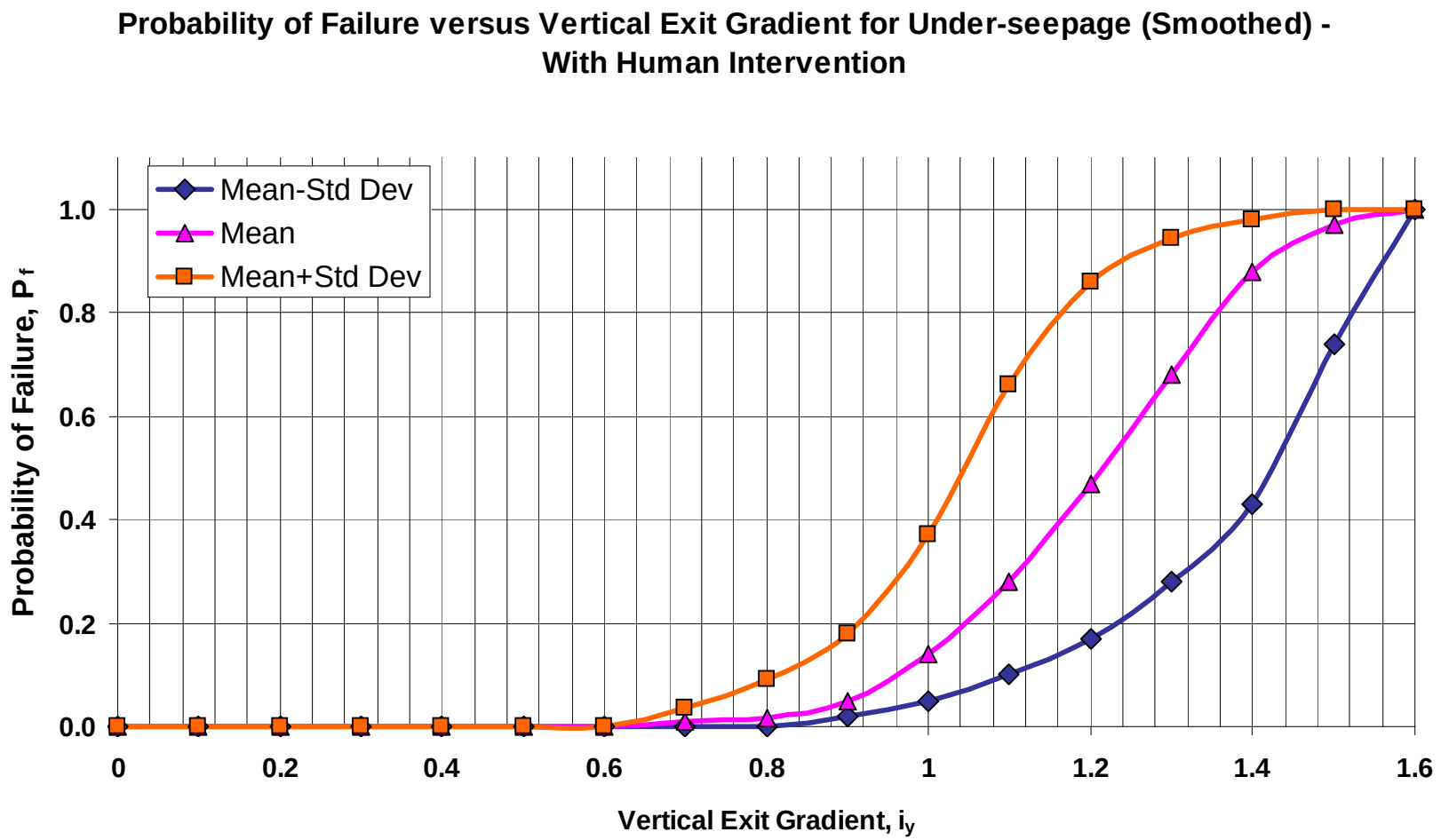

Delta Risk Management Strategy (DRMS) Levee Fragility		Probability of Failure versus Exit Gradient - With Human Intervention	Figure 7-72
URS	Project No. 26815621		

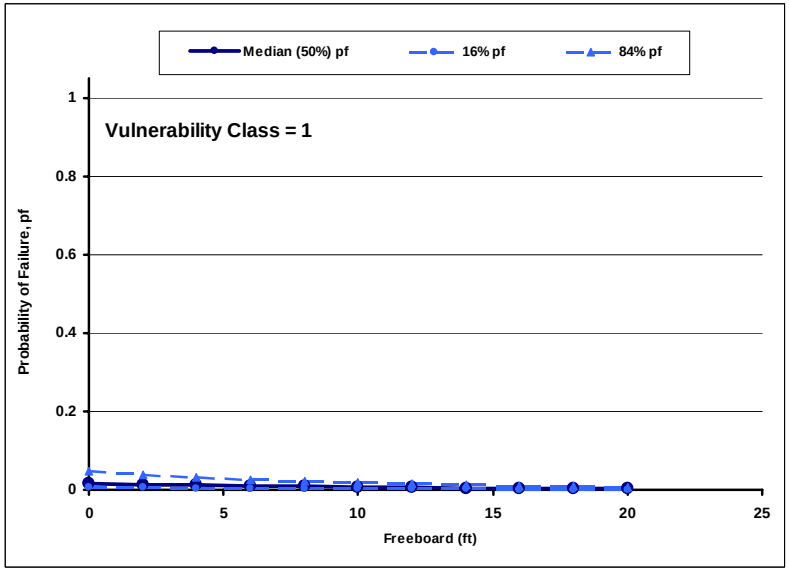

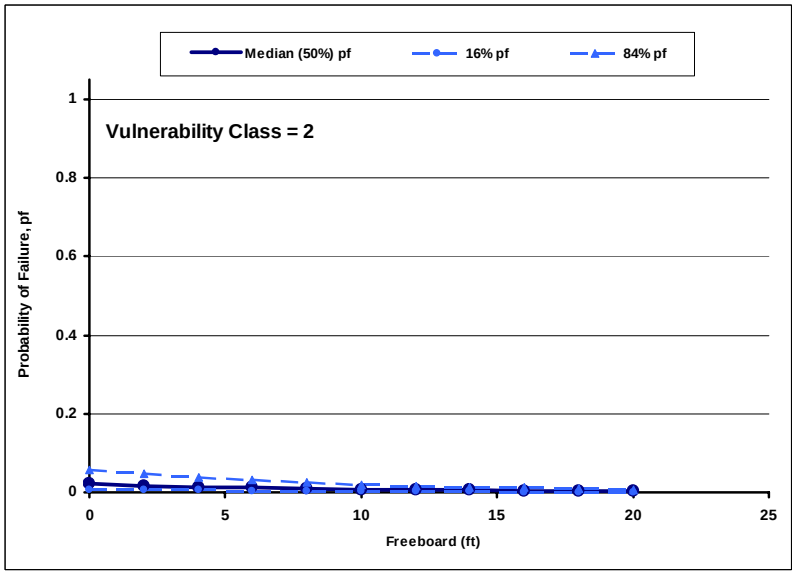

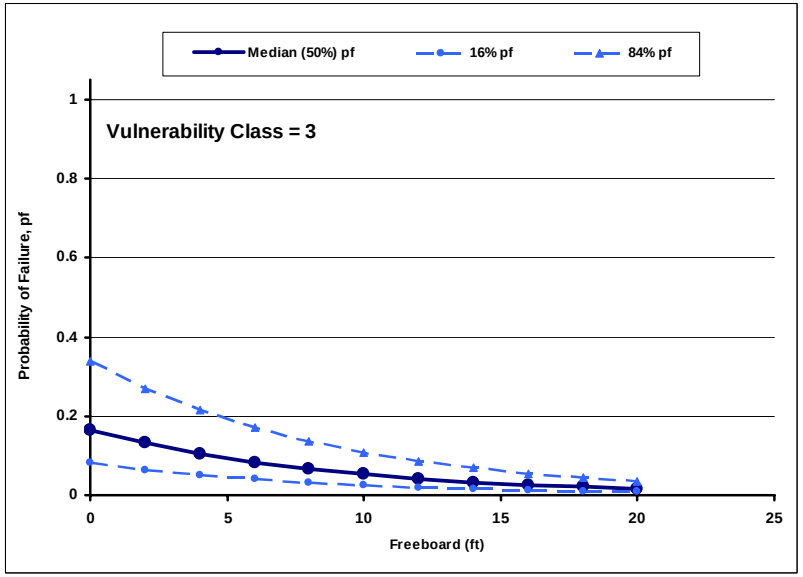

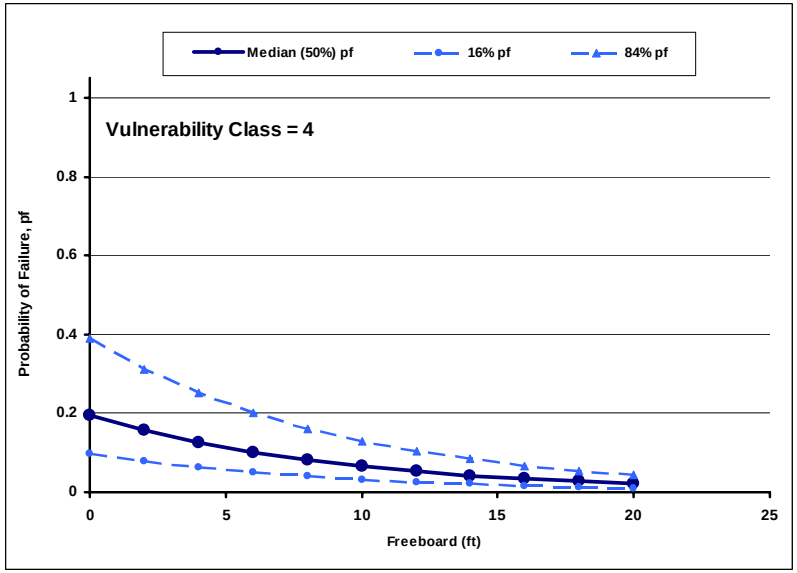

Delta Risk Management Strategy (DRMS) Levee Fragility		Estimated Failure Probability at 16%, 50%, and 84% Confidence Levels for Under-seepage Vulnerability Classes 1, 2, 3 and 4	Figure 7-73a
URS	Project No. 26815621		

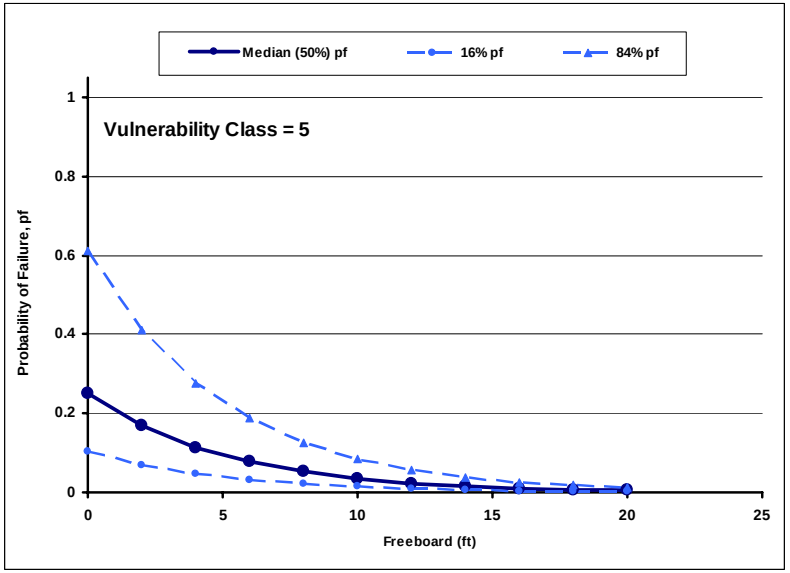

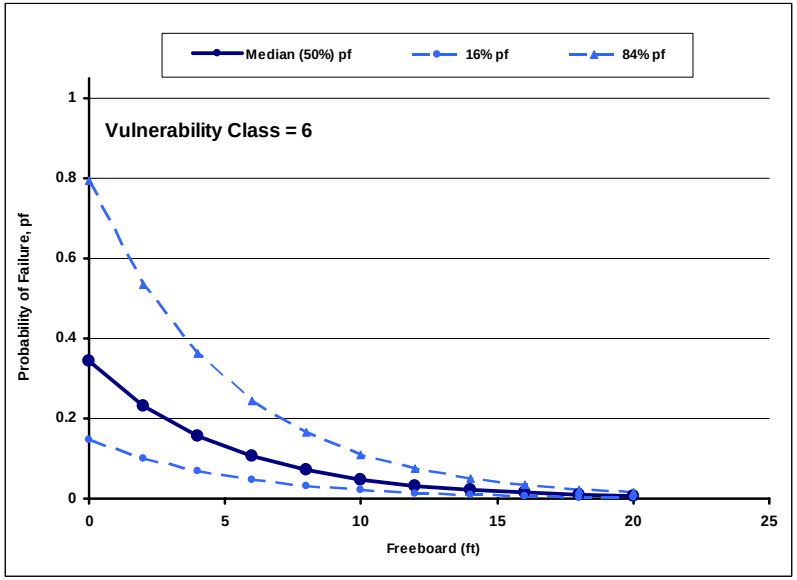

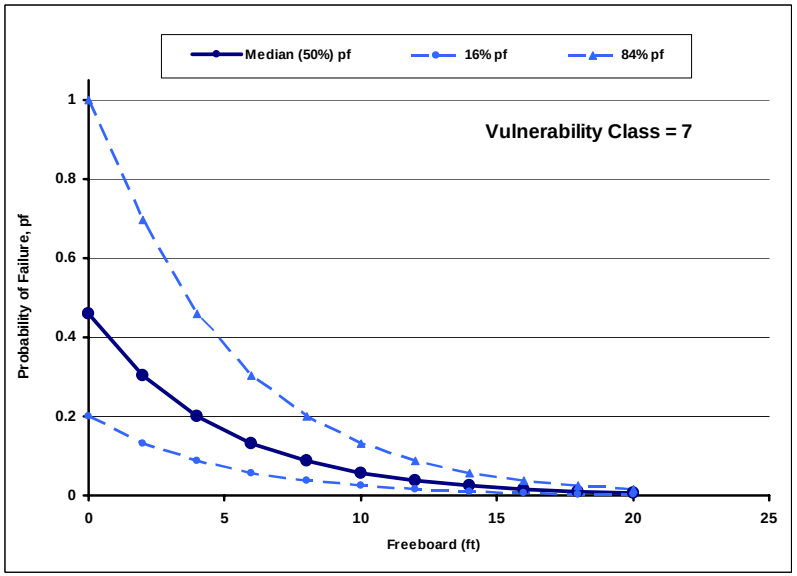

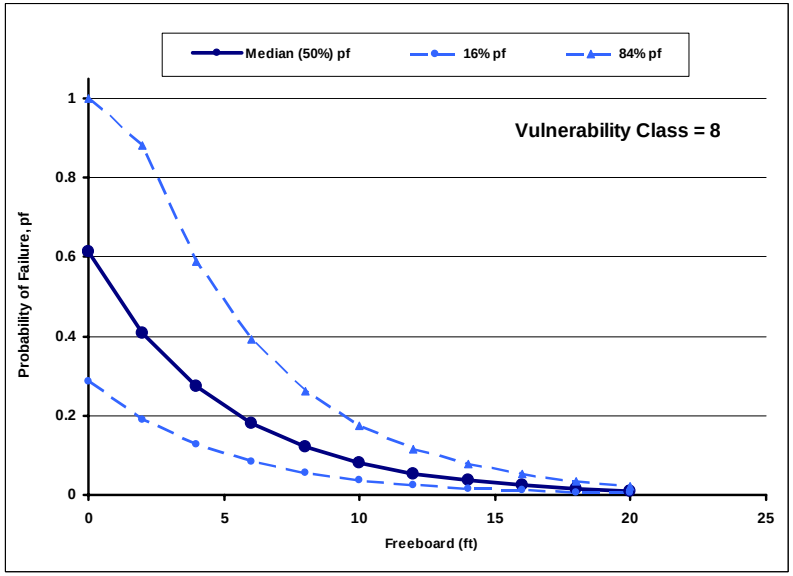

Delta Risk Management Strategy (DRMS) Levee Fragility		Estimated Failure Probability at 16%, 50%, and 84% confidence levels for Under-seepage Vulnerability Classes 5, 6, 7 and 8	Figure 7-73b
URS	Project No. 26815621		

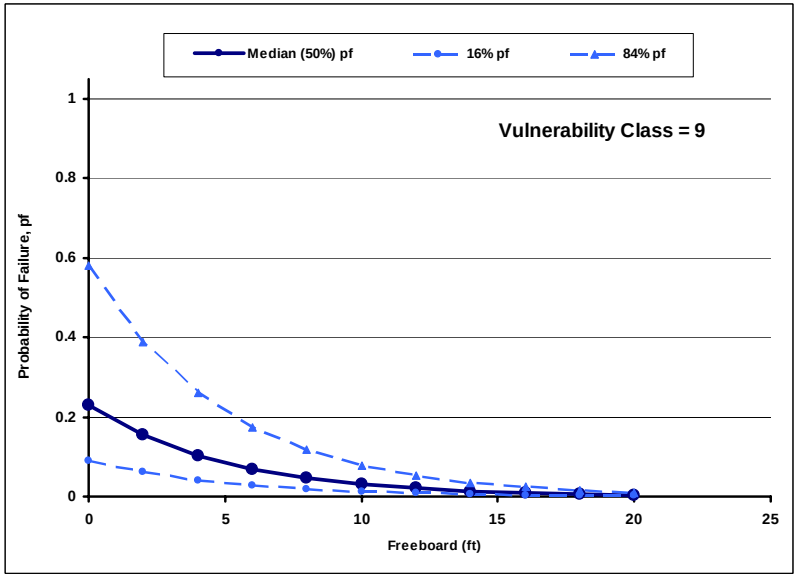

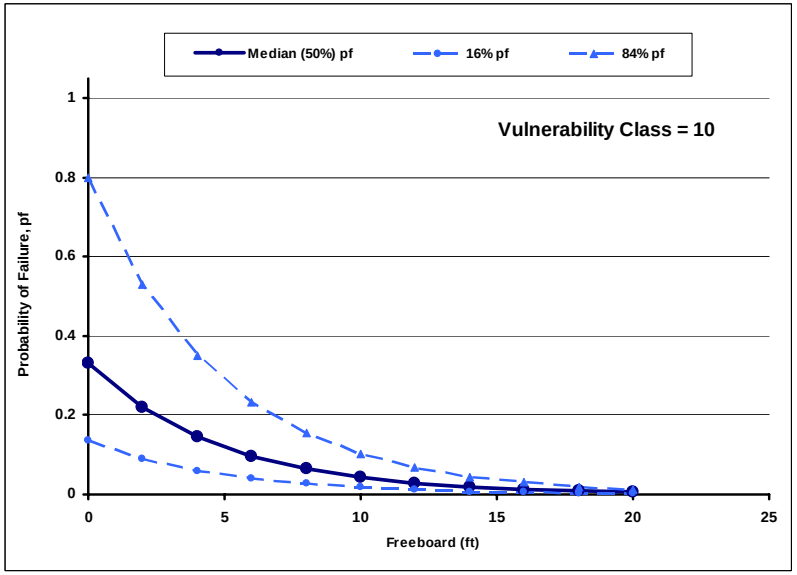

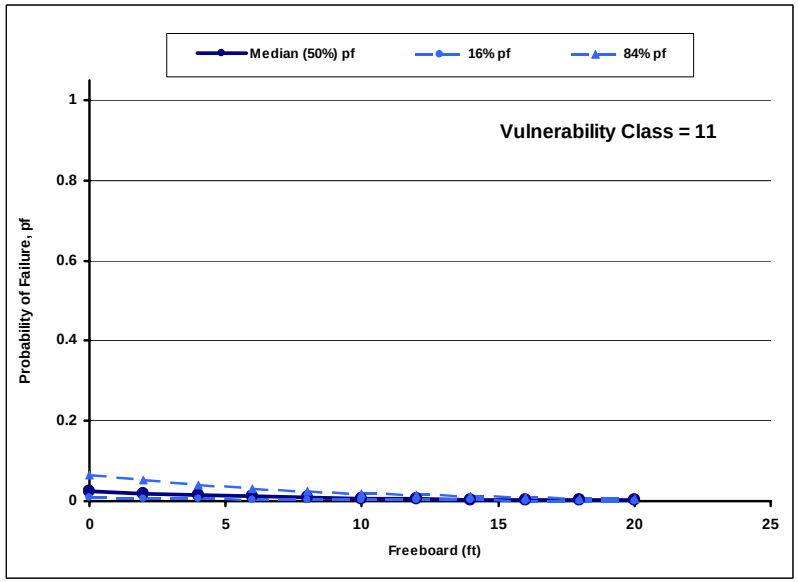

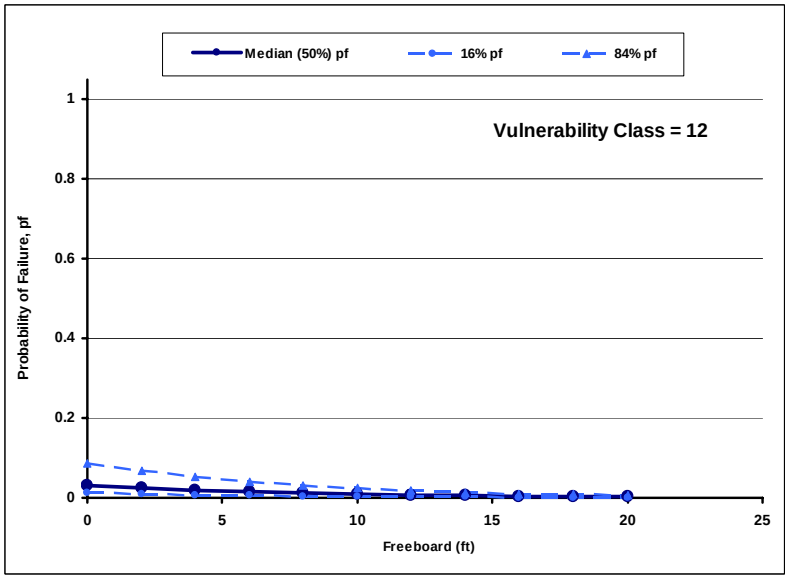

Delta Risk Management Strategy (DRMS) Levee Fragility		Estimated Failure Probability at 16%, 50%, and 84% confidence levels for Under-seepage Vulnerability Classes 9,10, 11 and 12	Figure 7-73c
URS	Project No. 26815621		

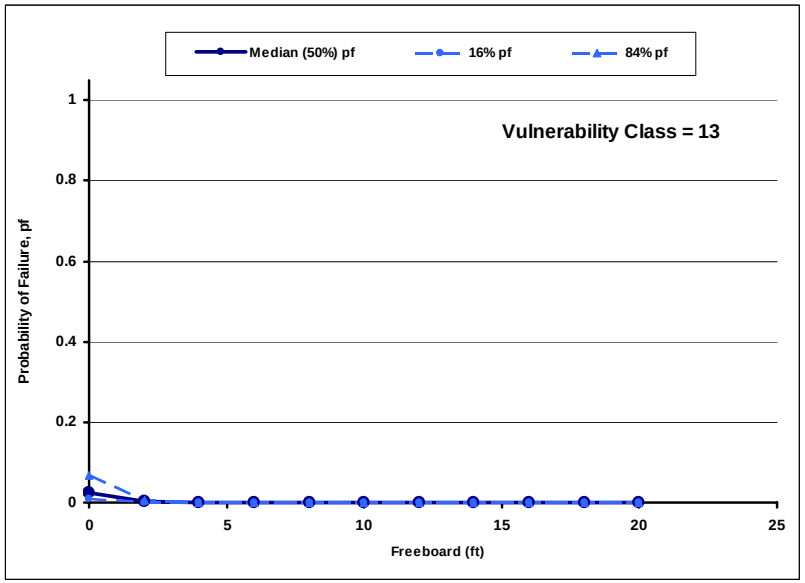

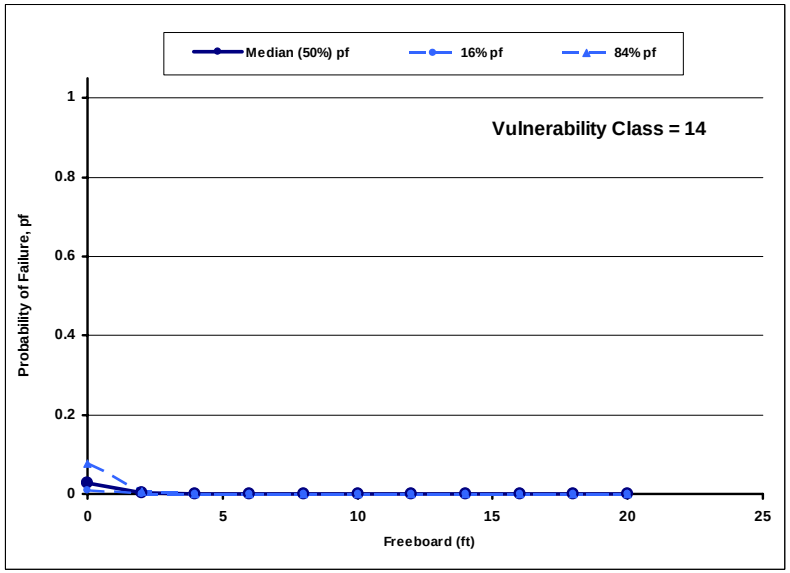

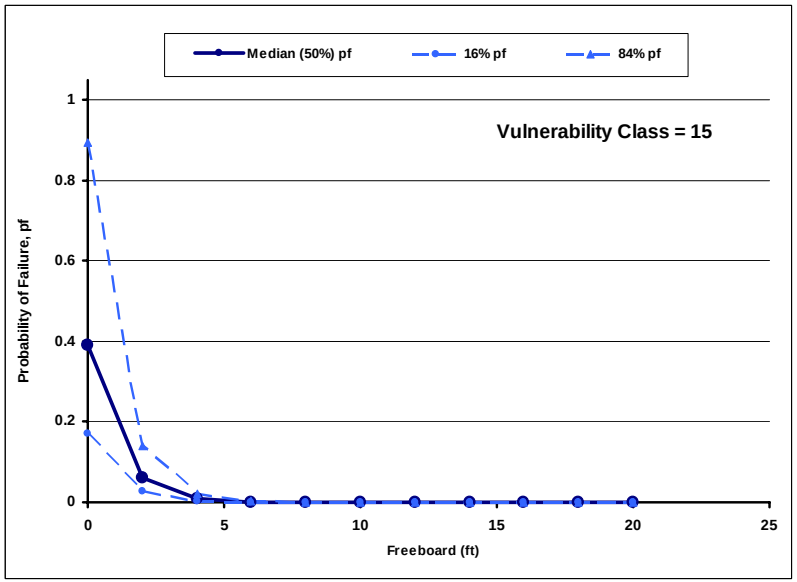

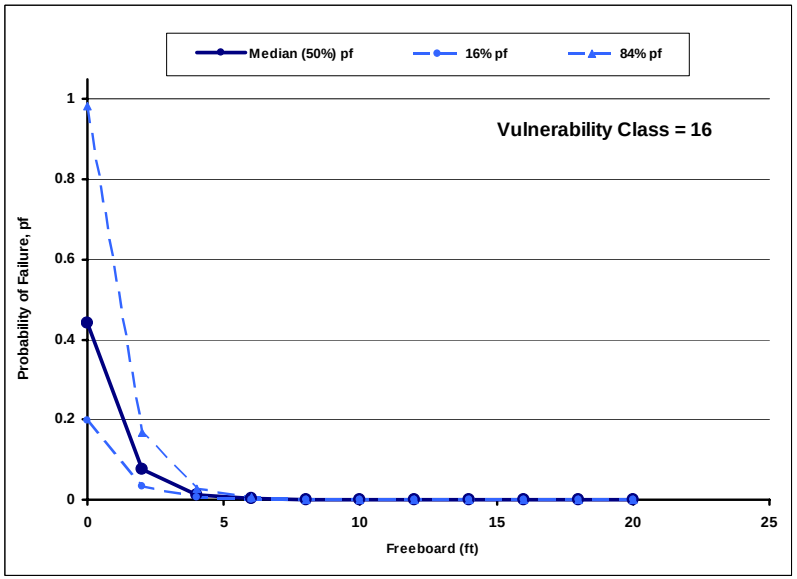

Delta Risk Management Strategy (DRMS) Levee Fragility		Estimated Failure Probability at 16%, 50%, and 84% confidence levels for Under-seepage Vulnerability Classes 13,14, 15 and 16	Figure 7-73d
URS	Project No. 26815621		

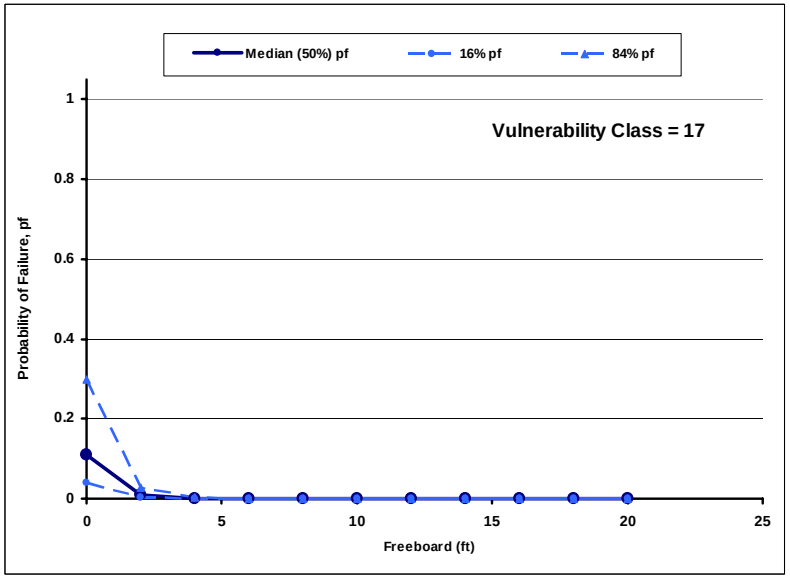

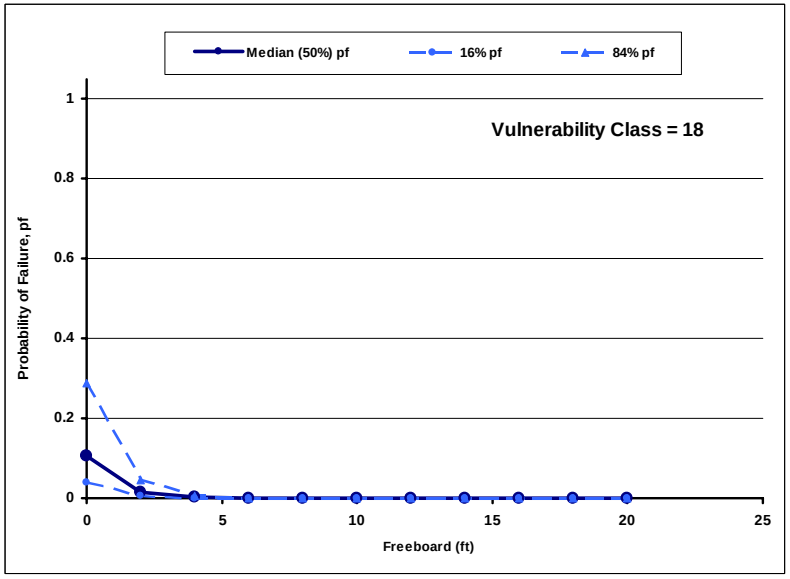

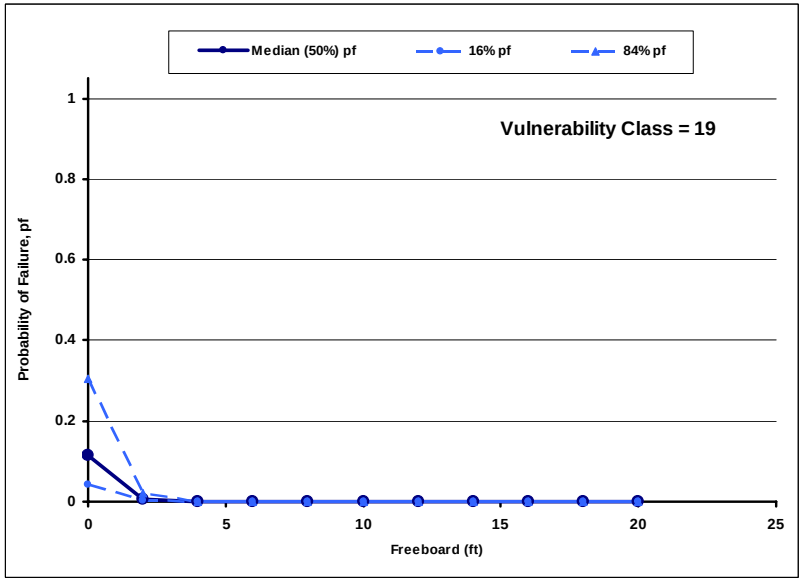

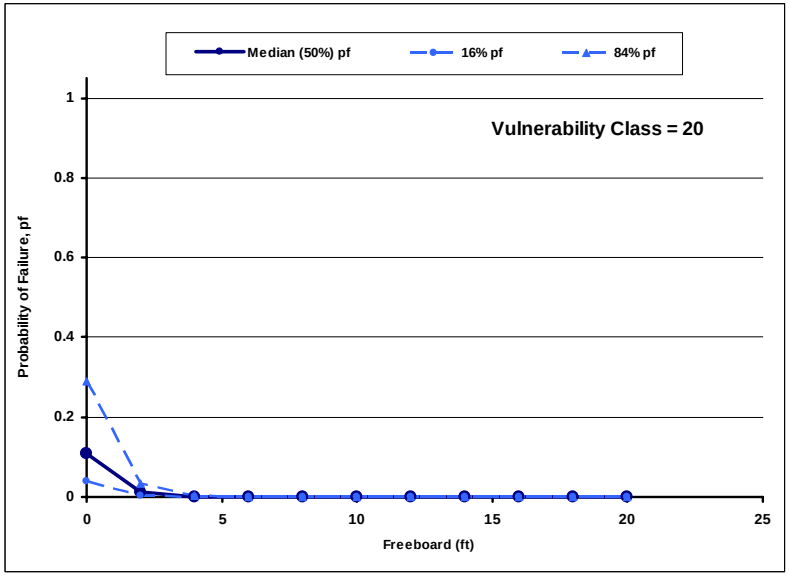

Delta Risk Management Strategy (DRMS) Levee Fragility		Estimated Failure Probability at 16%, 50%, and 84% confidence levels for Under-seepage Vulnerability Classes 17,18, 19 and 20	Figure 7-73e
URS	Project No. 26815621		

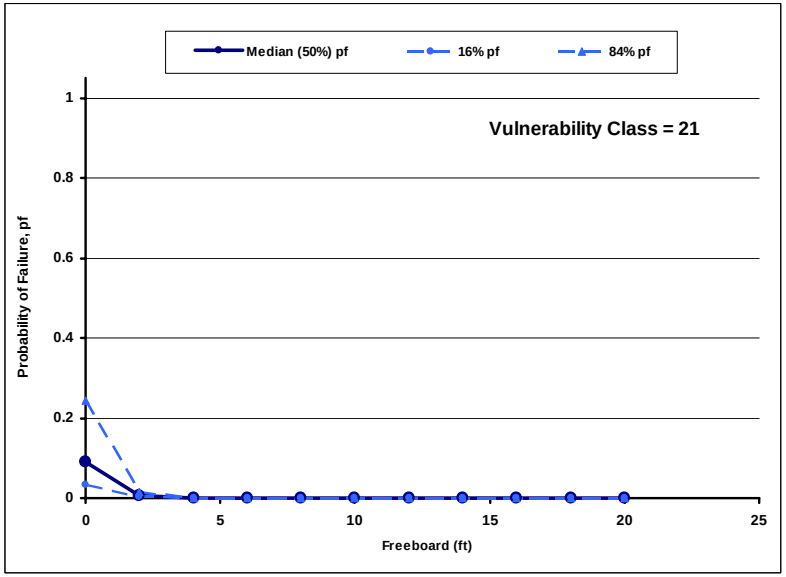

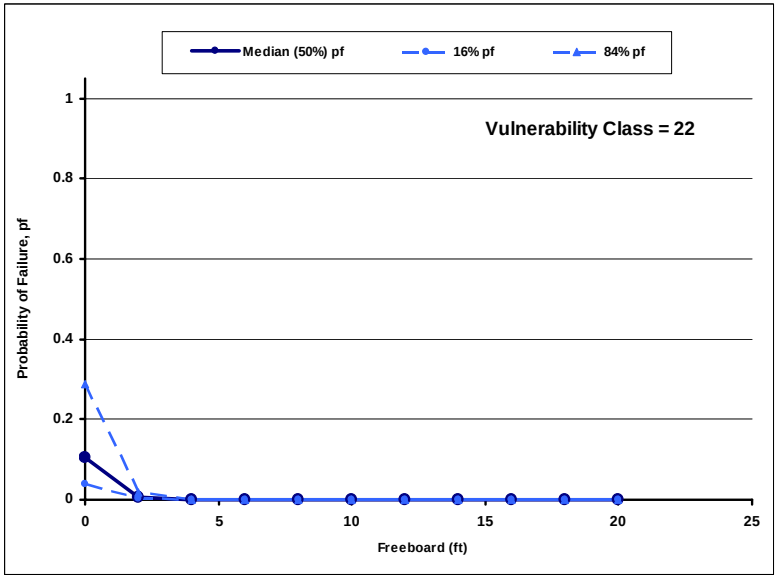

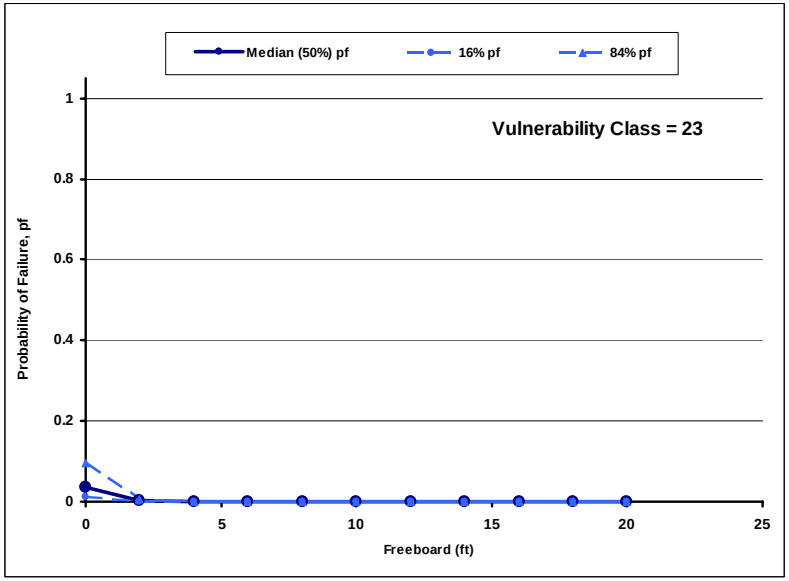

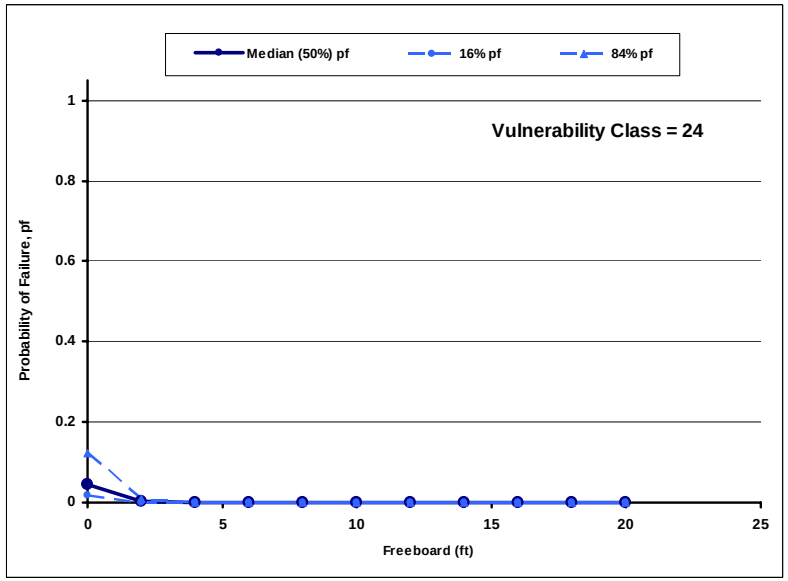

Delta Risk Management Strategy (DRMS) Levee Fragility		Estimated Failure Probability at 16%, 50%, and 84% confidence levels for Under-seepage Vulnerability Classes 21,22, 23 and 24	Figure 7-73f
URS	Project No. 26815621		

Landside toe through-seepage erosion, Sacramento Bypass South Levee (Jan. 2008)

Boil on landside slope, Bouldin Island, Delta (Feb. 1983)

Tension crack at levee crest, Staten Island, Delta (Jul. 2007)

Landside through-seepage erosion, Sac. River at Natomas Highway (Jan. 1986)

Boil on landside levee bench, Staten Island, Delta (Jul. 2007)

Figure 7-74 Through-Seepage Case Histories

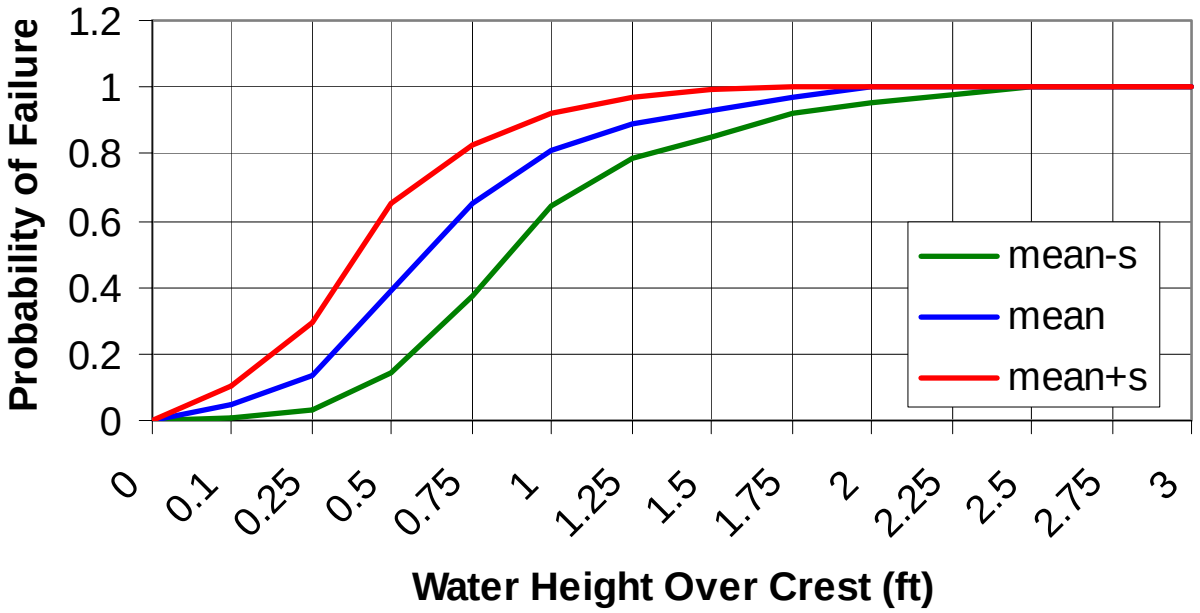

Delta Risk Management Strategy (DRMS) Levee Fragility		Probability of Failure versus Water Height over the Crest - Overtopping Failure Mode	Figure 7-75
URS	Project No. 26815621		